

ENHANCING PROGENITOR CELLS FOR CELL THERAPY AFTER MYOCARDIAL INFARCTION

SOPHIA MALANDRAKI-MILLER

Wolfson College
Department of Physiology, Anatomy and Genetics
University of Oxford

MT2012 - MT2016



Supervisors: Prof. Carolyn A. Carr & Dr. Nicola Smart

ACKNOWLEDGEMENTS

It is difficult to believe that 4 years have gone by and this study has come to an end. It has been a fascinating, enlightening and at times turbulent journey, which I could not have completed without the help and support of certain people and institutions.

First and foremost I owe a huge thank you to my main supervisor Prof. Carolyn Carr for her guidance, help and patience along the years. She has been extremely encouraging and willing to answer questions or to discuss scientific ideas, for all of which I am grateful. In addition, I express my gratitude to my co-supervisor, Dr. Nicola Smart, who has been a valuable supportive figure for me, always keen to offer help. To Prof. Kieran Clarke I owe special thanks for allowing me to be part of her group, and work in the laboratory facilities.

It goes without saying that I have had a lot of support by special people along these four years, who offered me encouragement, friendship, and help. A sincere thank you to my colleagues who have been a source of daily companionship, motivation and encouragement, making this a fun journey: Heba al-Siddiqi, Lucia Giles, Arne Bruyneel, Luz Maria Fialho, Colleen Lopez, Dragana Savic, Brianna Stubbs, Matt Kerr, Jack Miller, Filippo Perbellini, Kathy Pakzad, Lucy Ambrose, Beth Eggleston. I was very lucky to work with these people who, apart from being friends to me, have helped me and shared their knowledge on different techniques and technical matters. I would like to also thank Prof Damian Tyler, Dr. Mike Dodd, Dr. Rhys Evan, Mrs. Nicola Dixon, Mrs. Yvonne Green and the rest of the members of the Clarke group for being helpful.

A specific declaration of gratitude to Dr. Lisa Heather for sharing her wisdom on the metabolic study and offering guidance, and to Dr. Vicky Ball for her help with different lab instruments and for always being encouraging.

I definitely owe a big thank you to certain special people for being there for me Lewis Daly, Seema Chauhan, Roni Nudel, Joanna Kardari, Elpida Papatzanaki, Georgia Katsanevaki, Merja Rossi and Augustine Ajuo.

During this period I have also been privileged to meet some smart young students, who worked with me, along different parts of this project. It has been a pleasure working with Georgie Burrow, Eva Supit, Rita Alonaizan, Emma Smith and Saumya Jani, and of course Colleen Lopez. More specifically, I am thankful to

and I would like to acknowledge: Rita for her help with the caspase activity assay, and Georgie for her help with the Western Blot study on differentiation.

I would also like to extend my gratitude to certain groups in the Dept. of Physiology, Anatomy & Genetics for offering scientific and technical support to me at different point of this project. I would like to thank Prof. Paul Riley's group, and more specifically Dr. Richard Tyser for providing me with the mESC line, and Prof. Manuela Zaccolo's group, and more specifically Dr. Konstantinos Lefkimmatis, Dr. Oliver Lomas and Marcella Brescia, for sharing their knowledge on cardiac fibroblasts. Finally I am thankful to a very helpful individual in the department, Mrs. Sarah Noujaim.

A particular debt of gratitude is owed to the funding bodies and institutions which have supported me financially for the duration of my studies. namely I am grateful to Clarendon Fund for covering my DPhil costs, Rosetrees Trust and Primerdesign for supplying us with consumable funding, and last but not least Wolfson College.

Last but definitely not least, my family has been a source of great support, without which I could not have come this far. I am grateful beyond words to my parents: Helen and George, brother, George and grandmother, Maria for always believing in me, sending their love from afar and helping me any way they could.

ABSTRACT

Based on data from the World Healthcare Organisation, cardiovascular diseases are the primary cause of disease-related death globally, with myocardial infarction (MI) being the most prevalent. If not treated effectively, MI can progress to heart failure (HF). With 70 million prescriptions for HF in 2014 and 515 people in the UK being hospitalised daily with MI, the British Heart Foundation calls for novel robust treatments. Even though cardiac stem cell (CSC) therapy for MI has been under investigation for more than a decade, there still has not been a consensus over the identity of the adult endogenous CSC. Recent clinical trials, using selected Ckit+ cells or the cardiosphere-derived cells (CDCs) have shown moderate results.

The aim of this thesis was to develop a digestion-based method for isolation of cardiac progenitor cells (CPCs) from the mouse atria. The resulting “CTs” were isolated by collagenase/trypsin (where their name has resulted from) digestion with a prolonged period step for cell attachment. CTs were compared to isolated CDCs for their marker expression, using RT-PCR and Immunocytochemistry, showing cells with a mesenchymal phenotype which expressed SCA1 and CKIT. The CDCs had more of a fibroblast phenotype with higher Ddr2 and Wt1 expression.

Using a TGF- β 1 differentiation protocol, the CTs could be differentiated more effectively to a CM lineage than could the CDCs. In addition, Oleic acid (OA) supplementation stimulated the Peroxisome proliferator-activated receptor alpha pathway and led to maturation of the CT cells, both before and after differentiation. The differentiated CTs begin to express Tnnt2, while OA led to Myh7 increase and upregulated their oxidative metabolism. Finally, the CTs were more able to survive under serum-starvation than the CDCs, and transfection with miR-210 could enhance CT survival under these conditions and increased VEGF secretion.

By digestion of the whole atria and allowing a prolonged time for attachment, we have developed a novel isolation protocol which generates a cell population containing a range of progenitors. Cells within this population can survive under serum starvation and can be differentiated to a CM lineage, making them a promising therapeutic population.

Contents

ACKNOWLEDGEMENTS	2
ABSTRACT	4
1. INTRODUCTION	10
1.1. THE HEART, MI & HF.....	11
1.2. CELL THERAPY POST-MI.....	12
1.2.1. PLURIPOTENT STEM CELLS	13
1.2.2. ADULT PROGENITOR CELLS (PCs)	14
1.2.2.1. BONE MARROW-DERIVED STEM CELLS (BMSCs)	15
1.2.2.2. SKELETAL MYOBLASTS	15
1.2.2.3. MESENCHYMAL STEM CELLS	16
1.2.2.4. ENDOGENOUS CARDIAC PROGENITOR CELLS (CPCs)	17
1.2.2.4.1. CKIT+ CPCs	18
1.2.2.4.2. STEM CELL ANTIGEN (SCA1) CPCs	18
1.2.2.4.3. CARDIOSPHERE-DERIVED CELLS (CDCs).....	20
1.2.2.4.4. EPICARDIAL STEM CELLS.....	20
1.2.2.4.5. CELL COMBINATIONS	21
1.3. CARDIAC DEVELOPMENT & TRANSCRIPTION FACTORS	21
1.4. CAN THE HEART REGENERATE ITSELF?.....	24
1.5. OVERVIEW OF CARDIAC METABOLISM	26
1.6. STEM CELL THERAPY – CURRENT OBSTACLES	28
1.7. THESIS AIMS	29
ABBREVIATIONS.....	31
2. MATERIALS & METHODS	33
2.1 MICE	33
2.2 ISOLATION AND EXPANSION OF MOUSE CARDIAC PROGENITOR CELLS (CPCS)	33
2.2.1 CARDIOSPHERE-DERIVED CELLS (CDCS) ISOLATION	33
2.2.1.1 STANDARD ATRIAL EXPLANTING METHOD (CDCS)	33
2.2.1.2. CARDIOSPHERE FORMATION	34
2.2.1.3. CELL EXPANSION.....	35
2.2.2 COLLAGENASE-TRYPSIN DIGESTIONS (CTS).....	35
2.2.2.1. RE-PLATING ISOLATION METHOD (SLOWLY-ADHERING PROGENITORS).....	36
2.2.3. EXPLANT & CT CULTURE FROM THE SAME MOUSE ATRIA	36
2.3. STATISTICAL ANALYSIS.....	36
2.4. CELL PROLIFERATION ASSAY.....	37

2.5. RNA ISOLATION – CDNA CONVERSION.....	37
2.5.1 RNA EXTRACTION & QUANTIFICATION – QUALITY CHECK.....	37
2.5.2 REVERSE TRANSCRIPTION	37
2.6. REAL-TIME POLYMERASE CHAIN REACTION (RT-PCR).....	38
2.6.1. PRIMERS & PRIMER DESIGN.....	38
2.6.2. PRIMER EFFICIENCY TESTING	38
2.7. IMMUNOCYTOCHEMISTRY.....	40
2.7.1 CELL PREPARATION & FIXATION.....	40
2.7.2. ANTIBODY STAINING	40
2.7.3. CONFOCAL MICROSCOPY	41
2.8. FLOW CYTOMETRY	42
2.8.1. CELL PREPARATION	42
2.8.2. ANTIBODY STAINING & ANALYSIS	42
2.9. COLONY FORMING ASSAY	42
2.10. CARDIAC PROGENITOR DIFFERENTIATION TOWARDS CM LINEAGE.....	43
2.10.1. MOUSE-ESC DIFFERENTIATION	43
2.10.2. TGFB1 DIFFERENTIATION (GCDM).....	43
2.11. METABOLIC SUBSTRATE MANIPULATION	44
2.11.1. OLEIC ACID TREATMENT.....	44
2.11.2. ICARIIN TREATMENT.....	45
2.11.3. TGF-B1 DIFFERENTIATION + OLEIC ACID (GCDM+OA)	45
2.12. WESTERN BLOTS.....	46
2.12.1. CELL LYSATE PREPARATION.....	46
2.12.2. PROTEIN ASSAY	46
2.12.3. POLYACRYLAMIDE GEL ELECTROPHORESIS & PROTEIN TRANSFER	46
2.12.4. IMMUNOBLOTTING AND DETECTION	47
2.13. METABOLIC ASSAYS.....	47
2.13.1. GLUCOSE- ¹⁴ C OXIDATION MEASUREMENT	47
2.14. CELL TRANSFECTIONS.....	48
2.14.1. FLUORINE-NANOPARTICLE CELL TRANSFECTION.....	48
2.14.2. NANOPARTICLE - MIRNA TRANSFECTION	49
2.14.3. DHARMAFECT – MIRNA TRANSFECTION.....	50
2.15. APOPTOSIS INDUCTION & CELL SURVIVAL ASSAY.....	50
2.17. METABOLITE MEASUREMENTS	51
2.18. MIRNA TARGET PREDICTION	51
3. MOUSE ATRIAL CARDIAC PROGENITORS.....	57

3.1. INTRODUCTION	58
3.2.1. SEEKING FOR THE IDEAL CPC <i>IN VITRO</i>	58
3.2.2. WHAT IS THE CARDIAC FIBROBLAST?	58
3.2.3. FIBROBLASTS & OTHER CELLS.....	60
3.2.4. WHERE DO CPCs LIVE?	62
3.2.5. ISSUES WITH ISOLATION PROTOCOLS FOR CPCS	63
3.2.6. STUDY AIMS.....	65
3.3. RESULTS.....	66
3.3.1. ATTEMPTS TO OPTIMISE THE EXPLANTING PROTOCOL.....	66
3.3.2. DEVELOPING A DIGESTION-BASED PROTOCOL FOR CPC ISOLATION.....	69
3.3.3. CTS INCREASE PROLIFERATION & HOMOGENEITY, WITH PASSAGING	73
3.3.4. CTS CONTAIN A POPULATION OF STRONGLY-ADHERENT CELLS WITH HIGH LEVELS OF STEMNESS MARKERS	77
3.3.5. CTS HAVE CONSISTENTLY HIGHER STEMNESS MARKER SCA1 THAN CDCs	79
3.3.6. CTS & CDCS SHOW SIMILAR LEVELS OF CARDIAC DEVELOPMENTAL MARKERS.....	84
3.3.7. CTS CONTAIN A POPULATION OF TELOCYTES	85
3.4. DISCUSSION	87
3.4.1. ATTEMPTS TO OPTIMISE THE EXPLANTING PROTOCOL.....	87
3.4.2. DEVELOPING A DIGESTION-BASED PROTOCOL FOR CPC ISOLATION.....	88
3.4.3. CTS SHOW INCREASED PROLIFERATION AND HOMOGENEITY, WHILE PASSAGE INCREASES	88
3.4.4. CTS CONTAIN A POPULATION OF STRONGLY-ADHERENT CELLS WITH HIGH LEVELS OF STEMNESS MARKERS	89
3.3.5. CTS HAVE CONSISTENTLY HIGHER STEMNESS MARKER SCA1 THAN CDCs	90
3.3.6. CTS AND CDCS SHOW SIMILAR LEVELS OF CARDIAC DEVELOPMENTAL MARKERS ..	91
3.3.7. CTS CONTAIN A POPULATION OF TELOCYTES	91
4. CARDIAC PROGENITOR DIFFERENTIATION	93
4.1. INTRODUCTION	94
4.2.1. CARDIAC DIFFERENTIATION <i>IN VITRO</i>	94
4.2.2. TGF- β & THE HEART.....	98
4.2.3. PEROXISOME PROLIFERATOR-ACTIVATED RECEPTORS (PPARS).....	99
4.2.4. OLEIC ACID.....	100
4.2.5. CARDIAC DEVELOPMENT - METABOLIC SWITCH (1)	101
4.2.6. CARDIAC METABOLISM IN MI & HF - METABOLIC SWITCH (2)	102
4.2.7. MITOCHONDRIA IN HEALTH & DISEASE	102
4.2.8. FROM STEM CELL TO ADULT CELLS - METABOLIC SWITCH (3).....	103

4.2.9. MITOCHONDRIA IN DEVELOPMENT & CELL DIFFERENTIATION	105
4.2.10. STUDY AIMS.....	105
4.3. RESULTS	106
4.3.1. STAGES OF mESC DIFFERENTIATION VIA EMBRYOID BODY FORMATION.....	106
4.3.2. TGF- β 1 DIFFERENTIATION INCREASES EXPRESSION OF TNNT2 IN BOTH CDCS AND CTS 108	
4.3.3. MANIPULATION OF CELL METABOLISM	112
4.3.3.1. OLEIC ACID SUPPLEMENTATION STIMULATES THE PPARA PATHWAY AND METABOLICALLY MATURES CT CELLS.....	112
4.3.3.2. PHARMACOLOGICAL TREATMENT WITH ICARIIN DOES NOT STIMULATE THE PPARA PATHWAY IN ATRIAL CPCS.....	120
4.3.3.3. STIMULATION WITH OLEIC ACID FOR 1 WEEK FURTHER MATURES DIFFERENTIATED CTS FUNCTIONALLY AND METABOLICALLY	122
4.3.3.4. PROLONGED STIMULATION OF DIFFERENTIATED CTS WITH OLEIC ACID FOR 1 MONTH FURTHER MATURES DIFFERENTIATED CTS METABOLICALLY	128
4.4. DISCUSSION	130
4.4.1. STAGES OF MESC DIFFERENTIATION VIA EMBRYOID BODY FORMATION	130
4.4.2. TGF- β 1 DIFFERENTIATION INCREASES EXPRESSION OF TNNT	132
4.4.3. OLEIC ACID SUPPLEMENTATION STIMULATES THE PPARA PATHWAY AND METABOLICALLY MATURES CT CELLS.....	135
4.4.4. PHARMACOLOGICAL TREATMENT WITH ICARIIN DOES NOT STIMULATE THE PPARA PATHWAY IN ATRIAL CPCS.....	137
4.4.5 STIMULATION WITH OLEIC ACID FOR 1 WEEK FURTHER MATURES DIFFERENTIATED CTS PHENOTYPICALLY AND METABOLICALLY	138
4.4.6. PROLONGED STIMULATION OF DIFFERENTIATED CTS WITH OLEIC ACID FOR 1 MONTH FURTHER MATURES DIFFERENTIATED CTS METABOLICALLY	139
5. ENHANCING THE POTENTIAL OF CARDIAC PROGENITORS WITH MICRORNAS.....	142
5.1. INTRODUCTION	143
5.1.1. STEM CELL THERAPY - ENHANCING CELL SURVIVAL	143
5.1.2. MICRORNAS.....	143
5.1.3. IN SILICO ANALYSIS OF MIRNA TARGETS.....	145
5.1.4. MIRNAS & THE HEART	145
5.1.5. MIRNA-210	146
5.1.6. CELL DEATH <i>IN VITRO</i>	146
5.1.7. MIRNA DELIVERY	149
5.1.8. STUDY AIMS.....	150
5.2. RESULTS.....	151

5.2.1. CONTROL CTS HAVE BETTER SURVIVAL POTENTIAL THAN CDCs UNDER SERUM STARVATION	151
5.2.2. NP170 NANOPARTICLES CAN EFFICIENTLY LABEL CTs	153
5.2.3. MIR-210 INDUCES CT SURVIVAL SERUM STARVATION	154
5.2.4. IGFR1 SIGNALLING INVOLVED IN SERUM STARVATION DEATH – MIR-210 TARGET?	158
5.2.5. MIR-210 CAN INDUCE VEGF SECRETION FROM CTs.....	160
5.3. DISCUSSION	162
5.3.1. CONTROL CTS HAVE BETTER SURVIVAL POTENTIAL THAN CDCs UNDER SERUM STARVATION	162
5.3.2. MIR-210 INDUCES CT SURVIVAL UNDER SERUM STARVATION	162
5.3.3. IGFR1 SIGNALLING INVOLVED IN SERUM STARVATION DEATH – MIR-210 TARGET?	164
5.3.4. MIR-210 CAN INDUCE VEGF SECRETION FROM CTs.....	165
6. CONCLUSION	166
6.1. CONCLUSION	167
6.2. STUDY LIMITATIONS	168
6.3. FUTURE WORK.....	168
REFERENCES	170

APPENDIX A – RT-PCR Primers (page 52)

APPENDIX B – Microscopy antibodies & Dyes (page 54)

APPENDIX C – Western Blotting Components (page 55)

APPENDIX D – Cluster of Differentiation (CD_) Molecules - Full Names (page 64)

1. INTRODUCTION

1.1. THE HEART, MI & HF

The heart is a four-chamber pump that contracts 60 – 100 times per minute. Apart from the cardiomyocytes (CMs), the cells involved in contraction, the heart has endothelial cells (ECs), smooth muscle cells (SMCs), and fibroblasts.

Myocardial infarction (MI) is the primary cause of disease-related death in the world with no reliable therapy¹. Acute coronary syndromes, like MI, account for half of all cardiovascular deaths in the industrialised world, with around 20% of patients developing heart failure (HF) and having a 1-year mortality rate^{2,3}. Other studies focusing on older MI patients suggest that this percentage may reach 64%⁴. Therefore, HF remains a rapidly growing problem in Western societies⁵.

In terms of physiology, MI is caused by an occlusion of a coronary artery of the heart, usually due to an atherosclerotic plaque, which leads to restricted perfusion of the ventricular muscles⁶. As a result, there is massive loss of CMs⁷ and a collagenous scar is formed in the infarcted region, which is electrically uncoupled from the rest of the myocardium and has impaired contractile ability⁶. This is followed by a complex inflammatory response involving the release of macrophages, monocytes and neutrophils, to clear the necrotic cells and subsequent neuro-hormonal signaling⁸ (Figure 1.1).

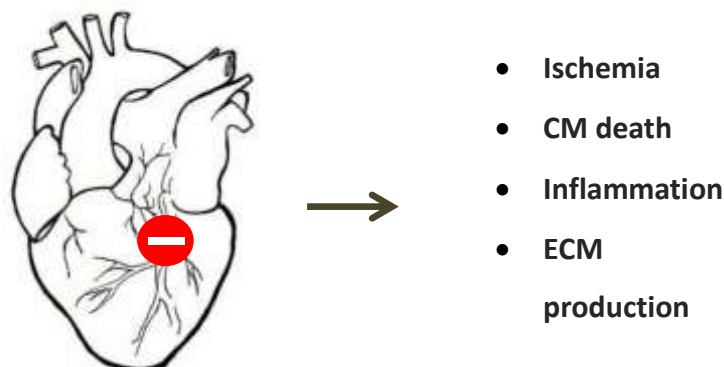


Figure 1.1. Schematic of MI, caused by occlusion at a coronary artery, leading to an ischemic fibrotic scar, CM loss and induction of inflammation and ECM production

The full involvement of the immune system in cardiac injury is still under investigation. It is considered to be one of the key players orchestrating the ventricular changes that follow MI, from the initial adaptive response to what is known as **left ventricular remodeling**⁹. Among these changes in myocardial structure and function are ventricular dilation, wall thinning, CM hypertrophy and poliploidisation, induction of extracellular matrix (ECM) protein synthesis and the eventual scar formation^{6,10}. The structural and functional remodeling, occurs along with metabolic remodeling, as will be explained later¹¹.

Current **therapeutic strategies** focus on reperfusion, thrombolysis and reducing the workload of the heart using pharmacological agents (such as b-blockers and angiotensin-converting enzyme inhibitors) or surgical procedures (such as bypass grafting or implanting a ventricular assist device)^{12,13,14}. Recent advances in treatment have improved time to reperfusion, but progress in identifying efficient therapies to offer more than symptom alleviation and support the surviving myocardium is yet to result in substantial clinical benefit^{15,16}. The long-term solution would be heart transplantation, but with the limited numbers of donors and the need for chronic immunosuppressants¹⁷, the search for finding an alternative solution to the problem of end stage HF is becoming increasingly more urgent.

1.2. CELL THERAPY POST-MI

MI can lead to a loss of up-to 1 billion CMs, which cannot be replaced, due to the insufficient degree of regeneration in the adult heart¹⁸. An attractive alternative solution could be offered by stem cell therapy (SCT), which has the potential to regenerate the damaged tissue and restore its contractility, harnessing the self-renewal and differentiation potential of stem cells (SCs)¹⁹. *In vivo*, the transplanted cells can act via a combination of the following mechanisms; a) replicate themselves and/or differentiate to mature CMs; b) stimulate the endogenous cardiac cells to regenerate; c) exert a beneficial effect via paracrine mechanisms of action²⁰ (Figure 1.2).

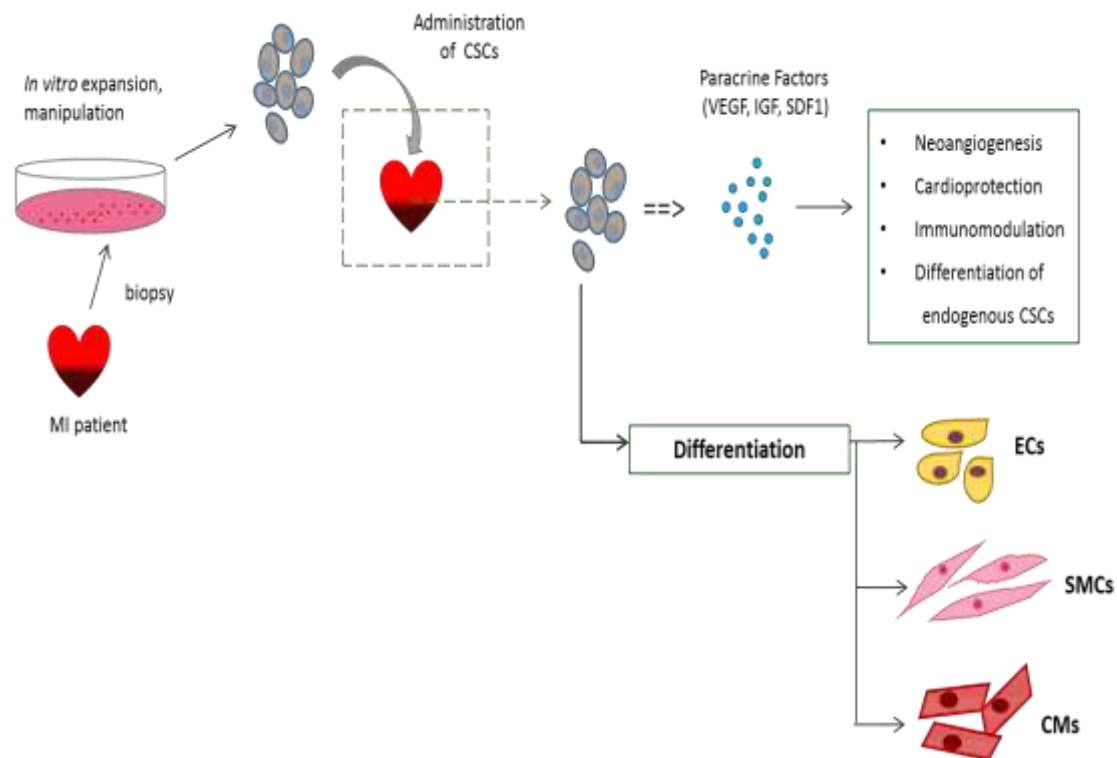


Figure 1.2. Schematic of SCT. The mechanisms of action of the transplanted cardiac stem cells (CSCs) can be by differentiation of the donor cells or via paracrine mechanisms

1.2.1. PLURIPOTENT STEM CELLS

Embryonic stem cells ESCs can be isolated from the inner cell mass (ICM) of pre-implantation embryos²¹ and are remarkable for their self-renewal potential, allowing them to be maintained and propagated *in vitro*, without losing their pluripotent SC phenotype²². The signalling pathways responsible for maintenance of ESC self-renewal involve leukemia inhibitory factor (LIF), bone morphogenic protein (BMP)²³, or fibroblast growth factor (FGF) and Nodal/Activin²⁴. With the right chemical cues, these cells can be differentiated into a plethora of cell types, as they are able to give rise to cells from all three germ layers²⁵. This 'ideal' SC type is not appropriate for SCT due to the risk of teratoma formation and the potential rejection of the allogeneic cells.

Induced-Pluripotent Stem Cells (iPSCs), introduced in 2006, are a promising source for *in vitro* CMs. They have an ESC-like phenotype and can be derived from the somatic cells of patients, originally via reprogramming with the

overexpression of pluripotency transcription factors: OCT4, SOX2, KLF4 and cMYC^{26,27}. Over the years the reprogramming process has become more efficient²⁸. iPSCs allow for autologous SCT treatment, disease modelling and drug screening²⁹. Several studies have shown their promising therapeutic potential for post-MI cardiac treatment^{30,31,32}. Even though this cell type offers an ethically-approved, autologous approach for cardiac SCT, there may still be immunological issues³³ and tumorigenicity concerns when using them.

An interesting tool for cell therapy that originated from the field of pluripotent SCs, mainly ESCs, are the pluripotent, *in vitro*-generated, **stem cell-derived cardiomyocytes (SC-CMs)**. These have been shown to integrate structurally and functionally with healthy host cardiac tissue *in vivo* in various studies^{34,35,36}. Despite the promising *in vivo* results, the initiation of beating in SC-derived CMs does not mean that these cells have the metabolic characteristics of mature CMs found in the healthy heart. Studies have shown that SC-CMs have immature calcium handling^{37,38} and a response to drugs more akin to CMs from the failing heart³⁹.

1.2.2. ADULT PROGENITOR CELLS (PCs)

Progenitor cells (PCs) are adult stem cells, with limited self-renewal and differentiation potential, as they are partially pre-committed to a specific lineage. They are found in small numbers at specific niches in adult organs, where they interact with ECM molecules⁴⁰. These interactions involve signalling pathways that offer cell protection and ensure a balance between self-renewal and division, thus providing the tissue with differentiated progeny^{41,42}. Even though the PCs are tissue-specific and pre-committed, studies have suggested that they have adequate plasticity to trans-differentiate *in vitro*, given specific chemical cues, to cell types of other lineages⁴³. This thesis will focus on PCs that have been proposed as candidates for SCT: bone marrow-derived stem cells, skeletal myoblasts, endothelial progenitor cells, mesenchymal stem cells, and endogenous cardiac progenitor cells.

1.2.2.1. BONE MARROW-DERIVED STEM CELLS (BMSCs)

BMSCs are a multipotent mixture of cell subtypes, comprised of a hematopoietic stem cell (HSC)-fraction and a mesenchymal stem cell (MSCs) fraction, with endothelial progenitor cells (EPCs)⁴⁴. They can differentiate into osteoblasts, chondrocytes and adipocytes, and contribute to the regeneration of mesenchymal tissues such as: bone, cartilage, muscle, adipose, and stroma⁴⁵. BMSCs were the first candidates to be extensively studied for cardiac SCT, because of pre-existing experience on bone marrow transplantations and availability of donor samples. Initially, mixed BMSCs⁴⁶ and lineage-negative (lin⁻) bone marrow-derived mesenchymal stem cells (BM-MSCs)⁴⁷ were used for *in vivo* cardiac regeneration studies, in both mice and rats, inducing improvement in cardiac function. Allogeneic lin⁻ BM-MSC transplantation resulted in short-term improvement in the post-infarcted mouse and rat heart^{48,49}, whereas other studies were not as encouraging⁵⁰.

Later studies investigating the therapeutic mechanism doubted the BMSCs cardiogenic potential, suggesting that the transplanted BM-HSCs⁵¹ or BM-MSCs⁵² fused with endogenous cells in the heart. Other studies suggested that the donor BM-MSCs stimulated the regenerative activity of endogenous CPCs⁵³ and did not differentiate themselves. More than 40 randomised control trials and 2700 patients later, the evidence for a beneficial effect of BM cell therapy for MI patients is still not sufficient. Even though Fisher *et al.* in a clinical trial review this year reported reduction in mortality after administering autologous BM-derived cells to HF patients⁵⁴, the analyses of MI trials offers controversial conclusions^{54,55,56}.

1.2.2.2. SKELETAL MYOBLASTS

While BMSCs were the extensively-studied and easily accessible candidates for SCT, skeletal myoblasts were the obvious and logical alternative, as they are able to generate muscle cells similar to those needed in the heart post-MI.

Transplantation of skeletal myoblasts improved cardiac function in animal studies, showing scar tissue replacement, reduced post-MI adverse remodeling and functional improvement^{57,58,59,60}. However, there have been several reports

doubting the capacity of myoblast-derived cardiac cells to form intercalated discs, eventually leading to their inability to couple electromechanically and synchronise with the recipient myocardium^{61,62,63}. This inadequacy of skeletal myoblasts was confirmed by the discouraging results from phase-II human clinical studies^{64,65}. Despite some studies suggesting reduction in arrhythmogenic incidents⁶⁶, the risk of arrhythmias implies a major problem of skeletal myoblasts transplantation. On the whole, despite the mixed results, the risk of reported arrhythmias makes skeletal myoblasts an un-ideal candidate for SCT.

1.2.2.3. MESENCHYMAL STEM CELLS

MSCs (other than BM-MSCs) are multipotent and have immunosuppressive properties and low tumorigenicity^{67,68}. They can be found in most post-natal organs and tissues^{69,70} and can be recognised by the expression of cell surface markers: CD73, CD90, CD105, CD44 and CD166 and the lack of CD34, CD31, CD14, CD45, CD133 and CD19⁷¹. This cell type has been described as immunomodulatory, and it is even suggested to be immunosuppressive and safe for allogeneic transplantations^{72,73}, but this property has been recently challenged⁷⁴.

Umbilical cord MSCs⁷⁵, adipose-derived MSCs⁷⁶ and amniotic fluid MSCs⁷⁷ are key MSC types for their differentiation and therapeutic potential, as well as the ease of their isolation. More specifically, both rat and pig **adipose-derived MSCs** have demonstrated therapeutic effect after infarction in preclinical studies^{78,79}. **Umbilical cord MSCs** had beneficial effect as well, when administered in the infarcted mouse heart, increasing capillary density and preserving cardiac function⁸⁰. Similarly, after human adipose-derived MSCs or human cord blood-derived MSCs had been injected into the rat heart post-MI, they led to higher ejection fraction and reduced scar size⁸¹.

A common characteristic of all the MSC subtypes is their pro-angiogenic and anti-apoptotic paracrine secretome, which might account for the observed improvement^{82,83,84}. Nonetheless, with proven safety and encouraging results, the adipose-derived MSCs have been tested in patients and showed improvement in left ventricular ejection fraction (LVEF) and perfusion as well as

reduced infarct size⁸⁵. The HUC-HEART trial, which uses umbilical cord MSCs, is currently ongoing⁸⁶. In summary, MSC SCT has proved to be efficient in improving cardiac function, thereby opening the door for larger clinical trials, with the vision of allowing for an off-the-shelf treatment.

1.2.2.4. ENDOGENOUS CARDIAC PROGENITOR CELLS (CPCs)

In the quest of finding the ideal progenitor cell type to regenerate the infarcted myocardium, the endogenous, adult, cardiac progenitor cells (CPCs) are an obvious and appealing candidate. The key players in this field, which have been extensively studied, made their appearance in the last 13 years (Figure 1.3), (for details on the markers see Table 1.1) with more cell types being added, based on different isolation methods, or being identified using different markers. The common characteristic of the suggested CPCs is a pre-commitment to the cardiac lineage, based on expression of cardiac transcription factors, and the ability to express contractile proteins after differentiation.

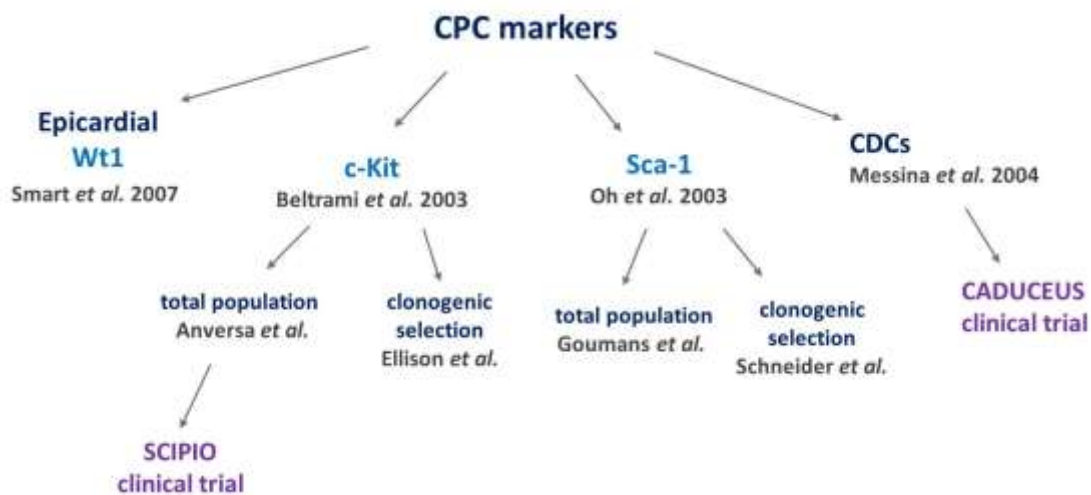


Figure 1.3. The main adult CPC populations, most extensively studied for ischemic cardiac disease treatment and the principal investigators involved in the studies

1.2.2.4.1. CKIT+ CPCs

A CPC type that has drawn a lot of attention are the **Ckit**⁺ CPCs (see Table 1.1). In 2003 Beltrami *et al.*, from the Anversa group, identified a Lin⁻ Ckit⁺ cell population able to differentiate to all three constituent cell types of the heart (CMs, ECs, SMCs) and showed cardiac regeneration in a rat MI model⁸⁷. Subsequent studies supported the beneficial effect after cardiac injury, but suggested that the Ckit⁺ cells were of BM origin⁸⁸. Other researchers suggested that the majority of Ckit⁺ cells in the heart are mast cells^{89,90}. Alongside that, studies specifically examining the lin⁻ Ckit⁺ population suggested that they are endothelial cells⁹¹ or maybe a mixed population of both⁹². Studies looking at the issue from a developmental perspective, suggested that Ckit⁺ cells contribute to new CMs after injury in the neonate, but they were unable to do so in the adult heart⁹³, in line with previous observations regarding the role of Ckit⁺ cells in the neonatal heart⁹⁴. In 2013, Ellison *et al.* showed that Ckit⁺ were necessary for cardiac recovery in rodent models of diffuse myocardial damage causing acute heart failure⁹⁵. Subsequent studies challenged this conclusion and showed opposing results^{96,97,98}. In 2011, the Anversa group used Ckit⁺ CPCs in a phase-I Stem Cell Infusion in Patients with Ischemic cardiomyopathy (SCIPIO) clinical trial showing encouraging results for post-MI treatment⁹⁹. However, in 2014 the results were questioned for their integrity¹⁰⁰.

1.2.2.4.2. STEM CELL ANTIGEN (SCA1) CPCs

Oh *et al.* in 2003 identified the **Sca1**⁺ (Table 1.1) endogenous CPCs in the mouse heart, having stem-like self-renewal characteristics and the ability to home to the injured myocardium¹⁰¹. Later it was shown that this cell population led to increased ejection fraction and neoangiogenesis, after injection into the acutely infarcted mouse heart¹⁰². It was also shown that Sca1⁺ CSCs contribute to the generation of CMs during normal ageing and after injury Sca1⁺ cells were induced to differentiate to three cardiac cell types¹⁰³. In line with these observations, a genetic deletion of Sca1 caused primary cardiac defects in heart contractility, repair and to the endogenous CPCs proliferation¹⁰⁴. A recent study by Nosedá *et al.* has shown that Platelet-Derived Growth Factor Receptor α

(**PDGFR α**) marks the clonogenic cardiogenic subtype of Sca1⁺ CPCs, which is able to differentiate into CMs, SMCs and ECs *in vivo*, with superior regenerative potential¹⁰⁵. The **cardiac side population (SP)** cells, identified by their ability to extrude a DNA-binding dye via the Abcg2 transporter, have been shown to be more than 80% Sca1⁺ ^{106,107}. Several studies have shown the ability for multipotential differentiation of SP CPCs¹⁰⁶, and for migration and homing into the injured rat heart¹⁰⁸. Although the human Sca1 isoform does not exist, a Sca1-like cell population has been isolated from the human heart using the murine antibody and has been extensively studied by the Goumans group¹⁰⁹.

Marker/ Transcription Factor	Full name	Type	Expressed in	Relevant cell Function	Effect of genetic deletion	Refs.
			(in rodents)			
Sca1	Stem cell antigen-1	Ly6 family of glycosyl phosphatidylinositol (GPI)-anchored cell surface proteins	HSCs, mammary SCs, mature T-cells, prostate, dermis, skeletal muscle, heart, liver	cell signalling, B & T cell activation	primary cardiac defects in myocardial contractility, impairment of CSC proliferation, cardiac dysfunction	104, 110, 111, 112
	lymphocyte antigen 6 complex Ly6a					
Ckit	proto-oncogene Ckit (CD117)	tyrosine-protein kinase Kit	HSCs, thymocyte progenitors, mast cells, cardiac progenitors, prostate SCs, tumour cells	cell survival, proliferation & differentiation	inhibited epithelial cell growth & impaired CSC migration	113, 114, 115, 116, 94
	stem cell growth factor receptor SCFR	cytokine receptor				
Wt1	Wilms tumour protein	transcription factor with proline / glutamine-rich DNA-binding domain	cardiac ECs, developing epicardium	epithelial to mesenchymal transition, vasculogenesis	Prenatal death, thin myocardial wall,	117, 118, 119, 120

Table 1.1. The main markers and transcription factors for the identification of CPCs; general information, role and function, related to the heart

1.2.2.4.3. CARDIOSPHERE-DERIVED CELLS (CDCs)

In 2004 Messina *et al.* isolated and cultured CSCs from mouse and human tissue explants¹²¹. The explant-derived cells (EDCs) cells were induced to form cell clusters, known as cardiospheres that were enriched for Ckit¹²¹. The spheres comprise of a mixture of progenitor cells, intermediate differentiating cells, fibroblasts and endothelial cells. Cells originating from them (CDCs) are clonogenic and self-renewing, characterised by Ckit/CD90/CD105 with low expression of: CD34, CD31¹²². Studies from the Carr group showed that they can also be isolated from patients¹²³, and rodent models of different co-morbidities^{124, 125}. In a study completed by our group, CDCs were shown to improve cardiac function when administered in rat heart following myocardial infarction¹²⁶, which was supported by other studies in both rat¹²⁷ and pig¹²⁸ hearts. In addition, human CDCs were shown to have superior, beneficial paracrine secretome, than BM-MSCs or adipose-derived MSCs¹²⁹. A study this year, by the Marban group, demonstrated that this cell type had a beneficial effect in a rat HF model, by decreasing fibrosis and inflammation¹³⁰. The ALLSTAR trial (NCT01458405) is currently assessing the use of allogeneic CDCs in MI patients.

However, the fact that CDCs are a mixed population, which may also contain fibroblasts (CD90⁺/Ddr2⁺) and immune/ hematopoietic cells (Ckit⁺/CD45⁺), has raised concerns as to whether this is the optimal CSC population for regenerative applications¹³¹. Also, there is considerable variability in the reported cell markers, among different studies, suggesting that this culture method may be unreliable¹²³.

1.2.2.4.4. EPICARDIAL STEM CELLS

The epicardium hosts a CPC niche^{132,119} and a well-established marker for epicardial cells, stemming from epicardial development, is Wilms Tumour protein 1 (Wt1)¹³³. Epicardial SCs have been shown to migrate and differentiate into CMs during development¹³⁴. In 2007 Smart *et al.* demonstrated that thymosin beta-4¹³⁵ can activate endogenous quiescent adult epicardial cells after myocardial infarction (MI), to migrate and induce neovascularization¹¹⁸,

later showing that these cells can also differentiate to CMs *in vivo* and regenerate the injured myocardium and express Wt1¹³⁶. Even though the epicardium-derived SCs can lead to the formation of new CMs in the developing heart, the level of such contribution post-MI, without exogenous pre-stimulation¹³⁷, requires further investigation.

1.2.2.4.5. CELL COMBINATIONS

Different approaches are investigating the delivery of combinations of cell types. A recent study showed that the injection of MSCs with Ckit+ CPCs in the infarcted myocardium led to a 2-fold greater reduction in scar size compared to either cell administered alone, and improved cardiac function¹³⁸.

In models of rat MI, co-culturing MSCs with skeletal myoblasts created cell sheets which, when transplanted, enhanced angiogenesis potential and functional recovery¹³⁹, and the co-transplantation of cord blood mononuclear cells and MSCs, led to enhanced reduction of scar tissue and improved regeneration¹⁴⁰. In another study comparing a range of human iPSC-derived cardiac cell ratios, the combination of 75% CMs and 25% non-CMs had the optimum tissue-remodelling properties¹⁴¹.

Recently, the Sussman group, has proposed 3D CardioClusters comprising CPCs, MSCs and EPCs and stem cell hybrids of MSCs and CPCs, known as CardioChimeras, in an effort to harness and combine the special characteristics of each individual cell type into a robust SCT treatment^{142,143}.

1.3. CARDIAC DEVELOPMENT & TRANSCRIPTION FACTORS

Several other CPC populations have been characterised based on the expression of cardiac transcription factors that are also involved in cardiac development (Table 1.2). Some of the main transcription factors are: NK class of homeodomain proteins (NKX2.5), Insulin gene enhancer protein (ISL1), GATA zinc-finger transcription factors (GATA4), the MADS domain transcription factor (MEF2C), T-box 5 (TBX5), as well as numerous other regulators. These factors are connected by complex regulatory relationships, which make unravelling the

earliest transcriptional circuits in the heart challenging and the identification of a "master regulator" for cardiogenesis so far impossible^{144,145}.

The necessity for understanding cardiogenesis is based on the notion that developmental paradigms are recapitulated during post-natal repair¹⁴⁶. An increasingly complex transcriptional-factor network emerges which guides the cardiogenic program from gastrulation through to the ultimate maturation of cardiac myocytes¹⁴⁷ (Figure 1.4).

Transcription Factor	Full name	Type	Expressed in	Relevant Function	Effect of genetic deletion	Refs.
			<i>(in rodents)</i>			
Mef2c	Myocyte-specific enhancer factor 2C	transcription factor of Mef2 family	skeletal & cardiac muscle	cardiogenesis vascular development, neurogenesis	prenatal death, abnormalities in the heart & vascular system	148, 149, 150
	MADS box transcription enhancer factor 2					
GATA4	GATA-binding factor 4	zinc finger transcription factor	CMs	embryogenesis & myocardial differentiation	mutations have been associated with cardiac septal defect	151, 152
Isl1	Insulin gene enhancer protein 1	transcription factor with two domains	SHF CPCs, cardiac neural crest	cardio-vascular development	severely deformed heart	153, 154
Nkx2.5	NK2 homeobox 5	Homeobox-containing transcription factor	prenatal heart, pharynx, thyroid, stomach	cardiogenesis	prohibits cardiac looping, defects in growth, haematopoiesis & angiogenesis	155, 156,
Tbx5	T-box 5	transcription factor of T-box family	prenatal heart, SHF	cardiogenesis, myogenesis & vascular development	Prenatal death, enlarged hearts, septation defects	157, 158, 159

Table 1.2. The main transcription factors involved in the development of the heart. Isl1, GATA4, Nkx2.5 and Mef2c are also used as markers for the identification of developmental stages of the CPCs

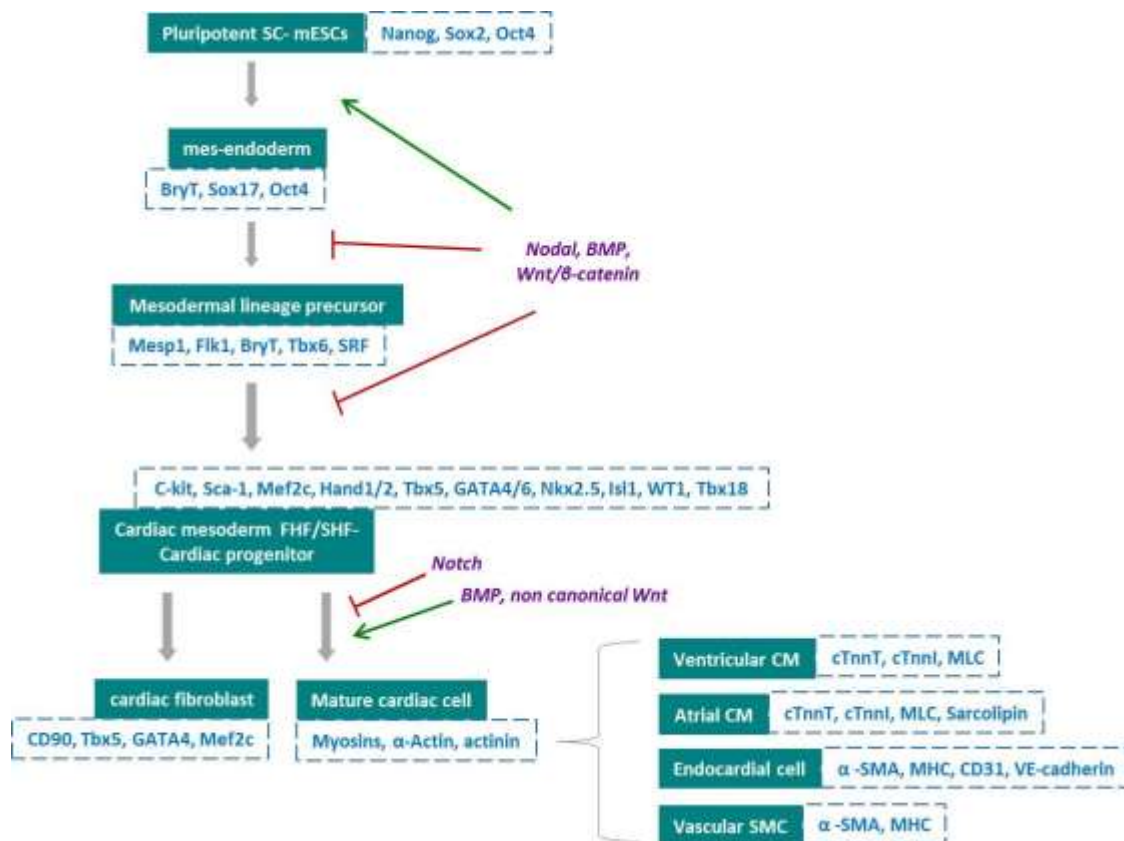


Figure 1.4. Schematic summarising the complex regulatory networks and signalling molecules that govern the differentiation of pluripotent SCs to mature cardiac cells.

In blue: the main transcription factors and genetic markers characterising each cell population. In purple: signalling molecules positively and negatively controlling the differentiation steps; green arrows indicate induction, whereas red ones indicate inhibition. Pluripotent SCs (mainly expressing *Nanog*, *Oct4* and *Sox2*) give rise to mes-endoderm, commit to the mesodermal lineage (characterised by *Mesp1*, *Flk1*, *Tbx6*), and then differentiate to cardiac progenitors. Cardiac progenitors (expressing a variety of markers: *Ckit*, *Sca1*, *Mef2c*, *Hand1/2*, *Tbx5*, *GATA4*, *Nkx2.5*, *Isl1*, *WT1*, *Tbx18*) can give rise to cardiac fibroblasts and mature cardiac cells. The latter express myosins (MHC/MLC), α -Actin and actinin. Ventricular CM, atrial CM, endocardial cell and vascular SMC, indicate some of the different types of mature cardiac cells that can originate from cardiac progenitors. The information shown in this figure can be found in the literature referenced in 1.3 (147, 144, 160, 161)

The extensive research that has been done, however, opens the way for crosstalk between the field of cardiac stem cell research and cardiac development, in an

effort to unravel the identity of the CSCs. The formation of the vertebrate heart is a complex morphogenetic process that depends on the spatio-temporally regulated contribution of cardiac progenitor cells¹⁶⁰. More specifically, in the **developing mouse embryo**¹⁶², cells migrate anteriorly from the primitive streak and form the cardiac crescent, with the second heart field lying medial to it. This step is followed by the formation of the heart tube, which begins to loop with the contribution of the cardiac neural crest cells. These cells migrate from the embryonic pharyngeal arches to the arterial pole, with the pro-epicardial organ forming next to the venous pole. The looped heart tube at this stage comprises of the following cardiac compartments: outflow tract, right atrium, left atrium, right ventricle and left ventricle. Subsequently, the heart 'matures' after septation, with the formation of the interventricular septum, the aortic arch, the aorta, the caval veins and the pulmonary vein.

The cell types that contribute to the formation of the developing heart originate from the first and second heart fields (FHF, SHF), with some contribution from epicardial progenitors. The FHF is reported to be characterised by the Tbx5, Isl1 and epicardial progenitors marked by Wilms tumour-1 (WT1) or T-box transcription factor 18 (Tbx18)¹³³. Other cardiogenic factors identified by embryonic lineage tracing or analysis of gene silencing include homeobox protein Nkx2.5, Mef2c and GATA4. The secretion of Wnt inhibitors and Bmp antagonists orchestrate the initiation of heart morphogenesis, together with signals from BMP and FGF, which activate the expression of cardiac specific transcription factors, such as: homeodomain protein Nkx2.5. Nkx2.5 activates a number of downstream transcription factors (such as MEF2 and GATA) which activate the expression of cardiac muscle specific proteins¹⁴⁵.

1.4. CAN THE HEART REGENERATE ITSELF?

For decades this question has caused a lot of debate. It started with observations of hypertrophied hearts in patients with certain medical conditions, which led to one's wondering what it was that allowed the enlargement of the heart. Around the early 1900s the answer was hyperplasia and hypertrophy of pre-existing CMs¹⁶³, because of the controversy as to what would be adequate evidence of

CM cell division^{164,165,166}. The notion of a heart that can survive and remain the same since birth clashes with cell death, in case of ischemic cardiac diseases and HF^{167,168}. Without CM replication or SC regeneration this would end up with complete deterioration of the cardiac muscle. First indications of cardiomyocyte proliferation started to appear right before the 2000s. With CMs being renewed in the mouse heart¹⁶⁹ and a suggested turnover of 7 - 40% per year in the human heart¹⁷⁰, having endogenous CPCs as a source for this renewal. In 2007, the Lee group used conditional genetic fate mapping in mice indicating that CMs renewed by the contribution of endogenous CPCs after injury - but not during normal aging¹⁷¹, with a much lower estimated rate. Similarly, the Bergman group, using nuclear carbon-14 (¹⁴C) integration in human DNA, showed <1% turnover per year in the adult heart, decreasing with age¹⁷². A similar annual rate, again declining with age but increasing after myocardial injury, was observed in mice using ¹⁵N imaging mass spectrometry by the Lee group¹⁷³. Interestingly, the latter showed that the new CMs originated from pre-existing ones, which contradicts their previous study reflecting discrepancies and difficulties with the techniques used¹⁷⁴. From a metabolic perspective, the postnatal switch from glycolysis to oxidative phosphorylation has been suggested to be the cause for the CM cell-cycle arrest¹⁷⁵, with the cycling CMs residing in protected hypoxic niches¹⁷⁶.

Coming back to the initial question, the postnatal heart has a degree of regenerative potential, especially after injury. As mentioned above, there are several studies suggesting a turnover of CMs of around 1%, supporting the hypothesis that the pre-existing CMs rather than CPCs, are responsible for the regeneration¹⁷⁷. At the same time, the SC field has supported evidence of endogenous CPC populations being able to give rise to the CM lineages in the heart, especially after injury^{87,103}. The above, along with differences between the animal/ human models, or the techniques for defining CM division, leave the question of *how* the heart regenerates unanswered.

1.5. OVERVIEW OF CARDIAC METABOLISM

The heart is a fascinating organ that beats 100,000 times a day and pumps 7200 L of blood through the body, in the same period, using 35 L of O₂ for energy production. It requires about 6 kg of adenosine triphosphate (ATP), which it utilises at a rate of 30 mg per second to sustain myocardial contraction and maintain ion homeostasis^{178,179}. Since the heart has low capacity for energy storage¹⁸⁰, an array of metabolic networks guides ATP production rates, based on demand. The heart has been characterised as a **metabolic omnivore**, being able to use a variety of substrates for energy production (see reviews^{181,182}). It is responsible for almost 10% of the whole body fuel consumption; with fats accounting for 70% of ATP production and carbohydrates for the remaining 30%. Glucose, pyruvate, TGs, glycogen, lactate, ketone bodies, FAs of different chain-lengths and certain amino acids, are among the energy-providing substrates of the heart.

Energy, in the form of ATP, can be produced in the cytosol via **glycolysis** (Figure 1.6); catabolism of glucose, derived from carbohydrates. The end-product of glycolysis is pyruvate, which can be further reduced to produce lactate. In case of carbohydrate shortage, gluconeogenesis of pyruvate, re-oxygenation of lactate or glycerol metabolism, can be used as sources of glucose synthesis^{183,181}.

Pyruvate can alternatively enter the mitochondria in the form of acetyl-coenzyme A (Acetyl-CoA) and be oxidised in the TCA cycle (also known as Krebs cycle), in a process called **oxidative phosphorylation**¹⁸⁴. The reducing equivalents of this chained reaction act as hydrogen carriers (Nicotinamide Adenine Dinucleotide Hydrogen; NADH and Flavin Adenine Dinucleotide Hydrogen; FADH₂), and enter the electron transport chain (ETC). There the coupled-transfer of electrons and H⁺ creates an electrochemical proton gradient that leads to the production of ATP. Under aerobic conditions more than 95% of ATP production comes from oxidative phosphorylation¹⁸⁵.

ATP can also be generated by the degradation of lipids (including triglycerides) into FAs, which are metabolized in the mitochondria via **beta-oxidation** (Figure 1.6). This metabolic pathway converts Fatty Acyl-CoA to Acetyl-CoA, allowing for its flux into the TCA cycle. Finally, the generated NADH and FADH₂ will lead to

ATP synthesis, through the ETC and oxidative phosphorylation¹⁸⁵. In the healthy heart 50-80% of the energy is generated via beta-oxidation¹⁸⁶.

Oxidative phosphorylation yields 36 ATP / glucose, being more efficient than glycolysis (4 ATP / glucose). Lipids, due to their reduced state are more oxygen-demanding than glucose (producing 2.8 ATP / O₂, versus 3.7 ATP / O₂), but on the other hand they are more energy-dense (high yield of ATP / carbon) ^{187,188}.

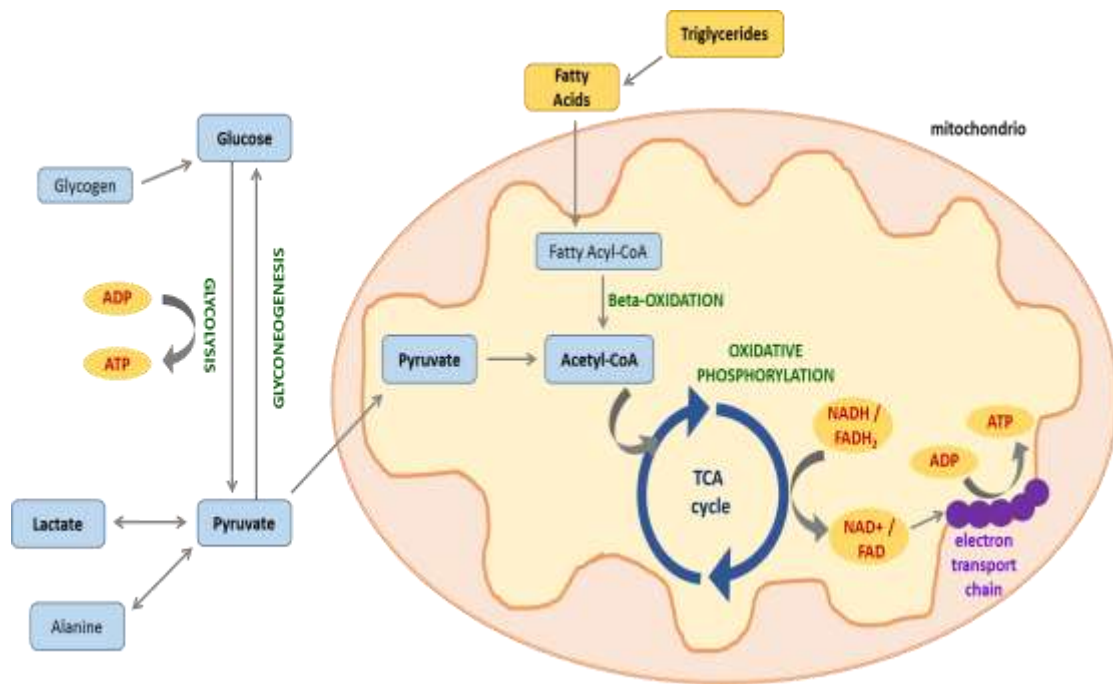


Figure 1.6. Schematic of basic cell metabolic pathways for energy production.

The heart has a remarkable ability to **adapt to changes** in its physiological state by selecting the most efficient substrate, depending on the conditions of its environment³. For example, as explained earlier, it is known that FAs require more oxygen than glucose, to generate the same amount of ATP ^{181,189}. Hypoxia leads to Hypoxia-inducible factor (HIF) upregulation, which has been shown to increase glycolysis and suppress mitochondrial oxidative metabolism^{182,190}. Thus, the heart regulates its substrate selection under hypoxic conditions, shifting towards the more oxygen-efficient fuel; glucose. In addition, a network of

interrelated mechanisms exists, that controls the interactions and the fluxes of glucose and fatty acid metabolism. It was first described as the glucose-fatty acid cycle by Randle (Randle cycle)¹⁹¹, and the complexity of this network is yet to be fully explored ¹⁹².

1.6. STEM CELL THERAPY – CURRENT OBSTACLES

The controversy and inconsistent results of the plethora of pre-clinical and clinical studies, could be because of differences in key aspects, including: cell dose, timing and routes of administration, detection time-points, disease models^{193,194,195,196}.

Despite remarkable advancements in the field of SCT for ischemic diseases, one of the main obstacles of successful therapeutic interventions is the extremely low cell retention of the transplanted cells. The harsh environment in the ischemic heart: of hypoxia, nutrient restriction, inflammation, with the additional issue of mechanical stress, lead to cell death and their being pumped outwards from the delivery sites. Several studies have demonstrated massive loss of the transplanted cells in a short period after administration¹⁹⁷; 90% of the injected MSCs were lost within the first day, and 99% in the first week¹⁹⁸, or about 85% of transplanted Ckit⁺ CPCs being lost after 1 day and 87% after 1 week post-transplantation¹⁹⁹, similar to that seen for rat neonatal CMs²⁰⁰.

Since cellular retention directly relates to the observed outcomes of SCT²⁰¹, strategies aimed at improving cell homing, survival and retention of infused cells within the heart are currently being investigated^{202,203}, such as pre-conditioning the transplanted cells with different signaling molecules^{204,205} and genetically²⁰⁶ or epigenetically²⁰⁷ modifying the cells ex vivo (see review²⁰⁸). In addition, tissue engineering and the use of different types of biomaterial scaffolds, has been demonstrated to increase cell retention at the ischemic region and improve the efficacy of SCT^{209,210,211}. Still, the inflammation, either due to the scaffold²¹² or the regional inflammatory environment of the scar, is likely to impact negatively on tissue engineering approaches. Studies have reported massive loss of cells, including 95% of the MSCs seeded in a collagen scaffold after one week²¹³.

1.7. THESIS AIMS

With the collective vision of enhancing stem cell therapy, this thesis focuses on assessing and optimizing different aspects of the culture and expansion of CPCs *in vitro*. Given the review on current knowledge provided in the introduction, the identity of the optimal CPC population is still unclear.

For this purpose this thesis:

1. designs an enzymatic digestion protocol for isolation of CPCs from the adult mouse atria
2. investigates the characteristics of unsorted isolated CPC populations, from the adult mouse atria, using a standardised (CDCs) and the newly developed protocol
3. evaluates the differentiation potential of these two CPC populations using an established TGF β 1 protocol, which has been applied previously to sorted CPCs
4. analytically assesses the metabolic profile of CPCs after fat supplementation, in an attempt to subsequently understand whether a forced shift in the CPC metabolism, by introducing fats as a substrate, can further mature the differentiated cells
5. compares the therapeutic potential of the two CPCs in an *in vitro* environment resembling the ischemic region, by assessing their capacity for survival and their paracrine secretome to induce neoangiogenesis
6. investigates the effect of miR-210, as a pre-conditioning factor, to increase the therapeutic potential of the CPCs, by reevaluating the aforementioned parameters

2. MATERIALS & METHODS

ABBREVIATIONS

ABBREVIATION	Full Name
5-AZA	5-Azacytidine
A.A.	Ascorbic Acid
APAF1	Apoptotic protease activating factor 1
A-SA	Alpha Sarcomeric Actin
ANF	Atrial Natriuretic peptide
ATG	Autophagy-related gene
ATP	Adenosine Triphosphate
BCL-2	B-cell lymphoma 2
BSA	Bovine Serum Albumin
BM	Bone Marrow
BMP	Bone Morphogenic Protein
CADUCEUS	Cardiosphere-Derived autologous stem Cells to reverse ventricular dysfunction
CANX	Calnexin
CEM	Complete Explant Medium
CDC	Cardiosphere-Derived Cell
CGM	Cardiosphere Growing Medium
CKIT	proto-oncogene Ckit / tyrosine-protein kinase Kit (CD117)
CNTRL	Control
CM	Cardiomyocyte
CO₂	Carbon Dioxide
CPC	Cardiac Progenitor Cell
CSC	Cardiac Stem Cell
CT	Collagenase Trypsin cell
CX43	Connexin 43
DDR2	Discoidin Domain Receptor 2
DH₂O	Distilled water
DIFF	Differentiation samples
DIFF + OA	Differentiation samples + Oleic Acid
DMSO	Dimethyl Sulfoxide
EB	Embryoid Body
ECL	Enhanced Chemiluminescence
ECM	Extracellular Matrix
EDC	Explant-derived Cell
EGF	Epidermal Growth Factor
EPC	Endothelial Progenitor Cell
ESC	Embryonic Stem Cell
FA	Fatty Acid
FADH₂	Flavin Adenine Dinucleotide Hydrogen
FBS	Fetal Bovine Serum
FGF	Fibroblast Growth Factor
HF	Heart Failure
HIF	Hypoxia-Inducible Factor
HRPT	Hypoxanthine-guanine phosphoribosyltransferase
HSC	Hematopoietic Stem Cell
GATA4	GATA binding protein 4
GCDM	Gouman's Cardiac Differentiation Medium
GLUT1	Glucose transporter type 1
GLUT4	Glucose transporter type 4

ICA	Icariin
ISL-1	ISL1 transcription factor, (Insulin gene enhancer protein – Islet1)
IMDM	Iscove's Modified Dulbecco's Medium
IPSC	Induced-Pluripotent Stem Cell
LV	Left Ventricle
LVEF	Left Ventricular Ejection Fraction
MEF2C	Myocyte Enhancer Factor 2C
MI	Myocardial Infarction
MIRNA / MIR	Micro-Ribonucleic Acid
MLC	Myosin Light Chain
MSC	Mesenchymal Stem Cell
mTOR	mammalian Target Of Rapamycin
MYH6	myosin, heavy chain 6, cardiac muscle, alpha
MYH7	myosin, heavy chain 7, cardiac muscle, beta
MYL2	myosin light chain 2
NADH	Nicotinamide Adenine Dinucleotide Hydrogen
NKX2.5	NK2 homeobox 5
NP	Nanoparticle
OA	Oleic Acid
OCT-3/4	Octamer-binding Transcription factor 4 / (POU5F1 ; POU domain, class 5, transcription factor 1)
P/S	Penicillin, Streptomycin
P/S/G	Penicillin, Streptomycin, L-Glutamine
PX	Passage x (x=number)
PBS	Phosphate Buffered Saline
PDH	Pyruvate Dehydrogenase
PDK4	Pyruvate Dehydrogenase Kinase-4
PGC1A	Peroxisome Proliferator-Activated Receptor Gamma Coactivator 1
PDGFRA	Platelet-Derived Growth Factor Receptor, alpha
PFA	Paraformaldehyde
PPARA	Peroxisome Proliferator Activated Receptor Alpha
ROS	Reactive Oxygen Species
RT-PCR	Real-Time – Polymerase Chain Reaction
RT	Room Temperature
RXR	Retinoid X Receptor
SC-CM	Stem Cell-Derived Cardiomyocyte
SCA1	Stem cells antigen-1
SCPIO	Stem Cell Infusion in Patients with Ischemic cardiomyopathy
SCT	Stem Cell Therapy
SDHA	Succinate Dehydrogenase complex, subunit A
SMC	Smooth muscle cell
SOX2	Sex (determining region Y)-box 2 / (SRY)
SP	Side Population
TBX	T-box family gene
TERT	telomerase reverse transcriptase
TG	Triglyceride
TGFB1	Transforming Growth Factor Beta 1
TM	Transition Medium
TNNT2	(Cardiac) Troponin T2
ULK	Unc-51 like autophagy activating kinase
VSEs	Very Small Embryonic-Like cells
WT1	Wilms Tumour protein 1

2. MATERIALS & METHODS

2.1 MICE

For this study wild type male; C57BL/6 mice, obtained from a commercial breeder (Harlan, Oxon, UK).

All animal procedures were reviewed and approved by the United Kingdom Home Office, conforming to the UK government regulations (Home Office License; PPL; 30/2755 & 30/3322 and PIL; 30/10405).

2.2 ISOLATION AND EXPANSION OF MOUSE CARDIAC PROGENITOR CELLS (CPCS)

2.2.1 CARDIOSPHERE-DERIVED CELLS (CDCS) ISOLATION

2.2.1.1 STANDARD ATRIAL EXPLANTING METHOD (CDCS)

The atrial explants cultures were based on the method of Smith *et al*¹²², modified as it is used in our lab²¹⁴. More specifically, the isolated mouse hearts were immediately washed with Dulbecco's phosphate buffered saline (DPBS) (Invitrogen, Fisher Scientific - UK Ltd), containing 15% Pen/Strep antibiotics and stored in Complete Explant Medium (CEM) on ice, until further processing. CEM comprised of Iscove's modified Dulbecco's medium (IMDM) (Invitrogen, Fisher Scientific - UK Ltd) supplemented with 20% foetal bovine serum (FBS) (Invitrogen, Fisher Scientific - UK Ltd), 1 U/ ml penicillin, 1 ug/ml streptomycin and 0.2 mM L-glutamine (P/S/G), (Gibco, Life Technologies, Fisher Scientific - UK Ltd) (Table 1). The atria were excised (Figure 1a), washed thoroughly in DPBS with Pen-Strep and minced mechanically into small pieces, after 3 minutes of 0.05% trypsin-EDTA (Invitrogen, Fisher Scientific - UK Ltd) digestion. The explant-pieces were plated on fibronectin-coated 6-well plates (coating solution comprised of fibronectin & DPBS in a 3 ul: 1 ml ratio) with 1 ml of CEM (Figure 1b) and cultured in an incubator at 37°C, 20% O₂ and 5% CO₂. The following day, 0.5 ml of medium was removed and replenished by fresh CEM. After an average of 6 days explant-derived cells appeared around the tissue pieces, termed as

Explant-derived cells (EDCs) (see Results 3.1). The explant cultures were fed every 2 days, with 0.5 ml of fresh CEM.

2.2.1.2. CARDIOSPHERE FORMATION

EDCs reached confluency around the tissue-pieces after approximately 1.5 months, on average, and were isolated using dissociation with Versene 1X (1:5000; Gibco) and subsequently, trypsin digestion. The average amount of 20,000 cells/ atrial explant was obtained each time. EDCs were either grown to passage 2 (P2) or cultured further through a cardio-sphere step, using the “Hanging Drop” method. Collected EDCs were re-suspended in Cardiosphere Growing Medium CGM (Table 2.1.) at a concentration of 2×10^4 cells/ml and plated in 25 ul droplets, hanging from the inside of the (un-coated) lid of plates (Figure 2.1c). The hanging drop cultures were kept for 4 days at 37 °C; the cardiospheres were collected by elution with PBS and were plated in fibronectin-coated 12-well plates, with CEM. Cardiosphere-derived cells (CDCs) could be observed coming out of the spheres and were cultured/passaged to P4 (see Results Chapter 3).

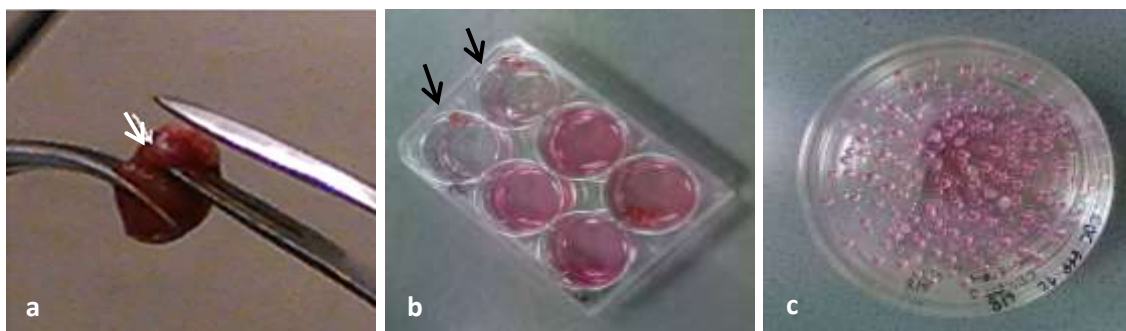


Figure 2.1. Technical steps of the isolation of atrial CPCs via the Cardiosphere-derived cells (CDCs) Isolation method; 1a. excision of the mouse atria, 1b. wells with explant atrial pieces, 1c. plates with hanging drops

<u>CEM</u> : Media & Components	Final Concentration	<u>CGM</u> : Media & Growth Factors	Final Concentration
IMDM	80%	DMEM/F12	63.4%
FBS	20%	IMDM	27.3%
L-Glutamine	2mM	FBS	6.8%
Pen/Strep	100U/ml	B27	2%
		Cardiotrophin	25 ng/ml
		FGF	20 ng/ml
		EGF	16 ng/ml
		Thrombin	25 ug/ml

Table 2.1. Concentration of solutions and growth factors in Complete Explant Medium (CEM) & Cardiosphere Growing Medium (CGM).

2.2.1.3. CELL EXPANSION

Both CDC and CT cultures were maintained at 37 °C in a humidified, 5% CO₂ incubator. The CEM medium was replaced every 3 days, and cells were passaged after reaching 90% confluency.

2.2.2 COLLAGENASE-TRYPSIN DIGESTIONS (CTS)

Mouse atria were excised, as before, washed thoroughly with PBS containing P/S and minced mechanically. The tissue-pieces were then transferred to a falcon tube containing 0.5 ml of the digestion solution (comprising of 0.1% trypsin & 0.1% Collagenase II (Calbiochem, 286 U/ mg)); and were incubated in a water bath at 37 °C for a total of 1 hour, with frequent shaking. Every 10 minutes the digestion-solution containing the tissue pieces was mechanically triturated with a syringe and needle, then left on ice for 1 minute to allow for the undigested tissue pieces to settle. Afterwards, the supernatant was collected, neutralized with the addition of FBS-containing medium, and plated on fibronectin-coated 6-well plates, after running it through a strainer. Fresh digestion solution was added to the remaining tissue pieces in the tube and incubated for another 10

minutes, as before, until 1 hour was reached. This intermittent digestion at 37 °C for 1 hour was the only way to get surviving fibroblast-like cells, resulting from the digestion protocol. The cells could be observed attaching after 2 days. They were collected and passaged when they reached 90% confluency, for further experiments and analysis.

2.2.2.1. RE-PLATING ISOLATION METHOD (SLOWLY-ADHERING PROGENITORS)

CTs were isolated as above (2.2.2) and cell suspension was plated in fibronectin-coated wells, as before. Then, the cell culture solution was subjected to a series of re-plating steps, as described in a study done on skeletal-muscle progenitors²¹⁵. More specifically, the cell culture solution was transferred to a new fibronectin-coated well, 2 hours post-isolation and then the same was done 24 hours later for the next 5 days. The cells that adhered in the well after the 6 x re-plating steps were expanded as slowly-adhering cardiac progenitor cells (SA-CPCs).

2.2.3. EXPLANT & CT CULTURE FROM THE SAME MOUSE ATRIA

Mouse atria were isolated, as before, washed thoroughly with PBS with P/S and minced mechanically. The atrial pieces were mixed and half of them were transferred in a petri dish with trypsin, as per the Standard Explant Culture Protocol (2.2.1.1.), the other half was added to the digestion solution, as per the Collagenase-Trypsin Digestions (2.2.2.). Both isolation protocols were performed simultaneously, to avoid any time-related variability during the isolation of the progenitors.

2.3. STATISTICAL ANALYSIS

For all the experiments in this thesis the n number refers to biological replicates. Results are presented as means \pm standard errors for RT-PCR and means \pm standard deviation for other analyses. Differences were considered significant at $p < 0.05$, determined using analysis of variance with a Student's *t*-test. Experiments with greater than 2 test groups were assessed by a one-way analysis of variance (ANOVA) with a Tukey post hoc test. GraphPad Prism 7.

2.4. CELL PROLIFERATION ASSAY

Cells isolated via Collagenase digestion (P0) were plated in 25 mm² fibronectin-coated flasks and were cultured in CEM (at 37 °C; 5% CO₂; being fed every 2 days), until reaching confluency. Then they were trypsinised and counted, using the Neubauer haemocytometer, under an inverted light microscope (Nikon, UK). Then 150,000 cells were plated in new fibronectin-coated flasks and cells were trypsinised and counted as before, after reaching confluency. This process was repeated until passage 7.

2.5. RNA ISOLATION – CDNA CONVERSION

2.5.1 RNA EXTRACTION & QUANTIFICATION – QUALITY CHECK

Collected cell pellets were kept at -80 °C, until analysis. Total RNA was extracted using the RNeasy Mini Kit (QIAGEN Ltd. - Manchester UK), following the manufacturer's protocol. Beta-mercaptoethanol was added in the RLT Lysis buffer (10 ul/ml) and, the extraction solution was treated with DNase, prior to RNA elution (RNase-Free DNase Set – QIAGEN Ltd. - Manchester UK), to degrade any residual DNA. The resulting RNA- yield and purity was defined using the NanoDrop spectrophotometer (for pure RNA; $A_{260}/A_{280} \approx 2$).

2.5.2 REVERSE TRANSCRIPTION

Complementary DNA (cDNA) was synthesized on the same day, from the isolated RNA solution, using the High Capacity cDNA Reverse Transcription kit (Life Technologies, Fisher Scientific - UK Ltd), following the manufacturer's protocol (Table 2.2.). cDNA aliquots were kept at -20°C for further use.

	Step 1	Step 2	Step 3	Step 4
Temperature (°C)	25	37	85	4
Time (minutes)	10	120	5	until sample collection

Table 2.2. Thermal cycler reverse transcription conditions

2.6. REAL-TIME POLYMERASE CHAIN REACTION (RT-PCR)

2.6.1. PRIMERS & PRIMER DESIGN

A custom-made primer-array for cardiac progenitor markers (Gata4, Nkx2.5, Ckit, Isl1, Mef2c, Flk1) was designed and validated by PrimerDesign (Southampton, UK). All the other primers used in this study were designed using the NCBI Primer-Blast online tool (www.ncbi.nlm.nih.gov/tools/primer-blast/). Selected criteria, for optimal primer design, for SYBR Green RT-PCR, include; primer length of ~20 nucleotides,

- melting temperature of 65-75°C,
- GC content of 50-60%,
- primers ending in G or C, and finally
- primers flanking the exon-exon border of the gene

The latter allows for avoiding the amplification of any genomic DNA (gDNA).

2.6.2. PRIMER EFFICIENCY TESTING

The designed primers' efficiency was assessed by performing Quantitative PCR, using serial dilutions of cDNA samples in RNase/DNase-free water, from mouse whole-heart samples. To these, 0.5 ul of each primer of the primer pairs were added. The resulting threshold cycles (Ct values) were plotted against the log₁₀ of the cDNA serial dilution. Primer efficiency is calculated as $E = (10^{(-1/s)-1}) \times 100\%$, where E is the amplification efficiency and s is the slope of the dilution curve.

2.6.3. RT-PCR REACTION PREPARATION

Real-time PCR was performed using the StepOnePlus Real-Time (Applied Biosystems, Life Technologies, Fisher Scientific - UK Ltd). Relative mRNA levels were normalized to Canx, Sdha, Hrpt housekeeping genes, as suggested through performing an initial comparative analysis of several reference genes (geNorm Kit; Primerdesign); including: B2M, Ywhaz, Atp5b, Ubc, Canx, Eif4a2, Rpli3a, Sdha, Cyc1, Gapdh, Actb, 18S and analysing the output with geNorm software, using "qBase+" (Biogazelle, Belgium). As detection system for the reaction SYBR green fluorescent intercalating dye was used (SYBR Green PCR mastermix, Life

Technologies, Fisher Scientific - UK Ltd). The fluorescence of the dye increases, once it binds to the DNA double helix. Thus, the more the PCR reaction amplifies the substrate (Table 2.3), the more DNA is created and the more the resulting fluorescence is generated.

Component	ul/reaction
AB Slow mix (dNTPS, RNA polymerase, SYBR fluorescent probe)	5
Primer forward	0.5
Primer reverse	0.5
RNase&DNase Free H ₂ O	1.5
cDNA template	2.5

Table 2.3. Volumes of components of RT-PCR reaction

Data was analysed using the published $\Delta\Delta Ct$ method Livak method, plotting the data as $2^{-\Delta\Delta Ct \pm SD}$ (on certain occasions $2^{-\Delta\Delta Ct \pm SE}$ was used, as stated)^{216,217} (Table 2.4).

1	Calculate ΔCt
2	Calculate Standard Deviation Of ΔCt
3	Calculate $\Delta\Delta Ct$
4	Calculate Standard Deviation $\Delta\Delta Ct$
5	Calculate Standard Error $\Delta\Delta Ct$
6	Calculate $\Delta\Delta Ct \pm SD$
7	Calculate $2^{-\Delta\Delta Ct \pm SD}$

Table 2.4. Calculation-steps that were followed for the qPCR data analysis.

2.7. IMMUNOCYTOCHEMISTRY

2.7.1 CELL PREPARATION & FIXATION

For Immunocytochemistry and Cell imaging purposes, the cells of interest (EDCs, CDCs, CTs) P2-P4 were seeded in 24-well plates, on fibronectin-coated cover slips (2×10^4 cells/well) and were fixed with 4% PFA for 30 minutes at 4°C and subsequently kept in PBS at 4°C. The fixation method was selected after evaluation of the quality of staining, after several methods (Table 2.5. – data not shown).

Method	Paraformaldehyde concentration (%)	Incubation time	Temperature
1	4%	10'	RT
2	1%	10'	RT
3	4%	30'	4 °C
4	1%	30'	4 °C
5	4%	2'	37°C (added in cell medium)
	4%	8'	RT

Table 2.5. Concentration of PFA and incubation conditions, of the tested fixation methods

2.7.2. ANTIBODY STAINING

After cell fixation, for intracellular staining, cells were permeabilised with 0.2% Triton X in PBS for 10 minutes. Then cells were blocked with a blocking solution comprising of 2% FBS and 2% Bovine serum albumin (BSA, Sigma-Aldrich Ltd. - Dorset, UK) for 30 minutes. Primary antibody staining followed (Appendix B); either overnight at 4 °C or for 1 hour at room temperature. After washing the cover slips with PBS for 4 times, in the case of non-conjugated antibodies; cells were labelled with secondary antibody (Appendix B) for 30 minutes at room temperature. In case of negative-control samples blocking solution alone was used, with the secondary antibody (where it applies). The slides were rinsed as before, and then stained with 150 ul of 4',6-diamidino-2-phenylindole (DAPI, Sigma-Aldrich Ltd. - Dorset, UK) 0,1% in PBS, for 5 minutes and mounted on glass slides, with a of 50% PBS and 50% Glycerol (Fisher Scientific - UK Ltd) as a

mounting medium. The slides were then kept at 4 °C, protected from light, until imaging.

2.7.3. CONFOCAL MICROSCOPY

Immunostaining was assessed using laser confocal microscopy (Inverted Olympus Fluoview FV1000 Confocal system). For image analysis FIJI software ('Fiji Is Just Image') was used. Positive staining was assessed comparing to a negative control; either cells stained only with DAPI or with just the secondary antibody and DAPI.

2.7.4. MITOCHONDRIAL STAINING

For mitochondrial imaging the MitoTracker® Red CMXRos (Fisher Scientific - UK Ltd) intracellular dye was used. The probe enters the live cells with passive diffusion, accumulates in active mitochondria and is retained after fixation. A working solution of 10 nM mitotracker, in non-FBS medium was incubated for 40 minutes with the cells. Then cells were washed with DPBS and fixed with PFA. After imaging the cells at Excitation/ Emission wavelengths of 579/599 nm, the fluorescence intensity was analysed using the FIJI image analysis software (Fiji is Just Image). More specifically, the outline of each cell was selected and the average fluorescence intensity was measured for each condition (Figure 2.2.).

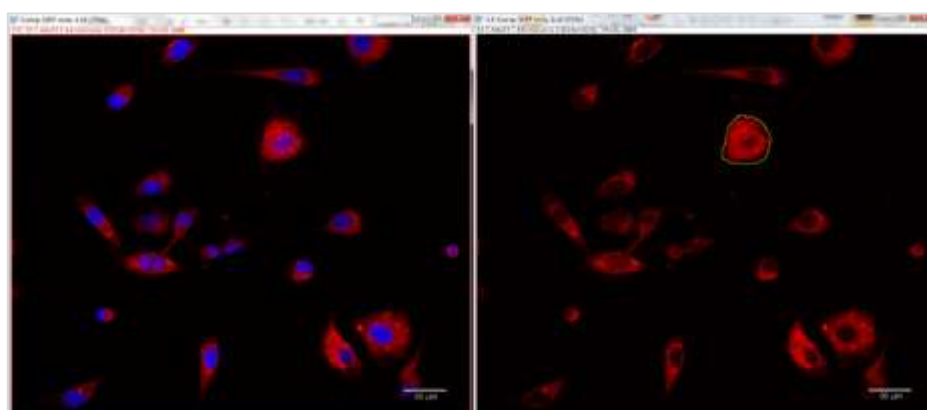


Figure 2.2. Representative cell images, after MitoTracker® Red CMXRos staining, under analysis with the FIJI software; the yellow outlines in each image mark each cell, allowing for the quantification of the fluorescence intensity per cell.

2.8. FLOW CYTOMETRY

2.8.1. CELL PREPARATION

For Flow Cytometry analysis, the cells of interest (DCs, CTs) were isolated and grown on coated surfaces, depending on the passage and experiment of interest. Subsequently, the cells were collected as a single suspension, washed with PBS and fixed with 4% PFA in tubes, at 4°C. Then, the cells were washed with PBS and used at a final concentration of at least 3×10^5 / ml.

2.8.2. ANTIBODY STAINING & ANALYSIS

Fixed cells were blocked with a blocking solution of 2% FBS and 2% BSA for 30 minutes. Then they were incubated with the appropriate concentration of primary antibody, either for 1 hour at room temperature or preferably overnight at 4°C, on a shaker. PBS was added in the tubes and then centrifugation at 1400 rpm for 5 minutes followed, to wash off the primary antibody. A 30 minute incubation with the secondary antibody at RT was done, where necessary, and then the cells were washed again with centrifugation. Finally the cell pellet was resuspended in 300 ul of PBS. Unstained cells or cells without a secondary antibody, resuspended in 500 ul of PBS, were used as a negative control and to calibrate the FACS machine. All the samples were kept on ice and in the dark until they were analysed. Flow Cytometric Analysis was done using a FACSCalibur flow cytometer (BD Biosciences, San Jose, CA). FlowJo software was used for data analysis. Each acquisition included 1×10^4 events. The percentage of positive cells was determined by setting a threshold excluding the negative population, as estimated via the negative control samples.

2.9. COLONY FORMING ASSAY

Cells were collected at the passages of interest P2 or P7 and subsequently replated in appropriate dilutions to assess colony-forming ability, based on protocol by Franken *et. al*²¹⁸. The assay is based on the ability of progenitor cells to proliferate and form colonies with unique morphology, as an indication of the heterogeneity of their progeny. Cell dilutions were made, so that 60, 180 and 360 cells were plated in duplicates in 6-well plates and cultured for 2 weeks. Afterwards, the wells were washed with DPBS and fixed with 70% cold Ethanol

for 2 hours at 4°C and then left to dry. Colonies were stained with a Crystal Violet dye solution (2 mg/ml) (Sigma-Aldrich Ltd. - Dorset, UK) for 5 minutes, which stains nuclei a deep purple colour. They were subsequently washed 2 times with tap water, they were drained inverted and left to dry overnight. The plates were then scanned for colony count and further characterisation. Colonies were defined to consist of at least 50 cells. Colony-forming capacity was expressed using the following formula:

$$\text{Colony – forming Capacity (\%)} = \left(\frac{\text{total number of colonies day 14}}{\text{total number of cells at day 0}} \right) * 100\%$$

2.10. CARDIAC PROGENITOR DIFFERENTIATION TOWARDS CM LINEAGE

2.10.1. MOUSE-ESC DIFFERENTIATION

The differentiated mouse-ESC which were used as a positive control for comparison with differentiated CDCs or CTs in RT-PCR experiments, were donated by Dr. Richard Tyser (Prof. Paul Riley group, DPAG, Oxford). The samples were collected either at day 4, day 7, or day 14 of differentiation. Differentiation was induced using the hanging drop culture – embryoid body formation method²¹⁹.

2.10.2. TGFβ1 DIFFERENTIATION (GCDM)

To differentiate cardiac progenitors, the TGFβ1 differentiation was used²²⁰. More specifically, CDCs or CTs were seeded in CEM on gelatine-coated flasks 0,1% (Sigma-Aldrich Ltd. - Dorset, UK); at a density of 25 x 10⁴ cells per 25cm² flask or at 2 x 10⁴ cells per well in a 24-well plate. The next day, when the cells were attached, the medium was replaced with Gouman's Cardiac Differentiation Medium (Table 2.6), containing 5 uM 5-Azacytidine. For the next 2 days, 5-Azacytidine was added, at a concentration of 5 uM. Then, at day 4 the medium was refreshed with plain "GCDM" and at day 6 the medium was replaced with GCDM supplemented with 10⁻⁴ M Ascorbic Acid and 1ng/ml TGFβ1. From that point forward, AA was added every 2 days and TGFβ1 twice weekly, while medium was refreshed every 2-3 days (Figure 2.3). The GCDM-differentiated

cells were collected after 25 days of differentiation. Cells grown in flasks were collected for qPCR analysis, while cells were grown in 24-well plates for either imaging or radiolabelled assays. Undifferentiated, but over-confluent cells were used as a control for the different assays.

GCDM : Media & Components	Final Concentration
IMDM	47%
Ham's F12 – GlutaMAX-I	47%
Horse serum	2%
MEM non-essential amino acids	1%
Insulin-Transferrin-Selenium	1%
Pen/Strep	2%
Drug supplementation	Final Concentration
5-Aza	5uM
TGF- β 1	1ng/ml
AA	1mM

Table 2.6. Concentrations of media and components added in the Goumans Cardiac Differentiation Medium (GCDM)

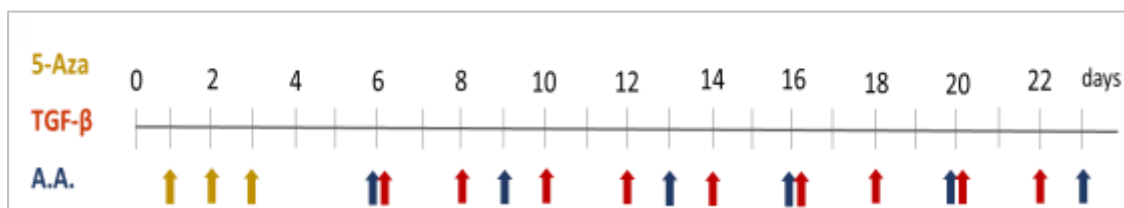


Figure 2.3. Schematic representation of the timeline of the TGF- β 1 differentiation protocol ²²⁰; yellow arrows mark the days when 5-Aza was added, whereas blue is for Ascorbic Acid and red for TGF- β 1.

2.11. METABOLIC SUBSTRATE MANIPULATION

2.11.1. OLEIC ACID TREATMENT

Both CDCs and CTs were metabolically manipulated by supplementation of the medium with Oleic Acid (OA). Cells were seeded in 6-well plated for either 48 hours, 1 week or 1 month, with the GCDM basal medium (without any drug

addition) supplemented with 75 μM , 150 μM and 300 μM OA conjugated to albumin (Sigma-Aldrich Ltd. - Dorset, UK). As a control CDCs or CTs were cultured in Bovine Serum Albumin (Sigma-Aldrich Ltd. - Dorset, UK) supplemented medium. (Table 2.7). Cells were initially kept for 48 hours, to determine the acute effects of OA on the transcriptome, and 1 week to look at the changes in the proteome.

Oleic Acid (μM)	BSA (μM)
300	20
150	10
75	5

Table 2.7. Concentrations of OA and the equivalent BSA concentrations, for the control conditions

2.11.2. ICARIIN TREATMENT

CTs were metabolically manipulated by supplementation of the medium with Icariin. Cells were seeded in 6-well plate for 48 hours with the GCDM basal medium (without any drug addition) supplemented with 5 μM and 20 μM of Icariin (concentrations decided based on^{221,222}), dissolved in DMSO (Table 2.8.). Since DMSO is toxic to the cells, testing of various ratios indicated the minimum effective amount, that allowed us to efficiently get Icariin powder into solution (data not shown) and was used for the experiments. As a control CTs were cultured in DMSO-supplemented medium.

Icariin (μM)	DMSO (μM)
20	0.5
5	0.125

Table 2.8. Concentrations of Icariin and the equivalent DMSO concentrations, for the control conditions

2.11.3. TGF-B1 DIFFERENTIATION + OLEIC ACID (GCDM+OA)

Following the 25-day TGF β 1 differentiation, as described in 2.10.2, the differentiating cells were cultured in OA 300 μM -supplemented GCDM, for either 1 week or 1 month. Subsequently samples were collected for further analysis.

2.12. WESTERN BLOTS

2.12.1. CELL LYSATE PREPARATION

Cells were trypsinised and kept at -80°C. The pellet was defrosted and the cells were lysed using lysis buffer (Appendix C). Subsequently, they were homogenised with a 21G needle, boiled for 5 minutes (95°C) and finally centrifuged for 10 minutes at 13,000 rpm.

2.12.2. PROTEIN ASSAY

The cell lysate was diluted 1:3 in distilled water and 50 ul of the working solution were analysed in duplicates on a 96-well plate. To determine the protein content of the samples the BCA protein kit (Perbio, UK) was used, according to the manufacturer's protocol. Standards were prepared for the standard curve, for the quantification. The absorbance was measured with a Multiscan FC plate-reader (Fisher Scientific - UK Ltd) at 550 nm and at 37°C. 5% b-mercaptoethanol was added to the remaining cell lysate supernatant of each sample, the sample was boiled at 95°C for 5 minutes, and then they were centrifuged at 13,000 rpm for 10 minutes at 4 °C. An aliquot, subsequently, was stored at -80 °C.

2.12.3. POLYACRYLAMIDE GEL ELECTROPHORESIS & PROTEIN TRANSFER

For the preparation of the electrophoresis gels, 10% APS was made first. A 1.5 mm thick 12.5% resolving gel was made up (Appendix C) and poured between the glass sheets of the electrophoresis apparatus. Stacking gel was prepared and poured on top of the resolving gel-layer. After both gels were set, 30 ul of each sample were loaded, along with the rainbow marker. The gel was run at 120 V and checked frequently, then transferred onto a nitrocellulose membrane (Pall Life Sciences) at 180 mA for 1 hour. SDS transfer buffer was used to soak up all the components used in the transfer apparatus. Ponceau staining (Sigma-Aldrich Ltd. - Dorset, UK) was used for 5' minutes on a rocker at RT, to check that the transfer was successful and protein loading was even.

2.12.4. IMMUNOBLOTTING AND DETECTION

Initially, the membrane was blocked, using TBS-Tween (Appendix C) with 5% milk powder, for 1 hour at room temperature, followed by incubation with the primary antibody (Appendix C) in 5% milk, overnight at 4 °C on a shaker. The following day, after washing the membrane in TBS-Tween for 1 hour the secondary antibody was added (Appendix C), for 1 hour at room temperature. For detection, ECL Western blotting detection solution (GE Healthcare, Amersham) was used. The films (Kodak) were exposed and developed in the dark room. The bands were analysed using a pixel counting programme (ImageStudioLite) and the pixel counts normalised to the control of each sample. After development, the membranes were washed in TBS-Tween and then placed in 15ml of stripping buffer (Sigma-Aldrich Ltd. - Dorset, UK) for 20 minutes, and then washed for 30 minutes in TBS-Tween before repeating the process above.

2.13. METABOLIC ASSAYS

2.13.1. GLUCOSE-¹⁴C OXIDATION MEASUREMENT

To measure the rates of glucose oxidation of the CTs in each condition, the Collins et al. method was followed²²³ with some modifications. CTs were seeded in gelatine-coated 24-well plates and were grown as an untreated CNTRL, differentiated or treated with OA for 48 hours, 1 week or 1 month. Subsequently, they were incubated for a total of 4 hours in the presence of radiolabelled glucose; 10 mM glucose containing 0.185 MBq D-U-¹⁴C-glucose, in a no-glucose basal medium DMEM (A14430, Gibco. Life Technologies, Fisher Scientific - UK Ltd). A total volume of 0.5 ml/well was used, of either DMEM-alone (negative CNTRL), or DMEM with ¹⁴C-glucose. In addition, wells without cells, containing DMEM with ¹⁴C-glucose were used as a second negative CNTRL. The ¹⁴CO₂, produced by the glucose oxidation was trapped on KOH-soaked filter papers covering the inside of the 24-well plate that was used as a lid for the apparatus (Figure 2.4.). A perforated rubber gasket, with holes corresponding to each well of the 24-well plate, was put between the two plates. A metallic contraption was screwed tightly around the “plate-sandwich”, so the whole apparatus with the cells and the media was sealed for the length of the experiment.

To trigger the release of the $^{14}\text{CO}_2$, perchloric acid was added to the well, at each desired time-point, to kill the cells. The samples were kept for 1 hour to allow for the release of dissolved $^{14}\text{CO}_2$. Filter papers containing trapped $^{14}\text{CO}_2$ were analysed using a scintillation counter.

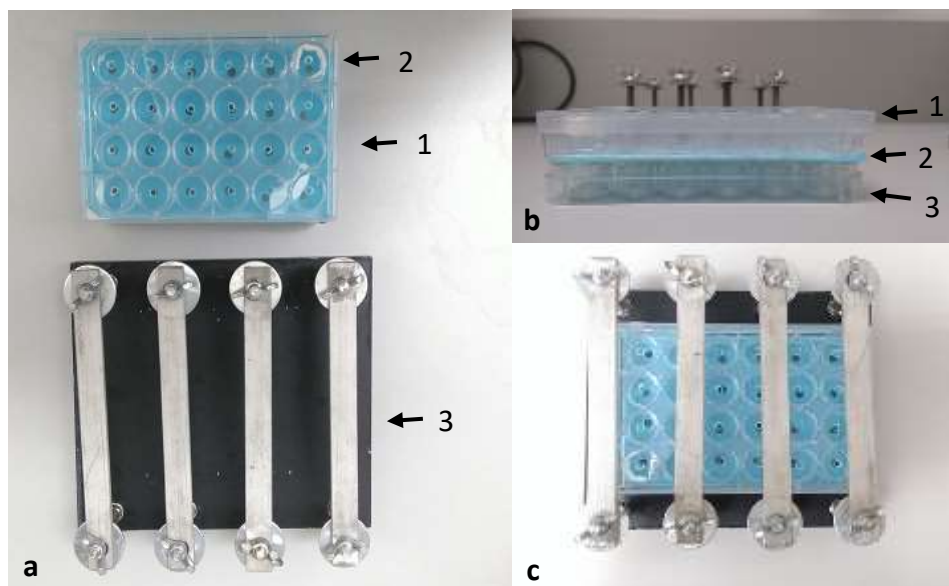


Figure 2.4. The apparatus constructed for trapping $^{14}\text{CO}_2$: a1. the plate-sandwich, with a blue rubber gasket, a2. with the KOH-soaked filter paper in the top right well. The plate-sandwich is placed in the metallic contraption (a3.). b: the plate-sandwich depicting the upper-plate (b1.), the rubber gasket (b2.) and the bottom-plate (b3.). c: the plate-sandwich positioned in the metallic contraption, ready to be placed in the incubator

2.14. CELL TRANSFECTIONS

2.14.1. FLUORINE-NANOPARTICLE CELL TRANSFECTION

The nanoparticles (NPs) used in this study were designed by Dr. R.S.M. Gomes²²⁴ during her DPhil with our group. They are biodegradable, of 170 nm diameter and consist of a poly (lactic acid-co-glycolic acid) (PLGA) core coated with protamine sulphate (PS), a small cationic agent. The later allows for miRNA loading on the NP170s, and further intracellular delivery²³. In addition, they are labelled with fluoresceinimine for imaging purposes (Figure 2.5). CDCs or CTs at P3-P4 were used for transfection with the NP170s. Both CPCs were seeded in gelatine-coated 24-well plates (80,000 cells/ well) and left to attach overnight.

NP170s were added at a concentration of 1.25 mg/ 10⁶ cells (standard dose) in 0,5 ml of 2%-serum CEM. An incubation of just 4 hours was reported to yield maximum transfection, so we examined 2 hours, 6 hours and 24 hours. In addition the NP170s concentration was checked at 2 x standard dose. After the end of the incubation, cells were washed with PBS and labelled with MitoTracker® Red CMXRos (Methods 2.5.3), to co-assess cell viability. Cells were washed with PBS and fixed with PFA 4% at 5°C, for Flow Cytometry analysis (Methods 2.6.). Cells double-positive for red (MitoTracker® Red CMXRos) and green (fluoresceinimine) were considered both alive and labelled with NP170s. Cells labelled with just MitoTracker® Red CMXRos were used as a negative control.

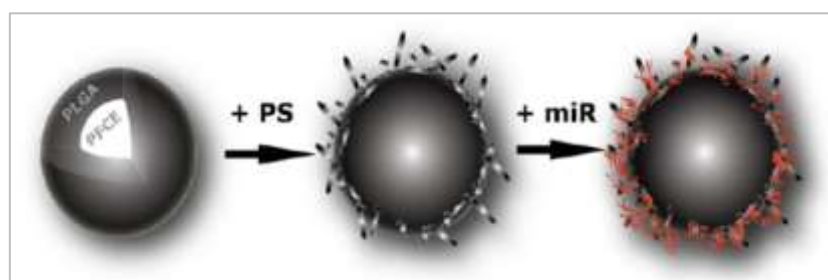


Figure 2.5. Schematic representation of the components comprising the 'NP170' NPs (image taken from R.S.M. Gomes et. al.)

2.14.2. NANOPARTICLE - MIRNA TRANSFECTION

NP170s were used (as in 2.14.1) with mirVana™ miRNA Mimics (Ambion, Life Technologies, Fisher Scientific - UK Ltd), following manufacturer's protocol. MiRNA Mimics were used at a final concentration of either 10 nM or 40 nM in serum-free IMDM containing P/S/G; (1 U/ ml penicillin / 1 ug/ml streptomycin / 0.2 mM L-glutamine. The miRNA solution was let to sit for 5 minutes at room temperature prior to further use. MiRNA were conjugated with the NP170s at a concentration of 12 ug miRNA/mg of NP170s, in DPBS for 1 hour on a shaker, at room temperature. CPCs, both CTs and CDCs, were seeded overnight in gelatine-coated 6-well plates (200,000 cells/ well). The cells were washed with DPBS and the NP170-miRNA solution was added in each well. Subsequently the cells were

kept at a 37°C incubator for 6 hours (optimal transfection time, see Results Figure 5.5).

2.14.3. DHARMAFECT – MIRNA TRANSFECTION

As a commercial transfection kit, DharmaFECT Reagent #1 (Fisher Scientific - UK Ltd) was used, according to manufacturer's protocol. MiRNA mimics were used at a final concentration of either 10 nM or 40 nM in serum-free IMDM with just P/S/G; (1 U/ ml penicillin / 1 ug/ ml streptomycin / 0.2 mM L-glutamine. DharmaFECT Reagent #1 was used at a 1:100 ratio, in serum-free IMDM. Both the miRNA mimic solution and the DharmaFECT Reagent #1 solution were left to sit for 5 min at room temperature prior to further use. Subsequently, the two reagent solutions were mixed together and were put at a shaker at room temperature for 20 minutes. CPCs, both CTs and CDCs, were seeded overnight in gelatine-coated 6-well plates (200,000 cells/ well). The cells were washed with PBS and the DharmaFECT-miRNA solution was added in each well. Subsequently the cells were kept at a 37 °C incubator for 48 hours.

2.15. APOPTOSIS INDUCTION & CELL SURVIVAL ASSAY

For induction of apoptosis the serum-starvation was used²²⁵. CTs or CDCs at P5, untreated or pre-transfected with mimics; miR-210 or negative-miR (depending on the experiment), were cultured in CEM without FBS for 3 days and 10 days. The non-serum CEM medium was refreshed every 2 days. After the end of the starvation the cells were washed with PBS twice and then counted, following the standard haemocytometer approach and the Countess Automated Cell Counter (Invitrogen, Fisher Scientific - UK Ltd).

2.16. ENZYME-LINKED IMMUNOSORBENT ASSAY (ELISA) FOR VEGF

CTs or CDCs were cultured in fibronectin-coated 6-well plates (100,000 cells/ well) or 24-well plates (25,000 cells/ well), in either CEM of CEM without FBS. Cell culture medium was collected after 24 hours of culture and stored at -20 °C until use. Before analysis, the samples were thawed and then spun down at 3000 rpm for 5 minutes, to remove cell debris. VEGF ELISA was performed, following

manufacturer's protocol (Bio-Techne, R&D Systems, Canada). The ELISA was measured using a Multiscan FC plate-reader (Fisher Scientific - UK Ltd).

2.17. METABOLITE MEASUREMENTS

Glucose and lactate levels were determined using the ABX Pentra 400 Chemistry Analyzer (Horiba Ltd., USA). To run this assay, cell culture medium was collected after each experiment and stored at -20 °C until use. Before analysis, the samples were thawed and spun at 3000 rpm for 5 minutes, to remove cell debris. Samples were analysed using the ABX Pentra with glucose reagent (Glucose PAP CP A11A01668, Horiba UK Ltd., Northampton) and lactate reagent (Lactic Acid A11A01721, Horiba UK Ltd., Northampton), which upon binding on the glucose and lactate molecules present in the medium, emit fluorescence. The fluorescence signal is detected and then the concentration of the metabolites is calculated, by the analyser, based on the calibrators that are loaded along with the samples of interest.

2.18. MIRNA TARGET PREDICTION

To investigate the mechanism of miR-210-induced survival, bioinformatics search was used. The predicted target genes for miR-210 were checked both the TargetScan and Miranda (MicroCosm) algorithms (see 5.1.3).

2.20. POLY-CASPASE ACTIVITY ASSAY

To measure caspase activity, CTs at P5 were seeded in a black 96-well plate in duplicates and were let to grow overnight in CEM. The next day wells were transfected (see 2.14.3) with miRNA mimics; miR-210 or negative-miR, while the rest were kept in normal cell culture medium. After the end of the transfection the miRNA-treated wells were serum-starved for 72 hours, and subsequently labelled for apoptotic cell staining with the FAM-FLICA Poly Caspase kit; FAM-VAD-FMK (637) (ImmunoChemistry Technologies, LLC, Bio-Rad, Kidlington UK), following manufacturers' protocol. For normalisation during analysis wells without a dye were used. Caspase activity was assessed as fluorescence intensity, using a plate reader (FLUOstar® Omega, BMG LABTECH Ltd., Aylesbury UK) at excitation/emission: 488/530 nm.

APPENDIX A – RT-PCR PRIMERS

Target gene	Sequence 5'-3'	Supplier
Acadm Forward	AGAACCAGACCTACAGTCGC	Sigma Aldrich
Acadm Reverse	CCTTCATCGCCATTTCTGCG	Sigma Aldrich
Fabp3 Forward	AGCATGACCAAGCCTACTACC	Sigma Aldrich
Fabp3 Reverse	CACCAGTGACTTGACCTTCCG	Sigma Aldrich
Glut1 Forward	CTGGCGGGAGACGCATAGTT	Sigma Aldrich
Glut 1 Reverse	GAACTCCTCAATAACCTTCTGGGG	Sigma Aldrich
Glut 4 Forward	GGCTCTGACGATGGGGAACC	Sigma Aldrich
Glut 4 Reverse	AAACTGAAGGGAGCCAAGCA	Sigma Aldrich
Pgc1 α Forward	TCTCAGAAGGGGCTGGTTG	Sigma Aldrich
Pgc1 α Reverse	AGCAGCACACTCTATGTCACT	Sigma Aldrich
Ppara α Forward	ACTACGGAGTTCACGCATGTG	Sigma Aldrich
Ppara α Reverse	TTGTCGTACACCAGCTTCAGC	Sigma Aldrich
Tnnt2 Forward	CTGAGACAGAGGAGCCAAC	Sigma Aldrich
Tnnt2 Reverse	ACCAAGTTGGGCATGAAGAG	Sigma Aldrich
Igfr1 Forward	GCTTCAGTCCCTTCCATTCCC	Sigma Aldrich
Igfr1 Reverse	TTTGGAGCAGTAGTTGTGCCG	Sigma Aldrich
Casp9b Forward	CTCCACCTTCCCAGGTTTTGTC	Sigma Aldrich
Casp9b Reverse	AATGCCATCCAAGGTCTCGAT	Sigma Aldrich
Cs Forward	TCCATCACAGCGGCGAC	Sigma Aldrich
Cs Reverse	AGGCAGGATGAGTTCTTGGC	Sigma Aldrich
Hprt Forward	TCAGTCAACGGGGACATAA	Sigma Aldrich
Hprt Reverse	GGGGCTGTACTGCTTAACCAG	Sigma Aldrich
Sdha Forward	AACTACAAGGGACAGGTGCTG	Sigma Aldrich
Sdha Reverse	CTCCCACAGGCATACAGAC	Sigma Aldrich
Pdk4 Forward	CAAAGACGGGAAACCCAAGC	Sigma Aldrich
Pdk4 Reverse	CACACTCAAAGGCATCTTGGAC	Sigma Aldrich
CD45 Forward	AGACAGGGTTGTTCTGTGCC	Sigma Aldrich
CD45 Reverse	GGTATTGCTCATAGCTGCACAC	Sigma Aldrich
Oct3/4 Forward	GAGAACCGTGTGAGGTGGAG	Sigma Aldrich
Oct3/4 3 Reverse	TCGAACCACATCCTTCTCTAGC	Sigma Aldrich
Wt1 Forward	TTCAAGGACTGCGAGAGAAG	Sigma Aldrich
Wt1 Reverse	GGGAAAACTTTCGCTGACAA	Sigma Aldrich
Myh7 2 Forward	CTACCAGACAGAGGAAGACAGGA	Sigma Aldrich
Myh7 2 Reverse	TTGGAGCTGGGTAGCACAGA	Sigma Aldrich
Myh6 2 Forward	CCTACCAGACAGAGGAAGACAAG	Sigma Aldrich
Myh6 2 Reverse	TGGAGAGGTTATTCCTCGTCG	Sigma Aldrich
Myl2 Forward	TCCAAAGAGGAGATCGACCA	Sigma Aldrich
Myl2 Reverse	CCAGAGCCAAGACTTCCTGTT	Sigma Aldrich
PDGFR α Forward	GCACCAAGTCAGGTCCATT	Sigma Aldrich
PDGFR α Reverse	TGTCCAGGTCTTCTTCGGC	Sigma Aldrich
Casp9 Forward	ACCTTCCCAGGTTTTGTCTCCTG	Sigma Aldrich
Casp9 Reverse	TGCAGGTCTTCAGAGCGAGC	Sigma Aldrich
Casp6 Forward	CTCGCGGGCAGGTGAAAGTA	Sigma Aldrich
Casp6 Reverse	TGTCTCTGTCTGCGTTGGTG	Sigma Aldrich
Casp3 Forward	GTCCACTGACTTGCTCCAT	Sigma Aldrich

Casp3 Reverse	AGCTTGGAACGGTACGCTAAG	Sigma Aldrich
Apaf1 Forward	CGCAAACACCCAAGGTCTCT	Sigma Aldrich
Apaf1 Reverse	CCACTCTCCACAGGGACAAC	Sigma Aldrich
Cd36 Forward	TTAATGGCACAGACGCAGCC	Sigma Aldrich
Cd36 Reverse	GGATTCTGGAGGGGTGATGC	Sigma Aldrich
Tert Forward	CTTGCGGTTGAAGTGTACG	Sigma Aldrich
Tert Reverse	CACACATGCATGGAACCTGT	Sigma Aldrich
Vimentin Forward	CAGCAGTATGAAAGCGTGGC	Sigma Aldrich
Vimentin Reverse	CAGAGAGGTCAGCAAACCTGG	Sigma Aldrich
Cx43 Forward	GAAGTACCCAACAGCAGCAG	Sigma Aldrich
Cx43 Reverse	TGGGCACCTCTCTTTCACTTAAT	Sigma Aldrich
CD34 Forward	CTGACTTGAGAAAGCTGGGGA	Sigma Aldrich
CD34 Reverse	CCATCAAGGTTCCAGCTCCAG	Sigma Aldrich
Acta2 Forward	CTGACAGAGGCACCACTGAA	Sigma Aldrich
Acta2 Reverse	CATCTCCAGAGTCCAGCACA	Sigma Aldrich
CD105 Forward	GGTACAGTGCATCGACATGG	Sigma Aldrich
CD105 Reverse	CAGAATCCCACAAGCTCCAA	Sigma Aldrich
Ddr2 Forward	ACTACAGTCGGGATGGCAAC	Sigma Aldrich
Ddr2 Reverse	ACACGTTTCATGGAGTGGTCA	Sigma Aldrich
CD90 Forward	CAGAATCCCACAAGCTCCAA	Sigma Aldrich
CD90 Reverse	GCCAGGAAGTGTTTTGAACC	Sigma Aldrich
Desmin Forward	GAGGTTGTCAGCGAGGCTAC	Sigma Aldrich
Desmin Reverse	GAAAAGTGGCTGGGTGTGAT	Sigma Aldrich

APPENDIX B – MICROSCOPY ANTIBODIES & DYES

IMMUNOCYTOCHEMISTRY

Primary antibody target	Manufacturer	Dilution	Secondary antibody	Dilution	Manufacture
CD90 - PE	Life technologies A14729	1:100	N/A	N/A	
DDR2	Santa Cruz sc-7555	1:200	AF488 Donkey anti goat	1:200	Invitrogen A11055
CD105	Santa Cruz sc-18893	1:100	AF488 Goat anti Rat	1:200	Life Technologies A11006
CD45	Invitrogen MCD4500	1:100	AF488 Goat anti Rat	1:200	Life Technologies A11006
CKIT	Santa Cruz sc-5535	1:100	AF568 Goat anti rabbit AF488 Donkey anti rabbit	1:200	Invitrogen A11011 Invitrogen A21206
SCA1 - FITC	Bd Pharmingen 557405	1:50	N/A	N/A	
Oct3/4	Santa Cruz sc-9081	1:50	AF568 Goat anti rabbit	1:200	Invitrogen A11011
SOX2	Santa Cruz sc-17320	1:50	AF488 Donkey anti goat	1:200	Invitrogen A11055
Cardiac TNNT2	Abcam Ab10214	1:200	AF488 Donkey anti mouse	1:1000	Invitrogen A21202
MHCb	Abcam Ab15	1:200	AF488 Donkey anti mouse	1:1000	Invitrogen A21202
DAPI (Nucleus)		1:5000	N/A	N/A	Life Technologies
Rodamine Phalloidin (fActin)		1:1000	N/A	N/A	Invitrogen

APPENDIX C – WESTERN BLOTTING COMPONENTS

Resolving Gel Buffer - 500ml (pH to 8.8)			
Component	Concentration	Amount (g)	Supplier
Tris	1.5M	90.83	Sigma-Aldrich
SDS	0.4%	2	Fluka BioChemika

Stacking Gel Buffer - 500ml (pH to 6.8)			
Component	Concentration	Amount (g)	Supplier
Tris	0.5M	30.28	Sigma-Aldrich
SDS	0.4%	2	Fluka BioChemika

Resolving Gel – 12.5 %		
Component	Amount	Supplier
Protogel (ml)	15	Sigma-Aldrich
Resolving gel buffer (ml)	12.5	
Water (ml)	10	
10% APS (ul)	250	Merk
TEMED (ul)	60	Sigma-Aldrich

Stacking Gel – 4 gels		
Component	Amount	Supplier
Protogel (ml)	3.4	Sigma-Aldrich
Stacking gel buffer (ml)	5	
Water (ml)	7.5	
10% APS (ul)	80	Merk
TEMED (ul)	40	Sigma-Aldrich

Transfer Buffer - 1.5L			
Component	Concentration	Amount	Supplier
Tris-Base (g)	25mM	4.54	Sigma-Aldrich
Glycine (g)	192mM	21.61	Sigma-Aldrich
Methanol (ml)	20%	300	Sigma-Aldrich

Sample Buffer Dye - 50ml			
Component	Concentration	Amount	Supplier
Tris-Base	187.5mM	1.136g	Sigma-Aldrich

Glycerol	30%	15ml	Sigma-Aldrich
SDS	6%	3g	Fluka BioChemika
Brilliant Blue	Dipped tip	Dipped tip	Sigma-Aldrich

10x TBS – 1L			
Component	Concentration	Amount	Supplier
Tris-Base	100mM	30.3	Sigma-Aldrich
NaCl	9%	90g	Sigma-Aldrich

10x TBS- Tween – 2L			
Component	Concentration	Amount	Supplier
10x TBS	10%	200ml	
Tween	0.05%	1ml	Sigma-Aldrich

10x electrophoresis buffer – 1L			
Component	Concentration	Amount	Supplier
Tris-Base	0.25M	30.3g	Sigma-Aldrich
Glycine	1.92M	144g	Sigma-Aldrich
SDS	1%	10g	Fluka BioChemika

Primary Antibody	Species	Dilution	Supplier	Secondary Antibody	Dilution	Supplier
Citrate Synthase	Rabbit IgG	1:1000	Alpha Diagnostics	Goat anti-rabbit	1:2000	Santa Cruz

3. MOUSE ATRIAL CARDIAC PROGENITORS

3.1. INTRODUCTION

3.2.1. SEEKING FOR THE IDEAL CPC *IN VITRO*

In Chapter 1 we discussed the main stem cell types used in cardiac cell therapy. We described the properties of MSCs, characterised by the presence of CD73, CD90, CD105, CD44 and CD166 and the lack of hematopoietic markers (1.2.3.3), as well as the different types of endogenous CPCs, with the popular markers for their recognition; Sca1, Ckit, Wt1 (Table 1.1). In addition to these markers, we mentioned the main cardiac transcription factors (MEF2c, GATA-4, NKX2.5, ISL1), (Table 1.2) that are being used for characterisation of the potential of cardiac progenitors. The identity of the CSC remains unclear. The Ckit⁺ or Sca1⁺ CSCs, as well as the CDCs, all share common mesenchymal markers, like CD90 and CD105, or some of the cardiac transcription factors (see 1.2.2.4). As the search for characterising the “best” endogenous cardiac cell population for treatment purposes continues, new studies introduce additional candidates, from outside the traditional CPC groups.

3.2.2. WHAT IS THE CARDIAC FIBROBLAST?

Any attempts to understand cardiac regeneration post-MI, or to characterise the endogenous CPCs (see 1.2.2.4), would not be fruitful without addressing the existence and identity of cardiac fibroblasts. Fibroblasts were introduced by Friedenstein AJ. in the late 1960s, described from spleen and BM as proliferative, adherent cells²²⁶. Soon after, Owen M. in 1988 was talking about “fibroplastic colonies” originating from BM stromal SCs, from a single colony-forming unit fibroblast²²⁷. Prockop DJ in 1997 described that these plastic-adherent cells could be useful for non-hematopoietic tissue therapy, differentiating *in vitro* into osteoblasts, chondrocytes, adipocytes, and myoblasts⁴⁴. Nowadays, we know fibroblasts are interstitial cells of mesenchymal lineage, found in almost every organ of the body²²⁸. They are believed to originate from cardiac MSCs that are activated and transdifferentiate²²⁹ or from circulating SCs (mainly BM-SCs)²³⁰, with the recent addition of the epicardial epithelial-to-mesenchymal transition as a source²³¹. All this could hint that fibroblasts are important for the good function of the heart, and therefore the organ has the ability to recruit them from various sources²³². Several studies have investigated the percentage of the

different cardiac cell populations. Fibroblasts have been found to take up about 60–70% of the human heart²³⁰ and 40 - 60% of the total cell population of the rat heart²²⁸. The murine adult heart was shown to be composed of 56% CMs and 27% fibroblasts²³³, indicating that the organism-models for cardiac research differ in the cellular composition of the organ.

Cardiac fibroblasts are involved in the production of ECM proteins, like collagen, and offer structural support to the tissues²³⁴. In addition, they are involved in processes like inflammation, fibrosis and tissue repair²³⁵. More specifically, post infarction cardiac fibroblasts are activated, by mechanical stress, alterations in the extracellular matrix environment and release of growth factors, chemokines and cytokines²³⁶. Alpha-smooth muscle actin (α -SMA) is an actin isoform that is expressed by fibroblasts upon differentiation to **myofibroblast**²³⁷. This process takes place upon wound healing, when myofibroblasts are involved in cardiac remodelling, in cases like infarction and fibrosis^{237,238}. The contractile and coupling ability of myofibroblasts (with the resident CMs) is still under debate, while further studies are needed to understand what happens *in vivo*²³⁹. Apart from α -SMA, activated fibroblasts can express a number of other markers under pathological conditions that are normally expressed in other cell types, such as fibroblast-specific protein 1 FSP1 (see below), or the epicardial WT1²³².

Morphologically fibroblasts are elongated, flat spindle-shaped cells, yet there are reports describing variability among different tissues^{230,228}. The lack of a definite **marker** that would allow their identification makes the study of cardiac cells and SCs more complicated. To begin with, Discoidin Domain-containing Receptor (DDR2), a collagen receptor, with a receptor tyrosine kinase function, is a popular cardiac fibroblast marker involved in their proliferation^{234,240}. In addition, vimentin is an intermediate filament protein involved in epithelial-to-mesenchymal transition²⁴¹ and has been reportedly involved in fibroblastic wound healing⁸¹. Another filament protein, FSP1, is involved in epithelial-to-mesenchymal transition and has been suggested as a fibroblast marker²⁴². The tyrosine kinase receptor PDGFR, involved in tissue fibrosis, is considered to be expressed by fibroblasts, such as lung myofibroblasts²⁴³. Finally, CD90 or Thymocyte antigen 1 (Thy-1), a cell surface glycoprotein with multiple functions²⁴⁴, has been used as a fibroblast marker. The marker has been shown

to label myofibroblasts in the adult heart, capable of differentiating into CM-like cells²⁴⁵. The identity of the fibroblast cell, though, is still elusive because of the lack of specificity of these markers, which are also expressed in several other cell types^{240,246,247} (see Table 3.1).

The lack of specificity, along with the fact that the marker expression changes under pathological conditions, makes the distinction of connective fibroblasts, activated myofibroblasts and other cells very challenging.

Gene	Full Name	Cell Types Expressed	Ref
Vimentin	Vimentin	fibroblasts, telocytes, ECs, macrophages, leukocytes, tumour cells, neuronal cells, SMCs	246
Ddr2	Discoidin Domain-containing Receptor 2	fibroblasts, osteocytes, leukocytes, tumour cells	240
Fsp1	Fibroblast-specific protein 1	fibroblasts, lymphocytes, macrophages, SMCs, myeloid cells	247
αSMA	alpha Smooth Muscle Actin	myofibroblasts, SMCs, MSCs	235
Pdgfra	Platelet-Derived Growth Factor Receptor alpha	BM-MSCs, MSCs, fibroblasts, skeletal muscle progenitors,	105, 248
CD90/Thy-1	Thymocyte antigen 1	fibroblasts, neuronal cells, BM-SCs, lymphocytes, CPCs, thymocytes, MSCs	249, 250, 232

Table 3.1. Table of common markers that have been used to identify fibroblasts

3.2.3. FIBROBLASTS & OTHER CELLS

As mentioned above, fibroblasts are considered to be of mesenchymal origin. Various studies have questioned the differences between MSCs or mesenchymal stromal cells and fibroblasts, since they have genetic, immunomodulatory and morphological similarities^{251,252}. The more cell types that are being introduced in the discussion, the less clear the distinctions become.

Pericytes, circulating perivascular cells involved in tissue repair, have been termed as cardiac MSCs²⁵³. They express hematopoietic and immune cell markers (CD45, CD34, CD68 etc), as well as CD146 and PDGFR α and b²⁵³. In addition, it has been shown that pericyte transplantation post-MI can lead to functional and structural recovery of the human heart²⁵⁴. Interestingly, a study comparing MSCs from adult or fetal tissues, fibroblasts and pericytes, for differentiation capacity, morphology, genetic and marker expression (all expressed FSP1 & CD146), demonstrated striking similarities²⁵⁵.

Another circulating cell type related to fibroblasts is the **fibrocyte**. Fibrocytes have been termed as mesenchymal progenitors, and are a collagen-producing, leukocyte sub-population of the peripheral blood²⁵⁶. They are mainly characterised by myeloid markers CD45, CD34, CD11b²⁵⁷, and have wound healing, and immunomodulatory properties. Studies have shown many similarities between fibrocytes and myofibroblasts, including α -SMA expression and secretion of pro-inflammatory factors²⁵⁷, with implication in the process of fibrosis in several tissues²⁵⁸.

Finally, a cell type introduced in 2010 is the cardiac **telocyte**. Upon discovery it was termed as an Interstitial Cajal-like Cell (ICLC) found in the mammalian heart²⁵⁹. These cardiac interstitial stromal cells have thin elongations called “telopodes”, that are composed of the “podomer” axons, with occasional “podom” clusters where mitochondria reside²⁶⁰. In the adult heart, telocytes, are in contact with CPCs and CMs, to support the normal function of the heart²⁶⁰. Their numbers and function decline post-MI²⁶¹, while after transplantation telocytes have been shown to aid cardiac regeneration²⁶². Taken all together, there are no clear distinctions between cell types that resemble fibroblasts, and “actual fibroblasts”, with the latter still being an undefined cell type itself^{263,228}.

In addition to the aforementioned cell types there are other less known adult stem cell populations, like the Very Small Embryonic Like (VSEL) stem cells²⁶⁴. These cells have been suggested to be epiblast-derived stem cells that reside in adult tissues, like the BM, blood, heart and brain²⁶⁵. VSELs express early cardiac and endothelial lineage markers (GATA4, Nkx2.5, and von Willebrand factor), and can be stimulated to migrate after injury, like MI and ischemic stroke²⁶⁶. This

cell population was found to be able to differentiate into HSCs, MSCs, epithelial cells, CMs and germ cells. Guidelines state that murine BM-derived and human umbilical cord VSELs are Sca1+/ Lin- and CD133+/ Lin-, respectively, and also express Oct4+ and Nanog+²⁶⁷. Despite the promising results and the initiation of a clinical trial for severe angina treatment, VSELs were soon questioned as researchers could not easily identify them in samples²⁶⁸. A study in 2012 on human umbilical cord-derived VSELs suggested that they represent a heterogeneous and inactive population that phenotypically resembled neither pluripotent nor adult stem cells. In addition these cells were unable to be expanded *in vitro*²⁶⁹. Since 2013, studies have refuted the very existence of VSELs in adult tissues²⁶⁸. Studies on the characteristics of human VSELs from peripheral blood continued in 2016, with a study using human peripheral blood samples showing that their number does not change with age²⁷⁰.

3.2.4. WHERE DO CPCs LIVE?

Cardiac SCs or CPCs have been isolated by various groups for a decade now (for this part of the introduction we will not revisit epicardial progenitors – see Introduction 1.2.2.4.4). However, in some cases including those referenced by many subsequent papers, studies neglect to specify which region of the heart the specimens originate from, including those conducted by the Anversa group^{271,272}. Others would digest the tissue using a perfusion method, and therefore would isolate from the ventricles, as in the initial description of Sca1+ cells by Oh H. *et al.*¹⁰¹. The CDC isolation protocol of Smith RR. *et al.* was also conducted using the ventricles¹²², while the initial Messina *et al.* study used both atrial and ventricular specimens, without distinguishing or comparing¹²¹. The human atria have been used as a source, like the Sca1+ cell of Smits A. *et al.*²²⁰ and the Bolli R. *et al.* SCIPIO clinical trial, where autologous Ckit cells were used from the RA appendage⁹⁹. Finally, many *in vitro* studies on rodent CSCs isolate them from the whole heart^{273,274,121,275}.

Interestingly, studies have shown that there are more stem cell niches found in the atria and apex of the adult mouse, than the ventricles²⁷⁶, or that more Ckit+ or Sca1+ CPCs can be isolated from them²⁷⁷ and that the atrial niches are more hypoxic and correlate with long-term quiescent repopulating CSCs²⁷⁸. Previous

data from our group have shown that EDCs isolated from the rat atria have significantly higher expression of Ckit than the ventricles²⁷⁹ and that agrees with observations the human right atrium is the most appropriate source for Ckit⁺ and Isl1⁺ CSCs²⁸⁰. Based on this short review of the isolation studies, we decided to focus our work on a specific compartment of the heart, the atria. Beside the encouraging results about the resident CSCs in the atria, it is also a compartment in the human heart that is commonly accessible for tissue biopsy.

3.2.5. ISSUES WITH ISOLATION PROTOCOLS FOR CPCs

In addition, to the complexity of identifying and characterising CPCs, the culture conditions also affect the phenotype of cells^{281,282}. For example in 2013, a new cell type was introduced from the human right atrial appendages, selected based on high aldehyde dehydrogenase (ALDH) enzymatic activity, which also expressed Ckit, CD34, Oct4 and Isl1²⁸³. These marker-selected cells, though, when expanded *ex vivo* alter their phenotype. They lose expression of CD34, while they start expressing CD13, CD44, and CD49c, starting to resemble CDCs or Ckit⁺ CSCs²⁸³. So, *in vitro* expansion techniques might account for some of the differences observed among the different CPC cell types. Still, it is impossible to use the adult CPCs for cell therapy, without expansion *in vitro*, because of large cell number that is required post-MI.

As shown in Figure 1.3., certain popular candidates are selected populations based on marker expression, or followed by clonogenic selection, or even total populations isolated via a specific protocol. The best possible isolation method would be one that would yield a big number without much time cost. The population should grow quickly and demonstrate a CPC phenotype. The clonogenic isolations, of Ckit⁺ CPCs from the Ellison G. group²⁸⁴ and the of Sca1⁺ CPCs from the Schneider MD. group¹⁰⁵ are promising, resulting in homogenous cardiogenic self-renewing populations. Nonetheless, the selected CSCs comprised 4% and 3% of the mouse heart and their success of generating single cell-derived clonal colonies was ~30% and 1% respectively (the former data are given from a P4 single cell, and not at P0, as the latter). This indicates a very low cell yield and a long time to grow the millions (if not billions) of cells required, starting from only one cell.

The Carr group has a long history of working with CDCs ^{285,126,124}, which are a mixed population of CPCs. The explanting protocol, as described by Messina *et al.*¹²¹, and later Smith RR *et al.*¹²², and used in our lab has a long expansion step²⁸⁶ and gives rise to a very heterogeneous cell population¹²³. In addition it is not a particularly robust protocol, as the cell yield is very variable¹²¹. More specifically, Dr. Perbellini F. (Thesis – unpublished data) explanted mouse atrial tissue and found a great variation in the yield of EDCs/ explant piece, as did Messina E *et al.*¹²¹, in addition to noticing explants without any EDC outgrowth. While, EDCs themselves had variable morphology and marker expression. Furthermore, Chan H *et al.*, in another study from our group noticed substantial differences in the time required to acquire EDCs from human atrial biopsies, spanning from 7 to 55 days¹²³.

APPENDIX D - Cluster of Differentiation (CD_) Molecules - Full Names

Cluster of Differentiation CD_ antigen	Official full name
CD11b	Integrin alpha M
CD14	CD14 antigen
CD19	CD19 antigen
CD31	Platelet and endothelial cell adhesion molecule 1 (PECAM-1)
CD34	CD34 antigen
CD36	CD36 antigen
CD44	CD44 antigen
CD45	Ptpcr protein tyrosine phosphatase, receptor type, C
CD49c	Integrin alpha 3
CD73	5' nucleotidase
CD90	Thymus cell (thymocyte) antigen 1
CD105	Endoglin
CD117	KIT proto-oncogene receptor tyrosine kinase
CD146	Melanoma cell adhesion molecule
CD166	Activated leukocyte cell adhesion molecule (ALCAM)

Table 3.2. Table of the official full names corresponding to the CD nomenclature for the CD molecules referenced in this thesis. The information was retrieved from the National Center for Biotechnology Information (NCBI) Gene website (<https://www.ncbi.nlm.nih.gov/gene>), for the house mouse CD molecules.

3.2.6. STUDY AIMS

As the cardiac stem cell field has been looking for the real cardiac progenitor, so did researchers in the skeletal muscle field. Gharaibeh *et al.*²⁸⁷, arguing that marker-selected isolations are not reliable, modified and used marker-independent method for isolating skeletal-muscle-derived progenitors with high stemness and therapeutic characteristics. Therefore, we were interested to try using this “preplate technique” on the cardiac tissue. Given our belief that a mixed cell population might survive and integrate better in the infarcted heart, supported by various approaches of mixed cell population, in this chapter:

- I tried alterations to the standard explanting protocol, to reduce the expansion time or obtain more stem-like CDCs
- In addition, I developed a new protocol for the isolation of CPCs from the mouse atria, based on enzymatic digestion
- I strived to phenotypically characterise the cell types obtained
- Finally, I compared the CPCs yielded with isolated CDCs, from same atrial tissue, on the premises of proliferation rate, heterogeneity, colony-forming capacity, marker expression

3.3. RESULTS

3.3.1. ATTEMPTS TO OPTIMISE THE EXPLANTING PROTOCOL

Initially, I attempted to alter the standard explanting protocol, developed by Messina E. *et al.*²⁸⁶ and optimised by Smith RR. *et al.*¹²², in order to make it more efficient. I focused on the Explant-derived cells (EDCs), the migratory cells that appear around the explants and are trypsinised to be processed at the cardiosphere step (Figure 3.1).

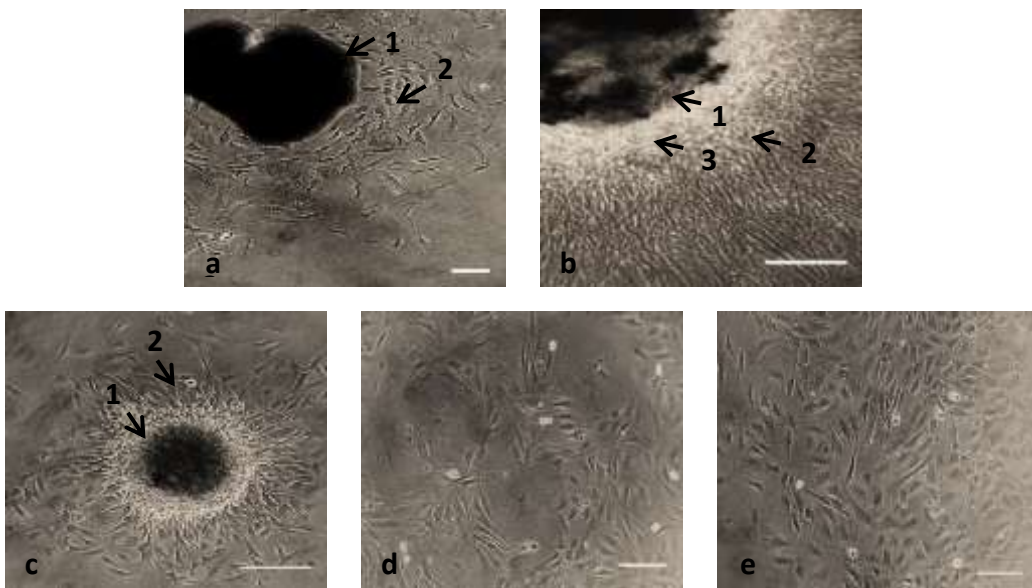


Figure 3.1. Different steps of the explanting protocol. (a) & (b) explants marked as 1. and EDCs coming out of the tissue explant marked as 2. (b3) indicates the very confluent region around the explants. (c1) plated cardiosphere and (c2) CDCs coming out of the sphere, (d) CDCs P2, (e) CDCs P4. (scale bars: a,d,e:100 μm , b,c: 200 μm).

Since multiple EDC harvests can be done it was important to understand the differences, in terms of the stemness markers, in order to use the most suitable one(s) to make CDCs. We noticed substantial gene expression changes among the different conditions (Figure 3.2), which led to the conclusion that we would not combine different harvests for our study, as it would increase the sample variability. Despite the fact that growing EDCs to P2 seemed appealing, as it

would allow us to obtain more CDCs from them, given the marked reduction of Ckit and Sca1 (Figure 3.2) we decided to proceed using harvest 1 P0 EDCs (H1 P0).

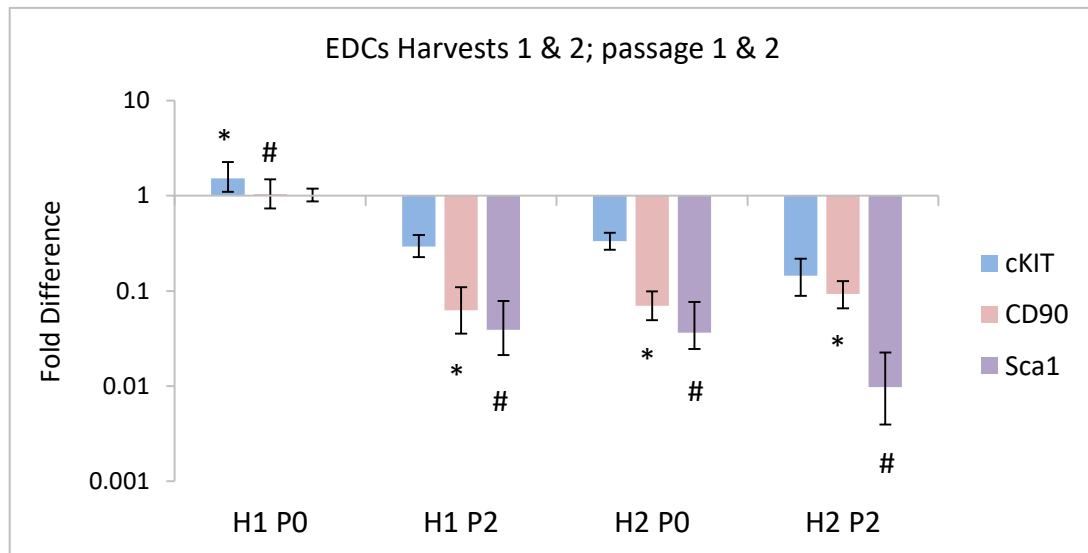


Figure 3.2. Gene expression changes between EDCs harvest 1 and 2, and passages P0 and P2. (n=4, error bars: standard error, p* <0.01 and p# <0.02 indicating difference to H1P0)

In order to better characterise the EDCs H1 P0 immunocytochemical analysis was conducted for CD45, CKIT, CD90, and SCA1 (Figure 3.3). CD90 was found strongly expressed in the imaged EDCs (57% +/- 28% n = 3 slides; 9/15 cells), while SCA1 was fainter and labelled a subset of the cells (30% +/- 7% n = 4 slides; 21/79 cells). 100% of the cells expressed CKIT (n = 3 slides; 72/72 cells), with a proportion double-stained for CD45 (56% +/- 24% n = 4 slides; 9/16 cells), suggesting a hematopoietic origin of the EDCs.

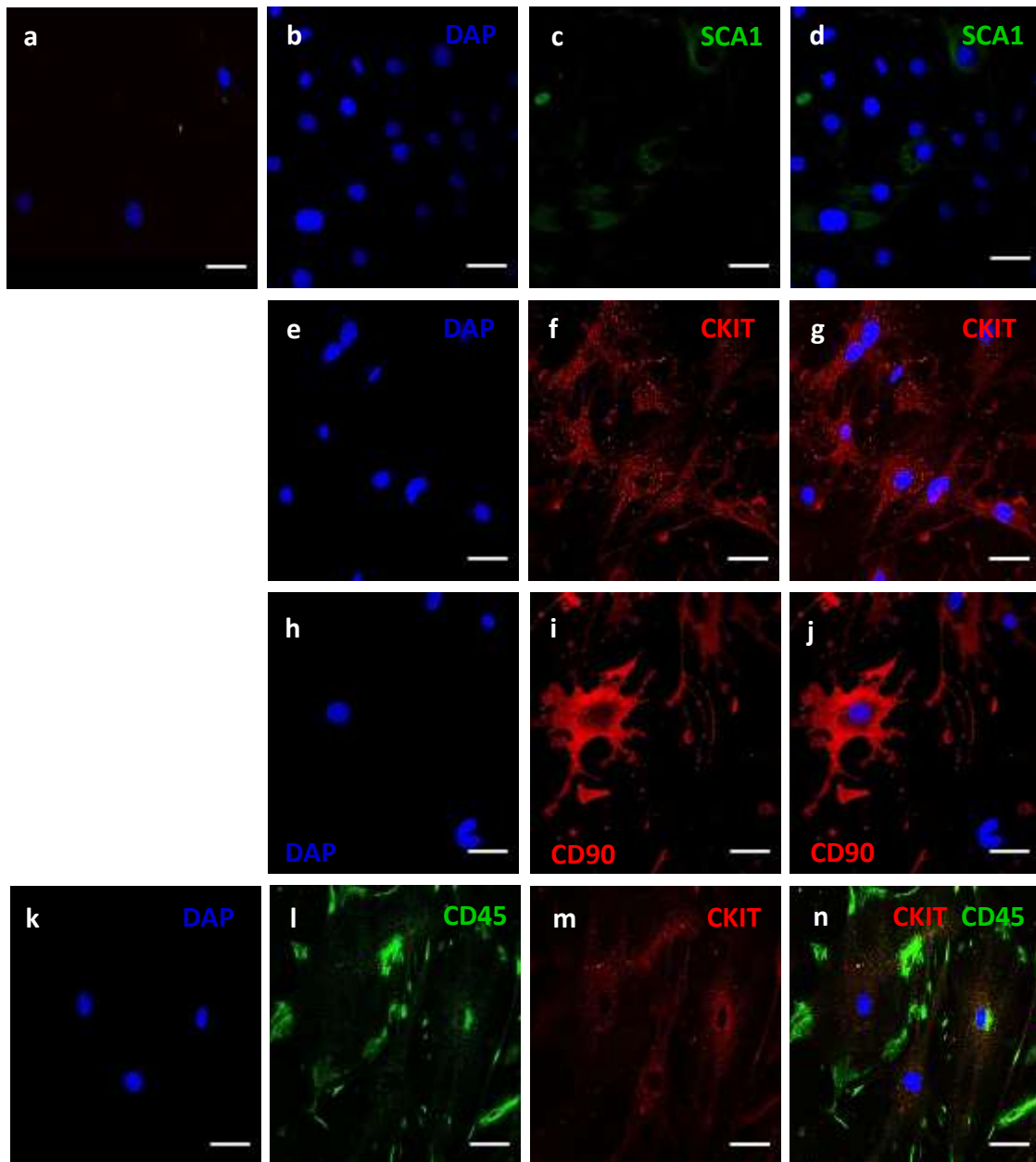


Figure 3.3. Immunocytochemistry on EDCs P0, stained with (a) secondary antibodies for negative control, (b-d) SCA1, (e-g) CKIT, (h-j) CD90 (k-n) CD45/CKIT double-staining, all co-stained with DAPI (b, e, h, k). Scale bars: 50 μ m.

Furthermore, the cardiosphere step, which is believed to enhance the Ckit expression of the CDCs because of the hypoxic conditions that take place in the core of the sphere¹²², was manipulated. The cardiospheres were kept at the

hanging drop stage for 5 days, and Ckit gene expression was significantly increased (Figure 3.4). Unfortunately, some of the droplets would dry out in the duration of 5 days or the retrieved cells would have reduced survival, therefore the study was continued using CDCs originating from a 3-day cardiosphere step, as before.

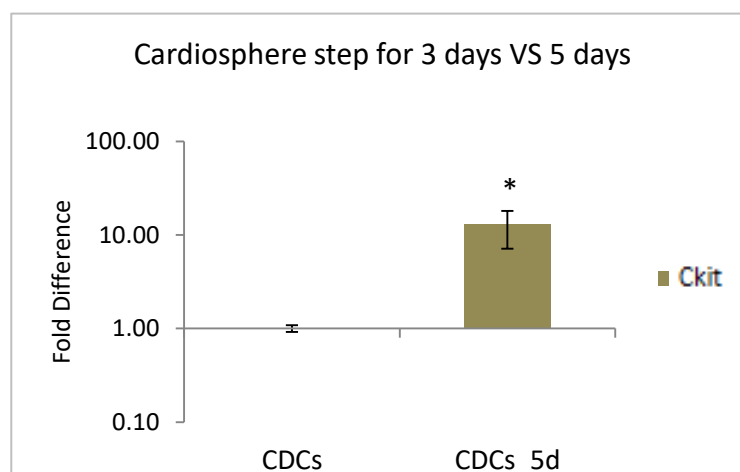


Figure 3.4. Ckit gene expression on CDCs P0 after 3 days or 5 days of the cardiosphere step (n=3, error bars: standard error, *p<0.04)

3.3.2. DEVELOPING A DIGESTION-BASED PROTOCOL FOR CPC ISOLATION

The two atrial CPC populations that this study focuses on are the collagenase-trypsin isolated cells and the CDCs. The former was a protocol designed after coming across the protocol from Gharaibeh *et al.*²⁸⁷ and Okada *et al.*²¹⁵ for isolating skeletal-muscle-derived progenitors with high stemness and therapeutic characteristics. The expansion method comprised of daily re-plating of the digestion suspension, in empty flasks, until only the slowly adhering cells remained (see 2.2.2.1).

Given that the cardiac muscle is different in composition to skeletal muscle, several digestion mixes were compared (see 2.2.2) looking for the one that allowed the yield of highest number of cells from mouse atria, as certain protocols were too harsh and lethal for the cells (Table 3.3). Cell viability was checked at various time points during each digestion protocol (every 5', 10', 30'), by observing Trypan blue-treated cells (which would stain blue only if dead)

under the microscope. After each digestion trial, the cultures were grown and checked for viable cells after one week.

PROTOCOL	Outcome after 1 week
30U/ ml Collagenase II ; 1h	debris only - No cells
30U/ ml Collagenase II ; 80' , then 0,1% Collagenase II ; 30'	debris only - No cells
0,1% Collagenase II ; 1h	very few fibroblast-like cells
0,1% Collagenase II ; 1h + then 0,1% trypsin ; 20' ³⁵	very few fibroblast-like cells
0,1% Collagenase II; 50' then add: 0,1% trypsin 20'	very few fibroblast-like cells
0,1% Collagenase II; 85'	debris only - No cells
trypsin in Krebs buffer + 0,1% Collagenase II	very few fibroblast-like cells
0,1% trypsin + 0,1% Collagenase II mix ; 1h	✓ highest number of fibroblast-like cells

Table 3.3. Different digestion protocols used for CPC isolation from the mouse atria

Applying this to digest mouse atria, a slowly attaching population of cells was identified that looked morphologically like the one described by Gharaibeh *et al.* ²⁸⁷ (Figure 3.5). However, the results of the isolation method were variable; some samples were quiescent over many weeks, before they started to proliferate. The lack of consistency of this protocol urged us to abandon it. Therefore the digestion method was adapted without purifying for only the fast or slow adhering fraction, and allowed all cells in the digestion to attach over 72 hours

without completely refreshing the medium (which would risk throwing away any slower adhering cells). Hereafter these cells will be the “CT” cells.

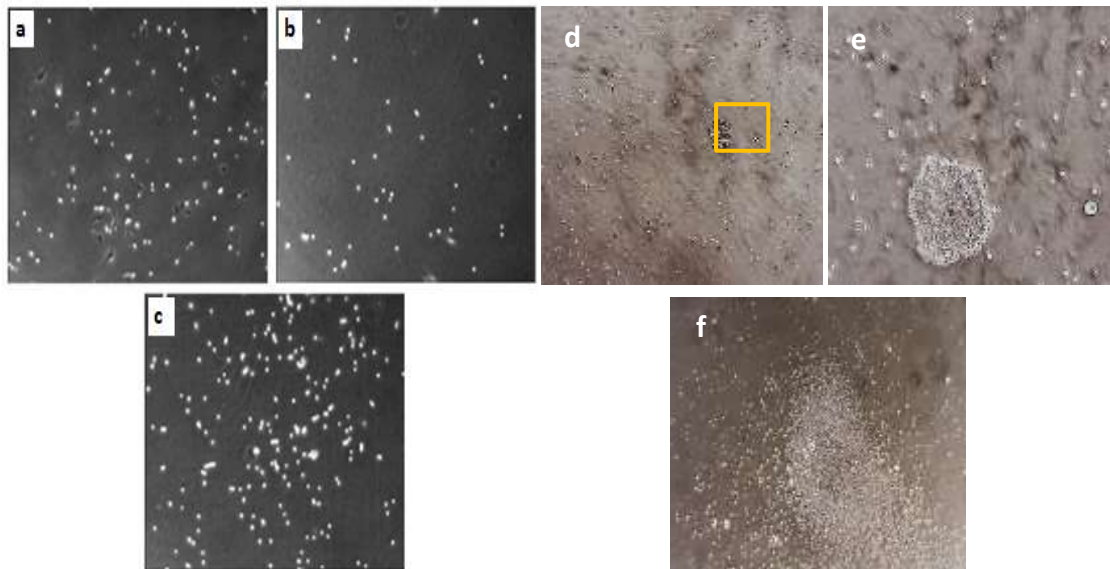


Figure 3.5. The cells isolated via the slow-adhering pre-plating protocol. (a)-(c) the skeletal muscle-derived cells isolated from Gharaibeh *et al.* and (d)-(f) the cells isolated by the same method applied on mouse atria. (d) cells 1 week after the last pre-plating step, (e) 40x zoom of initial magnification, aiming at the yellow square region, (f) 3 days after “awakening” of certain cell colonies, indicating rapid proliferation. Original magnification x10 for all images (except for (e)).

In an effort to increase the stemness and cardiogenic potential of CTs, they were processed via a cardiosphere step, as done in the explanting protocol (see 3.3.1). A population of cells was obtained that was labelled “CT_CDCs” and was initially checked for its gene expression profile, in comparison to CTs at P2 (Figure 3.6.). The cardiosphere formation led to an increase in *Ckit* gene expression, but a significant decrease in *Sca1*. The mesenchymal/fibroblast markers *CD90*, *Ddr2* and *CD105* decreased, with the latter changing significantly (Figure 3.6).

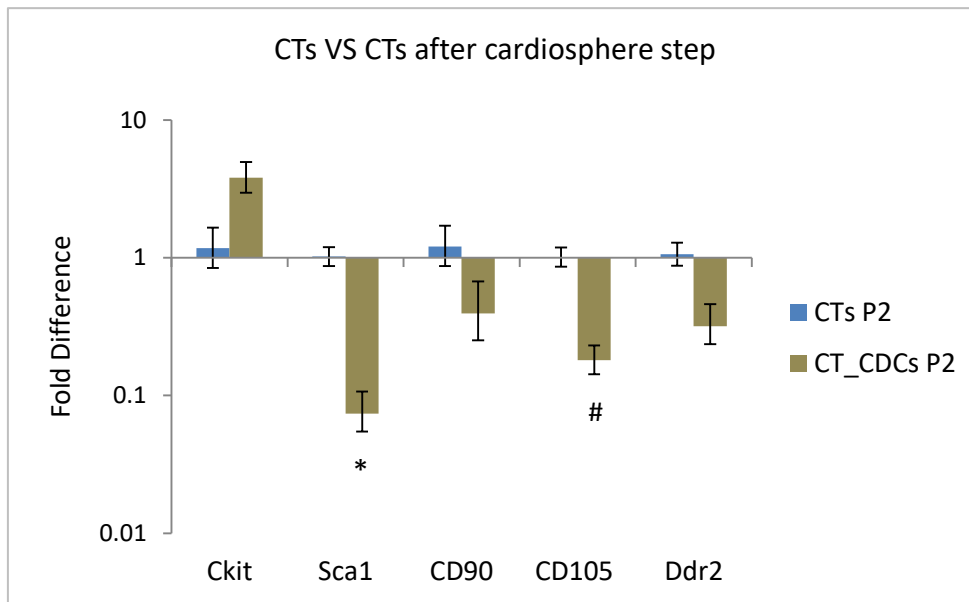


Figure 3.6. Gene expression changes at CTs after being processed via the cardiosphere step and reaching P2. (n=4, error bars: standard error, *p<0.04 , #p<0.02 indicating difference to CTs)

The interest in this population was soon hindered by the fact that the CTs would not form cardiospheres consistently, with a failure rate of 40%. Some samples would result in malformed clusters of cells that did not adhere to the wells to give rise to CDCs (Figure 3.7.). Therefore this approach was abandoned and the rest of the study was continued using CTs.

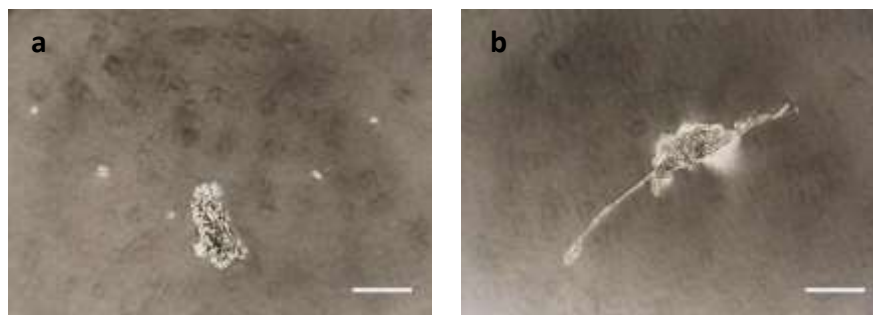


Figure 3.7. Phase contrast representative images, (a) and (b), of cardiospheres from CTs. (scale bars 200 μm)

3.3.3. CTS INCREASE PROLIFERATION & HOMOGENEITY, WITH PASSAGING

Since the first few isolations of CTs it was apparent that they were very proliferative and this allowed for a shorter expansion protocol, than the one required with CDCs (Table 3.4). Despite the variability among the different isolations, this observation was reproducible and confirmed by collaborators and colleagues that used the protocol of CT isolation.

	Average Time & Yield at P0	Average Time to P2
CDCs	40,000 cells/ 40 days	2 months
CTs	120,000/ 10 days	20 days

Table 3.4. Representative numbers stating the length of each protocol, for isolations from whole mouse atria/protocol and upon confluency at P0 and P2.

To understand the nature of the CT cells that were isolated, they were grown for more than 40 passages, surpassing the limit of somatic cells, to investigate their capacity for proliferation (see Methods 2.4). After passage 7, the cells became morphologically homogenous and their proliferative capacity increased substantially. At each successive passage, the number of cells in a confluent flask increased, indicating that the cell size was smaller (Figure 3.8. and 3.9.).

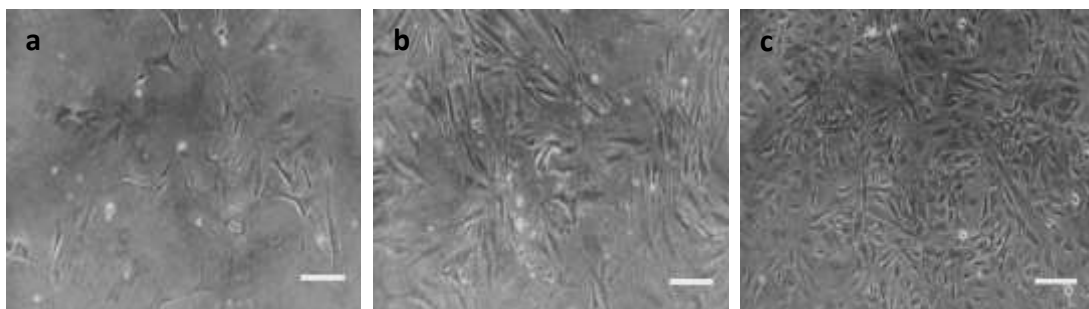


Figure 3.8. CTs under phase contrast microscope, as observed at (a) p2, (b) p4, and (c) p6. (scale bars 100 μ m)

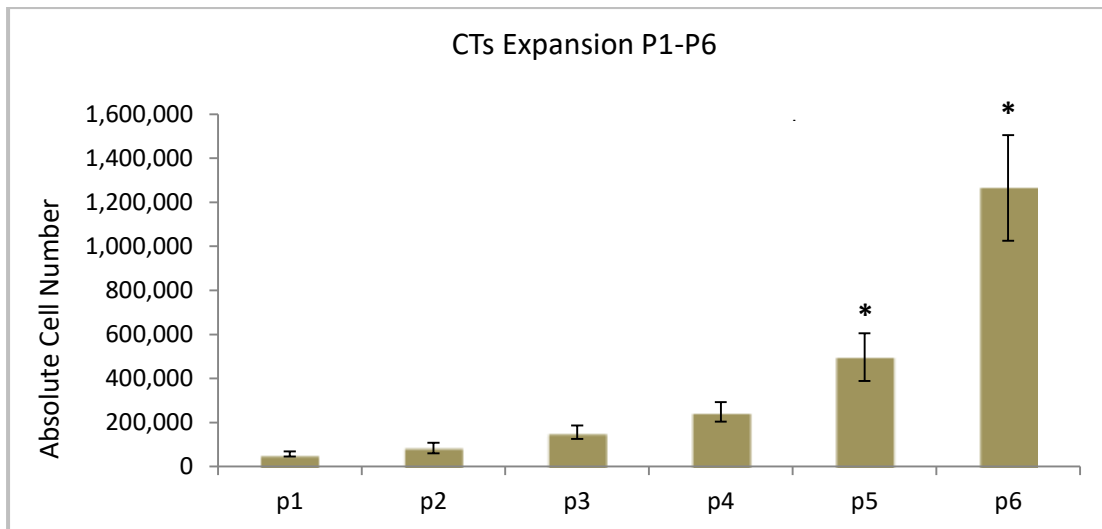


Figure 3.9. Absolute cell numbers of CTs, from a confluent flask, between the different passages (P1-P6). (n=4, *p<0.04 indicating difference to p2)

To compare the homogeneity of CTs to CDCs, we performed a Colony Forming Unit assay (see Methods 2.9). Looking into the images of the colony forming assay, after staining (see Methods 2.9), the CTs were more homogenous than CDCs, and became more homogenous at p7 in comparison to p2 (Figure 3.10). We also observed that CTs had higher colony forming capacity, at P7 than at P2 (Figure 3.11). This suggested that the change in proliferation rate that the CTs show after p6 could be associated with a change in their characteristics.

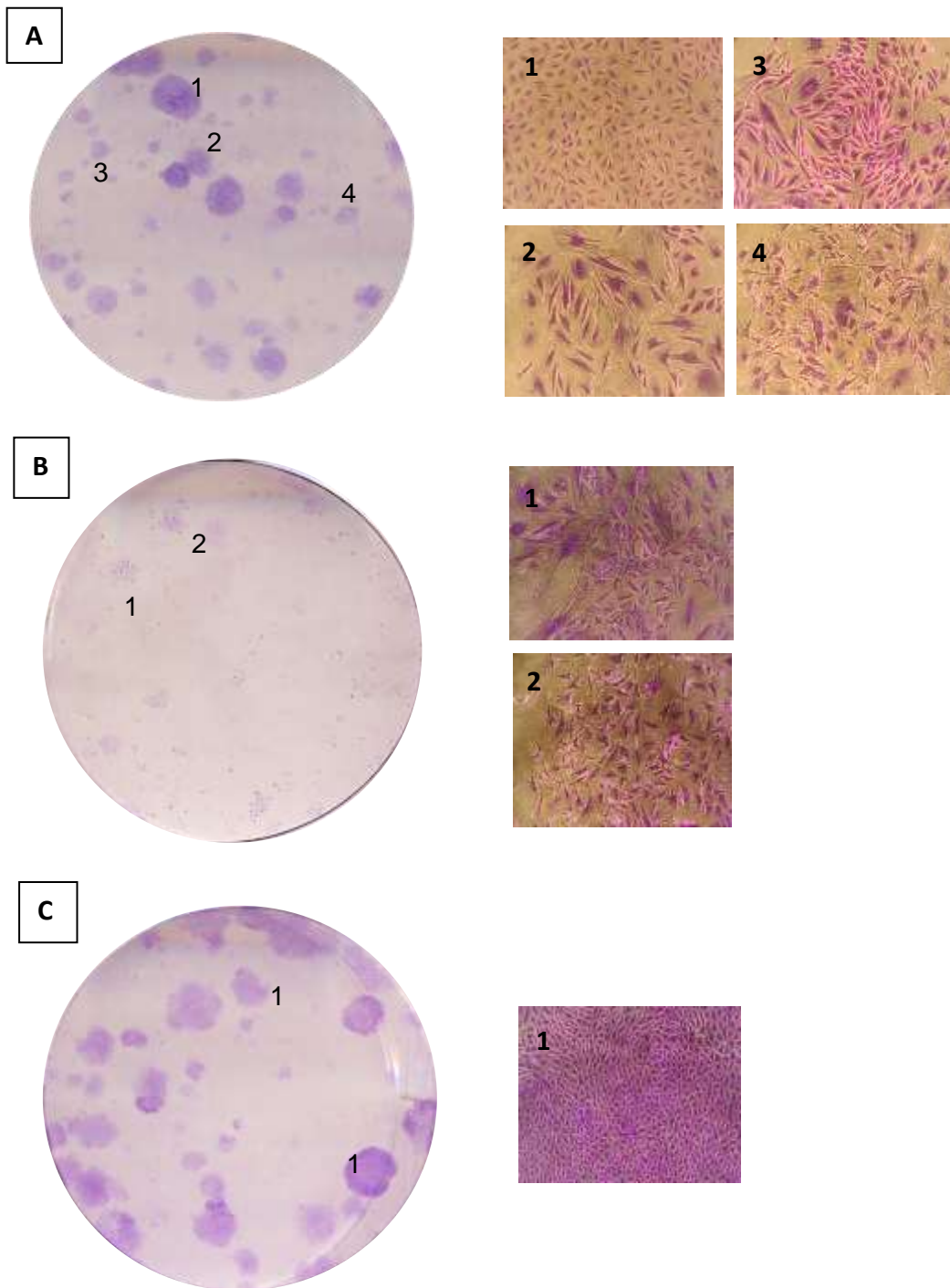


Figure 3.10. Colony Forming Unit Assay on A) CDCs P2, B) CTs P2, C) CTs P7. Right panel indicates the morphology of the colonies stained with crystal violet, numbers 1 - 4 correspond to different representative shapes and sizes, indicating variability of the populations

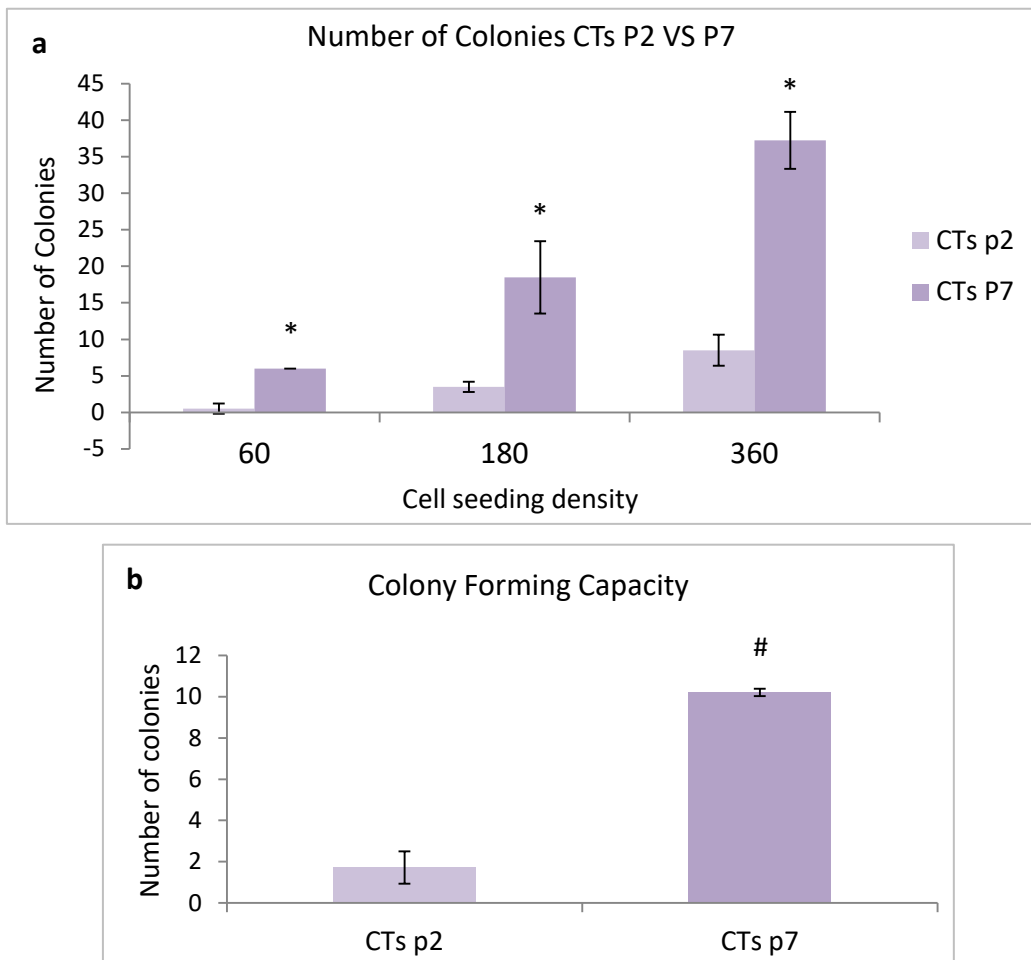


Figure 3.11. Comparison of the colony forming capacity of CTs p2 and p7. (a) the number of colonies by cell seeding density and (b) plot of colony forming capacity. (n=4, error bar: standard deviation, *p<0.002, and #p<0.01, compared to CTs p2)

Subsequently, the gene expression changes from P2 to P7 were checked, as the morphological and growth alterations of CTs (see above) could be associated with a selection of the stem-like colonies. The RT-PCR analysis showed reduction of Ckit, while Sca1 remained unchanged (Figure 3.12a). The rest of the cardiac transcription factors did not change significantly, except for Nkx2.5 that increased at P7 (Figure 3.12a). This could indicate differentiation towards a cardiac lineage, which would match the increase in Myh7 (MHCb) (Figure 3.12b).

In addition the hematopoietic marker CD45 was upregulated at P7 (Figure 3.12b).

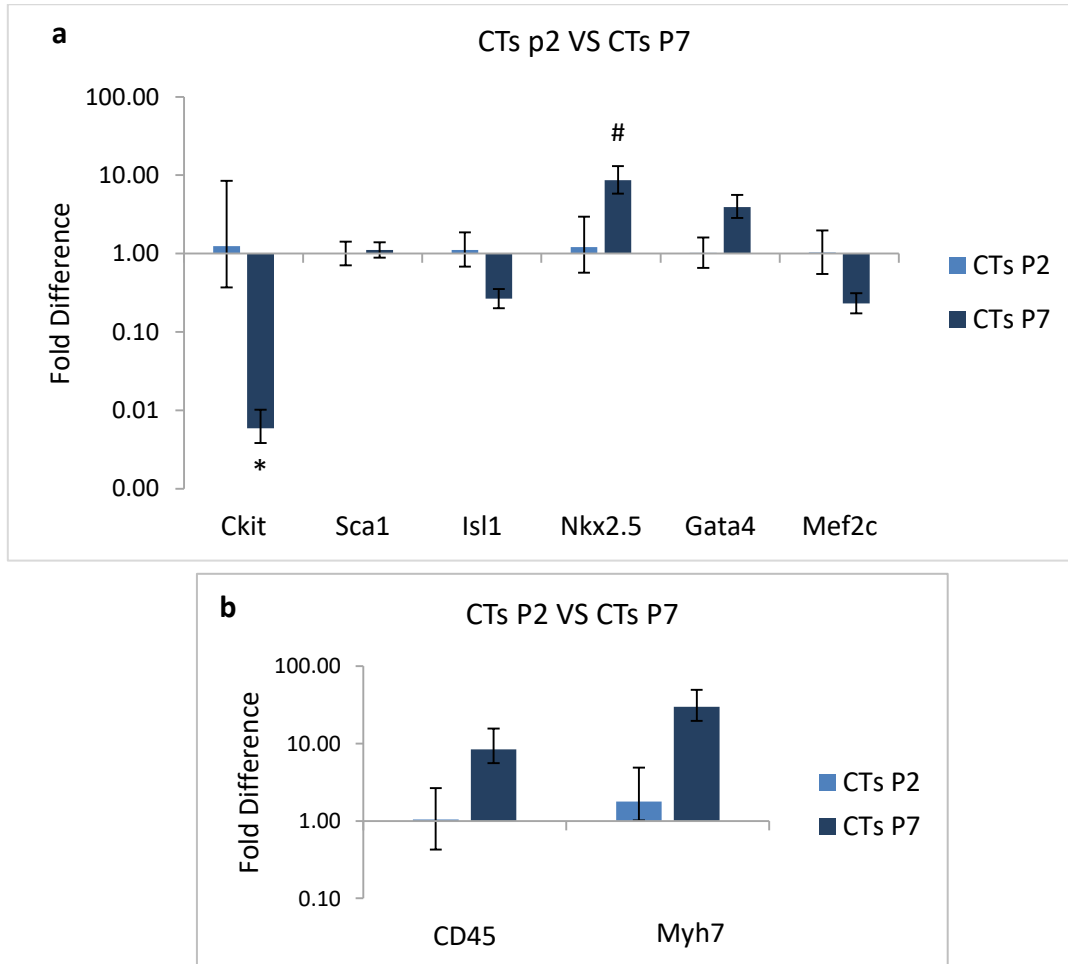


Figure 3.12. Gene expression changes of (a) SC markers and cardiac transcription factors, and (b) hematopoietic and mature cardiac markers, of CTs from P2 to P7. (n= 3, error bars: standard error, *p<0.03, #p<0.05 indicating difference to CTs P2)

3.3.4. CTS CONTAIN A POPULATION OF STRONGLY-ADHERENT CELLS WITH HIGH LEVELS OF STEMNESS MARKERS

While conducting CT isolations a small fraction of cells was observed that were strongly adherent on fibronectin at P0-P2 and would not detach with the normal trypsinisation process. They would require at least 3 x of 4' trypsinisations and would appear consistently in the CT culture. Their distinct morphology, with small, round bubble-like shape at P0 (Figure 3.13a) would make them

distinguishable. They would retain this shape until P2, at which stage the cells would spontaneously alter their morphology and start to proliferate (Figure 3.13b). Looking into their gene expression profile, these cells (“CTs adh”) had high levels of stemness markers, especially Oct4 (Figure 3.14).

In addition to RT-PCR, OCT4 and SOX2 were checked with immunocytochemistry (Figure 3.15), where 100% of cells (from 2 slides imaged; 7 cells) expressed OCT4 (SOX2 was not visible in any of the slides).

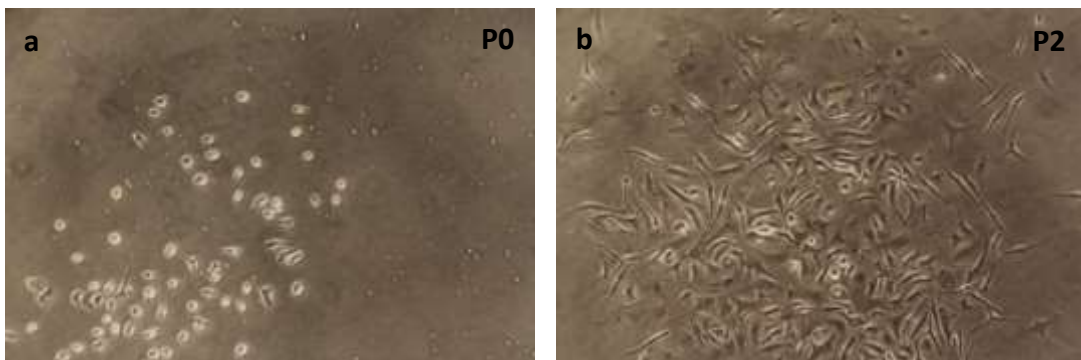


Figure 3.13. Strongly adherent CTs at (1) P0 and (b) P2 after being activated, under phase bright. Original magnification x10 for all images.

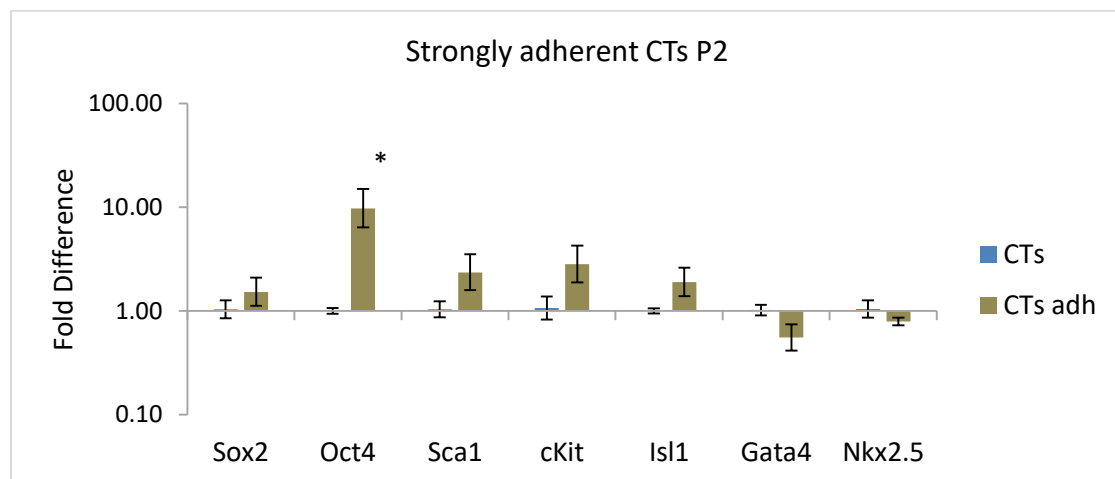


Figure 3.14. Gene expression changes of SC markers and cardiac transcription factors, of CTs and the strongly adherent CTs, both at P2. (n= 3, error bars: standard error, *p=0.01 indicating difference to CTs)

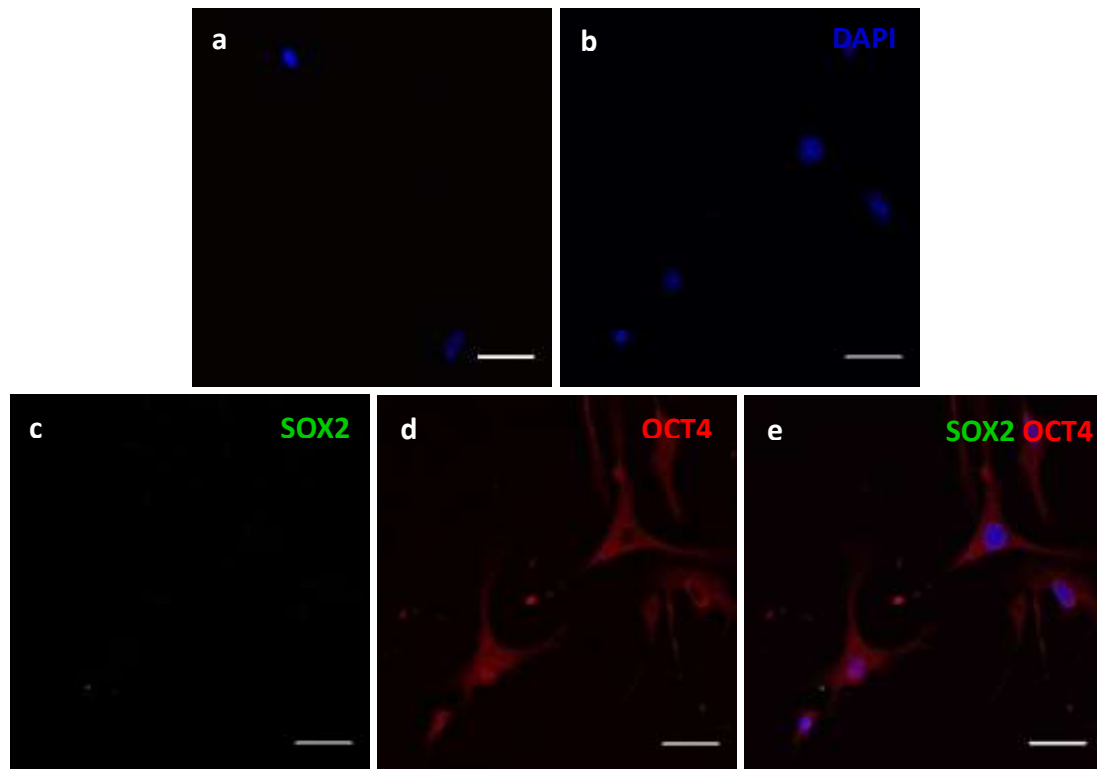


Figure 3.15. Immunocytochemistry on strongly adherent CTs P0, stained with (a) secondary antibodies for negative control, SCA1, (c-e) SOX2/OCT4 double-staining, (b) co-stained with DAPI. Scale bars: 50 μ m.

Despite our interest in expanding and working with this population of CTs alone, the variability in the time that the “strongly-adherent” CTs took to stop being quiescent, and start proliferating, was a major disadvantage of this approach. With an average time span from a few days to 4 weeks, the lack of robustness and reproducibility led us to resume working with the total population of isolated CTs, as previously.

3.3.5. CTS HAVE CONSISTENTLY HIGHER STEMNESS MARKER SCA1 THAN CDCs

After isolating CDCs and CTs, from mouse atria, and expanding them to P2 they were compared on their gene expression, using RT-PCR (Figure 3.16). CTs had significantly higher expression of the fibroblast-mesenchymal marker CD90, and the stemness marker Sca1, and reduced expression of the fibroblast marker

Ddr2. The hematopoietic marker CD45 and the mast cell marker Tryptase, as well as the stemness markers Oct4 and Sox2 were checked and found not expressed (or “undetermined”), as was Myh7 (MHCb).

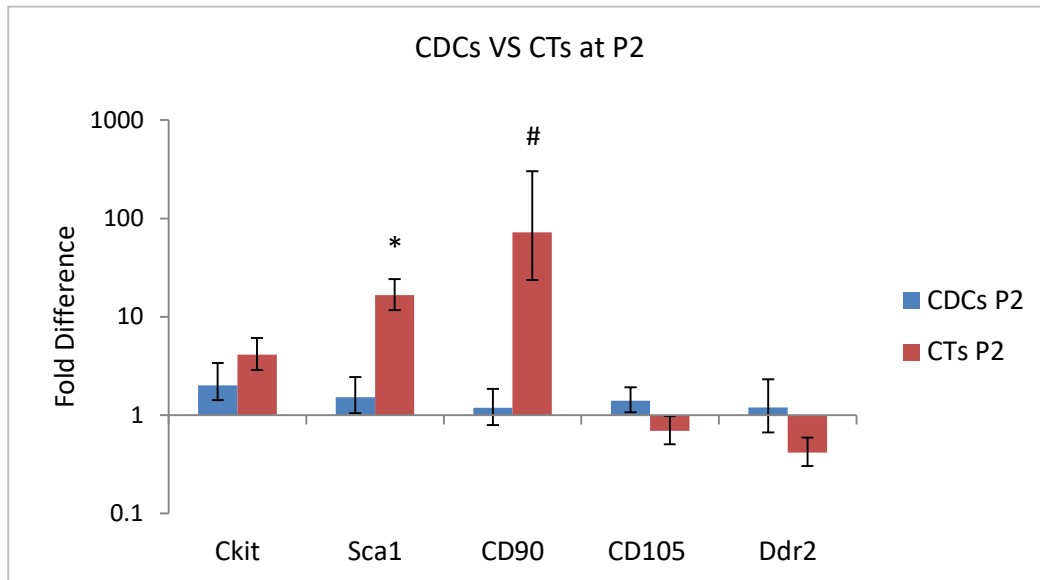


Figure 3.16. Representative graph of gene expression differences of CTs P2 compared to CDCs P2 (n= 5, error bars, standard error, *p=0.0001, #p=0.002, indicating difference to CDCs P2)

While conducting more isolations we decided that in order to avoid the observed variability in our populations we should isolate both CTs and CDCs from the same tissue atria (see Methods 2.2.3) and characterise the cells at P4, as that was the passage that would allow us to obtain enough cells for different comparisons. The comparison of gene expression, with RT-PCR, at P4 (Figure 3.17) showed that CTs had significantly higher Sca1 expression, but lower Ckit, than CDCs. Both mesenchymal markers CD90 and CD105 were increased, the former significantly. Looking into the fibroblast markers, a reduction in Ddr2 gene expression was observed, compared to CDCs, whereas Vimentin, did not change. Also, gene expression levels of Tnnt2, an indicator of spontaneous differentiation, were the same. Finally, Wt1, an epicardial marker, was significantly reduced in CTs compared to CDCs (Figure 3.17).

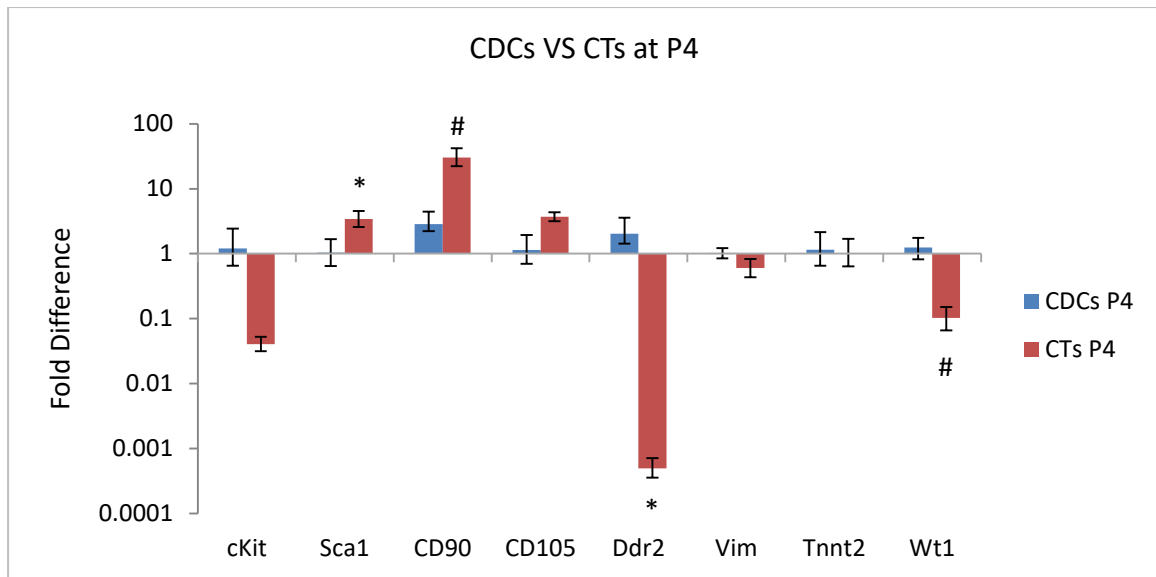


Figure 3.17. Gene expression differences of CTs P4 compared to CDCs P4, from the same mouse atria (n= 3, error bars, standard error, *p=0.05, #p<0.02 indicating difference to CDCs P4)

To confirm the expression of certain markers of interest immunocytochemistry was used on CTs and CDCs at P4 (Figures 3.18 & 3.19, respectively).

CTs expressed SCA1 (94% +/- 9% n = 8 slides; 151/162 cells) and CKIT (96% +/- 7% n = 3 slides; 81/86 cells), while we noticed that a portion of Sca1 cells were CD90⁺ (47% +/- 19% n = 4 slides; 12/22 cells) were Sca1 double-positive, while not all Sca1⁺ cells were CD90⁺ (Figure 3.18j).

CDCs (Figure 3.19) did not express Sca1 (n = 2 slides; 33 cells imaged). CKIT was found very faintly expressed in 96% of the imaged CDCs (96% +/- 9% n = 4 slides; 111/117 cells). 39% of the CDCs expressed CD90 (n=3 slides; +/- 10%).

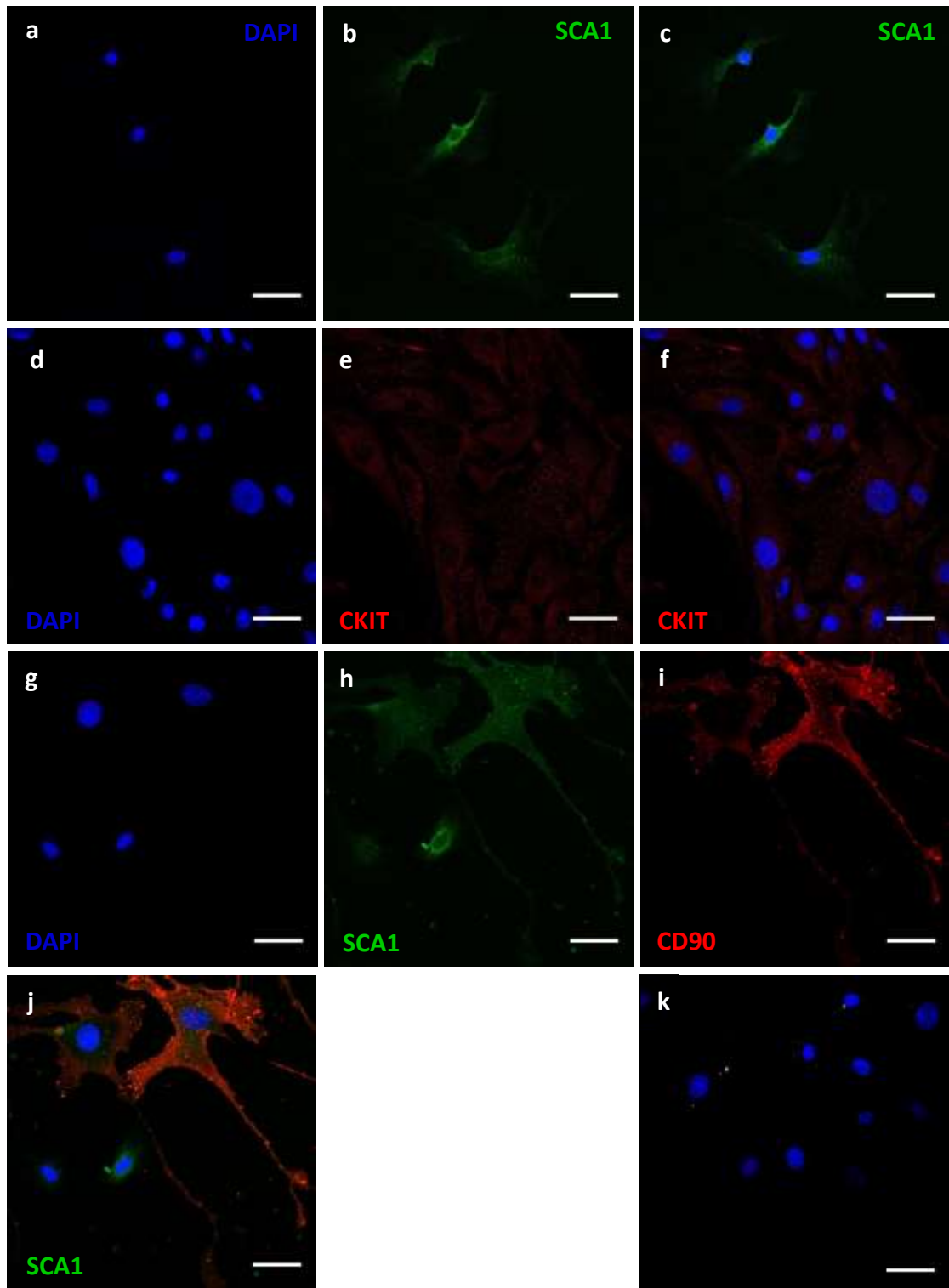


Figure 3.18. Immunocytochemistry on CTs for (a-c) SCA1, (d-f) CKIT, (g-i) CD90 and SCA1 double staining, co-stained with DAPI (a, d, g), (k): secondary antibodies for negative control,. Scale bars: 50 μm.

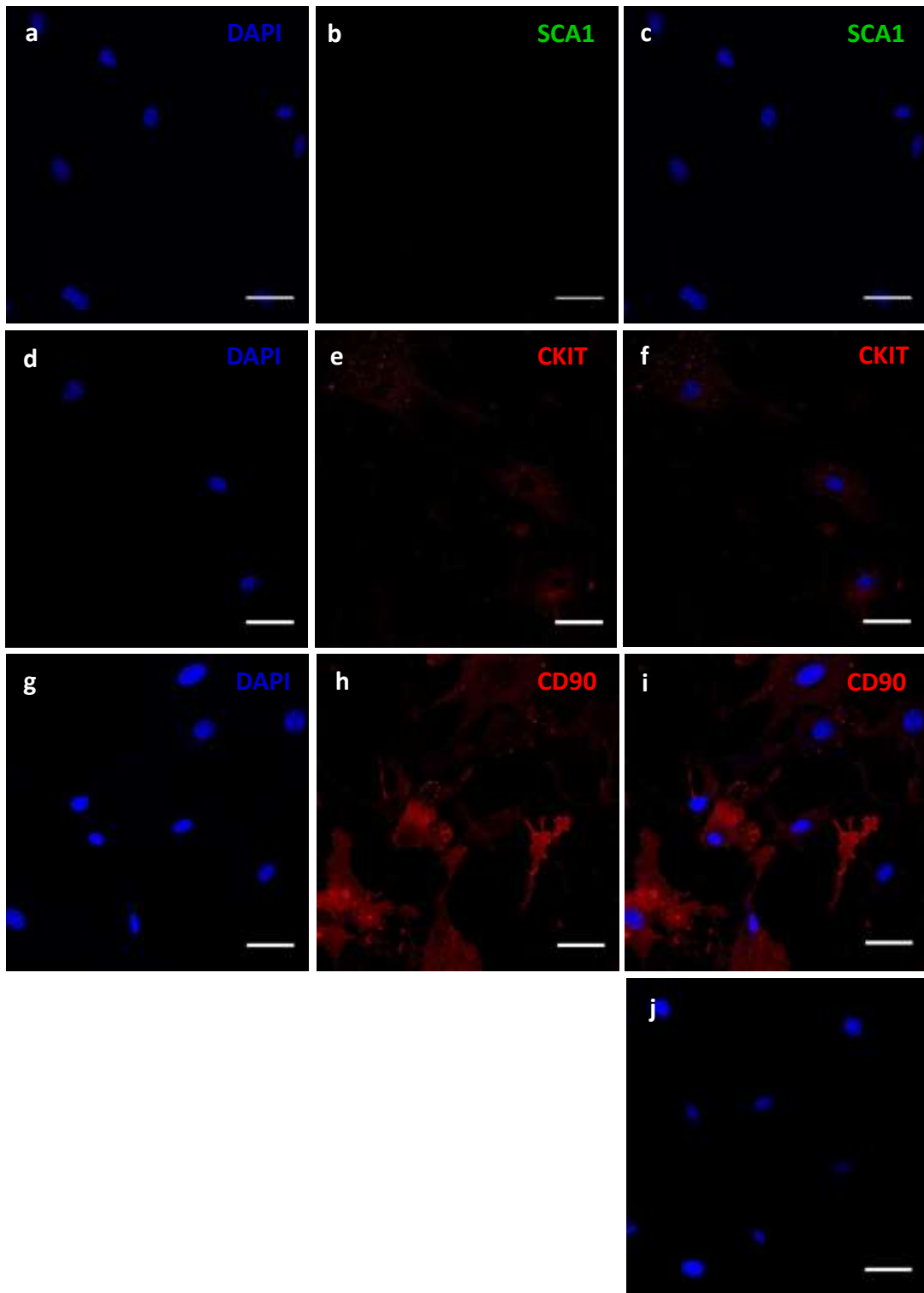


Figure 3.19. Immunocytochemistry on CDCs, for (a-c) SCA1, (d-f) CKIT, (g-i) CD90, co-stained with DAPI (a, d, g), (j): secondary antibodies for negative control. Scale bars: 50 μm .

3.3.6. CTS & CDCS SHOW SIMILAR LEVELS OF CARDIAC DEVELOPMENTAL MARKERS

To assess the stage of maturity of the isolated CPCs along the cardiac lineage, gene expression at P4 was compared with a mESC cell line at day 4 and 7 of differentiation via embryoid body (EB) formation (see Methods 2.10.1.), as a positive control. The early-onset cardiac genes that are involved in the development of the embryonic mouse heart (Introduction Table 1.2), could allow us to characterise and position the CPC population at a developmental stage.

Agreeing with the genetic changes during differentiation, the stemness genes (Oct4, Ckit and Tert) reduced their expression as mESCs progressed from day 4 (EBs d4) to day 7 (EBs d7) of differentiation, while the early-onset cardiac markers (Nkx2.5, Gata4, Mef2c, Isl1) increased (Figure 3.20). Furthermore, the CTs and CDCs did not differ substantially in the gene expression pattern of the cardiac developmental markers at P4 (Figure 3.20). The stemness markers were reduced in the CPC populations, which had more comparable cardiac lineage gene expression levels to mESCs at d7 of differentiation.

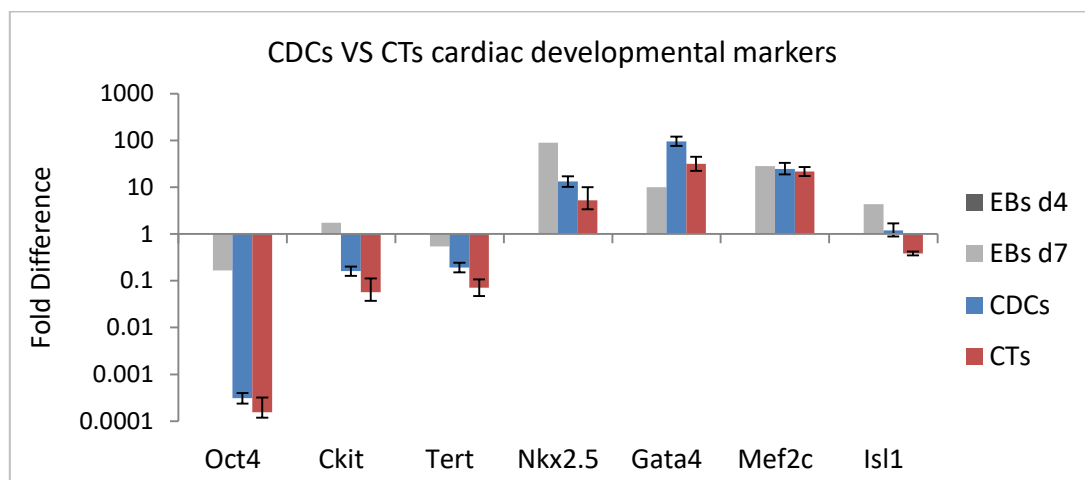


Figure 3.20. Gene expression levels of stemness and cardiac developmental markers of CDCs and CTs, compared to mESCs at day 4 and day 7 of differentiation to CMs. (n=3 for the CPC population, normalised to EBs d4, no significant difference of CTs to CDCs).

3.3.7. CTS CONTAIN A POPULATION OF TELOCYTES

As described in 3.2.3. telocytes are mesenchymal cells with distinct morphology from that of any other cell type. Observing our primary isolation cultures of CTs we were baffled by some cells with elongated branches, different to the common fibroblast- or CM-morphology (Figure 3.21).

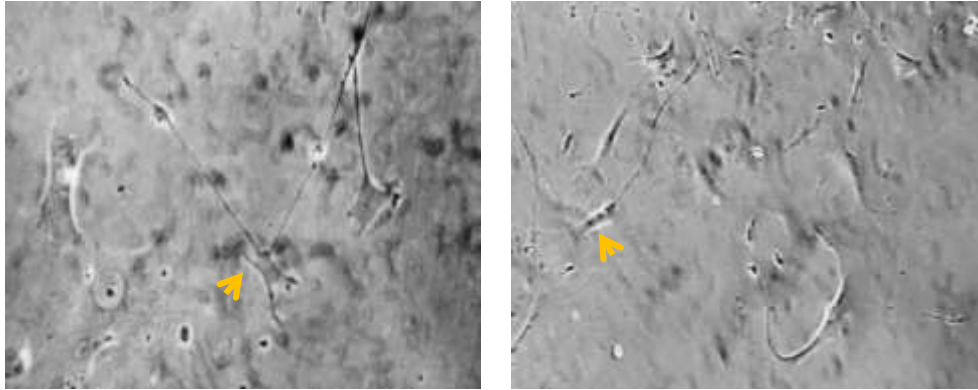


Figure 3.21. (a) CTs P0 and (b) CTs P2. Yellow arrows indicating cells with elongated branches

After doing a literature search and coming across the telocyte references in a couple of papers, we decided to use Immunocytochemistry to identify whether we had telocyte populations in our CT cultures (see 3.2.3). Using the combination of Ckit/CD34 antibody staining (see Methods 2.7), we could identify telocytes in non-confluent cultures (Figure 3.22). In addition we stained with MitoTracker® Red CMXRos and we could observe mitochondria located at the podoms of the telocytes (see Methods 2.7.4) (Figure 3.23).

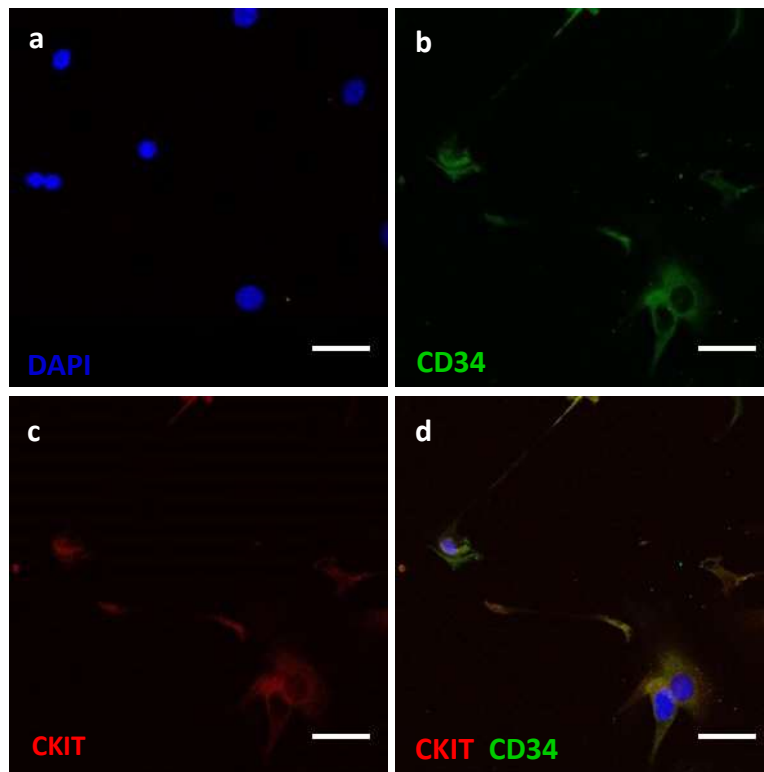


Figure 3.22. Immunocytochemistry of telocytes, double-stained for CKIT and CD34, (a) secondary antibodies for negative control, (b) CD34, (c) CKIT, (d) CKIT and CD34 double staining. Scale bars: 50 μ m.

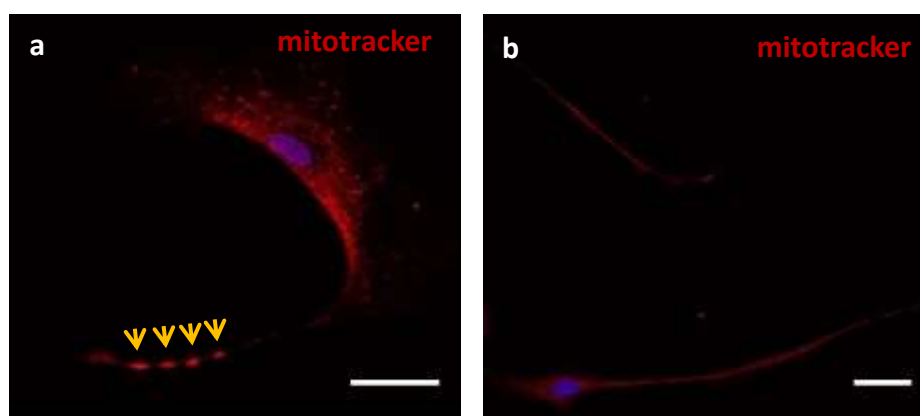


Figure 3.23. (a), (b) Immunocytochemistry of telocytes, stained with MitoTracker® Red CMXRos for mitochondrial labelling. Yellow arrows at (a) marking the podoms with mitochondrial clusters. Scale bars: 50 μ m.

3.4. DISCUSSION

3.4.1. ATTEMPTS TO OPTIMISE THE EXPLANTING PROTOCOL

This study compares CDCs and CTs isolated from the atria of adult mice. As described in 3.2.5, previous findings from our group have demonstrated an unpleasant variability in the protocol outputs, including lack of robustness in the cell isolation, variable cell yield, and cell characteristics. Davis DR. *et al.*²⁸⁸ used this method to explant tissue from rat, mouse, pig and human heart, and stated that the EDCs varied in their time of growth and proliferation, as seen by Smith RR. *et al.*¹²² Also, the cell yield would be affected by cell culture media or differences in animal strains²⁸⁹.

I, therefore, decided to attempt to optimise the explanting protocol. To my knowledge there has been one published modification, focusing on the cardiosphere step, whereby after obtaining the CDCs, they were processed again via a cardiosphere step, to obtain what was called "secondary cardiospheres"²⁹⁰. This was tested in cells from mice and later from human tissue²⁹¹, and gave rise to cells with higher differentiation potential, better engraftment and paracrine activity.

EDCs were subsequently checked, given that no study to this day has compared the EDC harvests, and that studies have combined 2¹²³- 5²⁸⁹ harvests in order to obtain more cells, for CDC formation. The different EDC harvests that were analysed were variable, with reduction in stemness markers with later harvest or higher passage (Figure 3.2). Markers like CKIT, CD45, SCA1 were expressed, being strongly positive for CD90 (Figure 3.3), similar to those observed by Dr. F. Perbellini from our lab (thesis - unpublished data). Dr. Perbellini saw CKIT, CD90, CD45, and SCA1 expression, as well as Chan H *et al.*¹²³. These are similar to other studies that found CKIT⁺/CD90⁺/CD34⁺/CD45⁺ EDCs^{123,288}. Any variations could be explained by the fact that we used H1 P0 EDCs from mice, whereas other studies were done in rats, combining harvests. Finally, a higher Ckit expression was achieved, by increasing the length of the cardiosphere step (Figure 3.4). This, as Smith RR *et al.*¹²² suggested, maybe due to the hypoxic core of the cardiosphere. Unfortunately this reduced cell viability, which agrees with what Bartosh *et al.* who made hanging drop spheres from human MSCs for more

than 3 days and found the cells were dying because of nutrient deprivation and medium acidity²⁹².

3.4.2. DEVELOPING A DIGESTION-BASED PROTOCOL FOR CPC ISOLATION

As described in the Introduction, several methods are used to isolate CPCs (Figure 1.3). Different groups isolate them with enzymatic digestion, followed by clonogenic selection or magnetic sorting, based on certain markers or use the explanting protocol. The digestion method involves Collagenase^{293,271,101,220} (often type II²⁹³) in all the studies, but the type or duration of isolation is not always clear. Therefore different combinations of digestion solutions were tested, aiming to obtain the highest amount of viable cells after 1 week (Table 3.4). A combination of 0,1% trypsin + 0,1% Collagenase II mix for 1 hour was eventually selected, conditions lethal to the sensitive CMs¹⁰¹. The idea of combining Collagenase and trypsin originated from the Gharaibeh *et al*²⁸⁷. study on slow-adhering Skeletal muscle CPCs. As shown in Figure 3.5., we identified cells with that morphology, but the protocol was sufficiently robust to use for cell therapy purposes.

Cardiospheres were attempted to be formed from the CTs, and the resulting CT_CDCs had increase Ckit expression, although Sca1 and CD105 were significantly reduced, as well as CD90 (Figure 3.6). Interestingly, not all CTs could form cardiospheres. The sphere assay was developed to increase stemness markers, but it is now known that it is not sufficient to establish it²⁹⁴. This assay has not been used in other CPCs, apart from EDCs. Bartosh *et. al.*, made spheres from MSCs that had advanced immunomodulatory potential, using the hanging drop approach²⁹². In a subsequent paper, they state that approximately 30–50% of the initial amount of cells can be recovered from the spheres, and that cells have 80-90% viability²⁹⁵. This lack of robustness is similar to what we observed in our CT hanging drop spheres.

3.4.3. CTS SHOW INCREASED PROLIFERATION AND HOMOGENEITY, WHILE PASSAGE INCREASES

The digestion-based isolation protocol yielded more cells and in shorter time, than the explanting method (see Table 3.4). The latter depends on the migratory

ability of cells out of the explants and it is very variable. As described in 3.2.5., studies from our group have shown that certain explants did not have any EDC outgrowth or the number of EDCs varied a lot among the pieces of tissue or the samples²⁷⁹, (Dr. Filippo Perbellini thesis, unpublished data).

Studies on MSCs and BM stromal cells have discussed the importance of cell size, suggesting that smaller cells have greater multipotentiality and differentiation capacity than larger cells^{296,297}. The CTs became more proliferative, smaller in size and homogenous, as they progressed from P2-P7 (Figure 3.9, 3.10). Interestingly, colony-forming capacity reduces with passage in the MSCs studies, which is not what we observed, probably because p7 is not high-enough a passage to observe this in CTs. A study in UCB MSCs described very high proliferation at P7, but the cell morphology became gradually more irregular and bigger²⁹⁸. To our knowledge there have not been studies of passaging and morphology done on CPCs, Dr. Perbellini though, did notice increased colony forming capacity in CDCs with higher passage (thesis – unpublished data), similar to what we see in CTs here (Figure 3.11).

The CTs at P7, had decreased expression of the stemness marker Ckit, while Sca1 remained at the same levels (Figure 3.12). At the same time the hematopoietic CD45, as well as Nkx2.5, Gata4 and Myh7 were increased. The CTs are a mixed population, and it seems that with time in culture they begin to differentiate, interestingly, without losing their proliferative capacity.

3.4.4. CTS CONTAIN A POPULATION OF STRONGLY-ADHERENT CELLS WITH HIGH LEVELS OF STEMNESS MARKERS

In CT primary cultures we consistently noticed cells that would strongly adhere to the bottom on the flasks, and had distinct morphology that would not change (Figure 3.13). These cells increased expression of stemness markers, especially Oct4 (Figure 3.14), which was later verified with immunocytochemistry (Figure 3.14). They would remain quiescent over variable lengths of time and would then be activated to proliferate at some point at P2 (Figure 3.13 b), the inconsistent nature of the method made it unappealing for cell therapy. We later realised that the characteristics of these cells resemble the Oct4⁺/ Sca1⁺ Very Small Embryonic Like (VSEL) Stem Cells, that have been isolated from BM, blood,

heart and brain tissues²⁶⁵. What drew our attention was the fact that these cells do not proliferate *in vitro* if cultured alone, and they are quiescent²⁶⁶. Even though there is not enough evidence to call these strongly-adherent CTs "VSELs", it would explain what we observed. Finally, the expression pattern of Oct4, at Figure 3.14, shows that it is not only localised in the nucleus. This could be explained by the fact that Oct4 can be found in two isoforms, with different localisation patterns (nucleus and cytoplasm) representing different levels of activity²⁹⁹.

3.3.5. CTS HAVE CONSISTENTLY HIGHER STEMNESS MARKER SCA1 THAN CDCs

Using the digestion protocol that was developed CTs were isolated, and compared to CDCs at P2 (populations isolated from different atria, different mice), and later at P4 using the same atria for both isolations.

RT-PCR showed at both P2 (Figure 3.16) and P4 (Figure 3.17), that CTs had consistently significantly higher expression of Sca1 and CD90, than CDCs. Ddr2 was also found reduced in both cases, whereas CD105 levels were comparable. Endogenous Ckit cells, side population cells, colony-forming fibroblasts, and CDCs express Sca1, as well as Ckitt²⁹³. Loss of Sca1 expression from Ckit+ CPCs has shown to lead to decreased growth rate and increased differentiation marker expression¹⁰⁴, rendering this marker a very attractive one for cell therapy. The higher CD90 expression in CTs could indicate a more fibroblast nature (see 3.2.2) than CDCs, even though this is contradicted by the reduction in Ddr2 that we observed. CD90 has been previously been shown to be expressed in CDCs^{122,300124}.

The marker expression of SCA1, CKIT, CD90 was confirmed with immunocytochemistry in CTs (3.18) and CDCs (3.19), interestingly the former had a fraction of Sca1⁺ cells that did not express CD90 (Figure 3.18j), whereas CDCs did not express it (Figure 3.17c). Neither Oh *et al.*¹⁰¹ who introduced the Sca1⁺ murine CPCs, nor Smits A. *et al.*²²⁰. who isolated Sca1⁺ CPCs from human atria investigated CD90 expression. Both found Ckit expression in their Sca1⁺ cell populations. A recent paper from 2014 in human CSCs, shows that CD90 distinguishes two populations of CSCs with the positive fraction having better

differentiation potential to CMs²⁴⁵ (for differentiation comparison see Chapter 4). Finally, the higher expression of Wt1 in CDCs (Figure 3.17) suggests an epicardial origin of these cells. It could be that epicardial cells are predominantly migrating out of the explants and retain the Wt1 expression at the CDC stage, whereas they only form a small part of the CT cell digestion.

3.3.6. CTS AND CDCS SHOW SIMILAR LEVELS OF CARDIAC DEVELOPMENTAL MARKERS

The array of cardiac transcription factors that are present during cardiac development (see Introduction 1.3) could help us characterise the CPC population of this study. The RT-PCR analysis (Figure 3.20) showed that CTs and CDs had comparable level of gene expression of these markers, which resembled that of mESCs at day 7 of differentiation. The fact that CDCs express cardiac transcription factors, namely Gata-4 and Nkx2.5 has been shown by our lab previously¹²⁶. Also Smits A *et al.*²²⁰ showed that human Sca1⁺ atrial CPCs express Isl1, Ckit, Nkx2.5, Mef2c and Gata-4. The expression of cardiogenic markers by CPC populations (GATA4, NKX2.5, TBX5, and MEF2c), has been also review by Mercola M *et al.*¹⁴⁷. All these together indicate that CTs is a cardiac progenitor population comparable to CDCs, belonging to the cardiac lineage.

The fact that they express fibroblast markers is evident, and described in the literature. We are not currently certain to what extent they are fibroblasts, or could be called so, but even so a very interesting study by the group of Rosenthal's N. group³⁰¹, suggested that we should revisit the notion of cardiac fibroblasts. Focusing on a CD90⁺, Ddr2⁺, periostin⁺ "fibroblast" population from the mouse heart, they noticed that they also had "an unexpected enrichment in cardiogenic transcription factors" and suggested that they are useful for cardiac development and regeneration.

3.3.7. CTS CONTAIN A POPULATION OF TELOCYTES

Telocytes have been identified in cardiac tissue slices as supportive interstitial cardiac cells, with an important role in cardiac regeneration (see 3.2.3). In the heart, TCs have been observed in the myocardium, epicardium, endocardium and valves. Cells with the distinct telocyte morphology were found in the CT cultures

(Figure 3.21). Telocytes have been observed *in vitro* in CM primary cultures³⁰² and are mainly characterised by CD34/ CKIT double-expression, as was observed (Figure 3.22). Additionally we demonstrated the existence of mitochondria in telocyte podoms, as described previously²⁶⁰ (Figure 3.23). The existence of telocytes has not been mentioned in any other study describing other CPCs. CD34 has been observed as a marker in various studies, including the CDCs, whereas it is depleted in Ckit+/Lin- isolations. Oh *et al.* mentioned that the murine SCA1+/ CKIT+ CPCs expressed CD34¹⁰¹, whereas the human atrial Sca1+ did not²²⁰. It is possible that some of the CD34 cells in other isolation protocols are indeed telocytes.

In the world of cardiac regeneration the single-marker CPC isolation seems ideal, but it is time-consuming, with low cell yield and not consistently robust. In addition, approaches using mixed cell populations or combinations of cells have proven to allow for better engraftment and cell survival in the infarct region, which is important for stem cell therapy. This study had the aim to develop a digestion-based protocol to identify endogenous CPCs from the mouse atria, arising via a method independent of marker-selection. Both CTs and CDCs were of mesenchymal SC-like phenotype, and had comparable expression of cardiac transcription factors, while CDCs had higher fibroblast marker Ddr2 and the epicardial Wt1. The digestion method yielded a mixed type cell population that was comprised of OCT4+ quiescent cells and telocytes. With variations in the animal models, tissue origin, isolation methods, culture conditions, and even the criteria of analysing the isolated cells, we have not yet found the ideal CSC. In addition, different cell types with overlapping marker profile are coming to light, but are not consistently investigated in different isolation studies, making this quest even more difficult.

4. CARDIAC PROGENITOR DIFFERENTIATION

4.1. INTRODUCTION

4.2.1. CARDIAC DIFFERENTIATION *IN VITRO*

One of the main characteristics of pluripotent SCs is the ability for efficient differentiation to a plethora of cell types, after treatment with cytokines, growth factors or different chemicals. In the case of multipotent SCs, the differentiation is mainly confined to the lineage of origin. An ideal CPC type for cell therapy should be capable of robust differentiation to CMs, in the hope of replenishing the massive loss of CMs following MI. Therefore assessing the differentiation potential of CPC candidates *in vitro*, is a necessary prerequisite step.

Various methods and strategies have been applied, aiming to develop the optimal protocol for directing *in vitro* cardiac differentiation of stem cells. The most efficient ones to this day, either involve pluripotent SCs or co-culture, mainly with neonatal/ primary CMs (co-culture with visceral endoderm cells has also been successful³⁰³). **Co-culture** systems have led to trans-/ differentiation of adipose-derived SCs³⁰⁴, ECs³⁰⁵, CPCs^{306,307} into CMs. **Pluripotent stem cells** (ESCs and iPSCs) have great differentiation potential. Directed cardiac differentiation of human pluripotent SCs, yielding a population of pure CMs with >80% efficiency, can be achieved by altering between activation and inhibition of the Wnt signalling pathway^{308,309}. Which, in crosstalk with the Hippo and Notch pathways, is known to be major players in cardiogenesis^{310,311}. In addition, several approaches depend on growth factors (see Review³¹²) (see Table 1).

In vitro differentiation of adult **endogenous CPCs** is very challenging, due to their limited plasticity. Despite a variety of differentiation studies, the ability of adult progenitors for differentiation, is still under debate^{313,314}. Different approaches, utilising various differentiation factors have been used on both pluripotent SCs and CPCs, with the main ones being; DMSO, 5-Azacytidine, Ascorbic Acid, members of the TGF- β superfamily, oxytocin, dexamethasone and retinoic acid (see Table 4.1 & 4.2).

Cytokines/growth factors/chemical compounds	DIFFERENTIATION to CMs	
	Pluripotent SCs (ESCs)	Adult Progenitors (CPCs, MSCs)
TGF-β1 family (TGF-β1, BMP-2, -4)	Behfar <i>et al.</i> ³¹⁵ , Yuasa <i>et al.</i> ³¹⁶ , Slager <i>et al.</i> ³¹⁷ , Lian <i>et al.</i> ³⁰⁹ , Cagavi <i>et al.</i> ³¹⁸ , La Flamme <i>et al.</i> ³¹⁹ , Menard <i>et al.</i> ³²⁰ , Monzen <i>et al.</i> ³²¹ , Sachinidis <i>et al.</i> ³²²	Smits <i>et al.</i> ³²³ , Goumans <i>et al.</i> ³²⁴ , Ye <i>et al.</i> ²⁷³ , Choi <i>et al.</i> ³²⁵ .
Hepatocyte Growth Factor (HGF)	Roggia <i>et al.</i> ³²⁶	
Oxytocin	Paquin <i>et al.</i> ³²⁷ , Fathi <i>et al.</i> ³²⁸ .	Smith <i>et al.</i> ²⁹³ ., Matsuura <i>et al.</i> ³²⁹ , Oyoma <i>et al.</i> ¹⁰⁸ .
5-Azacytidine	Choi <i>et al.</i> ³⁰⁴ ., Yoon <i>et al.</i> ³³⁰ ,	Fukuda <i>et al.</i> ³³¹ , Rangappa <i>et al.</i> ³³² , Oh <i>et al.</i> ¹⁰¹ , Qian <i>et al.</i> ³³³ , Xu <i>et al.</i> ³³⁴ , Goumans <i>et al.</i> ³²⁴ , Naeem <i>et al.</i> ³³⁵
Ascorbic acid	Passier <i>et al.</i> ³³⁶ , Takahashi <i>et al.</i> ³³⁷ , Martinez <i>et al.</i> ³³⁸	
Retinoic acid	Slager <i>et al.</i> ³¹⁷ , Wobus <i>et al.</i> ³³⁹ , Zandstra <i>et al.</i> ³⁴⁰ ., Drab <i>et al.</i> ³⁴¹ . Lengerke <i>et al.</i> ³⁴² .	
DMSO	McBurney <i>et al.</i> ³⁴³ , Ventura <i>et al.</i> ³⁴⁴ , Skerjanc <i>et al.</i> ³⁴⁵ , Jasmin <i>et al.</i> ³⁴⁶ ,	
Dexamethasone		Bearzi <i>et al.</i> ²⁷¹ , Beltrami <i>et al.</i> ⁸⁷ , Linke <i>et al.</i> ³⁴⁷ , Smith <i>et al.</i> ²⁹³ , van Berlo ⁹⁷

Table 4.1. Most common differentiation approaches, used on different mESC lines and CPC cell types

Differentiation approaches	main studies	cell type
TGF-β1 family	323	human atria Sca1 ⁺ ; clonally isolated & magnetic-sorting
	324	human fetal & adult atrial biopsies, Sca1 ⁺ magnetic-sorting
	273	whole mouse heart Sca1 ⁺ / CD45 ⁻ magnetic-sorting CDCs (Isl1 ⁺)
Oxytocin	293	3-6 mouse & rat whole hearts per sample, Ckit ⁺ /CD45 ⁻ /Tryp ⁻ magnetic-sorting
	329	mouse whole heart Sca1 ⁺ magnetic-sorting
	108	rat, mouse ventricles side population (SP) cells
5-Azacytidine	331	mouse BM stroma MSCs
	332	human adipose MSCs
	101	mouse whole heart Sca1 ⁺ magnetic-sorting
	333	human umbilical cord MSCs
	334	human BM-MSCs
	324	human fetal & adult atrial biopsies, Sca1 ⁺ magnetic-sorting
	335	rat BM-MSCs
Dexamethasone	271	human atrial or ventricular Ckit ⁺ -sorted
	87	rats Ckit ⁺ / Lin ⁻ magnetic-sorting
	347	dog left ventricle Ckit ⁺ / Lin ⁻ & Sca1 ⁺ / Lin ⁻ magnetic-sorting
	293	mouse whole heart Sca1 ⁺ magnetic-sorting
	97	mouse whole heart Ckit ⁺

Table 4.2. Different CPC cell types differentiated to cardiac cells/ CMs

More specifically, **5-azacytidine** is a demethylating agent that was introduced as a treatment for myelodysplastic syndrome, via epigenetic gene silencing³⁴⁸. It allows for the exposure of genes that are normally silenced, due to hypermethylation, by inhibiting of DNA methyltransferase^{349,350}. Several *in vitro* studies suggested that 5-Aza can induce cardiac differentiation, on different MSC types, such as human umbilical cord-derived MSCs³³³, adult human BM-derived MSCs^{334, 351}. Other studies have demonstrated the inefficiency of 5-Aza as a cardiac differentiation agent, showing transdifferentiation to skeletal muscle cells, rather than cardiac cells,³⁵² as well as unsuccessful differentiation of adipose-derived stem cells (ASCs)³⁵³ and adult mouse Sca1+ CPCs³²⁹.

Ascorbic Acid (A.A. / Vitamin C), is an antioxidant compound. It has been shown to increase the expression of cardiac genes and their proteins and to lead to beating CMs in mouse ES cells, without the EB step³³⁷. Cao *et al.* in 2012 demonstrated that A.A. was able to induce cardiac differentiation and maturation in several human and mouse iPSC lines³⁵⁴. In addition, treatment of BM-derived MSCs with A.A. triggered their proliferation and differentiation into osteoblasts and adipocytes³⁵⁵. Even though its antioxidant activity has been credited for its cardiogenic differentiation effect, studies had questioned the mechanism since no other antioxidants could cause the same results³³⁷. In 2006 Sato H. *et al.* suggested the involvement of collagen in the process³⁵⁶. Indeed a study in 2012 on both human and mouse iPSCs suggested that A.A. triggered collagen synthesis, which in turn stimulated CPC-specific proliferation via the MEK-ERK1/2 pathway and cardiac differentiation³⁵⁴.

Another key player in cardiac differentiation, as will be explained in detail below, is transforming growth factor-beta 1 (**TGF- β 1**). TGF- β 1 has been shown to differentiate Ckit⁺ selected BM-derived MNCs into cardiac-like cells³⁵⁷. In a study by Lim *et al* in 2007, differentiation of a mESC carcinoma line to beating CMs, upregulated TGF- β 1 gene expression. This potentially drives cardiac differentiation by inducing the cardiac transcription factor Nkx2.5³⁵⁸. Goumans *et al.* used TGF- β 1 to induce differentiation of adult atrial Sca1⁺ CPCs, in combination with 5-Aza and A.A.^{324,220}. The mechanism of action involves phosphorylation of Smad2, that leads to the expression of cardiac-specific proteins³²⁴.

Dexamethasone is a glucocorticoid compound with immunomodulatory properties. Initial studies showed that it stimulates differentiation and maturation of osteogenic progenitor cells³⁵⁹. The osteogenic effect of dexamethasone has been since then demonstrated on MSCs^{360,361,362}. Interestingly, since then various groups have used it as the main agent of differentiation of adult selected Ckit+ CPCs to CMs^{347, 271,272,293}.

4.2.2. TGF- β & THE HEART

The TGF- β superfamily of growth factors comprises over 30 members, including TGF- β (TGF- β 1-3), bone morphogenetic proteins (BMP), Activins, and Nodal³⁶³. These cytokines regulate numerous processes, such as embryonic development, cell proliferation, differentiation and immune responses^{364,365}. TGF- β activates various intracellular signalling cascades³⁶⁶ and has been linked to several human pathological conditions, such as carcinogenesis and fibrosis^{367, 368}. More specifically in fibrosis, TGF- β has been shown to stimulate the transition of fibroblasts to myofibroblasts (see 3.2.2) A crosstalk between TGF- β signalling and the canonical Wnt pathway has been suggested to be involved in cardiac fibrosis³⁶⁹. Most studies have been conducted *in vivo* on rodents. For example, a study on mice in 2010 showed TGF- β signaling causes increased proliferation of non-myocytes and expression of the “pro-fibroblast differentiation molecule” periostin, leading to adverse fibrosis in a cardiac hypertrophy model³⁷⁰. The source of the elevated TGF- β in these hearts was not defined.

The crucial role of TGF- β s in cardiac development has been highlighted by a study of TGF- β 1 and TGF- β 2 gene knockout in mice, leading to cardiac defects³⁷¹. Of the TGF- β family, distinct TGF- β isoforms have different effects on cell lineage specification. For example, TGF- β 2 has a two-pronged effect on cardiac differentiation, with early expression being a positive cue and later expression being inhibitory³⁷². In the case of TGF- β 1, *in vitro* CM differentiation studies have shown that it promotes cardiac differentiation by increasing expression of cardiac markers and contractile proteins, on human adult cardiac progenitors³⁷³, mouse skeletal muscle-derived progenitors³⁷⁴, and mouse BM cells³⁵⁷. Finally, it is suggested that the coculture-induced CM differentiation phenomenon, might be mediated by TGF- β secreted by the neonatal CMs³⁷⁵.

4.2.3. PEROXISOME PROLIFERATOR-ACTIVATED RECEPTORS (PPARS)

In addition to signalling pathways that have a direct effect on differentiations, others can indirectly trigger a shift in the cell phenotype. Peroxisome Proliferator-Activated Receptors (PPARs) comprise a group of nuclear receptor proteins that are part of the subfamily 1 of the nuclear hormone receptor superfamily³⁷⁶. They function as ligand-activated transcription factors, so PPAR activity requires heterodimerization with the Retinoid X Receptor (RXR)³⁷⁷. This PPAR-RXR heterodimer can form in the absence of a ligand, however when activated by one, the dimer binds to specific DNA regions in the promoter of target genes, called peroxisome proliferator response elements (PPREs) and regulates their transcription³⁷⁸ (Figure 4.2). This activation of the PPAR-RXR heterodimer can occur either via an RXR- or a PPAR-ligand and it results in release by co-repressor proteins, and binding of co-activators³⁷⁹. **FAs** (including oleic, palmitic, linoleic, and arachidonic acid) are natural ligands for Ppar α ³⁸⁰. In addition, synthetic ligands have been chemically composed, such as; the ureidofibrate, GW2331³⁸¹, and GW9578³⁸², a ureidobutyric acid, and used in metabolic studies as Ppar α agonists. Other natural compounds, like the flavonoid icariin can activate P38 MAPK³⁸³, which in turn increases the transcription of Pgc1 α , which then stimulates the PPAR α pathway²²¹.

The **roles of PPARs** span far beyond the stimulation of peroxisome proliferation, as initially shown³⁸⁴, being the genetic regulators of different mammalian metabolic pathways and subsequently numerous diseases³⁸⁵. Of the 3 receptor isoforms, alpha, gamma, and delta, Ppar α and PPAR δ are highly expressed in the heart³⁸⁶. Ppar α functions in the **liver** as a master regulator of hepatic lipid metabolism and has been extensively researched (see Review³⁸⁷).

Its most prominent role is that of regulating FA oxidation and ketogenesis, as an adaptative response to fasting³⁸⁸. In a study in mice, conducted by Clarke K *et al.* exposure to hypoxia led to reduced Ppar α levels, which functioned as an adaptative mechanism, required to maintain contractile function¹⁸⁹. Studies have shown that Ppar α target genes are involved in fatty acid metabolism³⁸⁹, and glucose metabolism³⁹⁰. Ding L *et al.* in 2007 showed that Ppar α levels were upregulated during differentiation of ESCs to beating CMs and that inhibition of Ppar α prevented the differentiation³⁹¹.

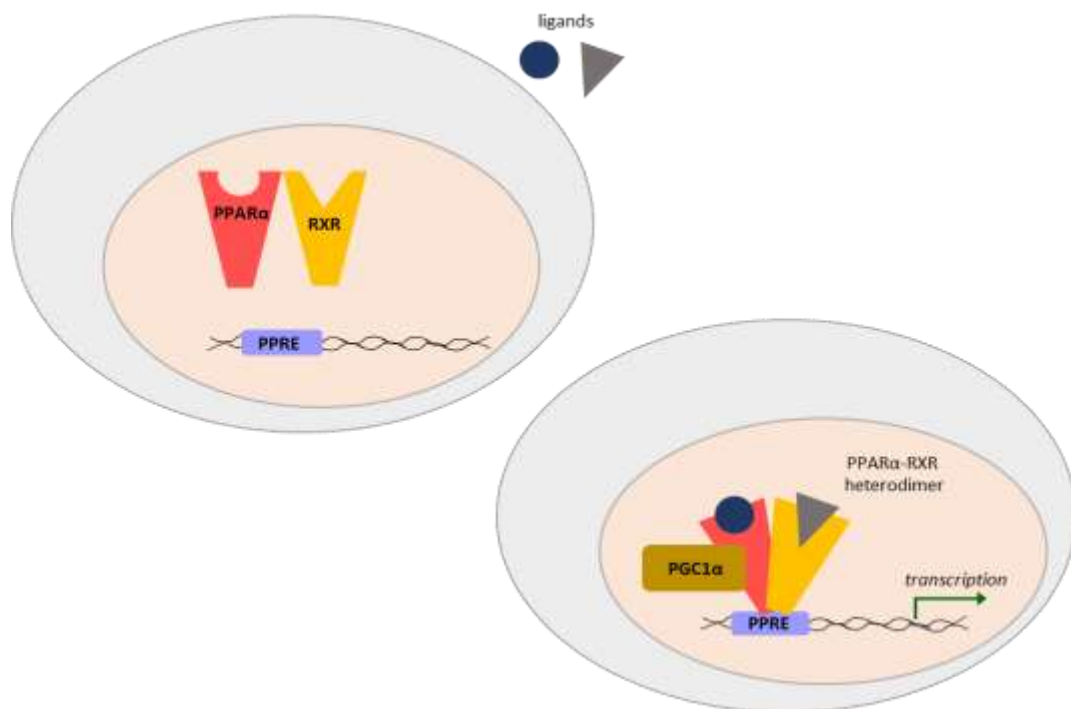


Figure 4.1. Ppar α binds to RXR, the heterodimer gets activated by ligands and Pgc1 α acts as a co-activator, for Ppar α . Then, the heterotrimer binds to the Ppar α response element (PPRE), in the promoter of target genes and increases the transcription rates of a number of metabolic proteins.

Finck *et al.* in 2002, showed that Ppar α is linked to FA-uptake in the CMs and up-regulation of the beta-oxidation pathway³⁹². In addition, PPAR coactivator 1 α (Pgc1 α) functions as a co-activator for Ppar α ³⁹³. PGC-1, was initially found enriched in brown adipose tissue and was characterised as a PPARg co-activator³⁹³. Later it was shown that Pgc1 α is involved in various metabolic processes³⁹⁴, primarily regulating of genes involved in FA oxidation³⁹⁵.

4.2.4. OLEIC ACID

As mentioned before, FAs are natural ligands for Ppar α ³⁸⁰. Oleic Acid (OA) is an 18-carbon-FA, one of the most abundant monounsaturated FAs in the body³⁹⁶. Binding of OA to Ppar α facilitates the formation of the heterotrimeric RXR-Ppar α -Pgc1 α transcription factor¹⁸⁶. A study conducted in 2014 on the HepG2 hepatic cell line, showed that not all FAs have the same binding affinity to Ppar α and therefore, do not necessarily result in its activation. While OA and

palmitoleic increased Ppar α transactivation, palmitic and stearic acid inhibited it. In addition others (arachidonic, eicosapentaenoic, and docosahexaenoic acid) exerted both effects dependent on their concentration³⁹⁷. Several studies have investigated the effect of OA on various cell types *in vitro*, focusing on; cancer cells proliferation^{398,399}, cell proliferation and inflammation on ECs^{400,401} and SMCs⁴⁰², oxidative stress on fibroblasts^{403,404}. Also it exerted a protective effect against lipotoxicity, in Skeletal MCs⁴⁰⁵ and insulin-producing cells⁴⁰⁶. The effect of OA on CMs *in vitro* has also been assessed. In one study, rat CMs showed myofibrillar disruptions after OA treatment, whereas in others it prevented TNF- α induced oxidative stress^{407,408}. In addition HL-1 CMs, incubated with OA developed calcium and sodium channel dysregulation⁴⁰⁹. Whereas, in mouse CMs it exerted a cardioprotective effect against cardiovascular insulin resistance and inflammation⁴¹⁰.

4.2.5. CARDIAC DEVELOPMENT - METABOLIC SWITCH (1)

The fetal heart is adapted to an environment of low oxygen and low fatty acid content, so, fetal CMs are highly dependent on glycolysis for ATP production⁴¹¹. In addition, lactate availability allows for energy production via lactate oxidation. During development, the heart undergoes a major metabolic alteration (Figure 1); the main physiological changes during the transition to the post-natal stage are the increased workload, and the demand for growth, that can not be met by glucose and lactate oxidation alone^{412,413}, though immediately after birth some studies suggest that the main energy biogenesis mechanism is still glycolysis⁴¹⁴. The parallel increase in circulating levels of free fatty acids (due to dietary alteration and lipid content in maternal milk) and in O₂ levels, after birth, mediate a switch from glycolysis-dependence, to predominantly relying on oxidative metabolism as mature CMs^{415,411}. During the early postnatal period, as cardiac energy demands increase, the **number of mitochondria** increases dramatically^{416,417}. Interestingly, the expression of the PGC-1 gene is also upregulated in the postnatal heart, before the increase in mitochondrial biogenesis and the metabolic switch to FA utilisation. Several studies demonstrated an increase in PGC-1, as well as Ppar α , mRNA levels in mice or rats during development^{418,419}. The suggested involvement of PGC-1a in

mitochondrial biogenesis was validated by studies showing that overexpression of PGC-1 in cardiomyocytes of transgenic mice resulted in mitochondrial proliferation⁴¹⁸. The regulatory mechanism involves genes encoding several key mitochondrial ETC proteins, specifically the transcription factors nuclear respiratory factors-1 and -2 (NRF-1 and -2)⁴²⁰. Along with their number, proteins related to mitochondrial functions, such as the ETC get upregulated. Disruption of the ETC function during cardiac development, leads to disrupted mitochondrial organisation in the CMs, resulting in perturbed sarcomere formation and contraction⁴²¹.

4.2.6. CARDIAC METABOLISM IN MI & HF - METABOLIC SWITCH (2)

Following myocardial infarction, tissue ischaemia leads to hypoxia, which in turn activates long-term HIF signaling at the myocardium⁴²². As previously described, HIF upregulation is related to increased glycolysis. During MI, the ischemic region relies solely on glycogen, as an anaerobic fuel for energy production⁴²³. Disrupted mitochondrial integrity and function, is another characteristic of HF, as mitochondria can be found with membrane and ETC defects^{424,425}, as well as reduced respiratory capacity^{425,426} and reduced oxidative phosphorylation^{427,428,429}. These findings are consistent with the concept that during HF, as happens in cardiac stress-induced hypertrophy, the metabolic state of the heart resembles that of the fetal stage, switching to glycolysis, over mitochondrial oxidative metabolism⁴³⁰. Studies have shown increased glucose uptake⁴³¹ and glycolysis¹⁸⁵ with either no change or a decrease in glucose oxidation^{432,431}.

4.2.7. MITOCHONDRIA IN HEALTH & DISEASE

Mitochondria are central organelles in energy production, so, their number, function, and dynamics affect ATP synthesis. The importance of mitochondrial integrity for maintenance of cardiac function has been also highlighted through several conditions which are characterised by mitochondrial mutations or abnormalities, causing among others; cardiomyopathy, neuromuscular dysfunction, diabetes mellitus and even sudden death^{27,28}. Impaired mitochondrial function also occurs with aging or with cardiac disease and

HF^{28,29}. The efficiency of the ETC is found to decline with age, which in turn decreases ATP generation^{433,434}.

4.2.8. FROM STEM CELL TO ADULT CELLS - METABOLIC SWITCH (3)

A well-studied metabolic switch in cardiac cells is that of the transition from the stem cell to the CM phenotype, which is characterised by a shift from anaerobic to oxidative metabolism⁴¹³. Similarly the Nobel laureate Otto Warburg suggested, in his paper in 1956, that cancer cells had perturbed cellular respiration, in contrast to non-cancerous adult cells⁴³⁵. He hypothesised that this difference in the metabolic state, is the fundamental drive of tumourgenesis. Since then the Warburg hypothesis has been well-established, characterising the metabolic difference between highly-proliferative (cancer cells or stem cells) and adult (terminally-differentiated) cells^{436,437}.

Basal cellular homeostasis involves processes like protein turnover, DNA repair, and vesicle trafficking. **Proliferating cells**, in addition to homeostasis maintenance, need more energy for anabolic processes such as cell division and growth. Stem and progenitor cells, as well as cancer cells, have been suggested to predominantly rely on glycolysis for ATP production, irrespective of oxygen presence; this metabolic paradox has been termed “aerobic glycolysis”³. Apart from Warburg’s observations on cancer cells, mouse fibroblasts⁴³⁸, human⁴³⁹ and mouse⁴⁴⁰ lymphocytes have been shown to utilise “aerobic glycolysis”, when stimulated to proliferate. ESCs derived from *in vitro* cultured ICMS⁴⁴¹ or ESCs cultured *in vitro*⁴⁴², show high rates of glycolysis and low oxidative phosphorylation. Possible explanations for this are that the cells might be damaged by low levels of intracellular reactive oxygen species (ROS), which would impair their capacity for self-renewal capacity and the maintenance of the stem cell phenotype⁴⁴³, therefore mitochondrial oxidation remains low⁴⁴⁴.

Adult endogenous stem cells reside in hypoxic niches, in a quiescent state. As mentioned before, hypoxia and HIF levels reinforce the increased glycolysis levels of HSCs, rather than oxidative phosphorylation⁴⁴⁵. The non-oxidative breakdown of glucose leads to the formation of pyruvate, which subsequently is broken down to lactate⁴⁴⁶. Various studies have supported that the major function of aerobic glycolysis is to supply glycolytic intermediates for anabolic

reactions in cells, thus being the metabolic pathway of choice during cell proliferation (for Review see⁴⁴⁷). Many proliferating mammalian cells also consume glutamine, to provide material for biosynthesis, such as human MSCs⁴⁴⁸. Glutamine, as a carbon source, can supply the TCA cycle with intermediates that can be used for the production of new macromolecules in cells. A recent study by Hosios *et al*, in 2016, argued that glutamine contributes most to protein, suggesting that anaplerosis of glutamine in the TCA cycle is serving mainly amino acid biosynthesis⁴⁴⁹. **Mature CMs** consume a huge amount of ATP to sustain contraction⁴⁵⁰. Due to their limited ability for storing energy, they need continuous fueling, which is mainly supported by FA oxidative phosphorylation⁴¹¹. Interestingly, the opposite switch is needed when terminally differentiated cells convert to iPS; the metabolic reprogramming entails shifting from oxidative phosphorylation to glycolysis⁴⁵¹. A shift in substrate availability is also experienced by stem/ progenitor cells during **transplantation *in vivo*** (Figure 4.2). Cells are transferred from the culture medium, which contains about 17-25 mM glucose (depending on the culture protocol) and no FFA, to substrates in plasma that vary substantially. Glucose levels in mice have been measured between ~3.4 - 9.6 mM (2.8 - 7.5 mM in rats) ^{452,453} and ~0.18 - 0.6 mM FFA²⁸⁵. This alteration is bound to cause changes in their metabolic machinery which might be one of the stimuli that induce differentiation following transplantation.

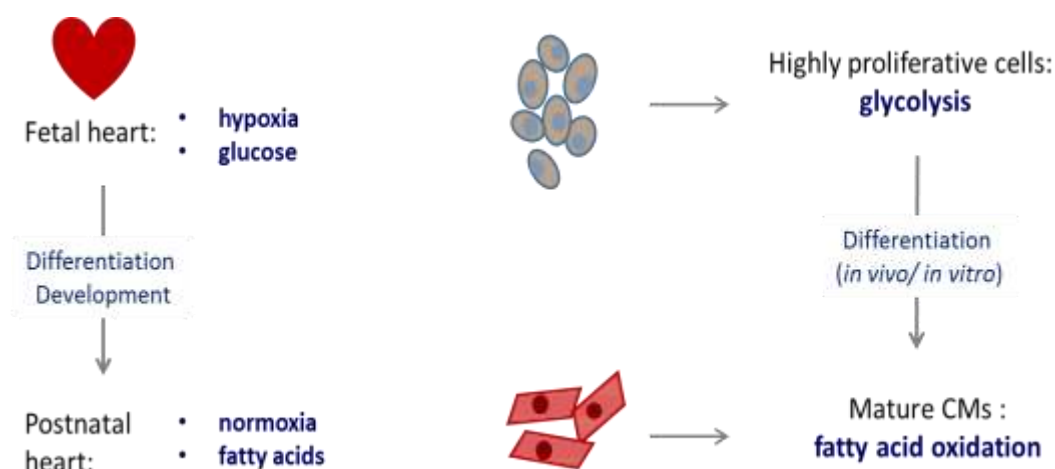


Figure 4.2. Schematic of metabolic switches during cardiac development (left) and cell differentiation (right).

4.2.9. MITOCHONDRIA IN DEVELOPMENT & CELL DIFFERENTIATION

When stem/ progenitor cells differentiate to CMs they need to increase mitochondrial numbers and fatty acid metabolism. Different studies have shown the importance of upregulating mitochondrial oxidative metabolism for cardiac differentiation^{454,455}. The idea that immature cells have under-developed mitochondria has been highlighted via studies in human and mouse ESCs, which revealed the presence of a small number of rounded and immature mitochondria with under-developed cristae^{456,421}. Moreover, multipotent stem/progenitor cells show the same characteristics; for example, mitochondria in HSCs are relatively inactive in lineage-committed progenitors than in HSCs^{457,458}. Interestingly, even ICM mitochondria have been shown to have a lower membrane potential, indicative of reduced mitochondrial function⁴⁵⁹. In addition, pluripotent ES cells derived from *in vitro* cultured ICMs show high rates of glycolysis^{441,460}.

4.2.10. STUDY AIMS

As described above, metabolic switches exist during development and differentiation. In addition, no cardiac differentiation protocol, to our knowledge, takes into account the lack of FAs as a cell culture substrate, despite the fact that there is a known shift to oxidative metabolism in mature cells. Both TGF- β 1, and OA are naturally found in the body, and so, in the context of SCT and transplantation of CPCs in the heart after injury, it is necessary to understand what effect these factors will have on the transplanted cells.

Therefore, in this chapter:

- I investigate which one of the isolated mixed-cell population of CPCs; CDCs and CTs, would differentiate better using an established protocol, in order to better characterise the optimal cardiac progenitor population.
- Also, I strive to answer the question of whether altering the metabolism would help the cells to differentiate further than a differentiation protocol allows.
- Finally, I assess the effect of fatty acid availability (OA) on undifferentiated and differentiated CPCs, as well as that of TGF- β 1 on undifferentiated CPCs.

4.3. RESULTS

4.3.1. STAGES OF mESC DIFFERENTIATION VIA EMBRYOID BODY FORMATION

To assess the differentiation potential of the CPCs, the Transforming Growth Factor - beta1 / 5-Azacytidine / Ascorbic Acid (TGF- β 1, 5-Aza, A.A.) differentiation protocol was used, as described by Gouman's *et al.* (see Methods 2.10.2). Based on previous work in our group (Dr. F. Perbellini thesis; unpublished data), this protocol resulted in enhanced differentiation of CDCs when compared to the 5-Aza/ DMSO protocol.

To assess the stage of maturity of the CPCs post-differentiation, gene expression was compared with a mESC cell line at day 4 and 7 of differentiation via embryoid body (EB) formation (see Methods 2.10.1.), as a positive control. These cells were initially checked with qPCR for the level of expression of: stemness genes, early-endothelial, as well as early-onset cardiac genes that are involved in the development of the embryonic mouse heart (Introduction Table 1.2). In addition, the level of gene expression of late-onset cardiac markers was checked in mESCs at day 14 of the embryoid body differentiation, which marks the endpoint of the protocol. Finally, since it has been shown before that mESCs do mature functionally following the 14-day protocol of differentiation (Dr. R. Tyser thesis, P. Riley group), it was interesting to check the metabolic genetic profile. More specifically, components of oxidative metabolism, which are seen in mature adult cardiac cells, were checked, along with the cardiac glucose transporters.

Agreeing with the genetic changes during differentiation, the stemness genes (Oct4, Sox2, Sca1, Ckit) reduced their expression as mESCs progressed from day 4 (EBs d4) to day 7 (EBs d7) of differentiation, while the early-onset (Gata4, Mef2c, Nkx2.5, Isl1) cardiac markers increased, as well as the endothelial Flk1 marker. (Figure 4.3).

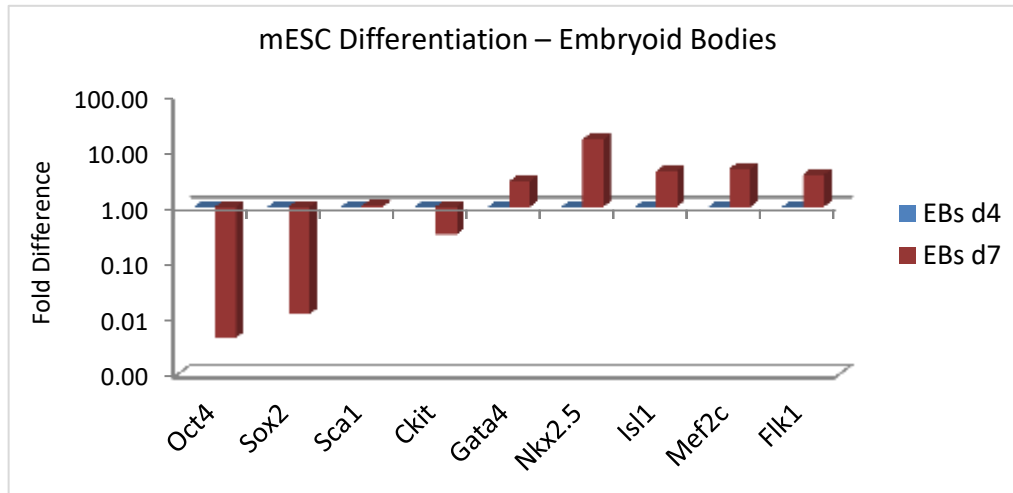


Figure 4.3. Gene expression levels of stemness markers (Oct4, Sox2, Sca1, Ckit), early-onset cardiac (Gata4, Mef2c, Nkx2.5, Isl1) and endothelial (Flk1) markers in mESCs at d4 and d7 of differentiation to CMs, normalized to EBs d4. (EBs: n=1)

At day 14 the mESCs are terminally differentiated and start to beat. As expected, the gene expression of late-onset cardiac markers (Tnnt2 and Myh7) increased from day 4, day 7 and day 14 (EBs d14) of differentiation. The same was observed for the glucose transporter Glut4, mainly found in the adult heart, and for the fatty acid transporter CD36, while the gene expression of the glucose transporter Glut1, predominant at the fetal stage, was reduced (Figure 4.4).

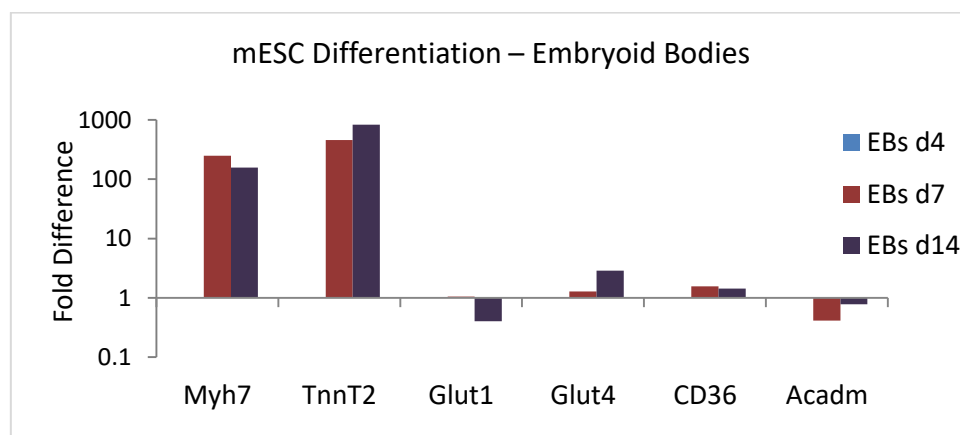


Figure 4.4. Gene expression levels of late-onset cardiac markers (Tnnt2 and Myh7) and Glut1, Glut4 in mESCs at d4, d7 and d14 of differentiation to CMs, normalized to EBs d4. (EBs: n=1)

To investigate further the metabolic changes, the genes involved in oxidative metabolism were checked. Ppar α expression initially decreased from day 4 to day 7 of embryoid body differentiation and then showed an 8-fold increase. Pgc1 α followed the opposite pattern, being upregulated early on and then downregulated when the cells terminally differentiated (Figure 4.5).

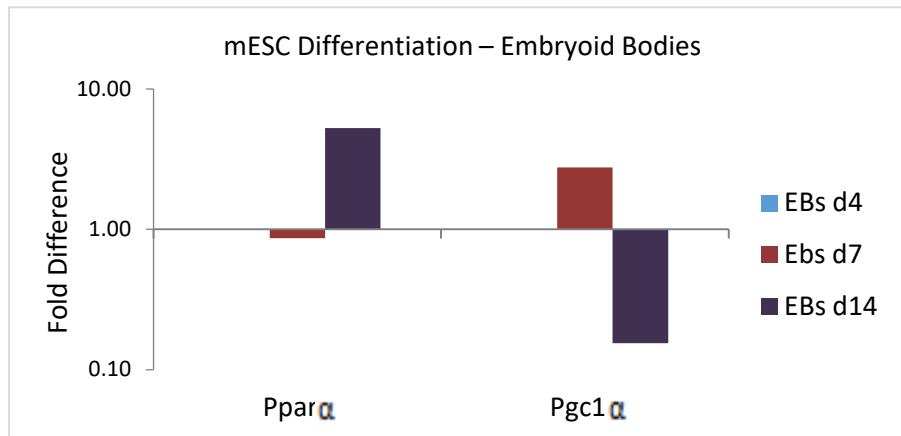


Figure 4.5. Gene expression levels of Ppar α and Pgc1 α in mESCs at d4, d7 and d14 of differentiation to CMs, normalized to EBs d4. (EBs: n=1)

4.3.2. TGF- β 1 DIFFERENTIATION INCREASES EXPRESSION OF TNNT2 IN BOTH CDCS AND CTS

Initially, CTs and CDCs at P4 were seeded in flasks and in 24-well plates, the following day the normal CEM medium was removed and were differentiated with CGDM and 5-Aza/ TGF- β 1/ A.A (see Methods 2.10.2). Based on Goumans *et al.* the endpoint of the differentiation was around 25 days, after which the differentiated human Sca1⁺ selected CPCs were shown to start to beat. There was no beating observed in any of our differentiations of the adult mixed atrial CPCs of this project, so the 1 month endpoint was selected. After 1 month of TGF- β 1/ 5-Aza/ A.A. differentiation CDCs and CTs at P4 were analysed using qPCR.

Cell morphology remained normal, relative to day 0 - prior to differentiation, although some changes were observed at day 20 (Figure 4.6 c). By day 30, the differentiated CTs formed clusters in all the samples checked (Figure 4.6 d1). The CTs continued to proliferate and there was a layer of cells that seemed to have

normal morphology (Figure 4.6. d2), suggesting that the differentiating cells could be located in the cluster and new undifferentiated cells continued to grow.

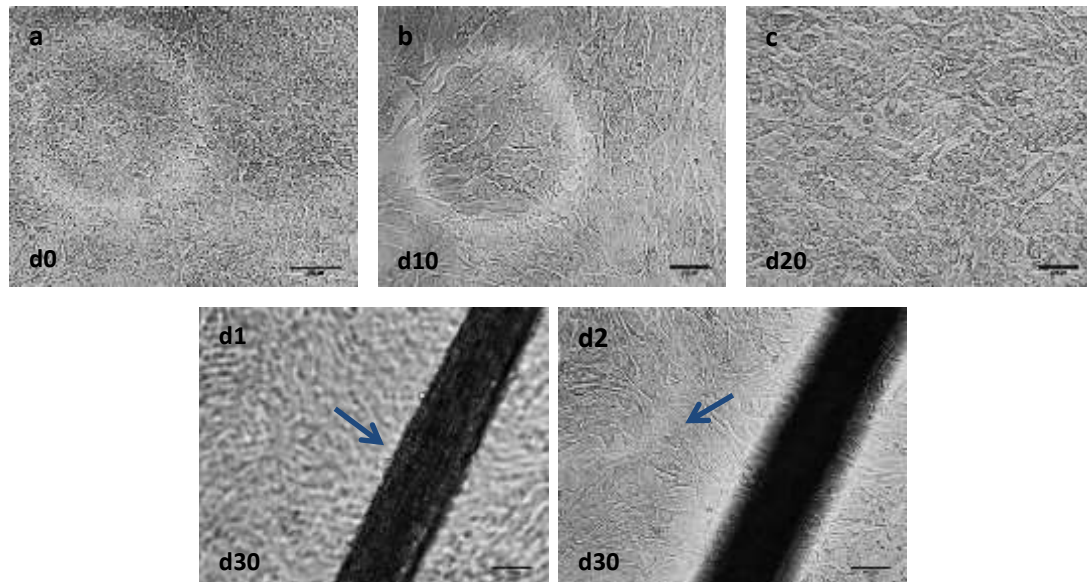


Figure 4.6. Cell morphology of differentiated CTs with the TGF- β 1 protocol, at day 0 (a), day 10 (b), day 20 (c) and d30 (d1, d2) under light microscope. Arrow at d1 indicating and focusing on the cell cluster, arrow at d2 indicating and focusing on the cell layer underneath the tubular cell cluster (scale bars: 100 μ m)

Both CTs and CDCs showed significantly increased gene expression of cardiac troponin-T (Tnnt2) of about 10-fold (Figure 4.7, 4.8), despite the different nature of the two populations and the fact they were heterogeneous. Myosin heavy chain beta (Myh7), Connexin-43 (Cx43) and Desmin did not change significantly. Myosin Heavy Chain alpha (Myh6) was not expressed at all in any of the tested cell types (data not shown).

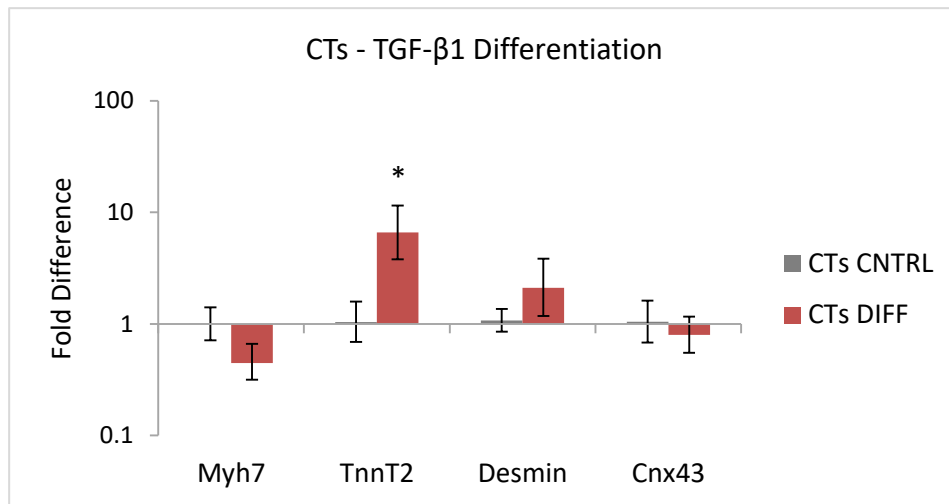


Figure 4.7. TGF-β1 differentiation of CTs at P4 compared to the respective undifferentiated control samples (n=4, *p<0.002, error bars: standard error), normalised to undifferentiated control.

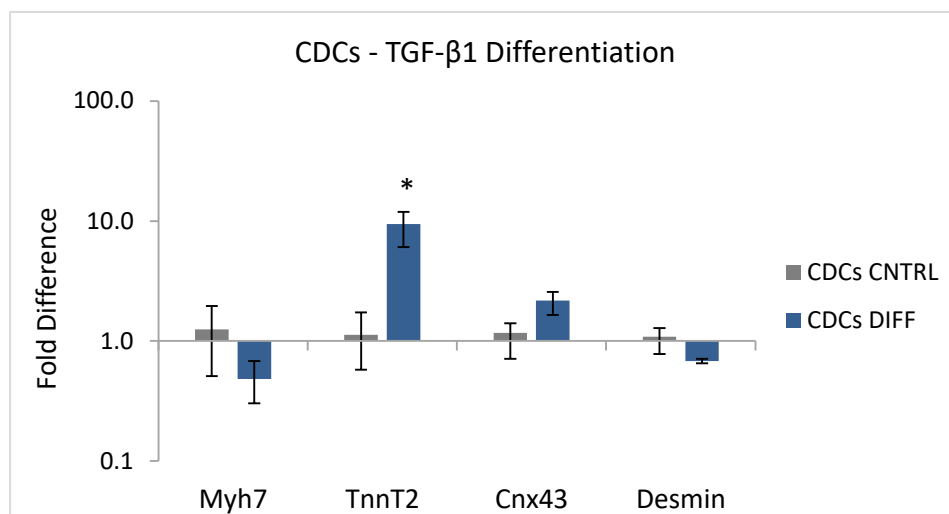


Figure 4.8. TGF-β1 differentiation of CDCs at P4 compared to the respective undifferentiated control samples (n= 3, *p=0.02, error bars: standard error), normalised to undifferentiated control.

The level of protein expression for TNNT2 and MHCb was assessed using Immunohistochemistry (Confocal Imaging) (Figure 3.9, 3.10). CPCs were seeded and differentiated, as above, at the same time as the cell samples for qPCR analysis.

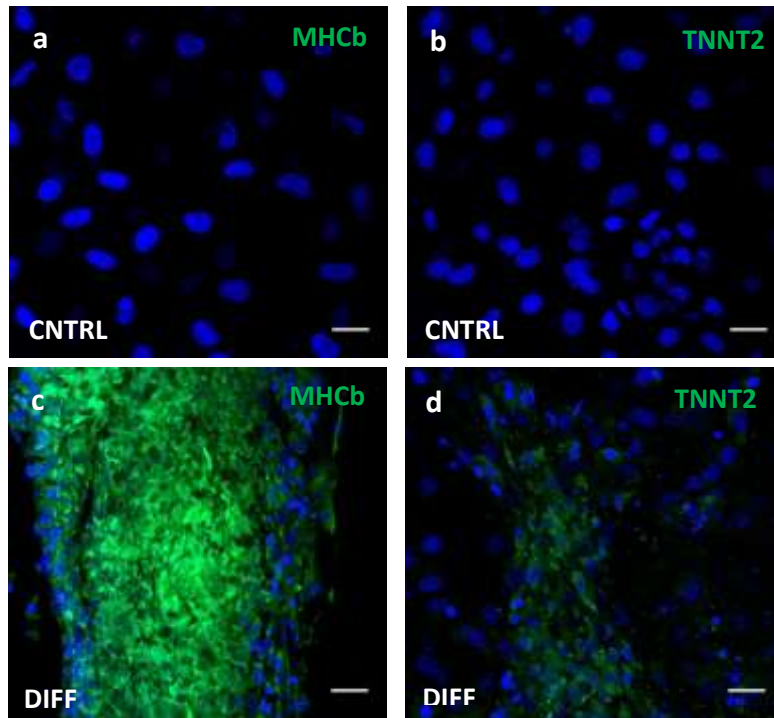


Figure 4.9. Differentiated CTs, with the TGF- β 1 protocol. Expression of MHCb and TNNT2 shown in green; a, b: control samples, c, d: differentiated samples. (blue: DAPI, scale bars: 30 μ m)

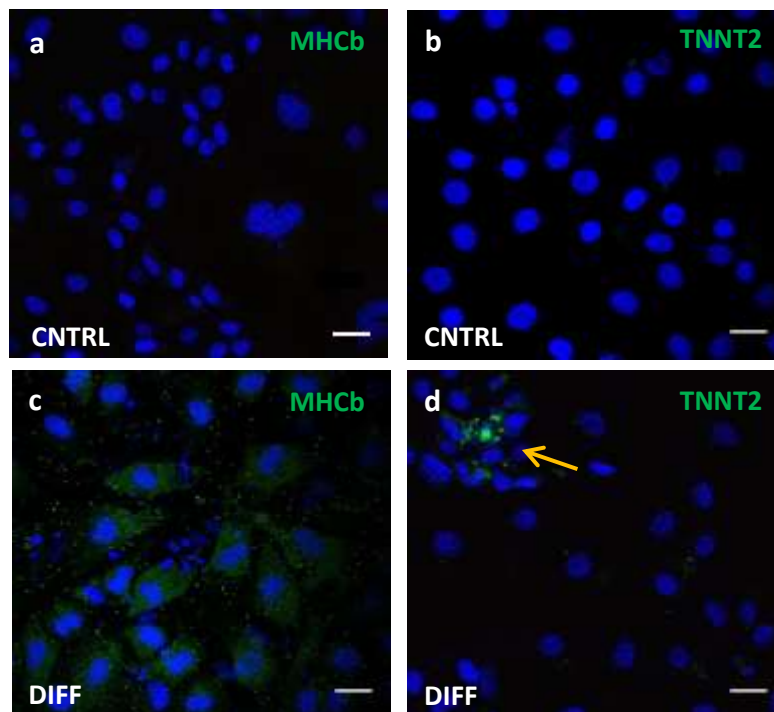


Figure 4.10. Differentiated CDCs, with the TGF- β 1 protocol. Expression of MHCb and TNNT2 shown in green; a, b: control undifferentiated samples, c, d: differentiated samples. (blue: DAPI, scale bars: 30 μ m)

The proteins were not detected in undifferentiated cells (Figure 3.10b). After differentiation, both CTs and CDCs showed localised expression of TNNT2 (Figure 3.9.d, 3.10.d). MHCb was expressed in CDCs and CTs; in the latter it was found in cell clusters that the CTs formed while differentiating (Figure 4.9.d and 4.10.d).

The CTs around the clusters did not express MHCb or TNNT2, suggesting that there was still a fraction of undifferentiated cells growing around the differentiating ones (Figure 4.6 d2).

4.3.3. MANIPULATION OF CELL METABOLISM

4.3.3.1. OLEIC ACID SUPPLEMENTATION STIMULATES THE PPARA PATHWAY AND METABOLICALLY MATURES CT CELLS

To increase the maturation of the differentiating CPCs in addition to the pharmacological agents (TGF- β 1 differentiation), the cell culture substrate content was altered. The aim was to harness the metabolic switch observed *in vivo*; both during normal embryonic development and post-implantation in the paradigm of cell therapy (see Introduction 4.2.5, 4.2.8). Ultimately the focus was to shift substrate metabolism from glycolysis and to increase FA oxidation by targeting the Ppar α pathway, as it has been linked to FA oxidative metabolism regulation (see Introduction 4.2.3). To achieve this, the CPC culture medium was supplemented with FAs, as they are endogenous activators of Ppar α . More specifically Oleic Acid (OA) was used, the predominant fatty acid normally found in the blood. The effect of increasing concentrations of OA were compared at 75 μ M, 150 μ M and 300 μ M. The 300 μ M was selected as the highest dose because high levels of FA have been shown to be toxic in cells⁴⁶¹. Also, based on previous work done in our group (Dr. Lucy Ambrose thesis; unpublished data) on the effect of OA on HL-1 CMs, a concentration of 500 μ M was found severely toxic, causing cell death. Also studies on adipose fibroblasts showed cytotoxicity at concentrations higher than 400 μ M for 24 hours⁴⁰³.

The effect of 75 μ M, 150 μ M or 300 μ M of OA on cell viability was checked, after 1 week of incubation, none of which were found toxic (Figure 4.11.a, 4.11.b).

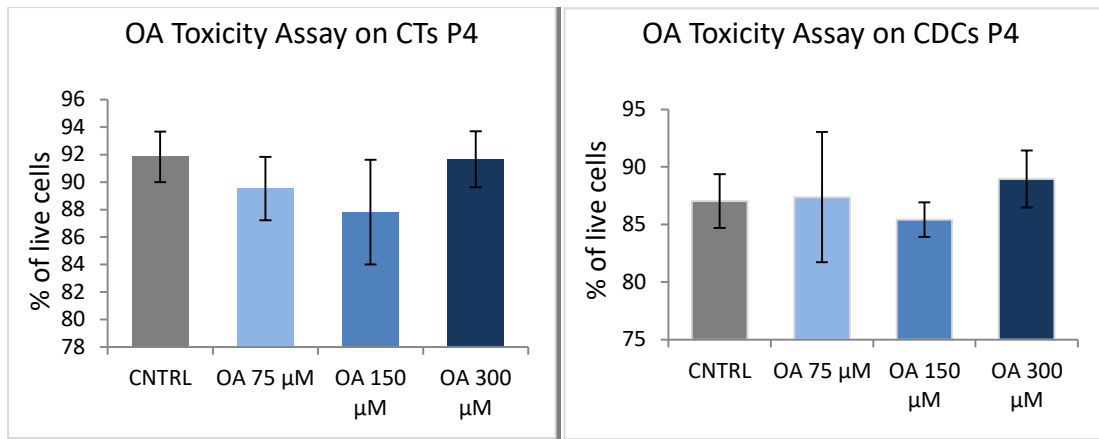


Figure 4.11. Effect of OA 75 μ M, 150 μ M and 300 μ M on the viability of CTs P4 and CDCs P4, compared to CNTRL untreated cells (n=3, error bars: standard deviation)

The gene expression of Ppar α was initially checked and its co-activator Pgc1 α in CTs P4 treated with OA 75 μ M, 150 μ M or 300 μ M for 48 hours (see Methods 2.10.1.), (Figure 4.12). Cells were cultured in GCDM basal medium, with added OA, so as to maintain the same level of glucose, amino acids and nutrients in the culture in all of our conditions, making the OA concentrations the only difference. Pgc1 α was significantly upregulated as the concentration of OA increased. Ppar α gene expression, on the other hand, did not change with increasing concentration of OA. This could mean that with short-term treatment with Oleic Acid Pgc1 α gets upregulated acutely, and not Ppar α .

As the OA supplement was pre-conjugated with BSA, the gene expression of Ppar α and Pgc1 α was also compared to the untreated controls which had been supplemented with Bovine Serum Albumin (BSA), at the respective concentrations.

Neither Ppar α , nor Pgc1 α showed any significant difference at 75 μ M of OA supplementation, but they did increase more than 5-fold at 300 μ M, when compared to the 20 μ M BSA control (Figure 4.13). This data show that Oleic acid does activate the Ppar α pathway.

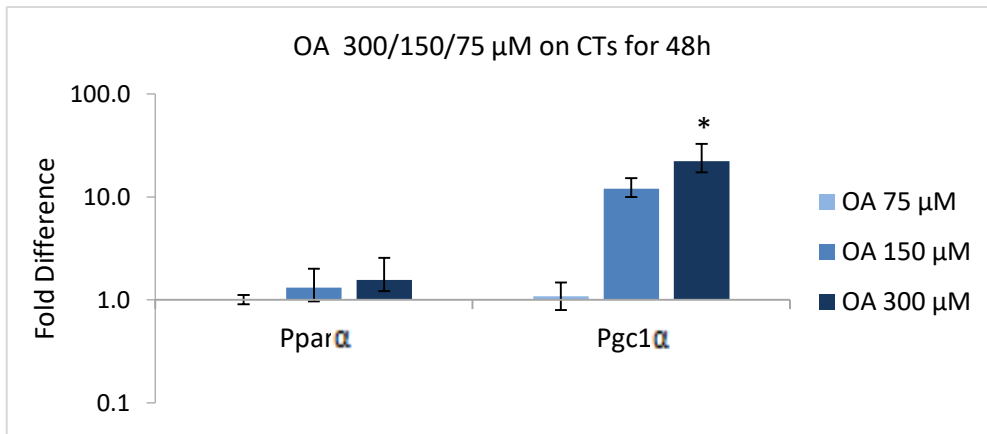


Figure 4.12. Effect of 48h supplementation with OA 75 μM, 150 μM, 300 μM on the expression of Pparα, Pgc1α, at CTs P4, normalised to OA 75μM. (n=4, *p<0.02, #p<0,01, indicating difference to OA 75 μM; error bars: standard error).

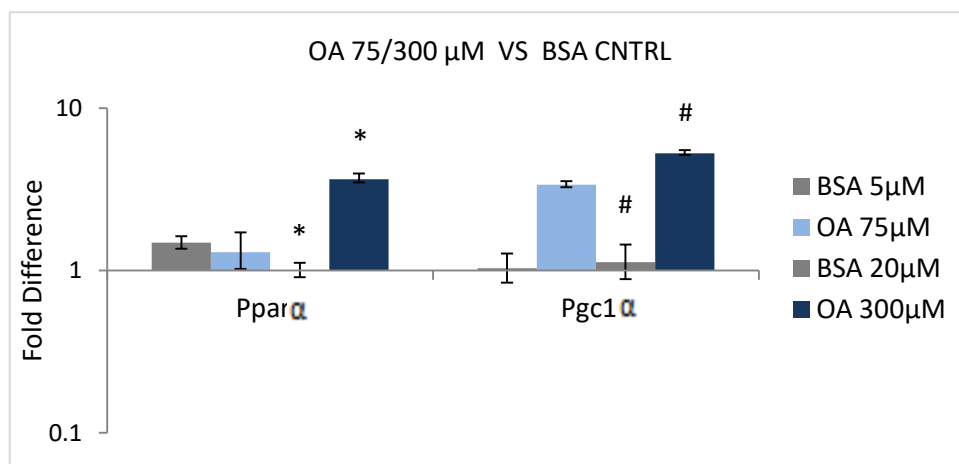


Figure 4.13.. Effect of 48 hour supplementation with OA 75 μM and 300 μM on the expression of Pparα, Pgc1α, on CTs P4. Normalised to 48h BSA supplementation with 5μM and 20μM, respectively. (n=4; error bars: standard error, *p<0.04, #p<0.03, indicating difference to the respective BSA CNTRLs).

Based on the aforementioned observations, to further test the long-term effect of OA treatment on the metabolism of the CTs the gene expression was investigated after treatment with OA 300 μM for 48 hours, 1 week and 1 month. Although a change in the CT morphology was observed after 1 month of incubation, no condition was found to be noticeably toxic (Figure 4.14).

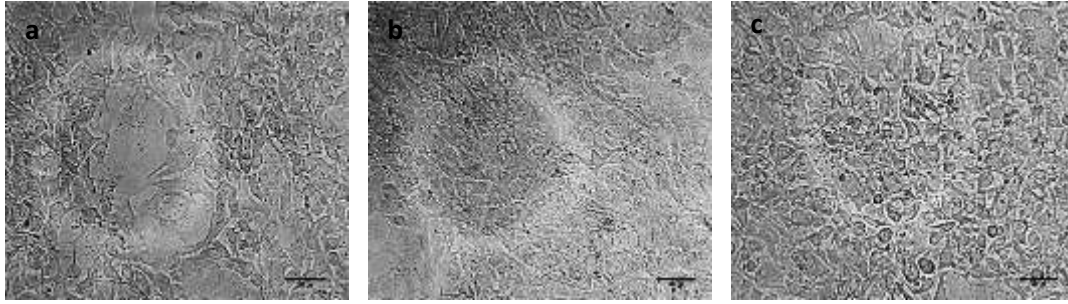


Figure 4.14.. CTs P4 treated with OA 300 μ M for 48 hours (4a), 1 week (4b) and 1 month (4c) (scale bars: 100 μ m)

Looking into the genetic changes of the metabolic genes (Figure 4.15 & 4.16); Pgc1 α gene expression gets significantly upregulated acutely after 48 hours and then drops. Ppar α becomes significantly upregulated with OA supplementation and, Glut4 shows the exact same pattern. The acute Pgc1 α increase in gene expression, followed by a decrease, could suggest a potential increase in mitochondria (see Introduction 4.2.5).

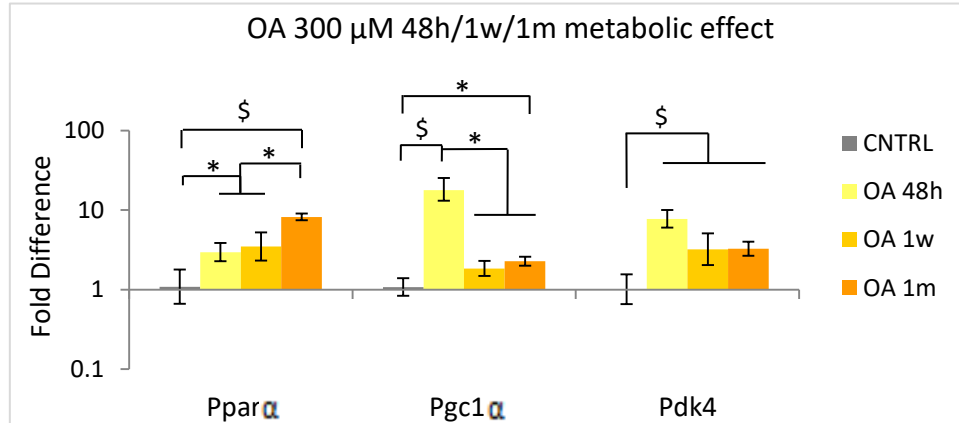


Figure 4.15. Effect of 48 hours, 1 week, 1 month supplementation with OA 300 μ M on the expression of metabolic genes, at CTs P4. Normalised to control untreated CTs. (n=3; error bars: standard error, *p<0.05, \$p<0.02).

Interestingly, Pyruvate Dehydrogenase Kinase (Pdk4), involved in FA oxidation, stays significantly upregulated with OA addition at all time-points, as does the fatty acid translocase receptor CD36, which functions as an OA receptor.

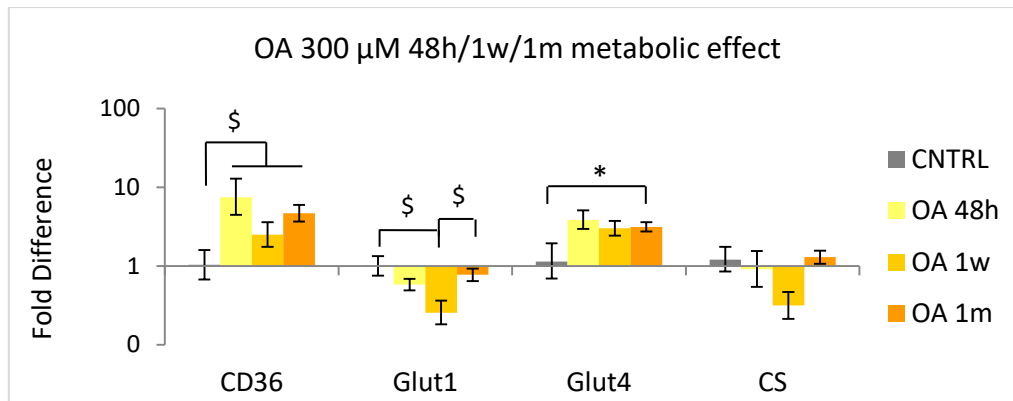


Figure 4.16. Effect of 48 hours, 1 week, 1 month supplementation with OA 300 μ M on the expression of metabolic genes, at CTs P4. Normalised to control untreated CTs. (n=3; error bars: standard error, *p<0.05, \$p<0.02).

But, looking into the citrate synthase gene expression (Cs), the first enzyme of the Citric Acid Cycle often used as a quantitative marker of mitochondria, no change in gene expression was observed (Figure 4.16).

To investigate the mitochondrial state, CTs were incubated with MitoTracker® Red CMXRos (see Methods 2.5.3.). The experiments were conducted in two separate parts; comparing CNTRL untreated cells with 48 hours of OA 300 μ M treatment (Figure 4.17) and subsequently the effect of 1 week of OA supplementation was compared to that of 48 hours (Figure 4.18). In both experiments an increase in the red fluorescence was observed, when the CTs had been exposed to OA for larger time periods.

The laser intensity and exposure parameters of the Confocal microscope, while imaging, were kept the same between the two comparing groups. Therefore, the observed signal increase can be due to more active mitochondria, since the CMXRos dye accumulates in live cells based on the mitochondrial potential⁴⁶².

It is important to mention at this point that the experiments were conducted at different time-points, using different parameters, following the investigation of the long-term and short-term effect, which accounts for the inconsistency in fluorescence between the two 48-hour OA samples.

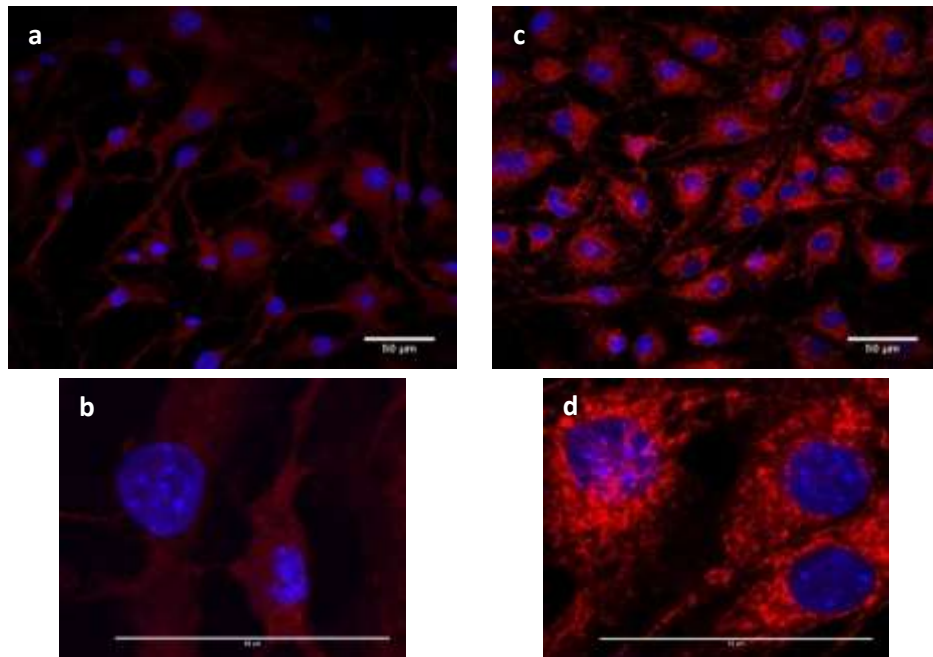


Figure 4.17. Short-term effect of OA in cell mitochondria; CTs P4; untreated CNTRL (a, b) and treated with OA 300 μ M for 48 hours (c, d), stained with MitoTracker® Red CMXRos. Images b, d are taken after 5% zoom of each respective group. (scale bars: 50 μ m)

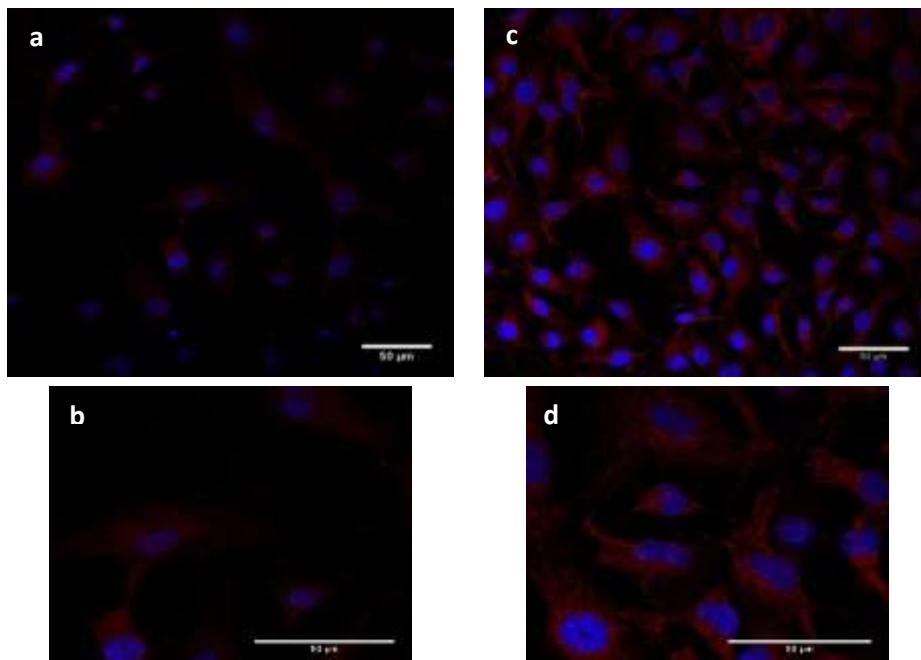


Figure 4.18. Long-term effect of OA in cell mitochondria; CTs P4; treated with OA 300 μ M for 48 hours (a, b) or 1 week (c, d), stained with MitoTracker® Red CMXRos. Images b, d are taken after 2.5% zoom of each respective group. (scale bars: 50 μ m)

To avoid confusion, the increase in fluorescence was measured using the Fiji Is Just Image J imaging software, in arbitrary units (Figure 4.19), which confirmed that there was a significant increase in fluorescence (see Methods 2.5.3).

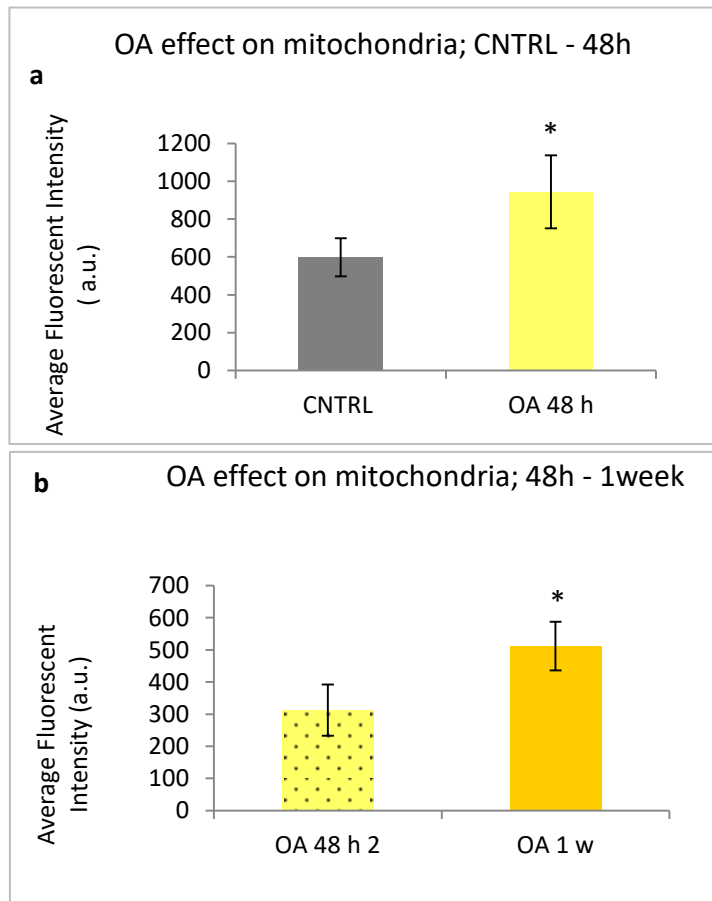


Figure 4.19. Effect of OA treatment 300 μ M for 48 hours (a) and 1 week (b), estimated as average fluorescent intensity, after staining with MitoTracker Red CMXRos red. Error bars: standard deviation, * $p < 0,00001$ compared to untreated CNTRL (a) and OA 48-hour treatment

To investigate further the changes in mitochondria, citrate synthase was checked with Western Blots (see Methods 2.12). CTs treated with Oleic Acid for 1 week, were compared to the untreated CNTRL cells. The assay showed that there was no change in citrate synthase protein levels (4.20). Therefore the effect of OA treatment could lead to an increase in the activity of mitochondria, rather than their number.

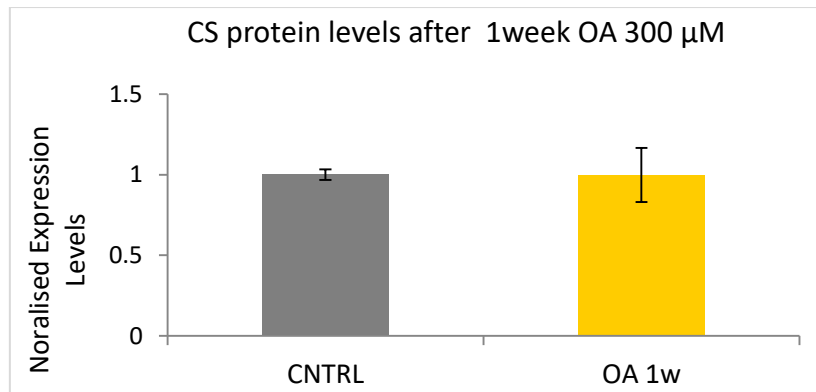


Figure 4.20. Protein levels of Citrate Synthase estimated with Western Blot, fold change of expression relative to the CNTRL samples.

It is known (see Introduction 4.2.8) that CPC maturation is marked by upregulation of oxidative metabolism and genes linked to mitochondrial number and activity. Given the observed changes after OA supplementation, the level of glucose oxidation was analysed. After culture in CDGM medium the CTs were supplemented with OA 300 μM for 48 hours and 1 week or no OA. Glucose oxidation was estimated by measuring the moles of labeled $^{14}\text{CO}_2$ that were produced after incubation with ^{14}C -glucose (see Methods 2.13.1). Interestingly, the level of glucose oxidation was increased significantly with increased time length of incubation with OA (Figure 4.21).

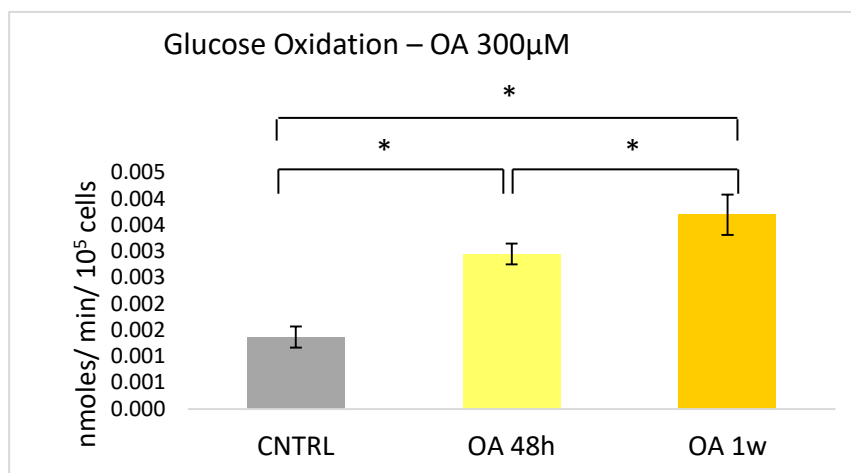


Figure 4.21. Effect of 48 hours, 1 week, 1 month supplementation with OA 300 μM on the glucose oxidation levels, measured as nMoles/ min/ 10^5 cells, compared to control untreated CTs. (n=4; *p<0,02 indicating differences amongst the groups, error bars: standard error).

A limitation of these experiments that required culture of the cells in 24-well plates was that the CTs that were grown for 1 month with OA, and became so over-confluent and formed sheets that detached from the slides and wells making any further analysis impossible. Our subsequent question was whether the observed metabolic maturation had any effect on or was any indication of a degree of functional maturation. Therefore, the effect of 48 hours, 1 week or 1 month treatment with 300 μ M OA was tested to assess any immediate effect on differentiating the CNTRL CTs. The RT-PCR data showed no significant change in the gene expression of Tnnt2 or Cx43. (Figure 4.22). Myh6, Myh7 and MLC were not expressed at any of the conditions checked.

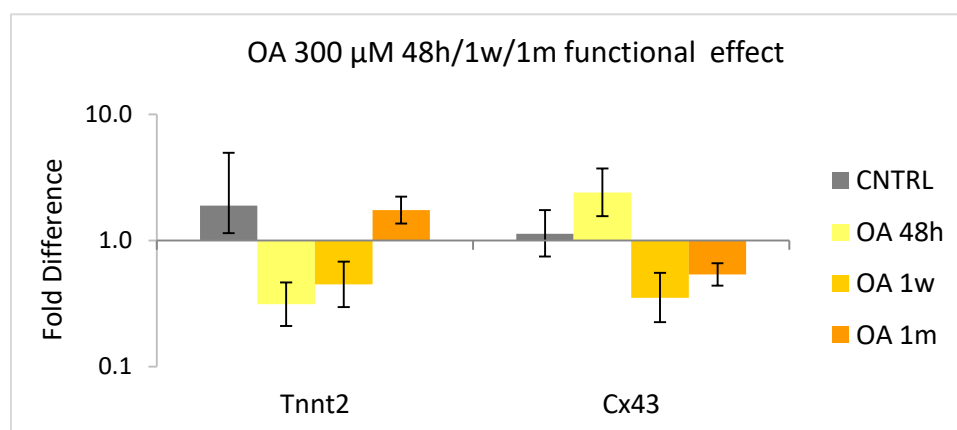


Figure 4.22. Effect of 48 hours, 1 week, 1 month supplementation with OA 300 μ M on the expression of differentiation genes, at CTs P4. Normalised to control untreated CTs. (n=3; error bars: standard error).

4.3.3.2. PHARMACOLOGICAL TREATMENT WITH ICARIIN DOES NOT STIMULATE THE PPARA PATHWAY IN ATRIAL CPCs

As a next step the stimulation of the Ppar α pathway was attempted using the pharmacological agent Icariin (referred to below as ICA). CTs P4 were tested, to compare with the effect of OA described in 4.2.4.1. DMSO treatment was used as a control, because Icariin is dissolved in DMSO (see Methods 2.11.2). Initially the cytotoxic effect of Icariin was assessed, showing no significant effect, compared to CNTRL cells (Figure 4.23).

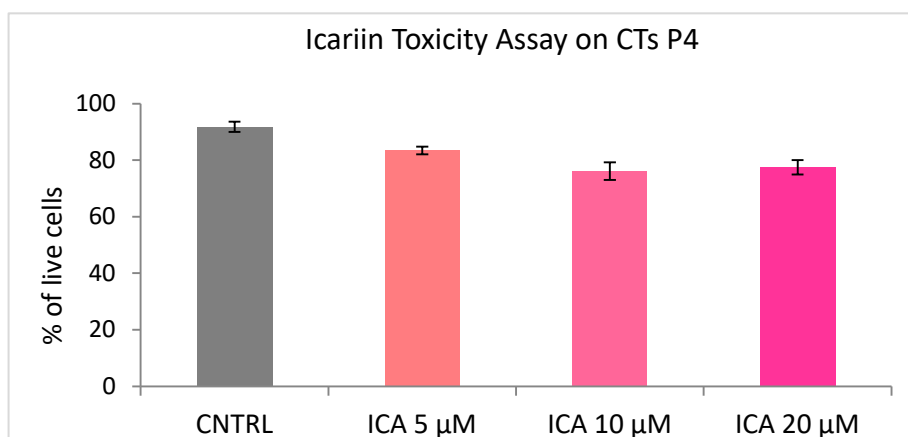


Figure 4.23. Effect of Icariin 5 μM , 10 μM and 20 μM on the viability of CTs P4, compared to CNTRL untreated cells (n=3, error bars: standard deviation)

Subsequently, the gene expression of *Ppar α* and *Pgc1 α* was checked in CTs P4 treated with 5 μM and 20 μM of Icariin for 48 hours (see Methods 2.11.2). Cells were cultured in GCDM basal medium, with added Icariin, or added DMSO for the CNTRL cell. The tested concentrations did not exert a significant effect on *Ppar α* or *Pgc1 α* gene expression (Figure 4.24), therefore the OA approach was taken forward, for subsequent experiments.

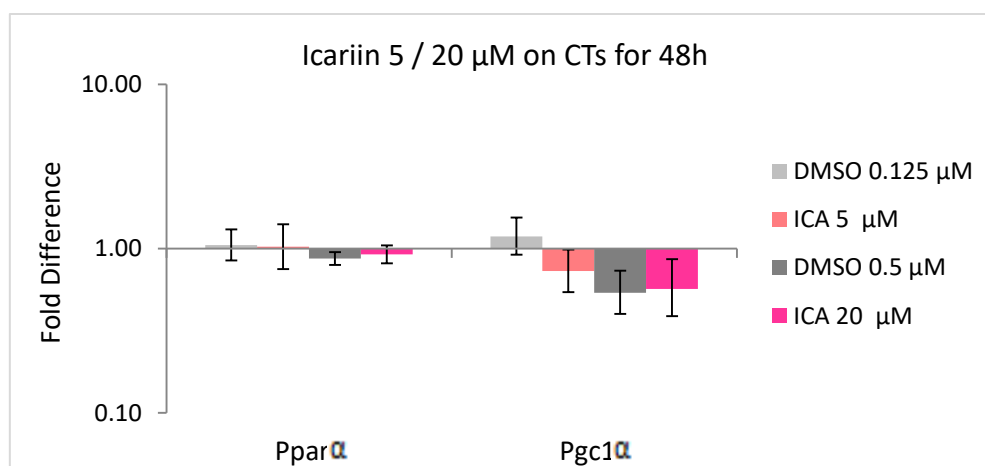


Figure 4.24. Effect of Icariin 5 μM and 20 μM on *Ppar α* , *Pgc1 α* gene expression on CTs P4. Normalised to 48h 0.125 μM and 0.5 μM DMSO treatment, respectively. (n=3; error bars: standard error).

4.3.3.3. STIMULATION WITH OLEIC ACID FOR 1 WEEK FURTHER MATURES DIFFERENTIATED CTS FUNCTIONALLY AND METABOLICALLY

Based on the encouraging data indicating upregulation of the Ppar α pathway after OA treatment in CT cells, OA was used after TGF- β 1 differentiation to assess whether the cells could be matured further than observed before (4.2.4). CTs were differentiated as before (2.10.2) and at the end of the TGF- β 1 differentiation protocol half of the cell population of each sample was supplemented with OA 300 μ M for a further period of 1 week (“DIFF+OA” samples) and half was collected (“DIFF” samples) (see Methods 2.10.2). The differentiating CTs formed cell clusters as before, but with the OA treatment the cells surrounding them were smaller in size than in the TGF- β 1 differentiation condition (Figure 3.6. and Figure 4.25), potentially suggesting that the OA addition could be having an additional effect on the differentiated CTs.

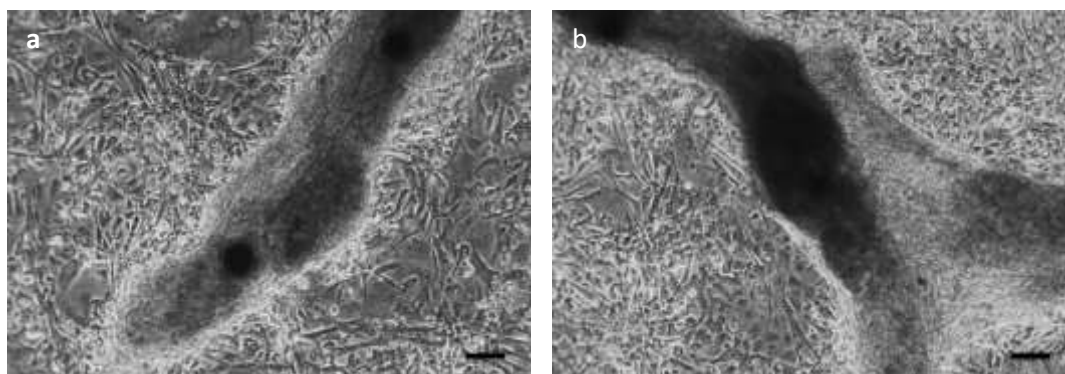


Figure 4.25. Cell morphology of differentiated CTs with the TGF- β 1 protocol, followed by 1 week of OA 300 μ M supplementation, under light microscope (scale bars: 100 μ M)

RT-PCR analysis of mature cardiac (Myh7, Myh6, Tnnt2, Cx43) genes was done, which showed that both Myh7 and Cx43 were significantly upregulated after OA treatment. Interestingly, Tnnt2 gene expression was not increased further (Figure 4.26). In order to assess the level of expression of the myocardial genes in the differentiated CTs they were compared to the mESCs at the day 14 of differentiation via EB formation (Figure 4.27). Tnnt2 gene expression was at similar levels as the EBs d14, but Myh7 was found much lower. The Cx43 levels, in both differentiation conditions, were higher than that of the EBs d14.

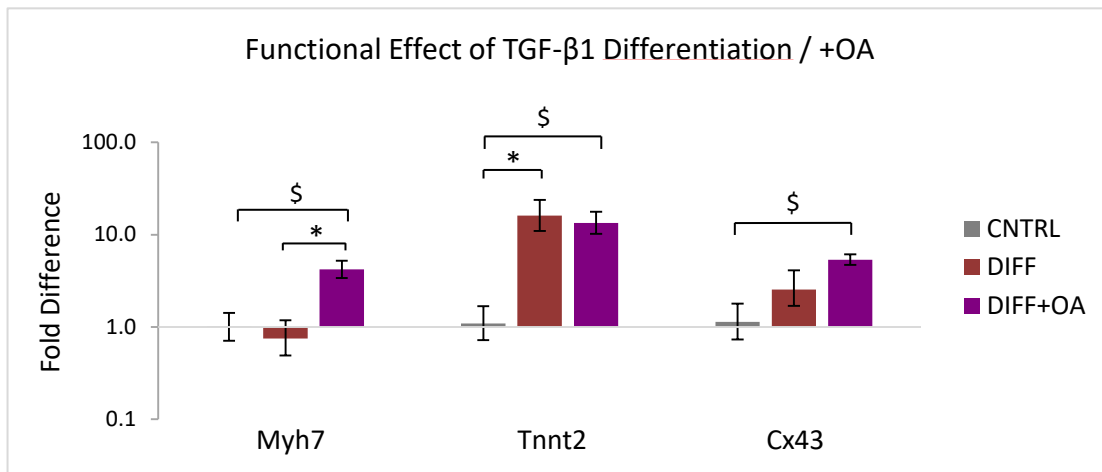


Figure 4.26. Effect of 1 week OA 300 μ M treatment post-differentiation on CTs at P4, compared to non-treated differentiated CTs and CNTRL undifferentiated CTs P4. (n=4, *p<0,02, \$p<0,01 compared to CNTRL, error bars: standard error)

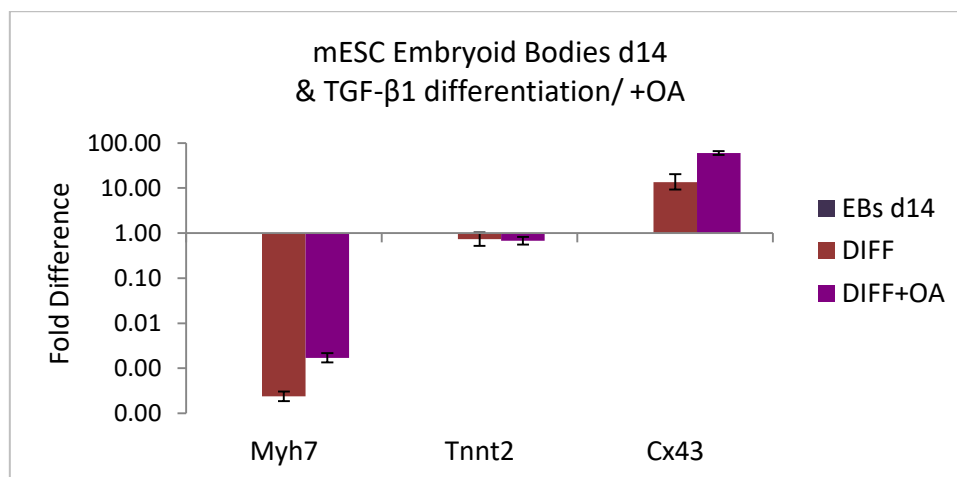


Figure 4.27. Gene expression levels of myocardial markers mESCs at d4, d7 and d14 of differentiation to CMs, normalized to EBs d14. (n=3 for DIFF and DIFF+OA, EBs: n=1, error bars: standard error)

Immunocytochemistry confirmed the expression of MHCb and TNNT2 in the differentiated CTs treated with OA (Figure 4.28). These cells were smaller than the undifferentiated controls and had formed clusters, as observed before (Figure 4.9.). Filamentous actin (fActin) staining, as well, to assess the shape and structural components of the cells, did not reveal CM shape or morphology, like striations (Figure 4.28).

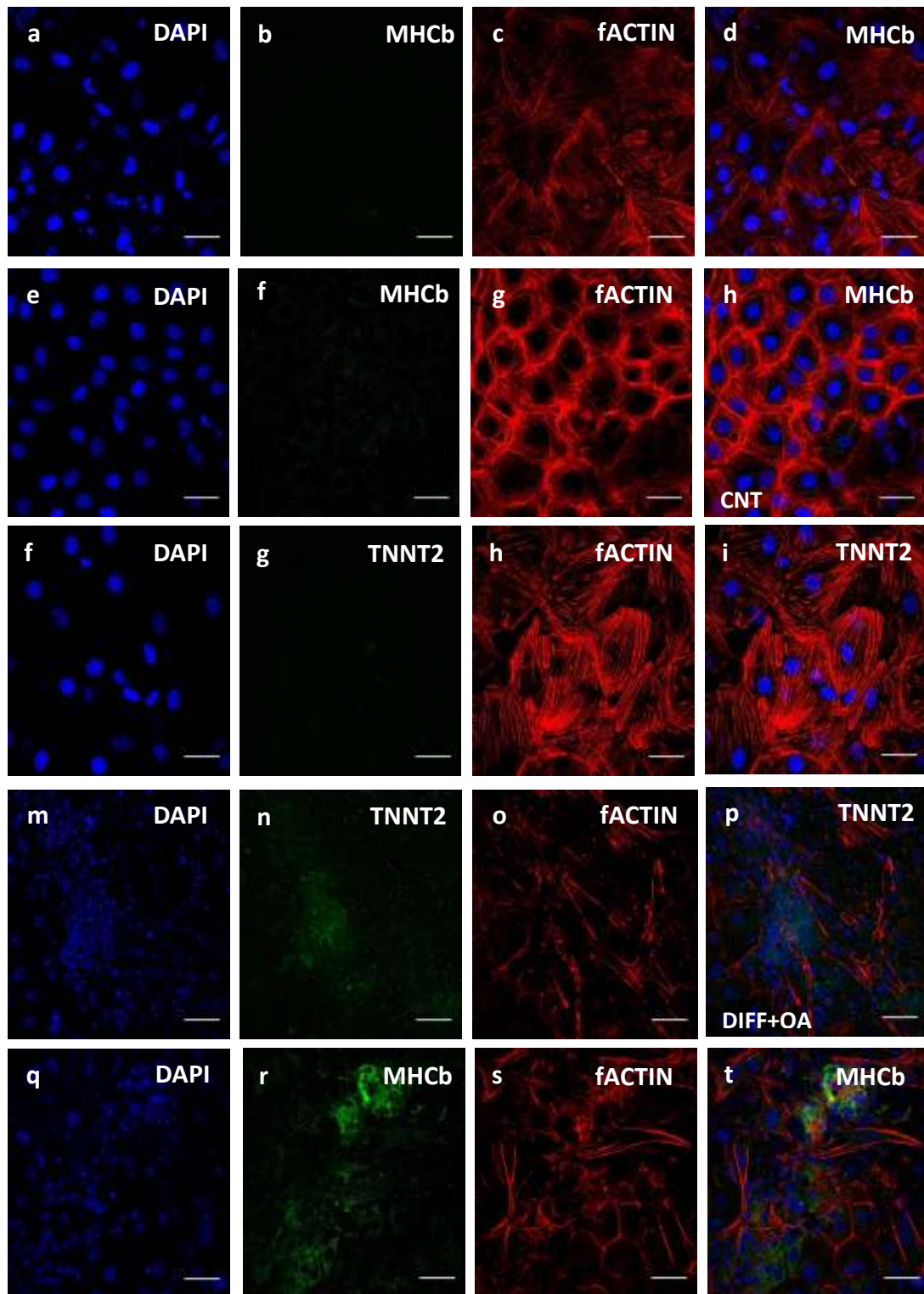


Figure 4.28. Differentiated CTs, with the TGF- β 1 protocol, followed by OA treatment 300 μ M for 1 week. Expression of MHCb and TNNT2 shown in green; a-d: negative control, m-t: differentiated CTs TGF- β 1+OA. (co-stained with DAPI, scale bars: 50 μ m)

Expression of metabolic genes after different differentiation conditions was assessed (Figure 4.29). The first interesting observation was that of the Pgc1 α - Ppara expression changes. To begin with, the TGF- β 1 protocol alone was sufficient to trigger gene expression increase of both Ppara and Pgc1 α . Further addition of OA for 1 week maintained the Ppara gene expression at the same level, but downregulated Pgc1 α expression.

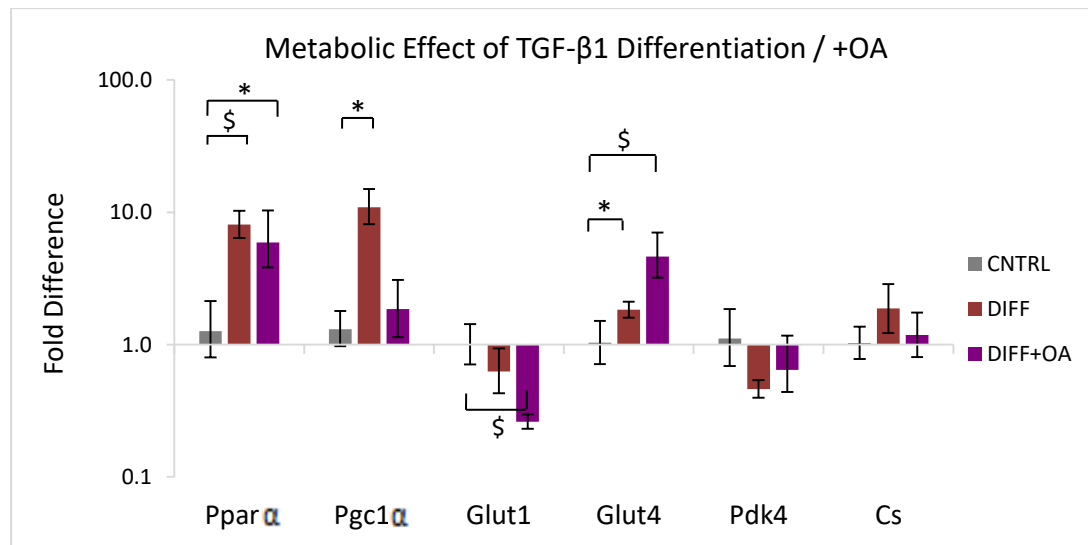


Figure 4.29. Metabolic effect of 1 week supplementation with OA 300 μ M post-differentiation on CTs, compared to non-treated differentiated CTs and CNTRL undifferentiated CTs, all at P4. (n=4, *p<0,05, \$p<0,01 indicating difference to CNTRL, error bars: standard error)

Glut1 gene expression was significantly downregulated after OA treatment, whereas a significant increase in Glut4 expression was observed after TGF- β 1 differentiation, which increased further following OA treatment. These changes, so far, suggested a metabolic maturation of the cells (more on Pgc1 α changes at Discussion 4.4.3). Pdk4 levels remained unchanged in both differentiation conditions, and did not increase as would be expected if there was upregulation in the FA oxidation pathway. Similarly to what was observed after OA treatment (Figure 4.15) on undifferentiated cells, Cs levels remained unchanged in both treatments. In addition, the protein levels of Cs were looked into, in differentiated cells with

subsequent OA treatment. The Western Blot analysis, did not demonstrated a significant increase (Figure 4.30).

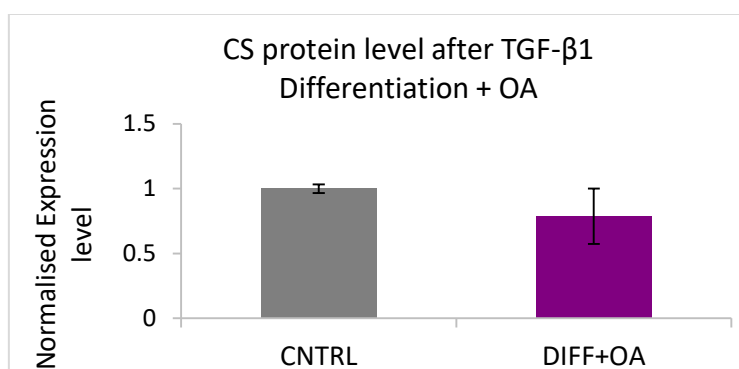


Figure 4.30. Protein levels of Citrate Synthase (CS) estimated by Western Blot analysis. Fold change of expression relative to the CNTRL samples.

To further understand the metabolic state, the levels of glucose oxidation were measured. The glucose oxidation rates were about 4 times more than those from CNTRL undifferentiated cells (Figure 4.31). This indicated that the DIFF+OA cells oxidized glucose at a higher rate, suggesting that the OA upregulated oxidative metabolism. Assessment of the mitochondrial membrane potential, with MitoTracker ® Red CMXRos, as before, suggested that there was an increase in the fluorescence between the CNTRL undifferentiated CTs and the DIFF+OA differentiated CTs (Figure 4.32).

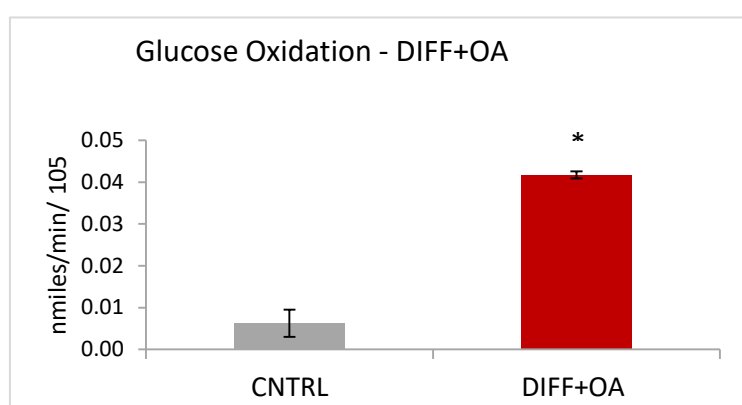


Figure 4.31. Effect of TGF- β 1 differentiation, followed by 1 week supplementation with OA 300 μ M, on the glucose oxidation levels, measured as nMoles/ min/ 10⁵ cells. Normalised to control untreated CTs. (n=3; *p<0,001 indicating differences amongst the groups, error bars: standard error).

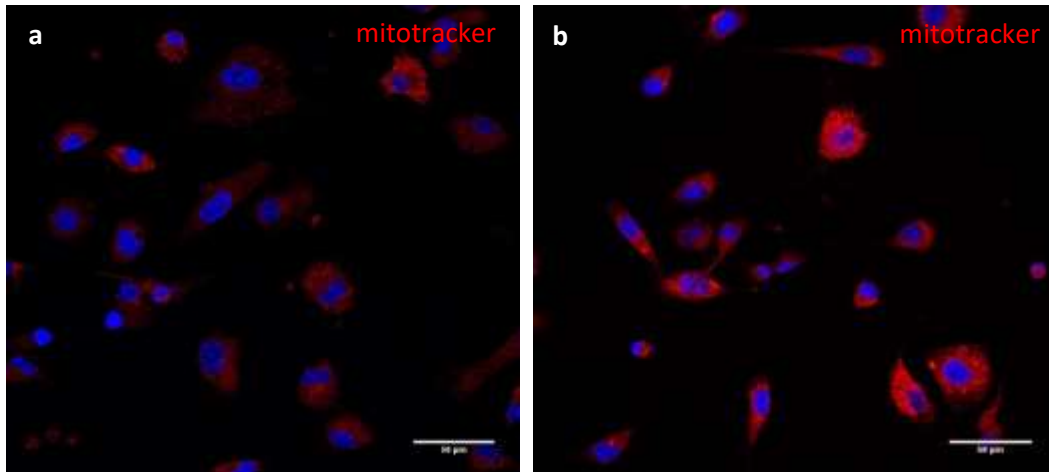


Figure 4.32. Effect of differentiation of CTs P4, followed by 1 week of OA 300 μ M, on cell mitochondria (b), compared with CNTRL undifferentiated cells (a). Both stained with MitoTracker® Red CMXRos. (scale bars: 50 μ m)

When the fluorescence intensity was calculated there was significant increase, indicating upregulated membrane potential in the differentiated group treated with oleic acid (Figure 4.33).

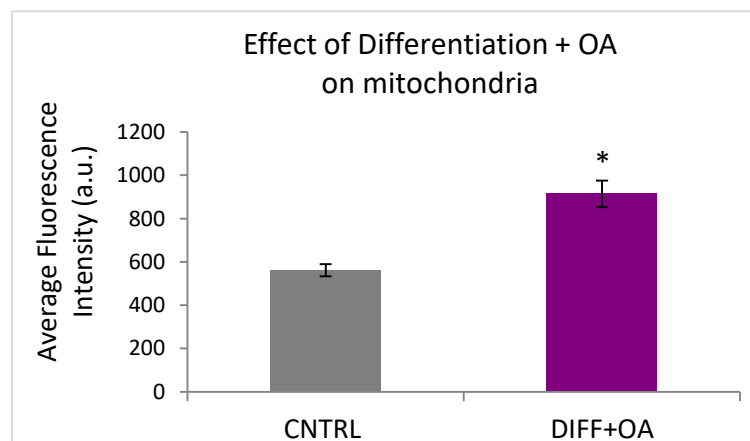


Figure 4.33. Effect of differentiation of CTs P4, followed by 1 week of OA 300 μ M, on cell mitochondria, estimated as average fluorescent intensity, after staining with MitoTracker Red CMXRos red. (n =20 cells, 2 repetitions, *p<0.01)

4.3.3.4. PROLONGED STIMULATION OF DIFFERENTIATED CTS WITH OLEIC ACID FOR 1 MONTH FURTHER MATURES DIFFERENTIATED CTS METABOLICALLY

Since the OA 300 μ M treatment of CNTRL cells for one month, showed the most promising results, in terms of metabolic changes (see Figure 4.15.) I investigated whether OA treatment pushes the cell differentiation further. To begin with the genetic changes of functional genes were checked (Figure 4.33.). Supplementation with 300 μ M OA for 1 month after TGF- β 1 differentiation resulted in significant upregulation of Cx43, whereas Tnnt2 and Myh7 did not change significantly, with the latter showing a slight decrease.

Finally, the metabolic changes that characterise the two conditions were looked into (Figure 4.34.). Both Pdk4 and Ppar α gene expression were significantly upregulated with long-term culture in OA-supplemented medium, post-TGF- β 1 differentiation. Cs gene expression did not change significantly.

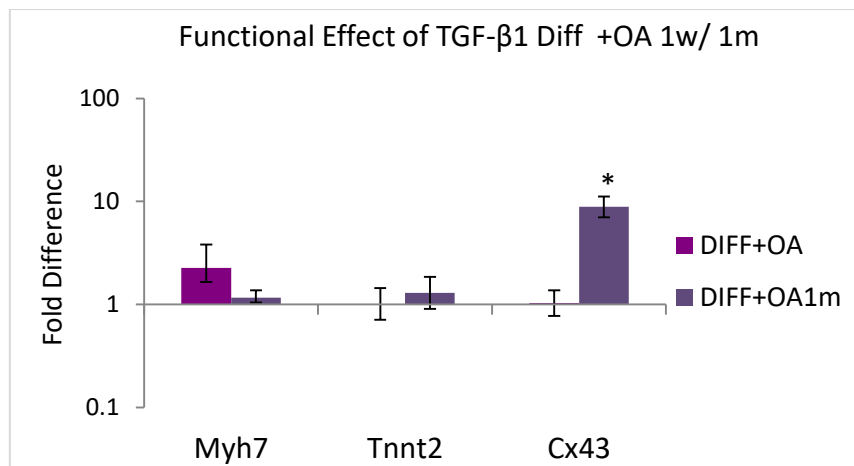


Figure 4.33. Effect of 1 month supplementation with OA 300 μ M post-differentiation of CTs at P4, normalised to 1 week supplementation of OA 300 μ M post-differentiation (n=4, *p<0,00001, error bars: standard error)

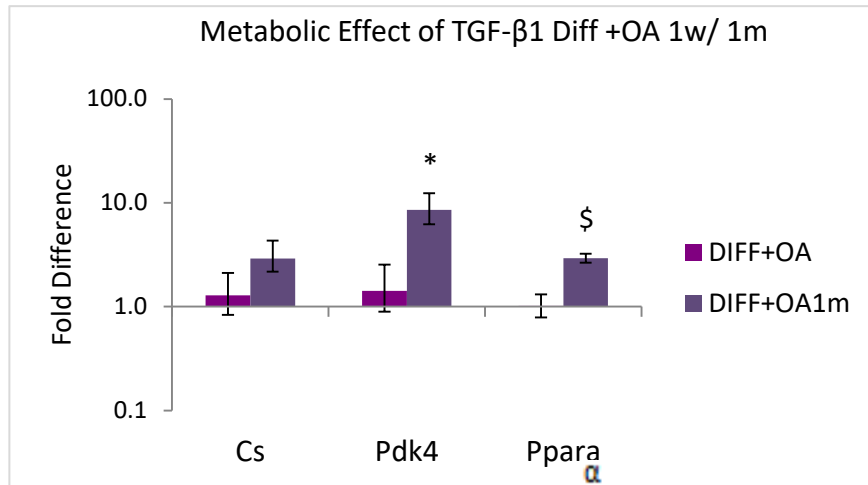


Figure 4.34. Metabolic effect of 1 month supplementation with OA 300 μ M post-differentiation on CTs, compared to 1 week supplementation on CTs at P4. (n=4, *p<0,05, \$p<0,01 indicating difference to DIFF+OA, error bars: standard error)

4.4. DISCUSSION

4.4.1. STAGES OF MESC DIFFERENTIATION VIA EMBRYOID BODY FORMATION

To evaluate the differentiation potential of the isolated adult atrial CPCs, I first aimed to identify the genetic changes that occur during successful *in vitro* differentiation to CMs. Based on previous work done by Prof. Paul Riley's group, differentiating mESCs were analysed at d4, d7 and d14 of differentiation, after which they are reported to be terminally differentiated. I observed that the gene expression of SC-markers (Oct4, Sox2, Ckit, Gata4) reduced, while transcription factors of the cardiac lineage (Nkx2.5, Isl1, Mef2c), the endothelial Flk1 (Figure 4.3) and genes characterising mature cardiac cells (Myh7 and Tnnt2) were upregulated (Figure 4.4). The gene expression of the fetal-tissue glucose transporter; Glut1 reduced, while Glut4 increased (Figure 4.4). Collectively these changes are following the expected pattern of markers of immature cell phenotype being downregulated, while those of mature cell phenotype upregulated (Table 4.3 & 4.4), as illustrated in the introduction (4.3 and Figure 4.4). This has been reported in studies of hESC differentiation^{34,463} and mESC^{322,464} into CMs, mentioning the upregulation of cardiac transcription factors, including GATA4, MEF2c and Nkx2.5, as well as cardiac markers MHCb and troponin^{322,219,465}. The downregulation of the gene expression of GLUT1 and upregulation of GLUT4, is a shift that has been reported in several studies, characterising the metabolic maturation of the cells^{466,467,468} (Figure 4.4). Finally, the CD36 and ACADM genes, related to FA metabolism, do not change substantially, since the fact that the cell medium does not have any lipids.

Looking into Ppar α and Pgc1 α expression (Figure 4.5), I saw that the former is upregulated at the end of differentiation (day 14), whereas the latter shows an increase at day 7 and then it decreases notably at day 14. This pattern could be explained by the need for upregulation of the mitochondrial metabolism early in the differentiating mESCs, which would require an increase in Pgc1 α gene expression (see Introduction 4.2.5). The involvement of both Ppar α and Pgc1 α in murine cardiac differentiation *in vitro* has been shown by different studies⁴⁶⁹.

Gene	Encoding Protein	Main Roles	Relevant expression sites	Ref.
Oct4	Octamer-binding transcription factor 4	maintenance of self-renewal & pluripotency, tumourgenesis, embryonic development	pluripotent SCs, progenitor cells	470, 471
Sox2	Transcription factor	maintenance of self-renewal & pluripotency, embryonic development	pluripotent SCs, progenitor cells	472, 472
Sca1	Cell surface protein	cell signalling	SCs, progenitor cells	101, 111
Ckit	Tyrosine-protein kinase, cytokine receptor	cell proliferation, survival	SCs, tumour cells	272, 113
Myh7	Myosin heavy chain beta (MHCb) "fast" isoform	cardiac muscle contraction	CMs	473, 474
Myh6	Myosin heavy chain alpha (MHCa) "slow" isoform	cardiac muscle contraction	CMs	475, 476
Tnnt2	tropomyosin-binding subunit of troponin complex	cardiac muscle contraction	CMs	477, 474
Cx43	Gap junction alpha-1 protein	intercellular communication, muscle contraction, development	CM gap junctions	478, 479
Desmin	type III intermediate filament	muscle cell function	striated muscles	480, 481

Table 4.3. Summary of the stem cell genes and the structural genes of cardiac lineage, characterising cardiac cells during development and differentiation.

In addition, initial low levels of $Ppar\alpha$, were demonstrated in undifferentiated ESCs by Ding L. *et al.*, that increased as beating clusters were formed³⁹¹, which

agrees with the increased levels at the day 14 samples. The involvement of these two genes in cardiac differentiation facilitates the shift to the oxidative metabolism that mature cells depend on³⁹⁵.

Gene	Encoding Protein	Main Roles	Relevant expression sites	Ref.
Glut1	Glucose transporter 1	glucose transportation	fetal tissues	482, 468
Glut4	Glucose transporter 4	glucose transportation	striated muscles	482, 468
CD36	Membrane scavenger receptor	FA transportation	striated muscles, capillaries	483, 484
Acadm	Acyl-CoA dehydrogenase	oxidation of FAs & amino acids	mammalian cells	485
Pdk4	Pyruvate dehydrogenase kinase	reduces pyruvate conversion to acetyl-CoA	mammalian cells	486
Cs	Tricarboxylic acid cycle enzyme	catalyses first step of TCA cycle	mammalian cells mitochondria	487
Pparaα	Transcription factor	promotes FA metabolism	liver, heart	488, 390
Pgc1α	Transcriptional coactivator	mitochondrial biogenesis & metabolism	liver, heart	489, 395

Table 4.4. Summary of metabolic genes involved in main metabolic pathways, investigated in this study

4.4.2. TGF- β 1 DIFFERENTIATION INCREASES EXPRESSION OF TNNT

In our differentiation study the TGF- β 1-based protocol, developed by the Goumans group, was selected based on previous studies in our lab (Dr. Kathy Pakzad and Dr. Filippo Perbellini; unpublished data). Signalling factors of the TGF- β 1 family, as well as 5-Aza, have been used by different groups and on different cell types (see Introduction Table 4.2.). The methods of assessment of

CPC differentiation, among the different studies reviewed in the introduction varies, but entails changes in cell morphology, as well as expression of markers such as Troponins, Myosin Heavy Chains and Connexins (see Table 4.5). In terms of cell morphology, various studies have shown that after a potential initial phase of cell death following the treatment with 5-Aza, the cells proliferate and differentiate^{108,333}.

Smits *et al.*²²⁰ observed multiple layers with different cell alignments and cell confluency, after the TGF- β 1 treatment. These reports agree with the observation of cell confluency in our differentiating cultures and the formation of cell clusters (Figure 4.6). Gene expression changed after TGF- β 1 differentiation showed significant upregulation of *Tnnt2* in the two different CPC groups (CTs and CDCs), but no changes in MHCb or Cx43 were observed (Figures 4.7, 4.8). Immunocytochemical analysis demonstrated accumulation of MHCb at the cell clusters that were formed during CT differentiation (Figure 4.9b). TNNT2 was observed, in CTs (Figure 4.9c), while the expression of the two proteins in CDCs was present, but weaker (Figure 4.10.c, d). Goumans *et al.*³²⁴ saw upregulation in Troponin, Cx43 and MHCb by staining and semi-quantitative RT-PCR, rather than RT-PCR. The observed pattern of MHCb expression (Figure 4.9d) in our study, may indicate that cells need to be highly confluent for efficient differentiation. Further to this, the cells were trypsinised before pelleting for RNA extraction. This did not work well with the cell clusters and clumps in the CT differentiated samples (Figure 4.6.), which may have been washed off or not been lysed efficiently (during RNA extraction), thereby producing conflicting results.

As we saw in chapter 3 both cell types express CD90, CDCs uniformly expressed it, while CTs had a subpopulation of Sca1⁺ /CD90⁻ cells. Interestingly, a study done on CDCs demonstrated that the CD90⁺ fraction differentiated less successfully to CMs than the CD90⁻ fraction⁴⁹⁰.

Differentiation approaches	studies	<i>in vitro</i> assessment of differentiation
TGF-β1 family	220	morphology, beating, staining: TnnI, a-SA
	324	morphology, beating, semi quantitative-PCR, staining: TnnI, MLC2, MHCb, a-SA, desmin, ANF, patch-clamp electrophysiology
	273	staining: TnnT, Cx43, a-SA expression
Oxytocin	293	morphology, beating, staining: TnnI, a-SA, Cx43 gap junctions, RT-PCR: reduction of Ckit & TERT, increase of Nkx2.5, Gata4, MHCb, TnnI
	329	morphology, beating, measurement of intracellular [Ca ²⁺], RT-PCR: Nkx2.5, Gata4, Mef2C, MHCa, MHCb, MLC2 & cardiac a-actin, staining: GATA4, ANF TnnT, a-SA, Cx43
	108	morphology, beating, staining: a-SA, GATA4, ANF, TnnT, MLC2v
5-Azacytidine	101	morphology, staining: a-SA, TnnI, Nkx2.5, MHCa, but not MHCb
	333	morphology, RT-PCR: increase of Nkx2.5, MHCb, cTnnT, ANP, desmin & decrease of Sox2, Nanog
	324	morphology, % of beating cells, RT-PCR & staining: TnnI, MLC2, MHCb, a-SA, desmin, ANF, staining for connexins at gap junctions, metabolic coupling; assessed by spreading of dye, patch-clamp electrophysiology, calcium-imaging
Dexamethasone	271	morphology, staining: a-SA, MHC, cardiac a-actin, contractile activity after electrical stimulation,
	87	morphology, staining: GATA4, Nkx2.5, Mef2, no sarcomeres, failed to contract even post-stimulation
	347	staining: a-SA, MHCb, TnnT, Cx43
	293	morphology, beating, staining: TnnI, a-SA, Cx43 at gap junctions, RT-PCR: reduction of Ckit & TERT, increase of Nkx2.5, Gata4, MHCb, TnnI
	97	staining: cardiac a-actinin & TnnT

Table 4.5. Main CPC differentiation studies and the methods for assessment of differentiation

4.4.3. OLEIC ACID SUPPLEMENTATION STIMULATES THE PPAR α PATHWAY AND METABOLICALLY MATURES CT CELLS

The hypothesis for manipulating the substrate availability of the cultured cells stemmed from the different layers of regulation that the Ppar α / Pgc1 α axis exerts during differentiation and maturation of metabolism (see Introduction 4.2.3., 4.2.5.). Based on our literature review, the various protocols of CPC differentiation focus on pharmacological reagents and cytokines, and do not refer to or take into account the substrate composition. This is a striking fact especially knowing how metabolic changes affect the function of the cells⁴³⁷ and how transition from glycolysis to FA oxidation affects cell maturation (see Introduction 4.2.8). The glucose concentration in culture media ranges from 5.5 mM - 25 mM, while there is no availability of lipids/ FAs (see Table 4.6).

Oleic acid was chosen for this a lipid substrates purpose in our study (see Introduction 4.2.4), at a range of non-toxic concentrations (Figure 4.11). Gene expression changes indicated that acute exposure (48 hours) to increasing concentrations of OA upregulated significantly Pgc1 α , without changes in Ppar α (Figure 4.12), but it was clear that both genes were upregulated when OA-treated cells were compared with the respective BSA controls (Figure 4.13). These results agree with studies showing that OA and FAs in general, activate the Ppar α pathway^{397,380}.

Based on the data so far the concentration of 300 μ M was selected and tested the metabolic effect of different lengths of incubation on CTs. Long term supplementation with OA leads to significant upregulation of Ppar α (Figure 4.15). Pgc1 α reached the maximum level of gene expression at 48 hours, as did Pdk4 which has been shown to be upregulated by Pgc1 α (Pgc1 α can induce the PDK4 gene expression in part through the interaction with the ERRA at the proximal part of the PDK4 promoter^{491,492,493}). Subsequently both decreased, but Pdk4 remained at significantly higher levels than the CNTRL samples. The response of the cells to OA addition induced upregulation of CD36, which mediates the uptake of fatty acids in a variety of cell types^{483,484}, at all of the investigated time-points (Figure 4.16).

Differentiation approaches	refs	main differentiation components	Glucose	FAs/lipid
TGF-β1 family	323, 324, 273	5 μ M 5-Aza, TGF- β 1 1 ng/ml, 10^{-4} M A.A. - IMDM/Ham's F12 GlutaMAX, 2% serum, 1% MEM amino acids, 1% insulin–transferrin–selenium	12.5 mM	0
Oxytocin	293	100 nM oxytocin acetate, 50 μ g/ml A.A., 2% serum, 1 μ M dexamethasone , beta-glycerol phosphate 10 mM, TGF- β 1, 5 ng/ml, BMP2 10 ng/ml, BMP4 10 ng/ml, Dkk1 150 ng/ml	5.5. mM	0
	329, 108	10% serum, 100 nm oxytocin	25 mM	0
5-Azacytidine	331	20% serum , 3 μ mol/L 5-Aza	25 mM	0
	332	1 - 112 μ mol/L 5-Aza	11 mM	0
	101	2% FBS, 3 μ M 5-Aza	5.5. mM	0
	333	10% FBS, 10 μ M 5-Aza	5.5. mM	0
	334	20% serum , 3 μ mol/L 5-Aza	25 mM	0
	324	5 μ M 5-Aza, MEM amino acids, insulin–transferrin–selenium, 10^{-4} M A.A.	12.5 mM	0
	335	3 & 10 μ M 5-Aza	25 mM	0
Dexamethasone	271, 87, 347	10% serum, 10^{-8} M dexamethasone	5.5 mM	0
	293	100 nM oxytocin acetate, 50 μ g/ml A.A., 2% serum, 1 μ M dexamethasone , beta-glycerol phosphate 10 mM, TGF- β 1, 5 ng/ml, BMP2 10 ng/ml, BMP4 10 ng/ml, Dkk1 150 ng/ml	5.5 mM	0
	97	10% serum, 10 nM dexamethasone	25 mM	0

Table 4.6. Main CPC differentiation studies and the media composition with glucose and FA concentration

The shift from Glut1 to Glut4 was similar to that seen with mESCs differentiation (Figure 4.4) and was consistent with cell maturation (4.4.1). Based on mitochondrial imaging, OA treatment seems to have an effect of mitochondrial membrane potential (Figures 4.17 & 4.18), which was significantly upregulated between 48 hours and 1 week of treatment (Figure 4.19). At this point it can be assumed that the OA treatment had an effect on mitochondrial activity, rather than the mitochondrial numbers, since CS was found unchanged even when the protein level was looked into (Figure 4.20). Citrate synthase differences in the estimated mRNA levels and enzymatic activity have been reported in studies⁴⁹⁴. So, the lack of changes in CS here could indicate no change in protein levels but there may have been increase in CS activity, since neither RT-PCR, nor the Western Blot conducted provide information about enzymatic activity. Both mitochondrial levels and activity are necessary for cell maturation⁴⁵⁵. When I looked into radio-labeled substrate utilisation, glucose oxidation was upregulated significantly at both 48 hours and 1 week of OA supplementation (Figure 4.21), indicating increase oxidative metabolism and suggesting a shift from Glycolysis, as expected in differentiating cells (see Introduction 4.2.5 & 4.2.8). All these changes suggested maturation of the OA-treated cells, but it was not enough to induce a differentiated phenotype to the cells (Figure 4.22).

4.4.4. PHARMACOLOGICAL TREATMENT WITH ICARIIN DOES NOT STIMULATE THE PPARA PATHWAY IN ATRIAL CPCS

Subsequently, the metabolic effect of the pharmacological agent Icariin was investigated, at non-toxic concentrations (Figure 4.23). There were no changes in Ppar α or Pgc1 α , contrast to what was seen with OA supplementation (Figure 4.24). There are only a few studies, so far, suggesting that Icariin stimulates the Ppar α pathway via a p38 MAPK mechanism⁴⁹⁵ (see Introduction 4.2.3), but other papers suggest that Icariin downregulates the expression of phosphorylated-p38 MAPK. Given the time-restrictions of this project and the positive results from OA treatment, further work on Icariin was not done.

4.4.5 STIMULATION WITH OLEIC ACID FOR 1 WEEK FURTHER MATURES DIFFERENTIATED CTS PHENOTYPICALY AND METABOLICALLY

To harness the metabolic maturation that was observed after 300 μ M OA treatment (see 4.3.3.1) the cell culture medium was supplemented for 1 week, following the TGF- β 1 differentiation protocol. The treated cells formed clusters, as seen with TGF- β 1 treatment and in published studies of TGF- β 1 differentiation²²⁰ (Figure 4.2.5). Gene expression changes revealed a more structurally mature phenotype, with *Tnnt2* remaining at higher levels than the CNTRL undifferentiated cells and both *Myh7* and *Cx43* (the first connexin to be expressed in developing mouse CMs⁴⁹⁶) being significantly upregulated (Figure 4.2.6). These changes in structural genes resemble more the observations of "successful" differentiation methods (see Table 4.5), than that which was achieved with TGF- β 1 differentiation alone. In addition, when the levels of myocardial markers of differentiated CTs were compared to mESCs at d14 of differentiation, *Tnnt2* levels were similar to that of the EBs d14 (Figure 4.2.7). *Myh7* expression was lower in the CTs, in both differentiation conditions, indicating that the differentiated CTs were not as structurally mature as EBs d14, but *Cx43* expression was higher. This have been the first study to compare the gene expression profile of mESCs and CPCs differentiated in vitro, in an attempt to assess the success of the differentiation. that Staining with fActin confirmed the change in cell size between undifferentiated CNTRL cells (Figure 4.28a,b) and the TGF- β 1+OA differentiated cells (Figure 4.28c,d) which are much smaller and formed clusters, was seen in MHCb accumulated cells (Figure 4.28c), but *TnnT2* imaging was less strong.

The profile of metabolic gene expression (Figure 4.29), after the two differentiation conditions, indicated that TGF- β 1 differentiation alone is enough to stimulate the *Ppara* α - *Pgc1* α pathway, as well as a shift from *Glut1* to *Glut4* gene expression, as seen during in our mESC differentiation (Figure 4.4, 4.5). As discussed before (4.4.1) *Ppara* α & *Pgc1* α are upregulated during differentiation, and the expression of *GLUT4* is higher in adult tissues. Addition of OA as a substrate after differentiation retained the levels of *Ppara* α , *Glut1* and *Glut4*, but led to a reduction in *Pgc1* α . This drop matches what was observed at d14 of mESC differentiation (Figure 4.4) and after long-term exposure of CNTRL cells

with OA (48h, compared to 1w and 1m; Figure 4.16). This suggests that Pgc1 α gene expression acts acutely and is not needed to be constitutively upregulated after changes have been induced. Alternatively, OA has been reported by one study in 2007 to suppress the expression of Pgc1 α levels in rat vascular smooth muscle cells⁴⁹⁷.

Cs gene expression levels did not change with any of the treatments, neither when checked at a protein level (Figure 4.30). Furthermore, glucose oxidation was significantly upregulated in the TGF- β 1-differentiated cells treated with OA, compared to untreated CNTRLs (Figure 4.31). Assessment of mitochondrial membrane potential indicated a significantly higher activity in the differentiated cells that were treated with OA (Figures 4.32 & 4.33), as seen after treatment on CNTRL cells (Figure 4.19). Taking these observations together I can suggest that OA treatment on differentiated cells leads to a moderate degree of structural and metabolic maturation, towards the cardiac lineage.

4.4.6. PROLONGED STIMULATION OF DIFFERENTIATED CTS WITH OLEIC ACID FOR 1 MONTH FURTHER MATURES DIFFERENTIATED CTS METABOLICALLY

Finally, given the time-dependent upregulation of metabolic genes after OA supplementation (Figure 4.15, 4.16) I was interested to obtain some preliminary data on the effect of 1 month treatment, after TGF- β 1 differentiation. The gene expression analysis showed significant upregulation of Cx43 (Figure 4.32) and the metabolic genes; Pdk4 and Ppar α (Figure 4.33). Despite these initial data being promising, more work needs to be conducted in order to understand whether this approach can mature the differentiated cells and on what level.

The lack of cell contraction in any of our differentiation studies and conditions could be because of the use of a mixed cell population, contrary to all other studies of CPC differentiation (Introduction; Table 4.2). The differentiation of CDCs, an established mixed-cell CPC population, to beating CMs¹²², was achieved after co-culture with neonatal CMs, or after transplantation in vivo^{498,499}. This suggests that successful initiation of contraction might be possible only in case of a homogenous, cell-sorted population. In any case, even in the initial report of

Goymans *et al.*³²⁴ only three of six clonally derived cell lines differentiated into spontaneous beating cells. *In vitro* contraction has not been robust even in other cell types, with Beltrami *et al.* failing to differentiate FACs sorted lin⁻kit⁺ rat CPCs⁸⁷ to a beating phenotype and Smith *et al.* observed a maximum rate of about 40%, dropping to 20% at day 14 of differentiation²⁹³.

To this date OA has been investigated on CNTRL cells *in vitro* and compared to saturated fatty acids, for its ability to act as an antioxidant and anti-inflammatory agent^{400,500}. In terms of differentiation, it has been used as a neurotrophic factor inducing neuronal differentiation in two studies^{501,502}, as well as in studies of maturation of mouse pre-adipocytes to adipocytes⁵⁰³. Its role as Ppar α ligand and activator has already been mentioned³⁸⁰ and the involvement of Ppar α /Pgc1 α in mESC differentiation to CMs^{221,504}, but there have been limited studies investigating substrate effects on cardiac differentiation. What is striking is the variability of glucose concentration among the differentiation studies (Table 4.6), especially bearing in mind that a glucose level of 25mM *in vivo* is considered hyperglycemic and leads to loss of mitochondrial networks^{505,506}.

The first report of supplementing the cell culture medium of a muscle cell type with OA takes us back in 1987, by Sauro *et al.*, investigating the oxidation rates between fatty acid-supplemented medium or normal medium, in short-term cultures of myoblasts, eventually concluding that the rate significantly increased after 6 days of cell growth⁵⁰⁷. A paper published in 2012 in Chinese²²², states in the abstract that "*fatty acid exposure after differentiation had no significant effects on differentiation of C2C12 and L6 myoblasts, while fatty acid exposure at 2 days before differentiation remarkably affected differentiation of the myoblasts*", but there was no way of assessing the study and contents properly. Finally, a study in 2013 demonstrated that oleic acid, but not long chain fatty acids, increased the expression of FA oxidation genes via a Pgc1 α -dependent mechanism, in skeletal muscle cells⁵⁰⁸.

This is the first study that combines analysis of the effect of FA supplementation *in vitro*, on both the Ppar α /Pgc1 α pathway, and on the functional and metabolic characteristics of the cells. It allows for a better understanding of the effect of fatty acids and the Ppar α in CPC differentiation towards CMs. The Ppar α pathway

was found stimulated by differentiation with TGF β 1. OA supplementation matured both control and differentiated cells metabolically. This opens the way for the development of a protocol that would allow for more efficient differentiation to mature CMs, from SCs.

5. ENHANCING THE POTENTIAL OF CARDIAC PROGENITORS WITH MICRORNAS

5.1. INTRODUCTION

5.1.1. STEM CELL THERAPY - ENHANCING CELL SURVIVAL

Cell retention directly affects the outcome of cell therapy²⁰¹ and, as described in Introduction 1.6., several studies have demonstrated massive loss of the transplanted cells shortly after administration to the infarcted heart^{199,200,197}. Approaches for the improvement of cell survival and engraftment are being actively investigated, involving pre-conditioning of the transplanted cells or the host tissue⁵⁰⁹. These will allow for increased adhesion, migration and survival of the donor cells or will induce endogenous CPC recruitment and long-term engraftment. In addition, bioengineered scaffolds that deliver and provide biomechanical support for the cells have shown promising results^{210,510}. For the purposes of this study, here we will focus on reviewing the main pre-treatment options for transplanted cells (for additional information refer to ^{202,511}). Among the methods employed, targeting adhesion molecules, like integrins and selectins to enhance engraftment of transplanted cells has been shown in bone⁵¹² and heart models⁵¹³. To enhance cell therapy, exposure to hypoxia via low rates of O₂ or the use of hypoxia-mimetic drugs can lead to enhanced cell migration^{514,515}, as well as survival^{516,517}. In addition, heat shock treatment has been demonstrated to improve cell survival of the transplanted cells in the infarcted area or to improve their therapeutic potential^{518,204}. Also, stimulating survival mechanism signalling, via preconditioning with different “therapeutic” kinases has been demonstrated⁵¹⁹.

5.1.2. MICRORNAS

MicroRNAs (miRNAs or miRs) are non-coding single-strand RNAs that post-transcriptionally regulate gene expression, by degradation and/or translational repression of the target mRNAs⁵²⁰. To this day, the human genome has been reported to encode for 1881 precursors and 2588 mature miRNAs, whereas the mouse genome for 1193 and 1915, respectively (miRBase v21 ⁵²¹). The target genes are predicted to be involved in almost every biological process⁵²², while individual miRs can affect many different target genes⁵²³.

The miRNA **biogenesis pathway** (Figure 5.1) begins in the nucleus with the transcription of a miRNA gene that leads to the formation of a primary miRNA transcript (pri-miRNA). The pri-miRNA is cleaved by the Drosha endonuclease,

which forms a complex with the DiGeorge syndrome Critical Region gene 8 (DGCR8), creating the precursor miRNA (pre-miRNA). The pre-miRNA hairpin is transported to the cytoplasm by Exportin 5 where cleavage by Dicer forms a miRNA duplex. One strand of it matures, known as guide (or lead) strand, and the other is degraded (passenger strand; marked usually by '*'). Argonaute proteins (Ago) bind to Dicer, interact with the miRNA duplex and induce the removal of one of the miRNA strands, preparing the complex to bind the target mRNAs⁵²⁴.

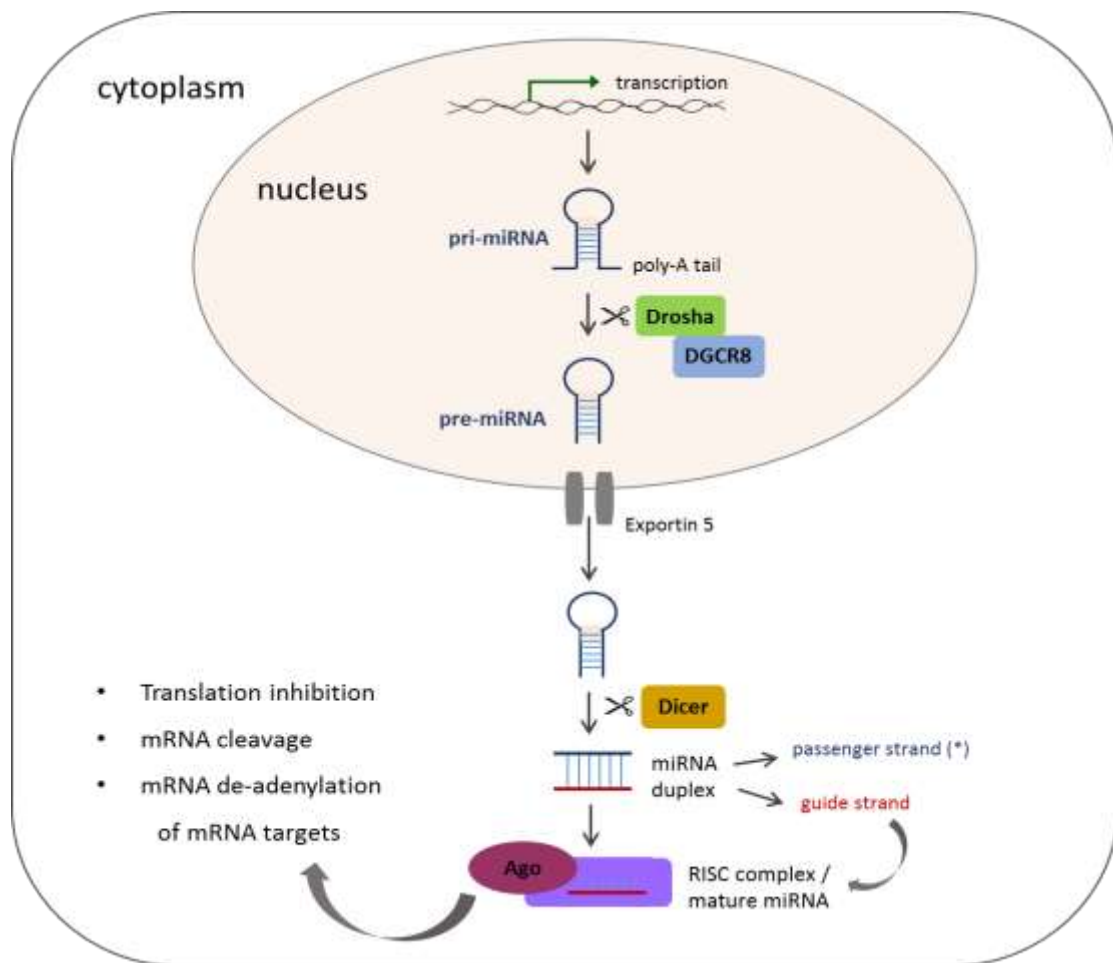


Figure 5.1. Schematic of the miRNA biogenesis pathway and the resulting effect of the mature miRNAs

5.1.3. IN SILICO ANALYSIS OF MIRNA TARGETS

As illustrated above, direct binding of the miRNA to the mRNA target is required for the post-transcriptional regulation to occur. MiRNAs bind to specific sites on the mRNA targets, that are commonly found within the 3'-untranslated region, but can also be found in the 5'-untranslated region⁵²⁵. The binding occurs by base-pairing of the nucleotides 2-7 of the miRNA "seed region"^{526,527} to the mRNA target.

Based on this knowledge, there are various online **bioinformatics tools** that allow for target recognition for all discovered miRNAs, with TargetScan⁵²⁸, PicTar⁵²⁹, Miranda⁵³⁰, and MirBase⁵³¹ being of the most popular ones (see also 2.18). The recognition algorithms vary but all take into account various criteria like; seed pairing, site number and site conservation among species, as well as pairing stability⁵²⁶. This does not exclude false-positives completely, therefore the use of these tools in combination is advisable. In addition, more sophisticated approaches take into account spatio-temporal expression of the miRNA and/ or the mRNA of interest, as well as any physical configurations that might affect the accessibility of the binding sequences⁵²⁷.

5.1.4. MIRNAS & THE HEART

MiRNAs have been shown to be **involved in** various aspects of the heart; from cardiac development to different clinical conditions^{532,533}. Studies in knock-out mouse models, deleting different key components of the miRNA biogenesis pathway (see Figure 5.1) led to gestational lethality and severe cardiovascular defects⁵³⁴. Recent studies demonstrate the key roles of miRNAs in numerous types of ischemic diseases, hypertrophy and heart failure (see reviews ^{535,536}).

Most miRNAs are expressed in a tissue-specific manner⁵³⁷. The most abundant ones in the heart are; miR-1, miR-133, miR-208a, -b, and miR-499^{533,538}. The levels of miRNAs, though, changes in different conditions making their use as biomarkers for different medical conditions a possible approach^{539,540}. More specifically, post-MI miR-29 gets downregulated⁵⁴¹ resulting in increased fibrosis, while miR-126 acts as a critical regulator of neovascularisation⁵⁴².

Mir-133 is found to be downregulated in the infarcted heart, and a study showed that MSC transfected with this oligonucleotide had increased survival and

improved therapeutic effect⁵⁴³. In 2011, Hu *et al.* reported that CPCs treated with a pro-survival cocktail of miR-21, miR-24, and miR-221 had increased retention and enhanced cardiac regeneration after transplantation *in vivo*. These are a few of the numerous recent studies suggesting miRNAs as a novel and promising therapeutic approach for MI treatment⁵⁴⁴.

5.1.5. MIRNA-210

The guide or leading strand of the miRNA-210 duplex; miR-210-3p was selected for this study. Initially miRNA-210 was referenced in 2008 by Ivan *et al.*, who introduced it as a hypoxia-inducible miRNA⁵⁴⁵ that also had a major role in different cancer types⁵⁴⁶. Later, lentivirus transfection of miR-210 in HL-1 CMs had a pro-angiogenic and anti-apoptotic effect, as well as improving cardiac function post-MI in mice⁵⁴⁷. Interestingly, human CPCs have been shown to secrete vesicles containing miR-210, with the potential to assist the heart post-MI⁵⁴⁸. MiR-210 levels are increased with hypoxia and studies demonstrate its proangiogenic properties in endothelial cells *in vitro*^{549,550}. Recent studies in March 2016, proposed that the levels of miR-210 in humans can act as an indicative factor in response to hypoxic environments or as a biomarker for peripheral artery disease^{551,552}, which support its initial hypoxia-related role. The results of these studies suggest that miR-210 should be further examined for a potential cardioprotective role in ischemia.

5.1.6. CELL DEATH IN VITRO

MI is followed by massive cell death (Introduction 1.6) for this purpose several scientific attempts, aiming to tackle this, study cell death *in vitro*. The most investigated cell death mechanisms in the heart are apoptosis, autophagy and necrosis (for review see⁵⁵³). **Apoptosis** is a type of programmed cell death that can be induced by an extrinsic or an intrinsic pathway, both showing distinct morphological changes. These changes involve: cell shrinkage, nuclear condensation and fragmentation, and membrane blebbing. The latter ends up in apoptotic body formation, which get phagocytosed and finally cleared, protecting the surrounding cells from imminent inflammation and necrosis⁵⁵⁴. Mechanistically, the extrinsic or death receptor-mediated pathway involves a

death ligand binding to a death receptor, such as the TNF-1 (Tumour Necrosis Factor-1) receptor or the Fas receptor (tumour necrosis factor receptor superfamily member 6), leading to APAF-1 (Apoptotic Protease Activating Factor 1) and procaspase-9 increase, and the activation of the effector caspases (like caspase-3)⁵⁵⁵. The intrinsic or mitochondrial apoptosis pathway, has the mitochondria as the key player involving Bcl-2 (B-Cell Lymphoma 2) and cytochrome c, APAF-1, with subsequent activation of the caspase cascade⁵⁵⁶. Despite apoptosis being a controlled type of cell death, post-infarction studies have demonstrated that it might contribute to the observed subsequent adverse remodelling^{557,558}. **Necrosis** is characterised by loss of cellular integrity, mitochondrial and cellular swelling, release of inflammatory immune components and enzymes, and cell lysis⁵⁵⁹. It can be caused by acute injury, prolonged ischemia and often follows apoptosis⁵⁵⁹. Necrosis is accompanied by infiltration of damage-associated-molecular-pattern molecules (DAMPs) and inflammation⁵⁶⁰. **Autophagy** is another type of programmed cell death (often linked to apoptosis⁵⁶¹), for degradation of unnecessary or malformed organelles and proteins. It involves intracellular organelles like the autophagosome and the lysosome as a final destination, with the formation of autolysosome leading to degradation⁵⁶². Apart from dysfunctional cellular constituents, autophagy can be triggered by hypoxia⁵⁶³ and nutrient starvation⁵⁶⁴. Key players of the pathway are the ATGs (Autophagy-related genes), ULKs (Unc-51 Like autophagy-activating Kinase) and mTOR (mammalian Target Of Rapamycin), the latter being an inhibitor of the process⁵⁶⁴. Despite being a cell death mechanism, autophagy is considered protective under stress conditions, like MI⁵⁶⁵. In contrast to necrosis and apoptosis, various amino acids and other molecules can be recycled by this catabolic mechanism for use in other processes. Autophagy occurs at basal levels under normal conditions in the heart, contributing to clearance. In the context of ischemia autophagy is upregulated. It is believed to act as a compensatory mechanism, triggered by low oxygen levels ameliorating adverse remodelling^{566,567}. These suggest that there are different roles of autophagy in the heart, depending on the conditions⁵⁶⁸. In addition, inactivation of autophagy reportedly triggers apoptosis in certain cell lines⁵⁶⁹.

In the last decade several other types of cell death have been identified, these mechanisms could either be distinct to apoptosis, autophagy and necrosis, or merely different stages of the development of those. Entosis⁵⁷⁰ involves cell-cell invasion and is common in cancer, while pyroptosis⁵⁷¹ is an inflammatory caspase-dependent cell death. Finally, paraptosis⁵⁷² was described in 2000 by Sperandio *et al.*, as a programmed cell death distinct from apoptosis, involving the formation of intracellular vacuoles. This mechanism involves caspase-9 and was shown to be IGF1R-induced^{572,573}. A similar morphology has been suggested in methuosis⁵⁷⁴, characterised by intracellular vacuolisation and dependent on the Ras pathway.

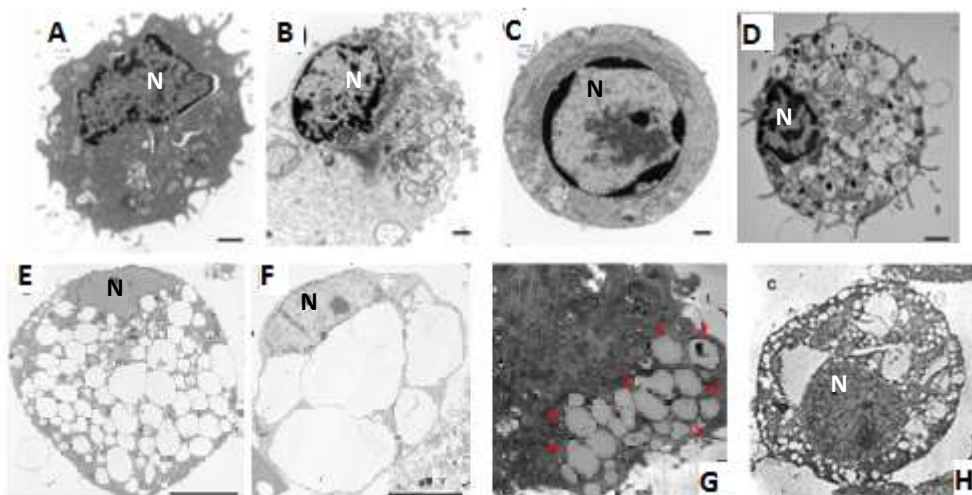


Figure 5.2. Morphological characteristics of A. a healthy cell, B. necrotic cell, C. apoptotic, D. autophagic, E., F. methuotic and G., H. paraptotic cell. Adapted from ⁵⁷⁵(for A-D), ⁵⁷⁴(for E & F), ⁵⁷⁶(for G), and ⁵⁷²(for H). N marks the nucleus, vacuoles can be seen in D-H

Autophagy, paraptosis and methuosis all display intracellular vacuoles, with the difference that the first displays apoptosis characteristics like nuclear fragmentation (see Figure 5.2).

The classification of cell death pathways based on morphological, biochemical and immunological factors, is not sufficient to characterise or explain the variety

of observed processes (under different conditions and tissues), nor does it cover the interplay and cross-regulation between the different types^{577,578}.

5.1.7. MIRNA DELIVERY

The levels of miRNAs can be efficiently artificially elevated by delivering miRNA “mimics”, which are commercially available synthetic oligonucleotides⁵⁷⁹. The efficacy of miRNA treatments is hindered by inherent obstacles such as low cellular uptake, poor *in vivo* stability and inappropriate compartmental distribution, therefore different methods for safe and targeted delivery are being explored^{580,581}. Biodegradable nanoparticles that are endocytosed by the cells, can be used as vector for the attachment of miRNAs²²⁴. A fluorine core would allow tracking of the delivery *in vivo*, by non-invasive imaging techniques, such as magnetic resonance imaging (MRI)⁵⁸². In 2012 Gomes *et al.* from the Carr group, developed a non-cytotoxic, biodegradable, FDA-approved nanoparticle (“NP170”) formed from poly-lactic acid-co-glycolic acid and perfluoro-1,5-crown ether; a fluorine compound that can be tracked using ¹⁹F-MRI. In a hind-limb ischemia study, they demonstrated that ECs treated with NP170s delivering miR-132 had higher survival and pro-angiogenic activity than cells without the miRNA. MiRNAs can be rapidly internalised by the NP170s, and remain within the endolysosomal compartment²²⁴, allowed for interaction of the miRNA with Ago which is necessary for its proper function (see Figure 5.1).

5.1.8. STUDY AIMS

As described in the Introduction (1.1 & 5.1.1) post-MI the heart suffers from loss of CMs and blood perfusion is restricted at the area of the scar. *In vivo* studies have reported that the number of cells surviving and engrafting at the injury-site after transplantation is miniscule. Improved survival of the cells and induction of neo-angiogenesis, via preconditioning, could enhance the cell therapy approach.

Therefore, in this chapter:

- I investigate the survival potential of both CTs and CDCs under serum starvation.
- I assess the neoangiogenesis potential of both cell types, via VEGF measurement.
- I attempt to label cells with the NP170s, for delivery of miRNAs.
- I investigate the effect of miRNA-210-3p transfection on the survival of CTs, under short-term and long-term serum starvation.
- I use preliminary analysis to introduce a potential, novel miRNA-210-3p target.

5.2. RESULTS

5.2.1. CONTROL CTS HAVE BETTER SURVIVAL POTENTIAL THAN CDCs UNDER SERUM STARVATION

To determine the anti-apoptotic effect of miR-210-3p (hereafter referred to as miR-210) no-serum conditions were used, to recapitulate the nutrient restriction in the infarct. Initially, the survival potential of control CTs and CDCs was analysed, in non-serum CEM medium for 72 hours and 10 days (see Methods 2.15). Removing serum from the cell culture medium hindered the growth of CTs, which, nevertheless, continued growing very slowly until the 10-day time-point (Figure 5.1a ,b, c).

The CDCs, on the other hand, started dying from the first 3 days and continued decreasing in number. So, after 3 and 10 days the CTs demonstrated superior survival potential (Figure 5.1a, b, c) (Figure 5.2).

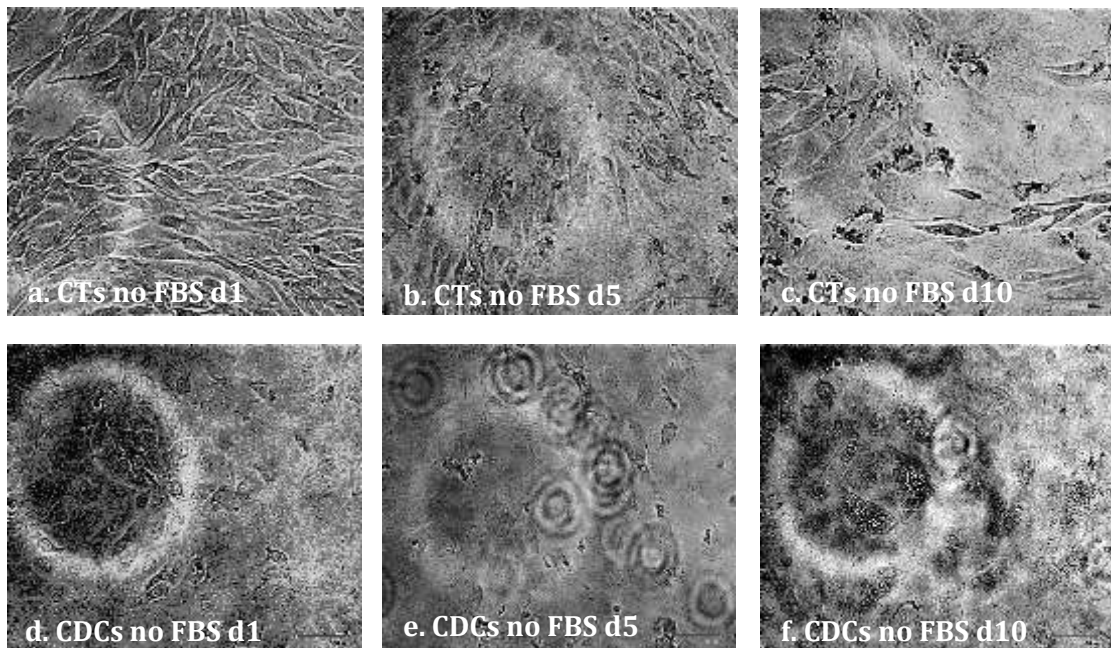


Figure 5.1. Cell morphology of CTs serum-starved for 1 days (a), 5 days (b), 10 days (c). CDCs serum-starved for 1 day (d), 5 days (e), 10 days (f). Scale bar: 100 um

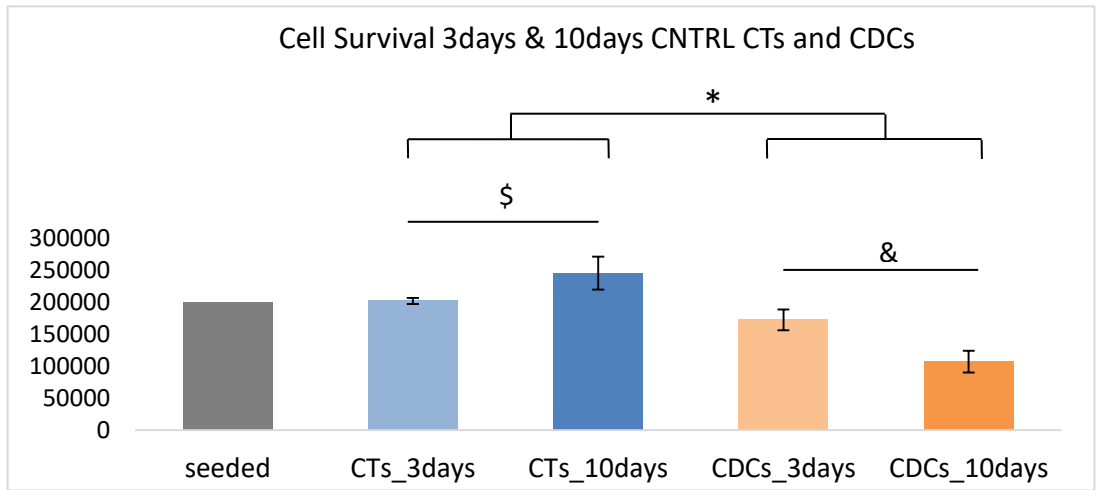


Figure 5.2. Cell Survival under serum starvation for 3 and 10 days, as assessed by cell counting, in control CTs and CDCs. (n=3, P4, *p<0.03, #p<0.01 in comparison to CTs; error bars: standard deviation)

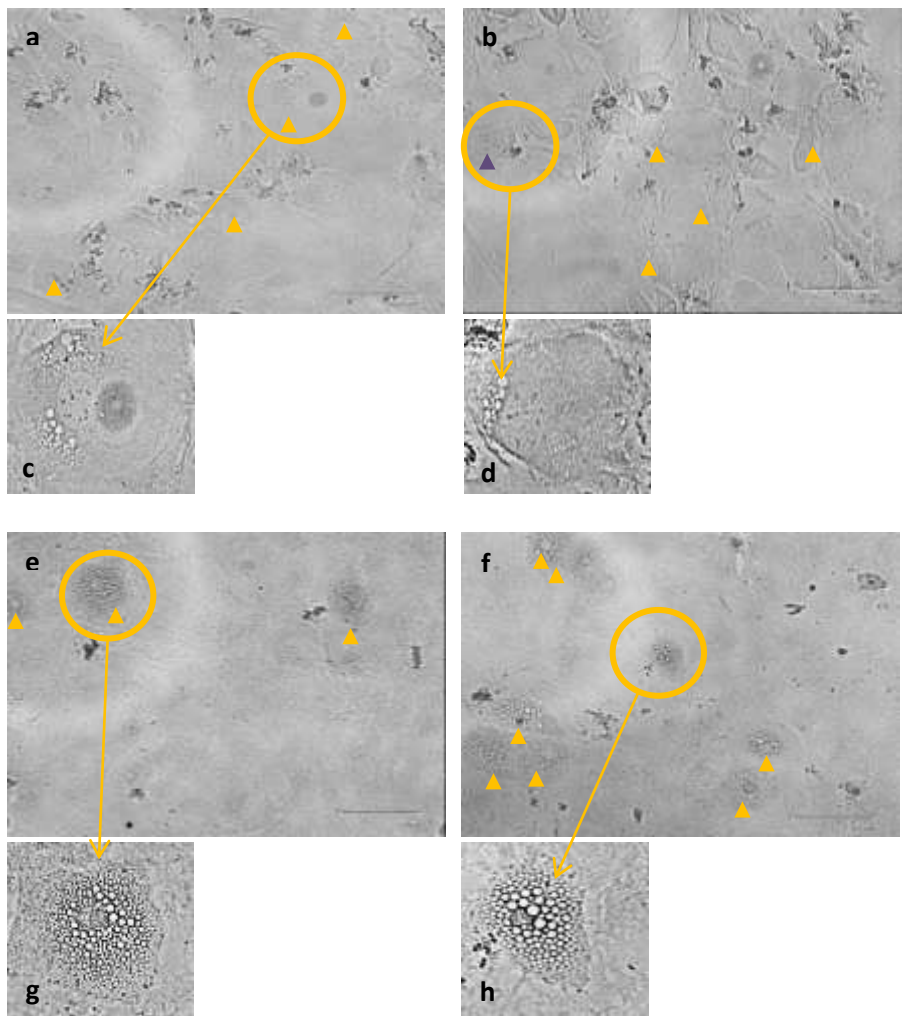


Figure 5.3. CTs (a-d) and CDCs (e-h) after 3 days of serum starvation. Signs of intracellular vacuoles observed, marked with yellow arrows. c,d and g,h: magnifications of vacuoles in a single cell. Scale bar: 100 um

5.2.2. NP170 NANOPARTICLES CAN EFFICIENTLY LABEL CTs

Based on the greater cell survival potential of the CTs in contrast to CDCs, under no-serum conditions, for the rest of the miR-210 experiments CT cells were used. To begin with, CT cells were transfected with the fluoresceinimine-NP170s (see Methods 2.14.1). Following the miRVana mimics guidelines the miRNA concentrations of 10 nM and 40 nM were tested. The miRVana mimic negative control 1, was used as a negative miRNA control to verify whether the transfection process itself, rather than the miRNA have an effect.

Imaging under fluorescent microscope confirmed the presence of NPs 72 hours after transfection, based on the green fluorescence of the fluoresceinimine (Figure 5.4).

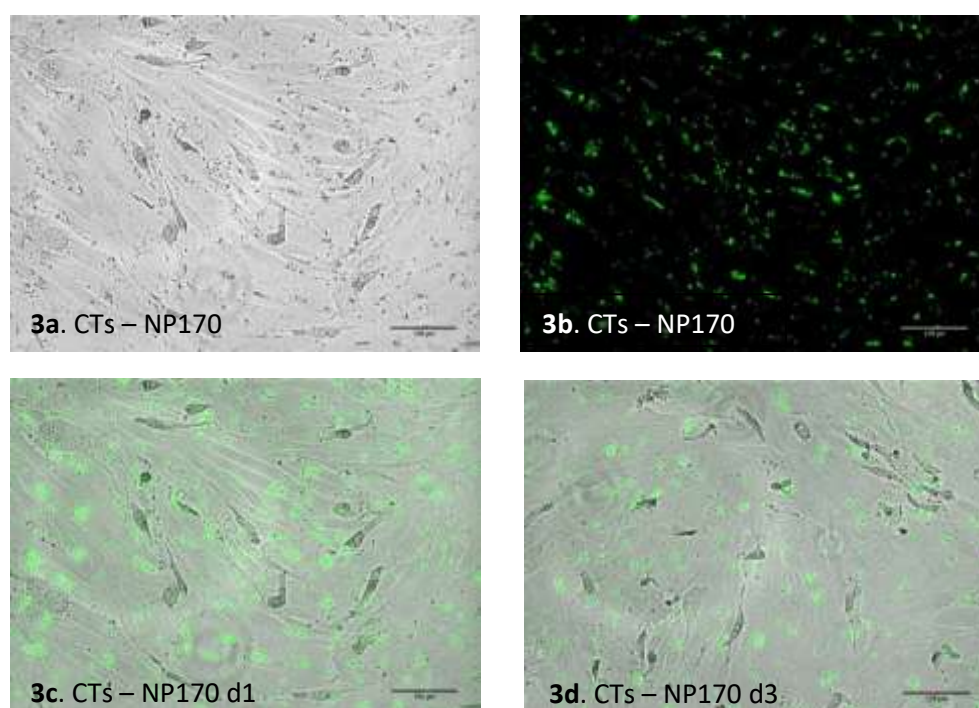


Figure 5.4. CTs transfected with NP170 nanoparticles carrying a GFP label; at day 1 of transfection (a, b, c). And at the end of 72 hours (d.), indicating retention of the NPs intracellularly. Scale bar: 125 um

To verify the labelling efficiency of the NP170s, Flow Cytometry was conducted at 2 hours, 6 hours, 24 hours post-transfection. MitoTracker® Red CMXRos was

used as a viability assessment. Based on these measurements (Figure 5.5) the incubation time of 6 hours was selected, with an efficiency of 85.1% alive and labelled cells (Figure 5.5B). Prolonged incubation for 24 hours did not result in superior labelling, instead the transfection conditions probably affected the cells negatively, resulting in 54% of labelled cell survival (Figure 5.5C) The use of the double dose gave the same results (data not shown).

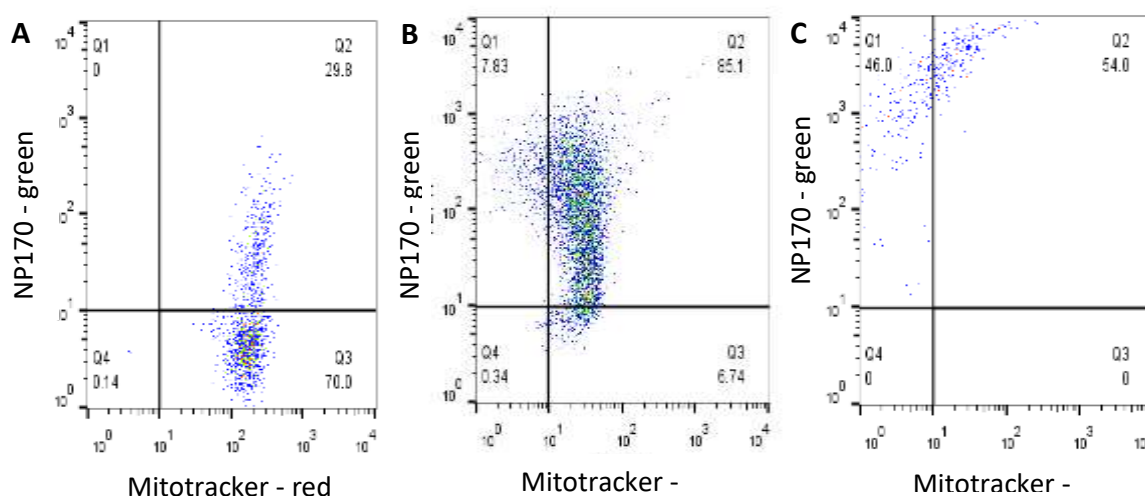


Figure 5.5. Indicative flow cytometry dot plots demonstrating the transfection yield and survival of the CTs, at 2 hours, 6 hours and 24 hours post-transfection, after incubation with the standard dose of NP170s (see Methods 2.14.1). FL1-H: fluoresceinimine fluorescence of NP170s and FL2-H: red fluorescence of MitoTracker® Red CMXRos. Q2 indicates percentage of alive and labelled cells.

5.2.3. MIR-210 INDUCES CT SURVIVAL SERUM STARVATION

To assess the protective effect that miR-210 could have under no serum conditions, CTs were transfected with a miR-210-3p mimic at 10 nM and 40 nM (see Methods 2.14.3). Both the commercial transfection reagent DharmaFECT formulation 1, and the NP170s (see Methods 2.14.2) were used.

The cell survival assessment showed no significant difference between the different miRNA conditions with the NP170-transfection method, whereas the

DharmaFECT transfection showed significant difference at the 40nM concentration of miR-210 in comparison to 10 nM or the negative-miRNA (Figure 5.6 and 5.7, respectively).

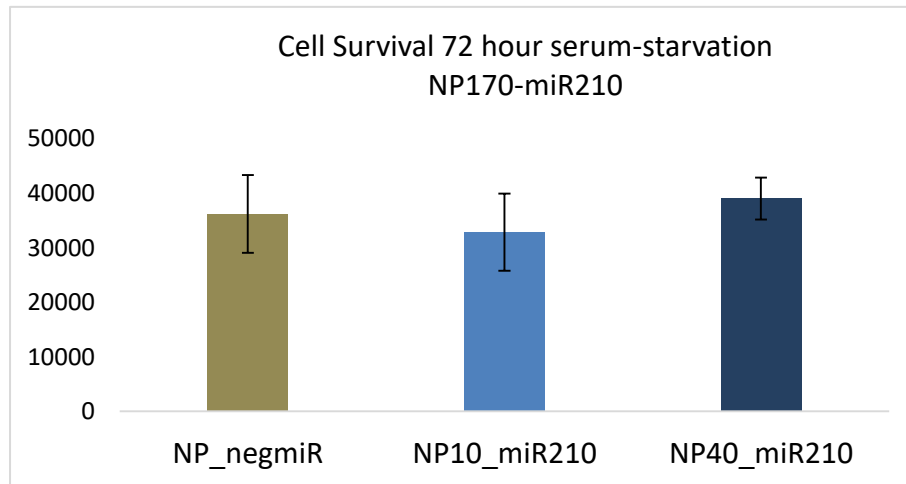


Figure 5.6. CT Survival under 72 hours serum starvation, after NP170 transfection with the miR-210, at 10 nM and 40 nM and with negative-miRNA, as assessed by cell counting. (n=3 CTs P4; error bars: standard deviation)

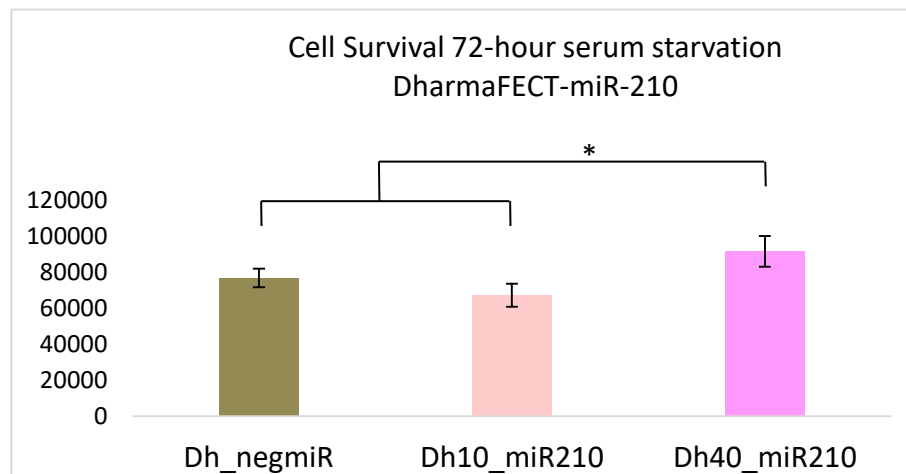


Figure 5.7. CT survival under 72 hours serum starvation, after DharmaFECT transfection with the miR-210, at 10nM and 40 nM and with negative-miRNA as assessed by cell counting. (n=3 CTs P4, *p<0,01 in comparison to miR210 40 nM; error bars: standard deviation)

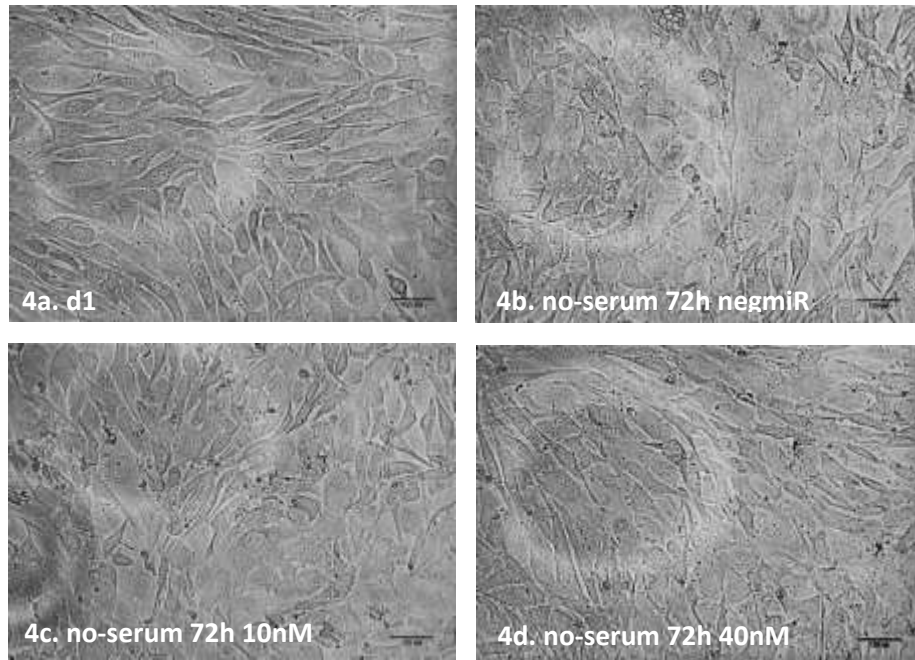


Figure 5.8. CTs transfected with DharmaFECT transfection; at day 1 (a) and after 72 hours (b, c, d). 4b. 72 hour transfection with the negative miR, 4c. 72 hour transfection with miR-210, 4d. 72 hour with 40 nM miR-210. Scale bar: 125 μ M

After contacting our collaborator who manufactured the NP, we were informed that the storage conditions used for this batch were not appropriate, and hence the protamine sulfate coating (see Methods Figure 2.5) integrity may have been jeopardised, hindering successful labelling.

For analysis of the long term pro-survival effect of miR-210, CTs were transfected with 10 nM and 40 nM miR-210 and subsequently were serum-starved for 10 days. The negative miRNA was used as a transfection control, as well as a negative (non-transfected CTs) and positive (20% serum media) control.

The negative control and the negative-miRNA condition showed the same results, confirming the fact that the DharmaFECT transfection alone does not have an effect (data not shown). In contrast, the cell number at both concentrations of miR-210 was significantly higher than the negative control or the negative-miRNA (Figure 5.9).

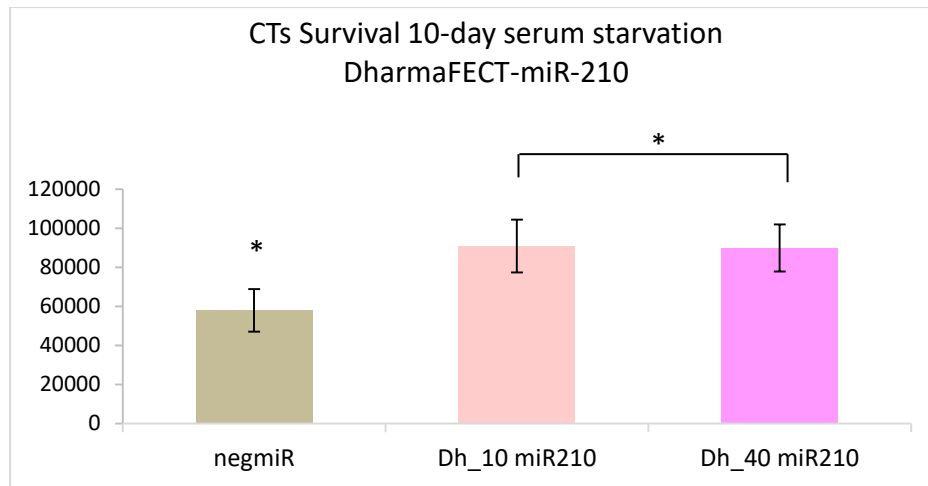


Figure 5.9. CT survival under 10 day serum starvation of CTs P4, transfected with 10 nM and 40 nM miR-210, using DharmaFECT (n=3, *p<0,05 ; error bars: standard deviation)

To further investigate the effect of miR-210 on CTs survival, the gene expression of caspases was analysed, in addition to the apoptotic assessment of activated caspases, after 72 hours of serum starvation. The gene expression levels of caspase-3 were significantly downregulated after miR-210 transfection, compared to negative miRNA transfection (Figure 5.10).

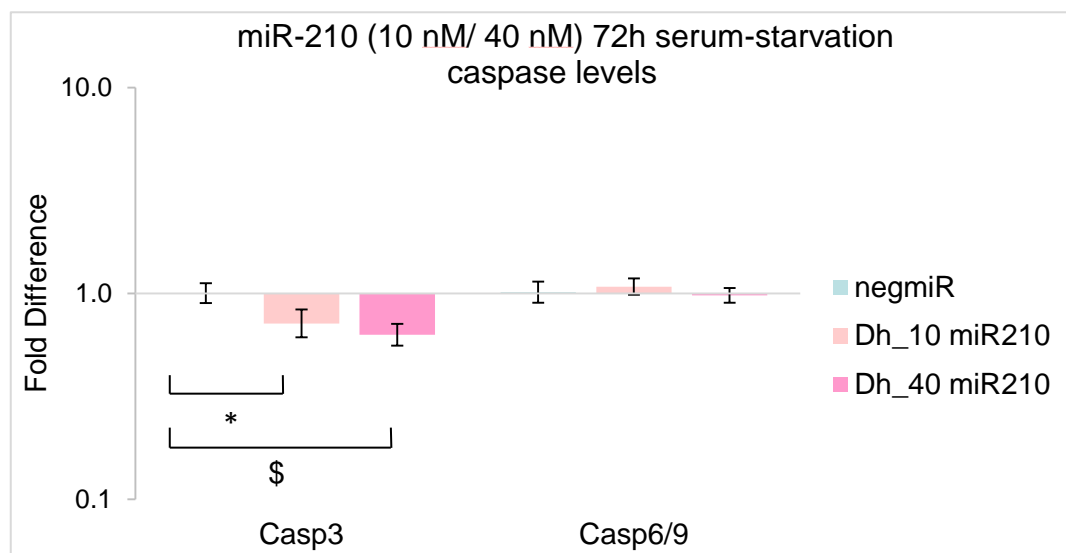


Figure 5.10. Gene expression of apoptosis-related caspases after transfection with negative miRNA or miR-210 at 10 nM and 40 nM (\$p<0,001, *p<0,04, n=4, error bars: standard error)

The activity levels of multiple activated caspases were estimated, using a commercial kit dye (see Methods 2.18), and we found that transfection with miR-210, at 40 nM, induced a reduction in their levels (Figure 5.11).

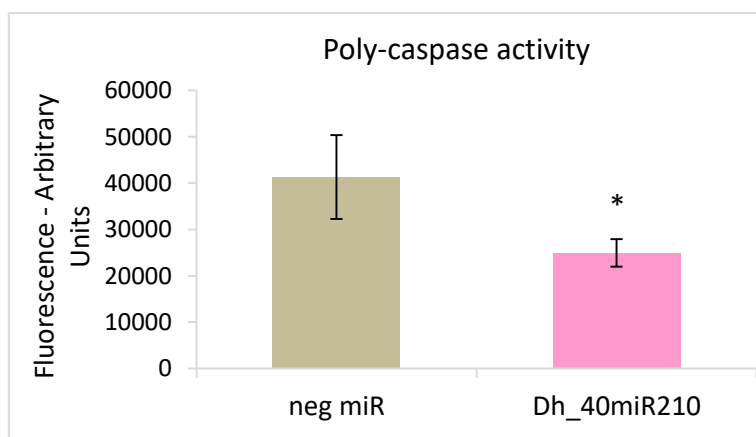


Figure 5.11. Poly-caspase activity levels ,after 72h of serum-starvation, in CTs transfected with the negative miRNA or miR-210 at 40 nM of serum-starvation. (* $p < 0.05$, $n = 4$, error bars: standard error)

5.2.4. IGFR1 SIGNALLING INVOLVED IN SERUM STARVATION DEATH – MIR-210 TARGET?

So far the data suggest that serum starvation of 72 hours induces cell death, involving apoptosis, and miR-210 can rescue the cells to a certain extent. Subsequently, the pro-survival effect of miR-210 was investigated, to understand the observed morphological changes that follow serum-starvation (see intracellular vacuoles, Figure 5.3). In an effort to understand the autophagy/paraptosis-like phenotype, the related genes were investigated. ATGs, ULKs and mTOR are key effectors of autophagy pathway, as well as IGFR-1 signalling which is involved in paraptosis (see 5.1.6).

To conduct a preliminary investigation and the effect of miR-210 on the survival effect, the aforementioned genes were checked with respects to being predicted targets of the miRNA. TargetScan and MicroCosm online bioinformatics tools were used, to cross-compare the results (see Methods 2.18, and 5.1.3).

Selecting the mouse miR-210-3p, using TargetScan we identified 32 mRNA transcripts with conserved sites (in the model species: human, mouse, chimpanzee, rhesus, cow, dog, opossum, chicken and frog), and 6 poorly conserved sites were suggested as targets. Microcosm identified 31 transcripts conserved among 8 model species, for the mouse miR-210.

Of the genes of interest neither ULKs nor mTOR were found as predicted targets (data not shown). Of the ATGs, ATG7 and ATG4C, as well as IGF1, IGFBP-3 and -5 of the IGFR1 signalling pathway were reported (see Table 5.1).

		Binding position of mmu-miR-210 on target mRNA	Predicted consequential pairing of target region (top) & miRNA (bottom)
TargetScan	IGF1	Position 5822-5828 of IGF1 3' UTR	5' ...GGAAUCUGGAUUACAACGCACAU... 3' AGUCGGCGACAGUGUGCGUGUC
	IGFBP5	Position 2348-2354 of IGFBP5 3' UTR	5' ...GUAUACCAUCACCCCGCACAAC... 3' AGUCGGCGACAGUGUGCGUGUC
	ATG7	Position 1503-1509 of ATG7 3' UTR	5' ...CUCUGUACAUUCUUUACGCACAG... 3' AGUCGGCGACAGUGUGCGUGUC
Microcosm	IGFBP3	Position 391-413 of IGFBP3 3' UTR	5' GUCGGCGACAGUGUGCGUGU 3' ...CAGATCTGTGTCTGATGCACA...
	ATG4C	Position 1078-1099 of ATG4C 3' UTR	5' AGUCGGCGACAGUGUGCGUGUC 3' ...TTAGGAGCTGAGACATGTACAG....

Table 5.1. Interactions of mouse miR-210-3p with the predicted targets: IGF1, IGFBP5, ATG7, IGFBP3, ATG4C, based on the TargetScan and Microcosm bioinformatics tools

Since the IGF1 signalling pathway components converge in the IGFR1 – IGF1 interaction, we checked the IGFR-1 gene expression levels with RT-PCR. As before, CTs were transfected with miR-210, and then serum-starved for 72 hours. The gene expression levels of IGFR-1 were found to significantly decrease

after miR-210 transfection, at both tested concentrations, compared to the negative miR control (Figure 5.12).

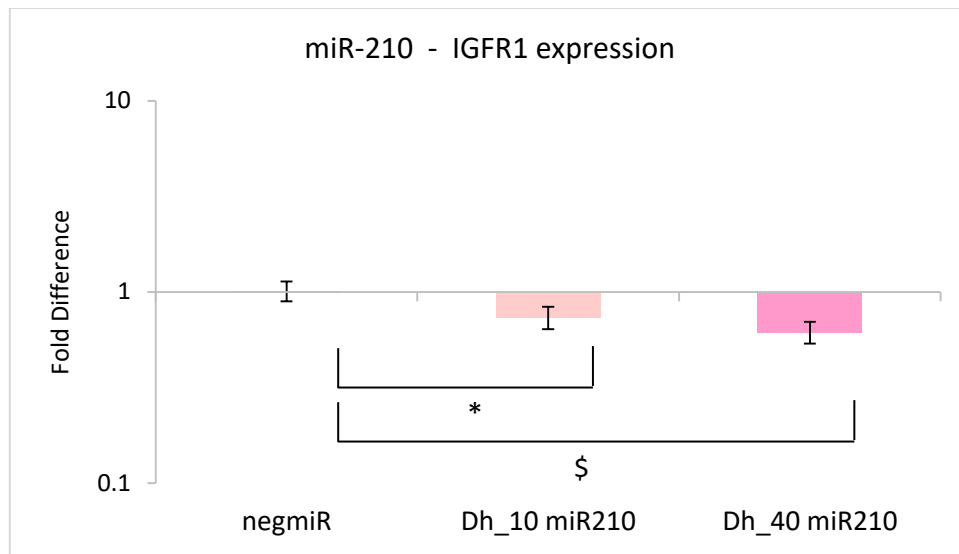


Figure 5.12. Gene expression of IGFR1 after transfection with negative miRNA or miR-210 at 10 nM and 40 nM (\$ $p < 0,001$, * $p < 0,04$, $n = 4$, error bars: standard error)

5.2.5. MIR-210 CAN INDUCE VEGF SECRETION FROM CTs

The ability of miR210 to increase VEGF secretion was assessed, in CTs and CDCs under ischaemic conditions. Initially, the VEGF secretion potential of both CDCs and CTs was checked. CDCs and CTs were serum-starved for 3 days, then the VEGF secretion over 24 hours was measured (see Methods 2.16). There was no significant difference between the two cell types. Even though the CDCs seemed to release more VEGF, the amount was more variable, in contrast to CTs (Figure 5.13).

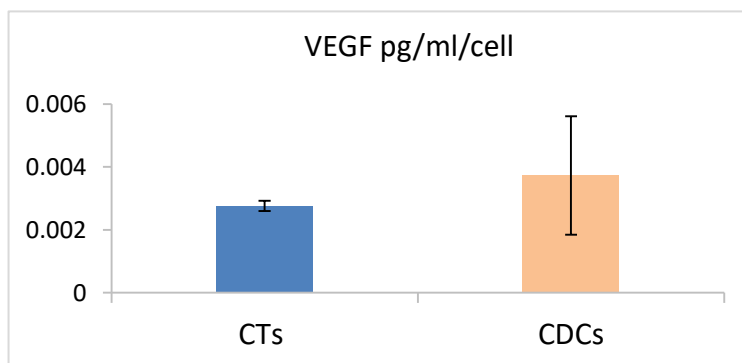


Figure 5.13. VEGF secretion in 24 hours, after 72 hours of serum starvation, of CDCs and CTs.

When CTs were transfected with miR-210, using DharmaFECT, an increase of VEGF secretion was observed after 72-hour serum starvation, compared to the transfection with the negative miRNA (Figure 5.14).

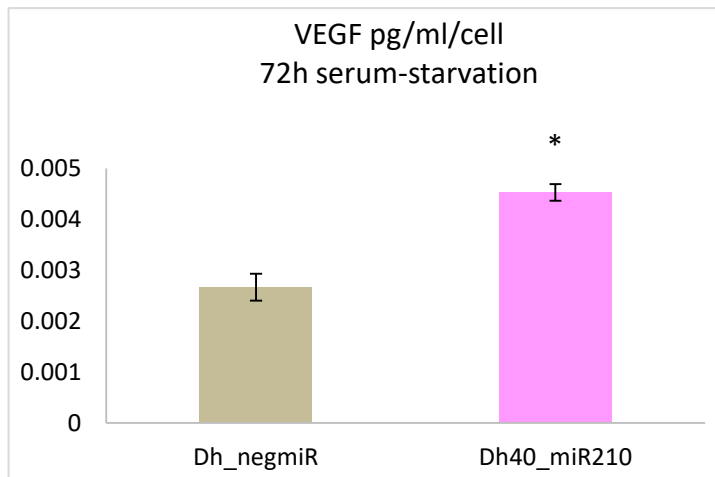


Figure 5.14. VEGF secretion (pg/ml/cell) in 24 hours, after miR-210 at 40 nM or negative-miR transfection. (n=3 CTs P4, *p<0,02 in comparison to miR-210 40 nM; error bars: standard deviation)

Finally, the amount of VEGF released by the CTs after 10 day serum starvation was checked. Interestingly, only the miR-210 at 40 nM showed a significant difference to the no-serum control, but the difference was abolished when compared to the negative-miRNA, which had very similar levels of expression to the miR-210 10 nM treatment (Figure 5.15).

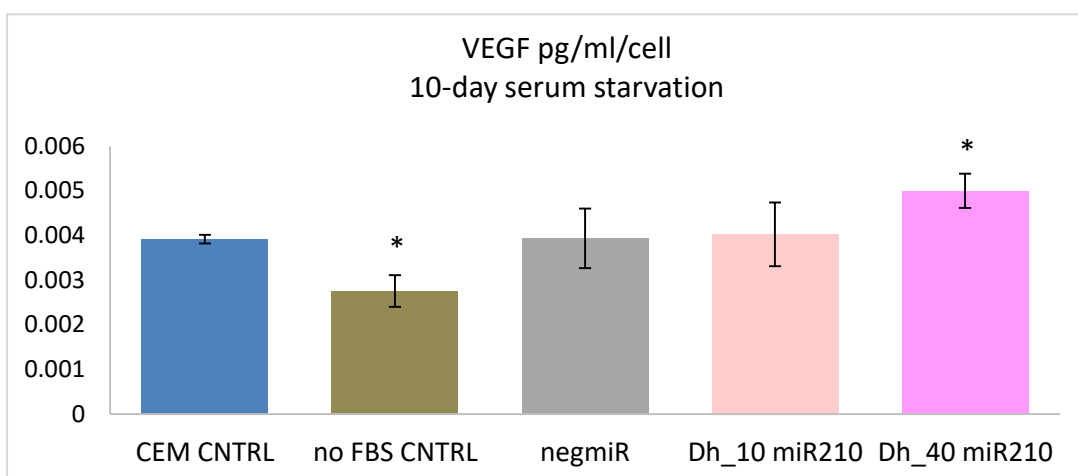


Figure 5.15. VEGF pg/ml/cell of CTs P4 transfected with 10nM and 40nM miR210, and subsequently serum-starved for 10 days. (*p<0,01 ; error bars: standard deviation)

5.3. DISCUSSION

5.3.1. CONTROL CTS HAVE BETTER SURVIVAL POTENTIAL THAN CDCs UNDER SERUM STARVATION

To study the issue of progenitor cell death *in vivo*, that occurs after transplantation in ischemic conditions, the combination of hypoxia and serum-deprivation is commonly used as an *in vitro* assay. Previous work from our group investigating the pro-survival effect of a specific miRNA against ischemia, on HUVECs, used a combination of 0.1% oxygen and no serum for 48 hours²²⁴. Progenitor cells are very different to terminally differentiated cells. The positive effect of hypoxia on the growth of SCs has been reported in studies. Indeed studies investigating the survival potential of MSCs have highlighted the importance of serum or nutrient deprivation in addition to hypoxia⁵⁸³, with some suggesting that if provided with nutrients, MSCs could survive hypoxia⁵⁸⁴. Given that serum withdrawal alone has been reported to induce apoptosis in several studies^{225, 585, 586}, we used that approach here.

The comparison of the two atrial progenitor cell types, CTs and CDCs, showed that the former were more tolerant to serum-starvation, at both 3 days and 10 days (Figure 5.2). Interestingly at the 3 day time-point CTs demonstrated hindered growth, whereas at the 10 day time-point they had a slow rate of growth. This was strikingly different to CDCs that were declining gradually in number during the length of the experiment (Figure 5.2). Such tolerance of harsh conditions has been observed before, with human umbilical cord MSCs being resistant to both hypoxia and serum deprivation⁵⁸⁷, and human adipose derived MSCs showing resistance to serum starvation⁵⁸⁸.

When we looked into the morphology of the serum-starved cells we observed intracellular vacuoles hinting at an autophagy- / paraptosis-related type of death (see 5.1.6 and Figure 5.3). Given that different cell death mechanisms operate in tandem, or regulate each other, this required further investigation (see below 5.3.3).

5.3.2. MIR-210 INDUCES CT SURVIVAL UNDER SERUM STARVATION

The pro-survival effect of miR-210 has been reported by several studies (see 5.1.5). In order to investigate its effect on CTs we decided to use the NP170

nanoparticles, that were designed by our collaborators (see 5.1.7). To compare the efficiency of the transfection and miRNA labeling, a commercial transfection kit; DharmaFECT was also used. Initially, fluoresceinimine-NP170s were used for transfection of CTs and we could observe retention of the green nanoparticles in the cells, after washing, for 72 hours (Figure 5.4) and we estimated that a 6 hour incubation was sufficient for efficient labeling (Figure 5.5). These results are similar to the labeling of HUVECs in the initial NP170 publication of Gomes *et al.*²²⁴, who used a 4-hour incubation and confirmed survival by the Mitrotracker CMXRos assay and FACS. Unfortunately, when we used NP170s for miRNA delivery the experiments showed no change (figure 5.6), and after communication with our manufacturer and collaborator we have strong concerns about the quality of the coating on the NPs used, that potentially hindered the miRNA loading on them (see Methods 2.14.2). The DharmaFECT-miRNA delivery showed positive results, with the highest concentrations of delivered miR-210 helping the cells survive better after the 72 hours of serum starvation, compared to both the lowest concentration and the negative control (Figure 5.7). Due to the difficulty of obtaining new NP170s and time constraints the commercial transfection approach was followed further. So, next the effect on 10-day serum-starved CTs was assessed and observed that both tested concentrations led to higher cell numbers than the CTs transfected with the negative miR (Figure 5.9). The prosurvival effect of miR-210 agrees with studies on rat BM-derived mesenchymal stem cells (MSCs) that were shown to be protected by ischemic preconditioning, via upregulation of miR-210⁵⁸⁹. Also when MSCs with overexpressed miR-210 or transfected with miR-210 were transplanted to infarcted heart, they transferred the miR-210 to the resident CMs and enhanced their survival⁵⁹⁰.

Subsequently, the cell death pathway in which miR-210 is involved was investigated. The apoptosis pathway was checked, based on the aforementioned papers suggesting that serum deprivation induces apoptosis. Indeed, both RT-PCR (Figure 5.10) and the polycaspase activity kit (Figure 5.11) showed that miR-210 transfection hindered apoptosis, since gene expression levels of effector caspase-3 and the activity of a combination of caspases was found reduced post-transfection, with 40 nM of miR-210. Indeed studies on BM-derived MSCs have

shown that miR-210 exerts its pro-survival effect by targeting the caspase-8-associated protein-2⁵⁸⁹. The lack of change of Caspase-9 (caspase-6/9), could be explained via a study stating that Caspase-9 plays a marginal role in serum starvation-induced apoptosis²²⁵. In any case caspase activity measurements are more reliable than gene expression analyses, as caspases get activated via proteolytic cleavage.

5.3.3. IGFR1 SIGNALING INVOLVED IN SERUM STARVATION DEATH – MIR-210 TARGET?

Serum starvation caused the formation of intracellular vacuoles (Figure 5.3), as commonly observed in autophagy or apoptosis (Figure 5.2). The characteristic morphology of both CTs and CDCs when cultured without serum could be because of autophagy, paraptosis or methuosis, therefore key players of these pathways were checked using bioinformatics target prediction tools (see 5.1.6). The autophagy-related proteins ATG-4C and -7 were predicted as targets by Microcosm and TargetScan, respectively.

What's more, we found that components of the IGFR1 pathway were identified as targets (Table 5.1). This signaling pathway has been reported to be involved in paraptosis⁵⁷³. IGF-1R gets activated by IGF1⁵⁹¹, and that in turn is modulated by IGFBPs. The IGFBP family has 6 members with a predominantly inhibitory role against IGF1, except for IGFBP-1, -3, and -5 known to stimulate IGF1 action⁵⁹². This suggested that miR-210 could exert its protective effect by blocking IGFR1 signaling, therefore we investigated further. To check this RT-PCR of IGFR1 levels was done and its gene expression was found decreased at both concentrations of the miRNA, compared to the negative control (Figure 5.12). This result is interesting because IGFR1 signaling is commonly inducing cell proliferation and is anti-apoptotic⁵⁹³. There has only been some evidence of IGFBP3 being pro-apoptotic⁵⁹³ and also IGFR1 being a player in the paraptosis pathway⁵⁷³, so results like ours are shedding further light in the multifaceted role of this signaling pathway in cell death.

A 2016 study by Wang *et al.*⁵⁵², from November 2015, demonstrated that inhibition of miR-210 expression improved the survival and cardiac function of MI mice. With the group where miR-210 levels were reduced demonstrating

improved cardiac function. Given the knowledge of the multiple roles of miRNAs and the cross-regulation of them by other, it comes at no surprise that the *in vitro* and *in vivo* results are occasionally clashing. This in any case does not render the use of miR-210 wrong, as a preconditioning agent *in vitro*.

5.3.4. MIR-210 CAN INDUCE VEGF SECRETION FROM CTs

Unless blood perfusion is restored at the area of the ischemic insult, the oxygen and nutrient supply will remain detrimentally low. Even with the use of cell therapy or other therapeutic agents, this condition will hinder regeneration, so the need for neoangiogenesis approaches is important. As a final point of interest, to support miR-210 as a pre-treatment approach in MI cell therapy approaches, the potential for neoangiogenesis was assessed. VEGF secretion estimated by ELISA, showed that there was no difference between CTs and CDCs (Figure 5.13). The miR-210 transfection of 40 nM led to an increase in the levels of secreted VEGF, after 3 and 10 days of serum starvation, compared to the negative miRNA transfection (Figure 5.14 and 5.15). This restored the levels of the growth factor to those of the control conditions (Figure 5.15) and did not increase them significantly more to that. The neo-angiogenesis effect of miR-210 in our study, agrees with reports from the literature on various cell lines (see 5.1.5).

All the above show that, CTs demonstrate good survival ability under low-serum conditions. In addition, miR-210 can be used as a preconditioning agent on CT cardiac progenitor cells, to protect them against apoptosis and non-apoptotic cell death (like paraptosis), and to stimulate VEGF secretion.

6. CONCLUSION

6.1. CONCLUSION

Our efforts in the field of cardiac stem cells could be resembled to the tale of “The men in the dark”. Based on the Indian story, a group of men enter a dark room to explore the features of an animal, the elephant. As each of them touches and described only one part of the animal, they compare notes and can not draw a uniform conclusion.

After more than a decade of research, the identity (and even existence) of the endogenous adult cardiac SC is still in question. Some scientists suggest that we are looking at the same cell population, but at different stages of development or activity (see quiescent VSELs or fibroblast/ activated myofibroblast). The use of different assessment techniques (see contradictory genetic lineage fate-mapping studies for Ckit cell analysis) and different culture conditions hinders the comparison of what happens *in vivo* and *in vitro*, and this is further confused by variability among animal models or even strains (see differences in explanting results among mouse strains).

In this thesis I attempt to develop a protocol for isolation of an adult atrial CPC population, independent of marker selection, which is highly proliferative and more homogeneous than the CDCs, that were being used hitherto. In an effort to “explore the whole elephant” I looked into the characteristics of populations that were found in the resulting digestion mix (strongly adherent CTs, VSEL-like cells). The CT population is of mesenchymal phenotype and expresses cardiac developmental markers. This is the first study, to our knowledge, that compares two isolation protocols from the same tissue of origin.

In an effort to assess the behaviour of the CPCs in an *in vitro* culture system that resembles the nutrient-restriction of the infarct, I found that CT cells survive better under serum starvation, than CDCs. In addition, the ability of miR-210 to enhance the CT survival and VEGF release gives encouraging data towards preconditioning CPCs prior to transplantation, with the hope to allow for better and long-term engraftment.

In addition, I demonstrated that fatty acid supplementation assists the maturation of CPCs for differentiation to CMs. To look at the whole picture, in terms of differentiation, I used a verified TGF- β 1 protocol and checked stemness and mesenchymal marker expression, as well as metabolic genetic profile and

radioactive metabolic assays. The data open the road for further studies that would allow the robust differentiation of CSCs to mature CMs. This is the first study, as far as I know, that holistically investigates molecular/cellular characteristics and the metabolism of an adult CPC population. Given that metabolic state affects marker expression and cellular function/ activity, I feel that it is of outmost importance to include metabolic assessments in the search of the endogenous cardiac progenitors.

6.2. STUDY LIMITATIONS

The efforts for characterisation of the isolated CTs would have been more complete with Flow Cytometry analysis or immunocytochemistry imaging at P0, when the cells have just attached following the 72-hour plating step. To complete this analysis a combination of different mouse hearts would have been required, to compile sufficient cells for the analysis. The characterisation at P0 would give us information about the initial cell types that survived the digestion and proliferated, giving rise to the population of CTs that the rest of experiments were conducted on. This would be useful because, as described in this thesis, the process of *in vitro* expansion alters the phenotype of the cells. It may be that some progenitor cells are lost between p0 and p2 and that might be retained with adjustment of the culture protocol.

Furthermore, time and funding constraints were a limiting factor at a couple of points in this study. It would have been interesting to have characterised all the different cell populations that the tested digestion solutions yielded. Furthermore, it would have been useful to acquire a new batch of nanoparticles “NP170” from our collaborators in Portugal, to transfect the cells with the NP170-miRNA complex. In both cases the time constraints did not allow for further investigation, and I was urged to focus on answering all the main questions of this study within the time I had available.

As explained below these points have been taken into consideration for the future work following this study.

6.3. FUTURE WORK

Study of the CTs is continuing in the Carr group. These cells should be characterised further by isolating and combining cells from different mouse atria

to yield enough cells for analysis at P0 using Flow Cytometry. In addition, an *in vivo* analysis of the regenerative potential of CTs, in comparison to CDCs, in a model of MI will allow for proper assessment of these cells in the context of cell therapy.

The valuable data on differentiation (Chapter 4) could be applied to optimise differentiation to CMs. Control CTs and iPSCs (that the Carr group also works with) could be treated with oleic acid prior to or during differentiation via the TGF β 1 protocol. Work in differentiating iPSCs within the Carr group, has shown that differentiation may be further matured by treatment with an agonist of the PPAR α pathway.

Based on the encouraging data from Chapter 5, the *in vivo* MI model could be used further to assess whether pre-conditioning CTs with miR-210 could increase their survival in the ischemic heart. This could be validated by revisiting the NP170 approach for labelling, which could allow us to use ^{19}F MRI to track the transplanted cells *in vivo*. Finally, based on preliminary analysis I have uncovered targets of miR-210, computationally, that would reveal another cell death mechanism that this miRNA potentially targets.

REFERENCES

1. Velagaleti RS, Pencina MJ, Murabito JM, et al. Long-term trends in the incidence of heart failure after myocardial infarction. *Circulation*. 2008;118(20):2057-2062. doi:10.1161/CIRCULATIONAHA.108.784215.
2. Go AS, Mozaffarian D, Roger VL, et al. Heart Disease and Stroke Statistics--2014 Update: A Report From the American Heart Association. *Circulation*. 2014;129(3):e28-e292. doi:10.1161/01.cir.0000441139.02102.80.
3. Fuster V. Global burden of cardiovascular disease: Time to implement feasible strategies and to monitor results. *J Am Coll Cardiol*. 2014;64(5):520-522. doi:10.1016/j.jacc.2014.06.1151.
4. Ezekowitz JA, Kaul P, Bakal JA, Armstrong PW, Welsh RC, McAlister FA. Declining In-Hospital Mortality and Increasing Heart Failure Incidence in Elderly Patients With First Myocardial Infarction. *J Am Coll Cardiol*. 2009;53(1):13-20. doi:10.1016/j.jacc.2008.08.067.
5. Dickstein K, Cohen-Solal A, Filippatos G, et al. ESC Guidelines for the diagnosis and treatment of acute and chronic heart failure 2008. *Eur Heart J*. 2008;29(19):2388-2442. doi:10.1093/eurheartj/ehn309.
6. Sutton MG, Sharpe N. Left ventricular remodeling after myocardial infarction: pathophysiology and therapy. *Circulation*. 2000;101(25):2981-2988. doi:10.1161/01.CIR.101.25.2981.
7. Hofstra L, Liem IH, Dumont EA, et al. Visualisation of cell death in vivo in patients with acute myocardial infarction. *Lancet*. 2000;356(9225):209-212. doi:10.1016/S0140-6736(00)02482-X.
8. Frangogiannis NG, Smith CW, Entman ML. The inflammatory response in myocardial infarction. *Cardiovasc Res*. 2002;53(1):31-47. doi:10.1016/S0008-6363(01)00434-5.
9. Epelman S, Liu PP, Mann DL. Role of innate and adaptive immune mechanisms in cardiac injury and repair. *Nat Rev Immunol*. 2015;15(2):117-129. doi:10.1038/nri3800.
10. Iyer R, Jung M, Lindsey M. MMP-9 Signaling in the Left Ventricle Following Myocardial Infarction. *Am J Physiol*. 2016;(Heart and Circulatory Physiology).
11. Ellen Kreipke R, Wang Y, Miklas JW, Mathieu J, Ruohola-Baker H. Metabolic remodeling in early development and cardiomyocyte maturation. *Semin Cell Dev Biol*. 2016;52:84-92. doi:10.1016/j.semcdb.2016.02.004.
12. Goldfinger JZ, Adler ED. End-of-life options for patients with advanced heart failure. *Curr Heart Fail Rep*. 2010;7(3):140-147. doi:10.1007/s11897-010-0017-5.
13. Kumar A, Cannon CP. Acute coronary syndromes: diagnosis and management, part I. *Mayo Clin Proc*. 2009;84(10):917-938. doi:10.1016/S0025-6196(11)60509-0.
14. Kumar A, Cannon CP. Acute coronary syndromes: Diagnosis and management, part II. *Mayo Clin Proc*. 2009;84(11):1021-1036. doi:10.4065/84.11.1021.
15. Kirklin JK, Naftel DC, Pagani FD, et al. Sixth INTERMACS annual report: A 10,000-patient database. *J Hear Lung Transplant*. 2014;33(6):555-564. doi:10.1016/j.healun.2014.04.010.
16. Perricone AJ, Vander Heide RS. Novel Therapeutic Strategies for Ischemic Heart Disease. *Pharmacol Res*. 2014;89:36-45. doi:10.1016/j.phrs.2014.08.004.
17. Toyoda Y, Guy TS, Kashem A. Present Status and Future Perspectives of Heart Transplantation. *Circ J*. 2013;77(5):1097-1110. doi:10.1253/circj.CJ-13-0296.
18. Laflamme M a, Murry CE. Heart regeneration. *Nature*. 2011;473(7347):326-335. doi:10.1038/nature10147.
19. Gersh BJ, Simari RD, Behfar A, Terzic CM, Terzic A. Cardiac cell repair therapy: a clinical perspective. *Mayo Clin Proc*. 2009;84(10):876-892. doi:10.1016/S0025-

- 6196(11)60505-3.
20. Vincent SD, Buckingham ME. How to make a heart. The origin and regulation of cardiac progenitor cells. *Curr Top Dev Biol.* 2010;90(C):1-41. doi:10.1016/S0070-2153(10)90001-X.
 21. Evans MJ, Kaufman MH. Establishment in culture of pluripotential cells from mouse embryos. *Nature.* 1981;292:154-156. doi:10.1038/292154a0.
 22. Smith AG. Embryo-derived stem cells: of mice and men. *Annu Rev Cell Dev Biol.* 2001;17:435-462. <http://www.ncbi.nlm.nih.gov/pubmed/11795272>.
 23. Qi X, Li T-G, Hao J, et al. BMP4 supports self-renewal of embryonic stem cells by inhibiting mitogen-activated protein kinase pathways. *Proc Natl Acad Sci U S A.* 2004;101(16):6027-6032. doi:10.1073/pnas.0401367101.
 24. Vallier L, Alexander M, Pedersen R a. Activin/Nodal and FGF pathways cooperate to maintain pluripotency of human embryonic stem cells. *J Cell Sci.* 2005;118(Pt 19):4495-4509. doi:10.1242/jcs.02553.
 25. Murry CE, Keller G. Differentiation of Embryonic Stem Cells to Clinically Relevant Populations: Lessons from Embryonic Development. *Cell.* 2008;132(4):661-680. doi:10.1016/j.cell.2008.02.008.
 26. Takahashi K, Yamanaka S. Induction of Pluripotent Stem Cells from Mouse Embryonic and Adult Fibroblast Cultures by Defined Factors. *Cell.* 2006;126(4):663-676. doi:10.1016/j.cell.2006.07.024.
 27. Takahashi K, Tanabe K, Ohnuki M, et al. Induction of Pluripotent Stem Cells from Adult Human Fibroblasts by Defined Factors. *Cell.* 2007;131(5):861-872. doi:10.1016/j.cell.2007.11.019.
 28. González F, Boué S, Izpisúa Belmonte JC. Methods for making induced pluripotent stem cells: reprogramming à la carte. *Nat Rev Genet.* 2011;12(4):231-242. doi:10.1038/nrg2937.
 29. Iglesias-García O, Pelacho B, Prósper F. Induced pluripotent stem cells as a new strategy for cardiac regeneration and disease modeling. *J Mol Cell Cardiol.* 2013;62:43-50. doi:10.1016/j.yjmcc.2013.04.022.
 30. Carpenter L, Carr C, Yang CT, Stuckey DJ, Clarke K, Watt SM. Efficient differentiation of human induced pluripotent stem cells generates cardiac cells that provide protection following myocardial infarction in the rat. *Stem Cells Dev.* 2012;21(6):977-986. doi:10.1089/scd.2011.0075.
 31. Lalit PA, Hei DJ, Raval AN, Kamp TJ. Induced pluripotent stem cells for post-myocardial infarction repair: Remarkable opportunities and challenges. *Circ Res.* 2014;114(8):1328-1345. doi:10.1161/CIRCRESAHA.114.300556.
 32. Mauritz C, Martens A, Rojas S V, et al. Induced pluripotent stem cell (iPSC)-derived Flk-1 progenitor cells engraft, differentiate, and improve heart function in a mouse model of acute myocardial infarction. *Eur Hear J.* 2011;32(21):2634-2641. doi:ehr166 [pii]\r10.1093/eurheartj/ehr166 [doi].
 33. Zhao T, Zhang Z-N, Rong Z, Xu Y. Immunogenicity of induced pluripotent stem cells. *Nature.* 2011;474(7350):212-215. doi:10.1161/RES.0b013e318232e187.
 34. Kehat I, Khimovich L, Caspi O, et al. Electromechanical integration of cardiomyocytes derived from human embryonic stem cells. *Nat Biotechnol.* 2004;22(10):1282-1289. doi:10.1038/nbt1014.
 35. Xue T, Cho HC, Akar FG, et al. Functional integration of electrically active cardiac derivatives from genetically engineered human embryonic stem cells with quiescent recipient ventricular cardiomyocytes: Insights into the development of cell-based pacemakers. *Circulation.* 2005;111(1):11-20. doi:10.1161/01.CIR.0000151313.18547.A2.
 36. Chong JJH, Yang X, Don CW, et al. Human embryonic-stem-cell-derived cardiomyocytes regenerate non-human primate hearts. *Nature.* 2014;510(7504):273-277. doi:10.1038/nature13233.
 37. Lee Y-K, Ng K-M, Lai W-H, et al. Calcium homeostasis in human induced

- pluripotent stem cell-derived cardiomyocytes. *Stem Cell Rev.* 2011;7(4):976-986. doi:10.1007/s12015-011-9273-3.
38. Satin J, Itzhaki I, Rapoport S, et al. Calcium handling in human embryonic stem cell-derived cardiomyocytes. *Stem Cells.* 2008;26(8):1961-1972. doi:10.1634/stemcells.2007-0591.
 39. Brito-Martins M, Harding SE, Ali NN. Beta(1)- and Beta(2)-Adrenoceptor Responses in Cardiomyocytes Derived from Human Embryonic Stem Cells: Comparison with Failing and Non-Failing Adult Human Heart. *Br J Pharmacol.* 2008;153(4):751-759. doi:10.1038/sj.bjp.0707619.
 40. Spradling A, Drummond-Barbosa D, Kai T. Stem cells find their niche. *Nature.* 2001;414(November):98-104. doi:10.1038/35102160.
 41. Li L, Xie T. Stem cell niche: structure and function. *Annu Rev Cell Dev Biol.* 2005;21(1):605-631. doi:10.1146/annurev.cellbio.21.012704.131525.
 42. Scadden DT. The stem-cell niche as an entity of action. *Nature.* 2006;441(7097):1075-1079. doi:10.1038/nature04957.
 43. Wagers AJ, Weissman IL. Plasticity of adult stem cells. *Cell.* 2004;116(5):639-648. doi:10.1016/S0092-8674(04)00208-9.
 44. Prockop DJ. Marrow Stromal Cells as Stem Cells for Nonhematopoietic Tissues. *Science (80-).* 1997;276(5309):71-74. doi:10.1126/science.276.5309.71.
 45. Ding D-C, Shyu W-C, Lin S-Z. Mesenchymal stem cells. *Cell Transplant.* 2011;20(1):5-14. doi:10.3727/096368910X.
 46. Orlic D, Kajstura J, Chimenti S, et al. Bone marrow cells regenerate infarcted myocardium. *Nature.* 2001;410(6829):701-705. doi:10.1038/35070587.
 47. Tomita S, Li RK, Weisel RD, et al. Autologous transplantation of bone marrow cells improves damaged heart function. *Circulation.* 1999;100(19 Suppl):II247--56. http://circ.ahajournals.org/cgi/content/full/100/suppl_2/II-247.
 48. Dai W, Hale SL, Martin BJ, et al. Allogeneic mesenchymal stem cell transplantation in postinfarcted rat myocardium: short- and long-term effects. *Circulation.* 2005;112(2):214-223. doi:10.1161/CIRCULATIONAHA.104.527937.
 49. Jackson KA, Majka SM, Wang H, et al. Regeneration of ischemic cardiac muscle and vascular endothelium by adult stem cells. *J Clin Invest.* 2001;107(11):1395-1402. doi:10.1172/JCI12150.
 50. Carr C a, Stuckey DJ, Tatton L, et al. Bone marrow-derived stromal cells home to and remain in the infarcted rat heart but fail to improve function: an in vivo cine-MRI study. *Am J Physiol Heart Circ Physiol.* 2008;295(2):H533-H542. doi:10.1152/ajpheart.00094.2008.
 51. Nygren JM, Jovinge S, Breitbach M, et al. Bone marrow-derived hematopoietic cells generate cardiomyocytes at a low frequency through cell fusion, but not transdifferentiation. *Nat Med.* 2004;10(5):494-501. doi:10.1038/nm1040.
 52. Alvarez-Dolado M, Pardal R, Garcia-Verdugo JM, et al. Fusion of bone-marrow-derived cells with Purkinje neurons, cardiomyocytes and hepatocytes. *Nature.* 2003;425(6961):968-973. doi:10.1038/nature02069.
 53. Loffredo FS, Steinhauser ML, Gannon J, Lee RT. Bone marrow-derived cell therapy stimulates endogenous cardiomyocyte progenitors and promotes cardiac repair. *Cell Stem Cell.* 2011;8(4):389-398. doi:10.1016/j.stem.2011.02.002.
 54. Fisher SA, Doree C, Taggart DP, Mathur A, Martin-Rendon E. Cell therapy for heart disease: Trial sequential analyses of two cochrane reviews. *Clin Pharmacol Ther.* 2016. doi:10.1002/cpt.344.
 55. Fisher SA, Zhang H, Doree C, Mathur A, Martin-Rendon E. Stem cell treatment for acute myocardial infarction. *Cochrane database Syst Rev.* 2015;9:CD006536. doi:10.1002/14651858.CD006536.pub4.
 56. Nowbar AN, Mielewicz M, Karavassilis M, et al. Discrepancies in autologous bone marrow stem cell trials and enhancement of ejection fraction (DAMASCENE): weighted regression and meta-analysis. *BMJ.* 2014;348:g2688.

- doi:10.1136/bmj.g2688.
57. Taylor D a, Atkins BZ, Hungspreugs P, et al. Regenerating functional myocardium: improved performance after skeletal myoblast transplantation. *Nat Med*. 1998;4(8):929-933. doi:10.1038/nm0898-929.
 58. Reinecke H, Murry CE. Transmural replacement of myocardium after skeletal myoblast grafting into the heart: Too much of a good thing? *Cardiovasc Pathol*. 2000;9(6):337-344. doi:10.1016/S1054-8807(00)00055-7.
 59. Menasché P. Skeletal Myoblasts as a Therapeutic Agent. *Prog Cardiovasc Dis*. 2007;50(1):7-17. doi:10.1016/j.pcad.2007.02.002.
 60. Ghostine S, Carrion C, Souza LCG, et al. Long-term efficacy of myoblast transplantation on regional structure and function after myocardial infarction. *Circulation*. 2002;106(12 Suppl 1):I131-6. doi:10.1161/01.cir.0000032889.55215.f1.
 61. Reinecke H, MacDonald GH, Hauschka SD, Murry CE. Electromechanical coupling between skeletal and cardiac muscle: Implications for infarct repair. *J Cell Biol*. 2000;149(3):731-740. doi:10.1083/jcb.149.3.731.
 62. Ferreira-Cornwell MC, Luo Y, Narula N, Lenox JM, Lieberman M, Radice GL. Remodeling the intercalated disc leads to cardiomyopathy in mice misexpressing cadherins in the heart. *J Cell Sci*. 2002;115(Pt 8):1623-1634.
 63. Reinecke H, Poppa V, Murry CE. Skeletal muscle stem cells do not transdifferentiate into cardiomyocytes after cardiac grafting. *J Mol Cell Cardiol*. 2002;34(2):241-249. doi:10.1006/jmcc.2001.1507.
 64. Lipinski MJ, Biondi-Zoccai GGL, Abbate A, et al. Impact of Intracoronary Cell Therapy on Left Ventricular Function in the Setting of Acute Myocardial Infarction. A Collaborative Systematic Review and Meta-Analysis of Controlled Clinical Trials. *J Am Coll Cardiol*. 2007;50(18):1761-1767. doi:10.1016/j.jacc.2007.07.041.
 65. Menasché P, Alfieri O, Janssens S, et al. The myoblast autologous grafting in ischemic cardiomyopathy (MAGIC) trial: First randomized placebo-controlled study of myoblast transplantation. *Circulation*. 2008;117(9):1189-1200. doi:10.1161/CIRCULATIONAHA.107.734103.
 66. Brickwedel J, Gulbins H, Reichenspurner H. Long-term follow-up after autologous skeletal myoblast transplantation in ischaemic heart disease. *Interact Cardiovasc Thorac Surg*. 2014;18(1):61-66. doi:10.1093/icvts/ivt434.
 67. Pittenger MF. Multilineage Potential of Adult Human Mesenchymal Stem Cells. *Science (80-)*. 1999;284(5411):143-147. doi:10.1126/science.284.5411.143.
 68. Wang X-J, Li Q-P. The roles of mesenchymal stem cells (MSCs) therapy in ischemic heart diseases. *Biochem Biophys Res Commun*. 2007;359(2):189-193. doi:10.1016/j.bbrc.2007.05.112.
 69. da Silva Meirelles L, Chagastelles PC, Nardi NB. Mesenchymal stem cells reside in virtually all post-natal organs and tissues. *J Cell Sci*. 2006;119(Pt 11):2204-2213. doi:10.1242/jcs.02932.
 70. Hass R, Kasper C, Böhm S, Jacobs R. Different populations and sources of human mesenchymal stem cells (MSC): A comparison of adult and neonatal tissue-derived MSC. *Cell Commun Signal*. 2011;9(1):12. doi:10.1186/1478-811X-9-12.
 71. Dominici M, Le Blanc K, Mueller I, et al. Minimal criteria for defining multipotent mesenchymal stromal cells. The International Society for Cellular Therapy position statement. *Cytotherapy*. 2006;8(4):315-317. doi:10.1080/14653240600855905.
 72. Ryan JM, Barry FP, Murphy JM, Mahon BP. Mesenchymal stem cells avoid allogeneic rejection. *J Inflamm (Lond)*. 2005;2:8. doi:10.1186/1476-9255-2-8.
 73. Nauta AJ, Westerhuis G, Kruisselbrink AB, Lurvink EGA, Willemze R, Fibbe WE. Donor-derived mesenchymal stem cells are immunogenic in an allogeneic host and stimulate donor graft rejection in a nonmyeloablative setting. *Blood*.

- 2006;108(6):2114-2120. doi:10.1182/blood-2005-11-011650.
74. Ankrum J a, Ong JF, Karp JM. Mesenchymal stem cells: immune evasive, not immune privileged. *Nat Biotechnol.* 2014;32(3):252-260. doi:10.1038/nbt.2816.
 75. Breymann C, Schmidt D, Hoerstrup SP. Umbilical cord cells as a source of cardiovascular tissue engineering. *Stem Cell Rev.* 2006;2(2):87-92. doi:10.1007/s12015-006-0014-y.
 76. Gimble JM, Katz AJ, Bunnell BA. Adipose-derived stem cells for regenerative medicine. *Circ Res.* 2007;100(9):1249-1260. doi:10.1161/01.RES.0000265074.83288.09.
 77. De Coppi P, Bartsch Jr G, Siddiqui MM, et al. Isolation of amniotic stem cell lines with potential for therapy. *Nat Biotech.* 2007;25(1):100-106. doi:10.1097/01.ogx.0000261640.52511.eb.
 78. Li B, Zeng Q, Wang H, et al. Adipose tissue stromal cells transplantation in rats of acute myocardial infarction. *Coron Artery Dis.* 2007;18(3):221-227. doi:10.1097/MCA.0b013e32801235da.
 79. Valina C, Pinkernell K, Song YH, et al. Intracoronary administration of autologous adipose tissue-derived stem cells improves left ventricular function, perfusion, and remodelling after acute myocardial infarction. *Eur Heart J.* 2007;28(21):2667-2677. doi:10.1093/eurheartj/ehm426.
 80. Gaebel R, Furlani D, Sorg H, et al. Cell origin of human mesenchymal stem cells determines a different healing performance in cardiac regeneration. *PLoS One.* 2011;6(2). doi:10.1371/journal.pone.0015652.
 81. Fang C-H, Jin J, Joe J-H, et al. In vivo differentiation of human amniotic epithelial cells into cardiomyocyte-like cells and cell transplantation effect on myocardial infarction in rats: comparison with cord blood and adipose tissue-derived mesenchymal stem cells. *Cell Transplant.* 2012;21(8):1687-1696. doi:10.3727/096368912X653039.
 82. Gong X, Wang P, Wu Q, Wang S, Yu L, Wang G. Human umbilical cord blood derived mesenchymal stem cells improve cardiac function in cTnTR141W transgenic mouse of dilated cardiomyopathy. *Eur J Cell Biol.* 2016;95(1):57-67. doi:10.1016/j.ejcb.2015.11.003.
 83. Rehman J, Traktuev D, Li J, et al. Secretion of Angiogenic and Antiapoptotic Factors by Human Adipose Stromal Cells. *Circulation.* 2004;109(10):1292-1298. doi:10.1161/01.CIR.0000121425.42966.F1.
 84. Yang D, Wang W, Li L, et al. The Relative Contribution of Paracrine Effect versus Direct Differentiation on Adipose-Derived Stem Cell Transplantation Mediated Cardiac Repair. *PLoS One.* 2013;8(3). doi:10.1371/journal.pone.0059020.
 85. Gutiérrez E, Sanz-Ruiz R, Alvarez EV, et al. General overview of the seventh international symposium on stem cell therapy and cardiovascular innovations. *J Cardiovasc Transl Res.* 2011;4(2):115-120. doi:10.1007/s12265-010-9247-x.
 86. A. C, A.T. U, O. C, et al. Human Umbilical Cord Mesenchymal Stromal Cell Transplantation in Myocardial Ischemia (HUC-HEART Trial). A Study Protocol of a Phase 1/2, Controlled and Randomized Trial in Combination with Coronary Artery Bypass Grafting. *Stem Cell Rev Reports.* 2015;11(5):752-760. doi:10.1007/s12015-015-9601-0.
 87. Beltrami AP, Barlucchi L, Torella D, et al. el. *Cell.* 2003;114(6):763-776. doi:10.1016/S0092-8674(03)00687-1.
 88. Fazel S, Cimini M, Chen L, et al. Cardioprotective c-kit+ cells are from the bone marrow and regulate the myocardial balance of angiogenic cytokines. *J Clin Invest.* 2006;116(7):1865-1877. doi:10.1172/JCI27019.
 89. Veinot JP, Prichett-Pejic W, Song J, et al. CD117-positive cells and mast cells in adult human cardiac valves--observations and implications for the creation of bioengineered grafts. *Cardiovasc Pathol.* 2006;15(1):36-40. doi:10.1016/j.carpath.2005.08.005.

90. Zhou Y, Pan P, Yao L, et al. CD117-positive cells of the heart: progenitor cells or mast cells? *J Histochem Cytochem*. 2010;58(4):309-316. doi:10.1369/jhc.2009.955146.
91. Sandstedt J, Jonsson M, Lindahl A, Jeppsson A, Asp J. C-kit+ CD45- Cells found in the adult human heart represent a population of endothelial progenitor cells. *Basic Res Cardiol*. 2010;105(4):545-556. doi:10.1007/s00395-010-0088-1.
92. Sandstedt J, Jonsson M, Dellgren G, Lindahl A, Jeppsson A, Asp J. Human C-kit+CD45- cardiac stem cells are heterogeneous and display both cardiac and endothelial commitment by single-cell qPCR analysis. *Biochem Biophys Res Commun*. 2014;443(1):234-238. doi:10.1016/j.bbrc.2013.11.086.
93. Jesty SA, Steffey MA, Lee FK, et al. c-kit+ precursors support postinfarction myogenesis in the neonatal, but not adult, heart. *Proc Natl Acad Sci U S A*. 2012;109(33):13380-13385. doi:10.1073/pnas.1208114109.
94. Tallini YN, Greene KS, Craven M, et al. C-Kit Expression Identifies Cardiovascular Precursors in the Neonatal Heart. *Proc Natl Acad Sci U S A*. 2009;106(6):1808-1813. doi:0808920106 [pii]\r10.1073/pnas.0808920106.
95. Ellison GM, Vicinanza C, Smith AJ, et al. Adult c-kitpos cardiac stem cells are necessary and sufficient for functional cardiac regeneration and repair. *Cell*. 2013;154(4):827-842. doi:10.1016/j.cell.2013.07.039.
96. Molkenstein JD, Houser SR. Are resident c-Kit+ cardiac stem cells really all that are needed to mend a broken heart? *Circ Res*. 2013;113(9):1037-1039. doi:10.1161/CIRCRESAHA.113.302564.
97. van Berlo JH, Kanisicak O, Maillet M, et al. c-kit+ cells minimally contribute cardiomyocytes to the heart. *Nature*. 2014;509(7500):337-341. doi:10.1038/nature13309.
98. Sultana N, Zhang L, Yan J, et al. Resident c-kit(+) cells in the heart are not cardiac stem cells. *Nat Commun*. 2015;6:8701. doi:10.1038/ncomms9701.
99. Bolli R, Chugh AR, D'Amario D, et al. Cardiac stem cells in patients with ischaemic cardiomyopathy (SCIPIO): initial results of a randomised phase 1 trial. *Lancet*. 2011;378(9806):1847-1857. doi:S0140-6736(11)61590-0 [pii]\r10.1016/S0140-6736(11)61590-0.
100. The Lancet Editors. Expression of concern: the SCIPIO trial. *Lancet*. 2014;383(9925):1279. doi:10.1016/S0140-6736(14)60608-5.
101. Oh H, Bradfute SB, Gallardo TD, et al. Cardiac progenitor cells from adult myocardium: homing, differentiation, and fusion after infarction. *Proc Natl Acad Sci U S A*. 2003;100(21):12313-12318. doi:10.1073/pnas.2132126100.
102. Wang X, Hu Q, Nakamura Y, et al. The role of the sca-1+/CD31- cardiac progenitor cell population in postinfarction left ventricular remodeling. *Stem Cells*. 2006;24(7):1779-1788. doi:10.1634/stemcells.2005-0386.
103. Uchida S, De Gaspari P, Kostin S, et al. Sca1-derived cells are a source of myocardial renewal in the murine adult heart. *Stem Cell Reports*. 2013;1(5):397-410. doi:10.1016/j.stemcr.2013.09.004.
104. Bailey B, Fransioli J, Gude NA, et al. Sca-1 knockout impairs myocardial and cardiac progenitor cell function. *Circ Res*. 2012;111(6):750-760. doi:10.1161/CIRCRESAHA.112.274662.
105. Nosedá M, Harada M, McSweeney S, et al. PDGFRalpha demarcates the cardiogenic and clonogenic Sca-1 stem cell. *Cardiovasc Res*. 2014;103:S107. <http://www.embase.com/search/results?subaction=viewrecord&from=export&id=L71588545> <http://dx.doi.org/10.1093/cvr/cvu098.25> <http://sfx.library.uu.nl/utrecht?sid=EMBASE&issn=00086363&id=doi:10.1093/cvr/cvu098.25&atitle=PDGFRalpha+demarcates+the+cardio>.
106. Pfister O, Oikonomopoulos A, Sereti K-I, et al. Role of the ATP-binding cassette transporter Abcg2 in the phenotype and function of cardiac side population cells. *Circ Res*. 2008;103(8):825-835. doi:10.1161/CIRCRESAHA.108.174615.

107. Martin CM, Meeson AP, Robertson SM, et al. Persistent expression of the ATP-binding cassette transporter, *Abcg2*, identifies cardiac SP cells in the developing and adult heart. *Dev Biol.* 2004;265(1):262-275. doi:10.1016/j.ydbio.2003.09.028.
108. Oyama T, Nagai T, Wada H, et al. Cardiac side population cells have a potential to migrate and differentiate into cardiomyocytes in vitro and in vivo. *J Cell Biol.* 2007;176(3):329-341. doi:10.1083/jcb.200603014.
109. van Vliet P, Rocco M, Smits AM, et al. Progenitor cells isolated from the human heart: a potential cell source for regenerative therapy. *Neth Heart J.* 2008;16(5):163-169. doi:10.1007/BF03086138.
110. Rosenblatt-Velin N, Ogay S, Felley a., Stanford WL, Pedrazzini T. Cardiac dysfunction and impaired compensatory response to pressure overload in mice deficient in stem cell antigen-1. *FASEB J.* 2012;26:229-239. doi:10.1096/fj.11-189605.
111. Holmes C, Stanford WL. Concise review: stem cell antigen-1: expression, function, and enigma. *Stem Cells.* 2007;25(6):1339-1347. doi:10.1634/stemcells.2006-0644.
112. Patterson JM, Johnson MH, Zimonjic DB, Graubert T a. Characterization of Ly-6M, a novel member of the Ly-6 family of hematopoietic proteins. *Blood.* 2000;95(10):3125-3132.
113. Roberts R, Govender D. Gene of the month: KIT. *J Clin Pathol.* 2015;68(9):671-674. doi:10.1136/jclinpath-2015-203207.
114. Westervelt BP, Ley TJ. The Journal of The American Society of Hematology. *Blood.* 1999;93(7):2143-2148.
115. Lennartsson J, Rönstrand L. Stem cell factor receptor/c-Kit: from basic science to clinical implications. *Physiol Rev.* 2012;92(4):1619-1649. doi:10.1152/physrev.00046.2011.
116. Bernex F, De Sepulveda P, Kress C, Elbaz C, Delouis C, Panthier JJ. Spatial and temporal patterns of c-kit-expressing cells in *WlacZ/+* and *WlacZ/WlacZ* mouse embryos. *Development.* 1996;122:3023-3033.
117. Duim SN, Kurakula K, Goumans MJ, Kruithof BPT. Cardiac endothelial cells express Wilms' tumor-1. *Wt1* expression in the developing, adult and infarcted heart. *J Mol Cell Cardiol.* 2015;81:127-135. doi:10.1016/j.yjmcc.2015.02.007.
118. Smart N, Risebro CA, Melville AAD, et al. Thymosin beta4 induces adult epicardial progenitor mobilization and neovascularization. *Nat.* 2007;445(7124):177-182. doi:10.1038/nature05383.
119. Smart N, Bollini S, Dubé KN, et al. De novo cardiomyocytes from within the activated adult heart after injury. *Nature.* 2011;474(7353):640-644. doi:10.1038/nature10188.
120. von Gise A, Zhou B, Honor LB, Ma Q, Petryk A, Pu WT. WT1 regulates epicardial epithelial to mesenchymal transition through β -catenin and retinoic acid signaling pathways. *Dev Biol.* 2011;356(2):421-431. doi:10.1016/j.ydbio.2011.05.668.
121. Messina E, De Angelis L, Frati G, et al. Isolation and expansion of adult cardiac stem cells from human and murine heart. *Circ Res.* 2004;95(9):911-921. doi:10.1161/01.RES.0000147315.71699.51.
122. Smith RR, Barile L, Cho HC, et al. Regenerative potential of cardiosphere-derived cells expanded from percutaneous endomyocardial biopsy specimens. *Circulation.* 2007;115(7):896-908. doi:10.1161/CIRCULATIONAHA.106.655209.
123. Chan HHL, Meher Homji Z, Gomes RSM, et al. Human cardiosphere-derived cells from patients with chronic ischaemic heart disease can be routinely expanded from atrial but not epicardial ventricular biopsies. *J Cardiovasc Transl Res.* 2012;5(5):678-687. doi:10.1007/s12265-012-9389-0.
124. Hsiao L-C, Perbellini F, Gomes RSM, et al. Murine cardiosphere-derived cells are

- impaired by age but not by cardiac dystrophic dysfunction. *Stem Cells Dev.* 2014;23(9):1027-1036. doi:10.1089/scd.2013.0388.
125. Perbellini F, Buchanan DA, Gomes RSM, et al. The effect of a high fat diet on cardiac and adipose mesenchymal cells. *Cardiovasc Res.* 2014;103:S107. <http://www.embase.com/search/results?subaction=viewrecord&from=export&id=L71588542> <http://dx.doi.org/10.1093/cvr/cvu098.22> <http://sfx.library.uu.nl/utrecht?sid=EMBASE&issn=00086363&id=doi:10.1093/cvr/cvu098.22&atitle=The+effect+of+a+high+fat+diet+on>.
 126. Carr CA, Stuckey DJ, Tan JJ, et al. Cardiosphere-derived cells improve function in the infarcted rat heart for at least 16 weeks--an MRI study. *PLoS One.* 2011;6(10):e25669. doi:10.1371/journal.pone.0025669.
 127. Tseliou E, Reich H, de Couto G, et al. Cardiospheres reverse adverse remodeling in chronic rat myocardial infarction: roles of soluble endoglin and Tgf- β signaling. *Basic Res Cardiol.* 2014;109(6). doi:10.1007/s00395-014-0443-8.
 128. Lee ST, White AJ, Matsushita S, et al. Intramyocardial injection of autologous cardiospheres or cardiosphere-derived cells preserves function and minimizes adverse ventricular remodeling in pigs with heart failure post-myocardial infarction. *J Am Coll Cardiol.* 2011;57(4):455-465. doi:10.1016/j.jacc.2010.07.049.
 129. Li TS, Cheng K, Malliaras K, et al. Direct comparison of different stem cell types and subpopulations reveals superior paracrine potency and myocardial repair efficacy with cardiosphere-derived cells. *J Am Coll Cardiol.* 2012;59(10):942-953. doi:10.1016/j.jacc.2011.11.029.
 130. Gallet R, de Couto G, Simsolo E, et al. Cardiosphere-Derived Cells Reverse Heart Failure With Preserved Ejection Fraction in Rats by Decreasing Fibrosis and Inflammation. *JACC Basic to Transl Sci.* 2016;1(1-2):14-28. doi:10.1016/j.jacbts.2016.01.003.
 131. Chimenti I, Forte E, Angelini F, Messina E, Giacomello A. Biochemistry and biology: Heart-to-heart to investigate cardiac progenitor cells. *Biochim Biophys Acta - Gen Subj.* 2013;1830(2):2459-2469. doi:10.1016/j.bbagen.2012.08.004.
 132. Limana F, Zacheo A, Mocini D, et al. Identification of myocardial and vascular precursor cells in human and mouse epicardium. *Circ Res.* 2007;101(12):1255-1265. doi:10.1161/CIRCRESAHA.107.150755.
 133. Zhou B, Ma Q, Rajagopal S, et al. Epicardial progenitors contribute to the cardiomyocyte lineage in the developing heart. *Nature.* 2008;454(7200):109-113. doi:10.1038/nature07060.
 134. Zhou B, Ma Q, Rajagopal S, et al. Epicardial progenitors contribute to the cardiomyocyte lineage in the developing heart. *Nature.* 2008;454(7200):109-113. doi:10.1038/nature07060.
 135. Bock-Marquette I, Shrivastava S, Pipes GCT, et al. Thymosin β 4 mediated PKC activation is essential to initiate the embryonic coronary developmental program and epicardial progenitor cell activation in adult mice in vivo. *J Mol Cell Cardiol.* 2009;46(5):728-738. doi:10.1016/j.yjmcc.2009.01.017.
 136. Smart N, Bollini S, Dubé KN, et al. De novo cardiomyocytes from within the activated adult heart after injury. *Nature.* 2011;474(7353):640-644. doi:10.1038/nature10188.
 137. Zhou B, Honor LB, Ma Q, et al. Thymosin beta 4 treatment after myocardial infarction does not reprogram epicardial cells into cardiomyocytes. *J Mol Cell Cardiol.* 2012;52(1):43-47. doi:10.1016/j.yjmcc.2011.08.020.
 138. Williams AR, Hatzistergos KE, Addicott B, et al. Enhanced effect of combining human cardiac stem cells and bone marrow mesenchymal stem cells to reduce infarct size and to restore cardiac function after myocardial infarction. *Circulation.* 2013;127(2):213-223. doi:10.1161/CIRCULATIONAHA.112.131110.
 139. Shudo Y, Miyagawa S, Ohkura H, et al. Addition of Mesenchymal Stem Cells Enhances the Therapeutic Effects of Skeletal Myoblast Cell-Sheet Transplantation

- in a Rat Ischemic Cardiomyopathy Model. *Tissue Eng Part A*. 2014;20(3-4):728-739. doi:10.1089/ten.tea.2012.0534.
140. Chen G, Yue A, Yu H, et al. Mesenchymal Stem Cells and Mononuclear Cells From Cord Blood: Cotransplantation Provides a Better Effect in Treating Myocardial Infarction. *Stem Cells Transl Med*. 2016;5(3):350-357. doi:10.5966/sctm.2015-0199.
 141. Thavandiran N, Dubois N, Mikryukov A, et al. Design and formulation of functional pluripotent stem cell-derived cardiac microtissues. *Proc Natl Acad Sci U S A*. 2013;1-10. doi:10.1073/pnas.1311120110.
 142. Quijada P, Salunga HT, Hariharan N, et al. Cardiac stem cell hybrids enhance myocardial repair. *Circ Res*. 2015;117(8):695-706. doi:10.1161/CIRCRESAHA.115.306838/-/DC1.
 143. Quijada P, Sussman M a. Making it stick: chasing the optimal stem cells for cardiac regeneration. *Expert Rev Cardiovasc Ther*. 2014;12(11):1275-1288. doi:10.1586/14779072.2014.972941.
 144. Van Weerd JH, Koshiba-Takeuchi K, Kwon C, Takeuchi JK. Epigenetic factors and cardiac development. *Cardiovasc Res*. 2011;91(2):203-211. doi:10.1093/cvr/cvr138.
 145. Srivastava D, Olson EN. A genetic blueprint for cardiac development. *Nature*. 2000;407(September):221-226. doi:10.1038/35025190.
 146. Steinhauser ML, Lee RT. Regeneration of the heart. *EMBO Mol Med*. 2011;3(12):701-712. doi:10.1002/emmm.201100175.
 147. Mercola M, Ruiz-Lozano P, Schneider MD. Cardiac muscle regeneration: Lessons from development. *Genes Dev*. 2011;25(4):299-309. doi:10.1101/gad.2018411.
 148. Lin Q, Schwarz J, Bucana C, Olson EN. Control of mouse cardiac morphogenesis and myogenesis by transcription factor MEF2C. *Science*. 1997;276(5317):1404-1407. doi:10.1126/science.276.5317.1404.
 149. Bi W, Drake CJ, Schwarz JJ. The transcription factor MEF2C-null mouse exhibits complex vascular malformations and reduced cardiac expression of angiotensin 1 and VEGF. *Dev Biol*. 1999;211(2):255-267. doi:10.1006/dbio.1999.9307.
 150. Iida K, Hidaka K, Takeuchi M, et al. Expression of MEF2 genes during human cardiac development. *Tohoku J Exp Med*. 1999;187(1):15-23. http://www.ncbi.nlm.nih.gov/entrez/query.fcgi?cmd=Retrieve&db=PubMed&dopt=Citation&list_uids=10458488.
 151. Molkenin JD, Lin Q, Duncan SA, Olson EN. Requirement of the transcription factor GATA4 for heart tube formation and ventral morphogenesis. *Genes Dev*. 1997;11(8):1061-1072. doi:10.1101/gad.11.8.1061.
 152. Watt AJ, Battle MA, Li J, Duncan SA. GATA4 is essential for formation of the proepicardium and regulates cardiogenesis. *Proc Natl Acad Sci U S A*. 2004;101(34):12573-12578. doi:10.1073/pnas.0400752101.
 153. Cai CL, Liang X, Shi Y, et al. Isl1 identifies a cardiac progenitor population that proliferates prior to differentiation and contributes a majority of cells to the heart. *Dev Cell*. 2003;5(6):877-889. doi:10.1016/S1534-5807(03)00363-0.
 154. Lin L, Bu L, Cai CL, Zhang X, Evans S. Isl1 is upstream of sonic hedgehog in a pathway required for cardiac morphogenesis. *Dev Biol*. 2006;295(2):756-763. doi:10.1016/j.ydbio.2006.03.053.
 155. Wu SM, Fujiwara Y, Cibulsky SM, et al. Developmental Origin of a Bipotential Myocardial and Smooth Muscle Cell Precursor in the Mammalian Heart. *Cell*. 2006;127(6):1137-1150. doi:10.1016/j.cell.2006.10.028.
 156. Tanaka M, Chen Z, Bartunkova S, Yamasaki N, Izumo S. The cardiac homeobox gene *Csx/Nkx2.5* lies genetically upstream of multiple genes essential for heart development. *Development*. 1999;126:1269-1280.
 157. Ogura T. *Tbx5* Specifies the Left/Right Ventricles and Ventricular Septum Position During Cardiogenesis. In: *Cardiovascular Development and Congenital*

- Malformations: Molecular & Genetic Mechanisms.* ; 2007:75-77.
doi:10.1002/9780470988664.ch18.
158. Takeuchi JK. Tbx5 specifies the left/right ventricles and ventricular septum position during cardiogenesis. *Development.* 2003;130(24):5953-5964.
doi:10.1242/dev.00797.
 159. Xie L, Hoffmann AD, Burnicka-Turek O, Friedland-Little JM, Zhang K, Moskowitz IP. Tbx5-Hedgehog Molecular Networks Are Essential in the Second Heart Field for Atrial Septation. *Dev Cell.* 2012;23(2):280-291.
doi:10.1016/j.devcel.2012.06.006.
 160. Van Vliet P, Wu SM, Zaffran S, Puc??at M. Early cardiac development: A view from stem cells to embryos. *Cardiovasc Res.* 2012;96(3):352-362.
doi:10.1093/cvr/cvs270.
 161. Milgrom-Hoffman M, Harrelson Z, Ferrara N, Zelzer E, Evans SM, Tzahor E. The heart endocardium is derived from vascular endothelial progenitors. *Development.* 2011;138:4777-4787. doi:10.1242/dev.061192.
 162. Buckingham M, Meilhac S, Zaffran S. Building the mammalian heart from two sources of myocardial cells. *Nat Rev Genet.* 2005;6(November):826-835.
doi:10.1038/nrg1710.
 163. Karsner HT, Saphir O, Todd TW. The State of the Cardiac Muscle in Hypertrophy and Atrophy*. *Am J Pathol.* 1925;1:351-372.1. doi:10.1016/S0002-8703(25)90020-8.
 164. Arula Jagat N, Aider NEH, R Enu V Irmani et al. APOPTOSIS IN MYOCYTES IN END-STAGE HEART FAILURE. *NEJM.* 1996;335(16):1182-1189.
doi:10.1056/NEJM199610173351603.
 165. Carvalho AB, de Carvalho ACC. Heart regeneration: Past, present and future. *World J Cardiol.* 2010;2(5):107-111. doi:10.4330/wjc.v2.i5.107.
 166. Soonpaa MH, Field LJ. Survey of studies examining mammalian cardiomyocyte DNA synthesis. *Circ Res.* 1998;83(1):15-26. doi:10.1016/S1566-0702(01)00339-3.
 167. Kang PM, Izumo S. Apoptosis in heart: Basic mechanisms and implications in cardiovascular diseases. *Trends Mol Med.* 2003;9(4):177-182.
doi:10.1016/S1471-4914(03)00025-X.
 168. Odashima M, Usui S, Takagi H, et al. Inhibition of endogenous Mst1 prevents apoptosis and cardiac dysfunction without affecting cardiac hypertrophy after myocardial infarction. *Circ Res.* 2007;100(9):1344-1352.
doi:10.1161/01.RES.0000265846.23485.7a.
 169. Hosoda T, D'Amario D, Cabral-Da-Silva MC, et al. Clonality of mouse and human cardiomyogenesis in vivo. *Proc Natl Acad Sci U S A.* 2009;106(40):17169-17174.
doi:10.1073/pnas.0903089106.
 170. Kajstura J, Gurusamy N, Og??rek B, et al. Myocyte turnover in the aging human heart. *Circ Res.* 2010;107(11):1374-1386. doi:10.1161/CIRCRESAHA.110.231498.
 171. Hsieh PCH, Segers VFM, Davis ME, et al. Evidence from a genetic fate-mapping study that stem cells refresh adult mammalian cardiomyocytes after injury. *Nat Med.* 2007;13(8):970-974. doi:10.1038/nm1618.
 172. Bergmann O, Bhardwaj RD, Bernard S, et al. Evidence for cardiomyocyte renewal in humans. *Science.* 2009;324(5923):98-102. doi:10.1126/science.1164680.
 173. Senyo SE, Steinhauser ML, Pizzimenti CL, et al. Mammalian heart renewal by pre-existing cardiomyocytes. *Nature.* 2012;493(7432):433-436.
doi:10.1038/nature11682.
 174. Bergmann O, Zdunek S, Felker A, et al. Dynamics of Cell Generation and Turnover in the Human Heart. *Cell.* 2015:1566-1575. doi:10.1016/j.cell.2015.05.026.
 175. Puente BN, Kimura W, Muralidhar SA, et al. The oxygen-rich postnatal environment induces cardiomyocyte cell-cycle arrest through DNA damage response. *Cell.* 2014;157(3):565-579. doi:10.1016/j.cell.2014.03.032.

176. Kimura W, Xiao F, Canseco DC, et al. Hypoxia fate mapping identifies cycling cardiomyocytes in the adult heart. *Nature*. 2015;523(7559):226-230. doi:10.1038/nature14582.
177. van Berlo JH, Molkentin JD. An emerging consensus on cardiac regeneration. *Nat Med*. 2014;20(12):1386-1393. doi:10.1038/nm.3764.
178. Bing RJ, Siegel a., Ungar I, Gilbert M. Metabolism of the human heart. *Am J Med*. 1954;16(4):504-515. doi:10.1016/0002-9343(54)90365-4.
179. Neubauer S. The failing heart--an engine out of fuel. *N Engl J Med*. 2007;356:1140-1151. doi:10.1056/NEJMra063052.
180. Neely JR, Morgan HE. Relationship Between Carbohydrate and Lipid Metabolism and the Energy Balance of Heart Muscle. *Annu Rev Physiol*. 1974;36:413-459. doi:10.1146/annurev.ph.36.030174.002213.
181. Evans RD, Heather LC. Metabolic pathways and abnormalities. *Surg*. 2016:1-7. doi:10.1016/j.mpsur.2016.03.010.
182. Taegtmeyer H, Young ME, Lopaschuk GD, et al. *Assessing Cardiac Metabolism A Scientific Statement From the American Heart Association.*; 2016. doi:10.1161/RES.0000000000000097.
183. Bar-Even A, Flamholz A, Noor E, Milo R. Rethinking glycolysis: on the biochemical logic of metabolic pathways. *Nat Chem Biol*. 2012;8(6):509-517. doi:10.1038/nchembio.971.
184. Madeira VMC. Overview of mitochondrial bioenergetics. *Methods Mol Biol*. 2012;810:1-6. doi:10.1007/978-1-61779-382-0_1.
185. Stanley WWC, Recchia F a, Lopaschuk GD. Myocardial Substrate Metabolism in the Normal and Failing Heart. *Physiol* 2005;85(3):1093-1129. doi:10.1152/physrev.00006.2004.
186. Lopaschuk GD, Ussher JR, Folmes CDL, Jaswal JS, STANLEY WC. Myocardial Fatty Acid Metabolism in Health and Disease. *Physiol Rev*. 2010;90(1):207-258. doi:10.1152/physrev.00015.2009.
187. Bing RJ, Siegel A, Ungar I, Gilbert M. Metabolism of the human heart: II. Studies on fat, ketone and amino acid metabolism. *Am J Med*. 1954;16(4):504-515. doi:10.1016/0002-9343(54)90365-4.
188. van der Vusse G, Glatz J, Stam H, Reneman R. Fatty acid homeostasis in the normoxic and ischemic heart. *Physiol Rev*. 1992;72:881-940.
189. Cole MA, Abd Jamil AH, Heather LC, et al. On the pivotal role of PPAR in adaptation of the heart to hypoxia and why fat in the diet increases hypoxic injury. *FASEB J*. 2016:1-14. doi:10.1096/fj.201500094R.
190. Kim JW, Tchernyshyov I, Semenza GL, Dang C V. HIF-1-mediated expression of pyruvate dehydrogenase kinase: A metabolic switch required for cellular adaptation to hypoxia. *Cell Metab*. 2006;3(3):177-185. doi:10.1016/j.cmet.2006.02.002.
191. Randle, P. J., Garland, P. B., Hales, C. N., Newsholme EA. The glucose fatty-acid cycle its role in insulin sensitivity and the metabolic disturbances of diabetes mellitus. *Lancet*. 1963;281(7285):785-789. doi:10.1016/S0140-6736(63)91500-9.
192. Hue L, Taegtmeyer H. The Randle cycle revisited: a new head for an old hat. *Am J Physiol Endocrinol Metab*. 2009;297(June 2009):E578-E591. doi:10.1152/ajpendo.00093.2009.
193. Zhang J, Huang X, Wang H, et al. The challenges and promises of allogeneic mesenchymal stem cells for use as a cell-based therapy. *Stem Cell Res Ther*. 2015;6(1):234. doi:10.1186/s13287-015-0240-9.
194. Golpanian S, Schulman IH, Ebert RF, et al. Concise Review: Review and Perspective of Cell Dosage and Routes of Administration From Preclinical and Clinical Studies of Stem Cell Therapy for Heart Disease. *Stem Cells Transl Med* . 2015. doi:10.5966/sctm.2015-0101.

195. Van Dijk A, Naaijkens BA, Jurgens WJFM, et al. Reduction of infarct size by intravenous injection of uncultured adipose derived stromal cells in a rat model is dependent on the time point of application. *Stem Cell Res.* 2011;7(3):219-229. doi:10.1016/j.scr.2011.06.003.
196. Bartunek J, Wijns W, Heyndrickx GR, Vanderheyden M. Timing of intracoronary bone-marrow-derived stem cell transplantation after ST-elevation myocardial infarction. *Nat Clin Pract Cardiovasc Med.* 2006;3 Suppl 1(March):S52-6. doi:10.1038/ncpcardio0417.
197. Hong KU, Li QH, Guo Y, et al. A highly sensitive and accurate method to quantify absolute numbers of c-kit+ cardiac stem cells following transplantation in mice. *Basic Res Cardiol.* 2013;108(3). doi:10.1007/s00395-013-0346-0.
198. Pons J, Huang Y, Takagawa J, et al. Combining angiogenic gene and stem cell therapies for myocardial infarction. *J Gene Med.* 2009;11(9):743-753. doi:10.1002/jgm.1362.
199. Hong KU, Guo Y, Li QH, et al. c-kit+ cardiac stem cells alleviate post-myocardial infarction left ventricular dysfunction despite poor engraftment and negligible retention in the recipient heart. *PLoS One.* 2014;9(5). doi:10.1371/journal.pone.0096725.
200. Müller-Ehmsen J, Whittaker P, Kloner RA, et al. Survival and development of neonatal rat cardiomyocytes transplanted into adult myocardium. *J Mol Cell Cardiol.* 2002;34(2):107-116. doi:10.1006/jmcc.2001.1491.
201. Vrtovec B, Poglajen G, Lezaic L, et al. Effects of intracoronary CD34+ stem cell transplantation in nonischemic dilated cardiomyopathy patients: 5-year follow-up. *Circ Res.* 2013;112(1):165-173. doi:10.1161/CIRCRESAHA.112.276519.
202. Li L, Chen X, Wang WE, Zeng C. How to Improve the Survival of Transplanted Mesenchymal Stem Cell in Ischemic Heart? *Stem Cells Int.* 2016;2016. doi:10.1155/2016/9682757.
203. Taghavi S, George JC. Homing of stem cells to ischemic myocardium. *Am J Transl Res.* 2013;5(4):404-411. doi:23724164.
204. McGinley LM, McMahon J, Stocca A, et al. Mesenchymal stem cell survival in the infarcted heart is enhanced by lentivirus vector-mediated heat shock protein 27 expression. *Hum Gene Ther.* 2013;24(10):840-851. doi:10.1089/hum.2011.009.
205. Tu TC, Nagano M, Yamashita T, et al. A Chemokine Receptor, CXCR4, Which Is Regulated by Hypoxia-Inducible Factor 2 α , Is Crucial for Functional Endothelial Progenitor Cells Migration to Ischemic Tissue and Wound Repair. *Stem Cells Dev.* 2016;25(3):266-276. doi:10.1089/scd.2015.0290.
206. Penn MS, Mangi AA. Genetic enhancement of stem cell engraftment, survival, and efficacy. *Circ Res.* 2008;102(12):1471-1482. doi:10.1161/CIRCRESAHA.108.175174.
207. Zakharova L. Transplantation of epigenetically modified adult cardiac c-kit+ cells retards remodeling and improves cardiac function in ischemic heart failure model. *Stem Cells Transl Med.* 2014;1-10. doi:10.5966/sctm.2014-0290.
208. Haider HK, Ashraf M. Preconditioning and stem cell survival. *J Cardiovasc Transl Res.* 2010;3(2):89-102. doi:10.1007/s12265-009-9161-2.
209. Kutschka I, Chen IY, Kofidis T, et al. Collagen matrices enhance survival of transplanted cardiomyoblasts and contribute to functional improvement of ischemic rat hearts. *Circulation.* 2006;114(SUPPL. 1). doi:10.1161/CIRCULATIONAHA.105.001297.
210. Traverse JH. Using biomaterials to improve the efficacy of cell therapy following acute myocardial infarction. *J Cardiovasc Transl Res.* 2012;5(1):67-72. doi:10.1007/s12265-011-9330-y.
211. Gaetani R, Feyen DAM, Verhage V, et al. Epicardial application of cardiac progenitor cells in a 3D-printed gelatin/hyaluronic acid patch preserves cardiac function after myocardial infarction. *Biomaterials.* 2015;61:339-348.

- doi:10.1016/j.biomaterials.2015.05.005.
212. Anderson JM, Rodriguez A, Chang DT. Foreign body reaction to biomaterials. *Semin Immunol.* 2008;20(2):86-100. doi:10.1016/j.smim.2007.11.004.
 213. Holladay C, Power K, Sefton M, O'Brien T, Gallagher WM, Pandit A. Functionalized scaffold-mediated interleukin 10 gene delivery significantly improves survival rates of stem cells in vivo. *Mol Ther.* 2011;19(5):969-978. doi:10.1038/mt.2010.311.
 214. Carr CA, Stuckey DJ, Tan JJ, et al. Cardiosphere-derived cells improve function in the infarcted rat heart for at least 16 weeks - an mri study. *PLoS One.* 2011;6(10). doi:10.1371/journal.pone.0025669.
 215. Okada M, Payne TR, Zheng B, et al. Myogenic Endothelial Cells Purified From Human Skeletal Muscle Improve Cardiac Function After Transplantation Into Infarcted Myocardium. *J Am Coll Cardiol.* 2008;52(23):1869-1880. doi:10.1016/j.jacc.2008.07.064.
 216. Livak KJ, Schmittgen TD. Analysis of relative gene expression data using real-time quantitative PCR and the 2⁻ ΔΔCT Method. *Methods.* 2001;25(4):402-408. doi:10.1006/meth.2001.1262.
 217. Biosystems A. Guide to Performing Relative Quantitation of Gene Expression Using Real-Time Quantitative PCR. *Gene Expr.* 2008;2009:1-60. doi:10.1007/978-3-642-31107-9.
 218. Franken N a P, Rodermond HM, Stap J, Haveman J, van Bree C. Clonogenic assay of cells in vitro. *Nat Protoc.* 2006;1(5):2315-2319. doi:10.1038/nprot.2006.339.
 219. Boheler KR, Czyz J, Tweedie D, Yang HT, Anisimov S V., Wobus AM. Differentiation of pluripotent embryonic stem cells into cardiomyocytes. *Circ Res.* 2002;91(3):189-201. doi:10.1161/01.RES.0000027865.61704.32.
 220. Smits AM, van Vliet P, Metz CH, et al. Human cardiomyocyte progenitor cells differentiate into functional mature cardiomyocytes: an in vitro model for studying human cardiac physiology and pathophysiology. *Nat Protoc.* 2009;4(2):232-243. doi:10.1038/nprot.2008.229.
 221. Ding L, Liang X-G, Zhu D-Y, Lou Y-J. Icariin promotes expression of PGC-1alpha, PPARalpha, and NRF-1 during cardiomyocyte differentiation of murine embryonic stem cells in vitro. *Acta Pharmacol Sin.* 2007;28(10):1541-1549. doi:10.1111/j.1745-7254.2007.00648.x.
 222. Cao H, Ke Y, Zhang Y, Zhang CJ, Qian W, Zhang GL. Icariin stimulates MC3T3-E1 cell proliferation and differentiation through up-regulation of bone morphogenetic protein-2. *Int J Mol Med.* 2012;29(3):435-439. doi:10.3892/ijmm.2011.845.
 223. Collins CL, Bode BP, Souba WW, Abcouwer SF. Multiwell (CO₂)-C-14-capture assay for evaluation of substrate oxidation rates of cells in culture. *Biotechniques.* 1998;24(5):803-808.
 224. Gomes RSM, Pires R, Cochlin L, et al. Efficient Pro-survival/angiogenic miRNA Delivery by an MRI-Detectable Nanomaterial. *ACS Nano.* 2013;7(4):3362-3372. doi:10.1021/nn400171w.
 225. Schamberger CJ, Gerner C, Cerni C. Caspase-9 plays a marginal role in serum starvation-induced apoptosis. *Exp Cell Res.* 2005;302(1):115-128. doi:10.1016/j.yexcr.2004.08.026.
 226. Friedenstein AJ, Petrakova K V, Kurolesova AI, Frolova GP. Heterotopic of bone marrow. Analysis of precursor cells for osteogenic and hematopoietic tissues. *Transplantation.* 1968;6(2):230-247. doi:10.1097/00007890-196803000-00009.
 227. Owen M. Marrow stromal stem cells. *J Cell Sci Suppl.* 1988;10:63-76. doi:10.1172/JCI10413.
 228. Souders CA, Bowers SLK, Baudino TA. Cardiac fibroblast: The renaissance cell. *Circ Res.* 2009;105(12):1164-1176. doi:10.1161/CIRCRESAHA.109.209809.
 229. Carlson S, Trial J, Soeller C, Entman ML. Cardiac mesenchymal stem cells

- contribute to scar formation after myocardial infarction. *Cardiovasc Res*. 2011;91(1):99-107. doi:10.1093/cvr/cvr061.
230. Porter KE, Turner NA. Cardiac fibroblasts: At the heart of myocardial remodeling. *Pharmacol Ther*. 2009;123(2):255-278. doi:10.1016/j.pharmthera.2009.05.002.
 231. Lighthouse JK, Small EM. Transcriptional control of cardiac fibroblast plasticity. *J Mol Cell Cardiol*. 2016;91:52-60. doi:10.1016/j.yjmcc.2015.12.016.
 232. Moore-Morris T, Cattaneo P, Puceat M, Evans SM. Origins of cardiac fibroblasts. *J Mol Cell Cardiol*. 2016;91:1-5. doi:10.1016/j.yjmcc.2015.12.031.
 233. Banerjee I, Fuseler JW, Price RL, Borg TK, Baudino TA. Determination of cell types and numbers during cardiac development in the neonatal and adult rat and mouse. *Am J Physiol Heart Circ Physiol*. 2007;293(3):H1883-91. doi:10.1152/ajpheart.00514.2007.
 234. Camelliti P, Borg TK, Kohl P. Structural and functional characterisation of cardiac fibroblasts. *Cardiovasc Res*. 2005;65(1):40-51. doi:10.1016/j.cardiores.2004.08.020.
 235. McAnulty RJ. Fibroblasts and myofibroblasts: Their source, function and role in disease. *Int J Biochem Cell Biol*. 2007;39(4):666-671. doi:10.1016/j.biocel.2006.11.005.
 236. Kong P, Christia P, Frangogiannis NG. The pathogenesis of cardiac fibrosis. *Cell Mol Life Sci*. 2014;71(4):549-574. doi:10.1007/s00018-013-1349-6.
 237. van den Borne SWM, Diez J, Blankesteyn WM, Verjans J, Hofstra L, Narula J. Myocardial remodeling after infarction: the role of myofibroblasts. *Nat Rev Cardiol*. 2010;7(1):30-37. doi:10.1038/nrcardio.2009.199.
 238. Vaughan MB, Howard EW, Tomasek JJ. Transforming growth factor-beta1 promotes the morphological and functional differentiation of the myofibroblast. *Exp Cell Res*. 2000;257(1):180-189. doi:10.1006/excr.2000.4869.
 239. Baum J, Duffy HS. Fibroblasts and myofibroblasts: what are we talking about? *J Cardiovasc Pharmacol*. 2011;57(4):376-379. doi:10.1097/FJC.0b013e3182116e39.
 240. Olaso E, Labrador J-P, Wang L, et al. Discoidin domain receptor 2 regulates fibroblast proliferation and migration through the extracellular matrix in association with transcriptional activation of matrix metalloproteinase-2. *J Biol Chem*. 2002;277(5):3606-3613. doi:10.1074/jbc.M107571200.
 241. Mendez MG, Kojima S-I, Goldman RD. Vimentin induces changes in cell shape, motility, and adhesion during the epithelial to mesenchymal transition. *FASEB J*. 2010;24(6):1838-1851. doi:10.1096/fj.09-151639.
 242. Strutz F, Okada H, Lo CW, et al. Identification and characterization of a fibroblast marker: FSP1. *J Cell Biol*. 1995;130(2):393-405. doi:10.1083/jcb.130.2.393.
 243. Bonner JC. Regulation of PDGF and its receptors in fibrotic diseases. *Cytokine Growth Factor Rev*. 2004;15(4):255-273. doi:10.1016/j.cytogfr.2004.03.006.
 244. Rege TA, Hagood JS. Thy-1 as a regulator of cell-cell and cell-matrix interactions in axon regeneration, apoptosis, adhesion, migration, cancer, and fibrosis. *FASEB J*. 2006;20(8):1045-1054. doi:10.1096/fj.05-5460rev.
 245. Gago-Lopez N, Awaji O, Zhang Y, et al. THY-1 receptor expression differentiates cardiosphere-derived cells with divergent cardiogenic differentiation potential. *Stem Cell Reports*. 2014;2(5):576-591. doi:10.1016/j.stemcr.2014.03.003.
 246. Ivaska J, Pallari HM, Nevo J, Eriksson JE. Novel functions of vimentin in cell adhesion, migration, and signaling. *Exp Cell Res*. 2007;313(10):2050-2062. doi:10.1016/j.yexcr.2007.03.040.
 247. Kong P, Christia P, Saxena A, Su Y, Frangogiannis NG. Lack of specificity of fibroblast-specific protein 1 in cardiac remodeling and fibrosis. *Am J Physiol Heart Circ Physiol*. 2013;305(9):H1363-72. doi:10.1152/ajpheart.00395.2013.
 248. Farahani RM, Xaymardan M. Platelet-Derived Growth Factor Receptor Alpha as a Marker of Mesenchymal Stem Cells in Development and Stem Cell Biology. *Stem*

- Cells Int.* 2015;2015:362753. doi:10.1155/2015/362753.
249. Ieda M, Tsuchihashi T, Ivey KN, et al. Cardiac fibroblasts regulate myocardial proliferation through beta1 integrin signaling. *Dev Cell.* 2009;16(2):233-244. doi:10.1016/j.devcel.2008.12.007.
 250. Haeryfar SMM, Hoskin DW. Thy-1: more than a mouse pan-T cell marker. *J Immunol.* 2004;173:3581-3588. doi:10.4049/jimmunol.173.6.3581.
 251. Haniffa MA, Collin MP, Buckley CD, Dazzi F. Mesenchymal stem cells: The fibroblasts' new clothes? *Haematologica.* 2009;94(2):258-263. doi:10.3324/haematol.13699.
 252. Hematti P. Mesenchymal stromal cells and fibroblasts: a case of mistaken identity? *Cytotherapy.* 2012;14(5):516-521. doi:10.3109/14653249.2012.677822.
 253. Chen WCW, Baily JE, Corselli M, et al. Human myocardial pericytes: Multipotent mesodermal precursors exhibiting cardiac specificity. *Stem Cells.* 2015;33(2):557-573. doi:10.1002/stem.1868.
 254. Chen CW, Okada M, Proto JD, et al. Human pericytes for ischemic heart repair. *Stem Cells.* 2013;31(2):305-316. doi:10.1002/stem.1285.
 255. Covas DT, Panepucci RA, Fontes AM, et al. Multipotent mesenchymal stromal cells obtained from diverse human tissues share functional properties and gene-expression profile with CD146 + perivascular cells and fibroblasts. *Exp Hematol.* 2008;36(5):642-654. doi:10.1016/j.exphem.2007.12.015.
 256. Quan TE, Cowper S, Wu SP, Bockenstedt LK, Bucala R. Circulating fibrocytes: Collagen-secreting cells of the peripheral blood. *Int J Biochem Cell Biol.* 2004;36(4):598-606. doi:10.1016/j.biocel.2003.10.005.
 257. Abe R, Donnelly SC, Peng T, Bucala R, Metz CN. Peripheral Blood Fibrocytes: Differentiation Pathway and Migration to Wound Sites. *J Immunol.* 2001;166(12):7556-7562. doi:10.4049/jimmunol.166.12.7556.
 258. Bellini A, Mattoli S. The role of the fibrocyte, a bone marrow-derived mesenchymal progenitor, in reactive and reparative fibroses. *Lab Invest.* 2007;87(9):858-870. doi:10.1038/labinvest.3700654.
 259. Popescu LM, Fausone-Pellegrini MS. TELOCYTES - a case of serendipity: The winding way from Interstitial Cells of Cajal (ICC), via Interstitial Cajal-Like Cells (ICLC) to TELOCYTES. *J Cell Mol Med.* 2010;14(4):729-740. doi:10.1111/j.1582-4934.2010.01059.x.
 260. Seif-Naraghi SB, Christman KL. Resident Stem Cells and Regenerative Therapy. *Resid Stem Cells Regen Ther.* 2013:43-67. doi:10.1016/B978-0-12-416012-5.00003-7.
 261. Zhao B, Chen S, Liu J, et al. Cardiac telocytes were decreased during myocardial infarction and their therapeutic effects for ischaemic heart in rat. *J Cell Mol Med.* 2013;17(1):123-133. doi:10.1111/j.1582-4934.2012.01655.x.
 262. Zhao B, Liao Z, Chen S, et al. Intramyocardial transplantation of cardiac telocytes decreases myocardial infarction and improves post-infarcted cardiac function in rats. *J Cell Mol Med.* 2014;18(5):780-789. doi:10.1111/jcmm.12259.
 263. Chang Y, Li C, Lu Z, Li H, Guo Z. Multiple immunophenotypes of cardiac telocytes. *Exp Cell Res.* 2015;338(2):239-244. doi:10.1016/j.yexcr.2015.08.012.
 264. Kucia M, Reza R, Campbell FR, et al. A population of very small embryonic-like (VSEL) CXCR4(+)SSEA-1(+)Oct-4+ stem cells identified in adult bone marrow. *Leuk Off J Leuk Soc Am Leuk Res Fund, UK.* 2006;20(5):857-869. doi:10.1038/sj.leu.2404171.
 265. Ratajczak MZ, Zuba-Surma EK, MacHalinski B, Ratajczak J, Kucia M. Very Small Embryonic-Like (VSEL) Stem Cells: Purification from Adult Organs, Characterization, and Biological Significance. *Stem Cell Rev.* 2008;4(2):89-99. doi:10.1007/s12015-008-9018-0.
 266. Wojakowski W, Kucia M, Liu R, et al. Circulating very small embryonic-like stem

- cells in cardiovascular disease. *J Cardiovasc Transl Res*. 2011;4(2):138-144. doi:10.1007/s12265-010-9254-y.
267. Shin D-M, Suszynska M, Mierzejewska K, Ratajczak J, Ratajczak MZ. Very small embryonic-like stem-cell optimization of isolation protocols: an update of molecular signatures and a review of current in vivo applications. *Exp Mol Med*. 2013;45(11):e56. doi:10.1038/emm.2013.117.
 268. Abbott A. Doubt cast over tiny stem cells. *Nature*. 2013;499(7459):390. doi:10.1038/499390a.
 269. Danova-Alt R, Heider A, Egger D, Cross M, Alt R. Very small embryonic-like stem cells purified from umbilical cord blood lack stem cell characteristics. *PLoS One*. 2012;7(4). doi:10.1371/journal.pone.0034899.
 270. Sovalat H, Scrofani M, Eidenschenk A, Hénon P. Human very small embryonic-like stem cells are present in normal peripheral blood of young, middle-aged, and aged subjects. *Stem Cells Int*. 2016;2016. doi:10.1155/2016/7651645.
 271. Bearzi C, Rota M, Hosoda T, et al. Human cardiac stem cells. *Proc Natl Acad Sci*. 2007;104(35):14068-14073. doi:10.1073/pnas.0706760104.
 272. Beltrami AP, Barlucchi L, Torella D, et al. Adult cardiac stem cells are multipotent and support myocardial regeneration. *Cell*. 2003;114(6):763-776. doi:10.1016/S0092-8674(03)00687-1.
 273. Ye J, Boyle A, Shih H, et al. Sca-1 + cardiosphere-derived cells are enriched for isl1-expressing cardiac precursors and improve cardiac function after myocardial injury. *PLoS One*. 2012;7(1). doi:10.1371/journal.pone.0030329.
 274. Rota M, Padin-Iruegas ME, Misao Y, et al. Local activation or implantation of cardiac progenitor cells rescues scarred infarcted myocardium improving cardiac function. *Circ Res*. 2008;103(1):107-116. doi:10.1161/CIRCRESAHA.108.178525.
 275. Davis DR, Kizana E, Terrovitis J, et al. Isolation and expansion of functionally-competent cardiac progenitor cells directly from heart biopsies. *J Mol Cell Cardiol*. 2010;49(2):312-321. doi:10.1016/j.yjmcc.2010.02.019.
 276. Urbanek K, Cesselli D, Rota M, et al. Stem cell niches in the adult mouse heart. *Proc Natl Acad Sci U S A*. 2006;103(24):9226-9231. doi:10.1073/pnas.0600635103.
 277. Saravanakumar M, Devaraj H. Distribution and homing pattern of c-kit+ Sca-1+ CXCR4+ resident cardiac stem cells in neonatal, postnatal, and adult mouse heart. *Cardiovasc Pathol*. 2013;22(4):257-263. doi:10.1016/j.carpath.2012.11.002.
 278. Sanada F, Kim J, Czarna A, et al. C-kit-positive cardiac stem cells nested in hypoxic niches are activated by stem cell factor reversing the aging myopathy. *Circ Res*. 2014;114(1):41-55. doi:10.1161/CIRCRESAHA.114.302500.
 279. Chan HHL, Meher Homji Z, Gomes RSM, et al. Human Cardiosphere-Derived Cells from Patients with Chronic Ischaemic Heart Disease Can Be Routinely Expanded from Atrial but Not Epicardial Ventricular Biopsies. *J Cardiovasc Transl Res*. 2012;5(5):678-687. doi:10.1007/s12265-012-9389-0.
 280. Itzhaki-Alfia A, Leor J, Raanani E, et al. Patient characteristics and cell source determine the number of isolated human cardiac progenitor cells. *Circulation*. 2009;120(25):2559-2566. doi:10.1161/CIRCULATIONAHA.109.849588.
 281. Ho a D, Wagner W, Franke W. Heterogeneity of mesenchymal stromal cell preparations. *Cytotherapy*. 2008;10(4):320-330. doi:10.1080/14653240802217011.
 282. Samuelsson H, Ringdén O, Lönnies H, Le Blanc K. Optimizing in vitro conditions for immunomodulation and expansion of mesenchymal stromal cells. *Cytotherapy*. 2009;11(2):129-136. doi:10.1080/14653240802684194.
 283. Koninckx R, Daniëls A, Windmolders S, et al. The cardiac atrial appendage stem cell: A new and promising candidate for myocardial repair. *Cardiovasc Res*. 2013;97(3):413-423. doi:10.1093/cvr/cvs427.
 284. Smith AJ, Lewis FC, Aquila I, et al. Isolation and characterization of resident

- endogenous c-Kit⁺ cardiac stem cells from the adult mouse and rat heart. *Nat Protoc.* 2014;9(7):1662-1681. doi:10.1038/nprot.2014.113.
285. Perbellini F, Gomes R, Vieira S, et al. Chronic High-Fat Feeding Affects the Mesenchymal Cell Population Expanded From Adipose Tissue but Not Cardiac Atria. *Stem Cells Transl Med.* 2015;4(12):1403-1414. doi:10.5966/sctm.2015-0024.
 286. Messina E, De Angelis L, Frati G, et al. Isolation and expansion of adult cardiac stem cells from human and murine heart. *Circ Res.* 2004;95(9):911-921. doi:10.1161/01.res.0000147315.71699.51.
 287. Gharaibeh B, Lu A, Tebbets J, et al. Isolation of a slowly adhering cell fraction containing stem cells from murine skeletal muscle by the preplate technique. *Nat Protoc.* 2008;3(9):1501-1509. doi:10.1038/nprot.2008.142.
 288. Davis DR, Zhang Y, Smith RR, et al. Validation of the cardiosphere method to culture cardiac progenitor cells from myocardial tissue. *PLoS One.* 2009;4(9). doi:10.1371/journal.pone.0007195.
 289. Davis DR, Kizana E, Terrovitis J, et al. Isolation and expansion of functionally-competent cardiac progenitor cells directly from heart biopsies. *J Mol Cell Cardiol.* 2010;49(2):312-321. doi:10.1016/j.yjmcc.2010.02.019.
 290. Cho H-J, Lee H-J, Youn S-W, et al. Secondary sphere formation enhances the functionality of cardiac progenitor cells. *Mol Ther.* 2012;20(9):1750-1766. doi:10.1038/mt.2012.109.
 291. Lee HJ, Cho HJ, Kwon YW, Park YB, Kim HS. Phenotypic modulation of human cardiospheres between stemness and paracrine activity, and implications for combined transplantation in cardiovascular regeneration. *Biomaterials.* 2013;34(38):9819-9829. doi:10.1016/j.biomaterials.2013.09.013.
 292. Bartosh TJ, Ylöstalo JH, Mohammadipoor A, et al. Aggregation of human mesenchymal stromal cells (MSCs) into 3D spheroids enhances their antiinflammatory properties. *Proc Natl Acad Sci U S A.* 2010;107(31):13724-13729. doi:10.1073/pnas.1008117107.
 293. Smith AJ, Lewis FC, Aquila I, et al. Isolation and characterization of resident endogenous c-Kit⁺ cardiac stem cells from the adult mouse and rat heart. *Nat Protoc.* 2014;9(7):1662-1681. doi:10.1038/nprot.2014.113.
 294. Barile L, Gherghiceanu M, Popescu LM, Moccetti T, Vassalli G. Human cardiospheres as a source of multipotent stem and progenitor cells. *Stem Cells Int.* 2013. doi:10.1155/2013/916837.
 295. Bartosh TJ, Ylostalo JH. Preparation of anti-inflammatory mesenchymal stem/precursor cells (MSCs) through sphere formation using hanging-drop culture technique. *Curr Protoc Stem Cell Biol.* 2014;1(SUPPL.28). doi:10.1002/9780470151808.sc02b06s28.
 296. Lo Surdo J, Bauer SR. Quantitative Approaches to Detect Donor and Passage Differences in Adipogenic Potential and Clonogenicity in Human Bone Marrow-Derived Mesenchymal Stem Cells. *Tissue Eng Part C Methods.* 2012;18(11):877-889. doi:10.1089/ten.tec.2011.0736.
 297. Colter DC, Sekiya I, Prockop DJ. Identification of a subpopulation of rapidly self-renewing and multipotential adult stem cells in colonies of human marrow stromal cells. *Proc Natl Acad Sci U S A.* 2001;98(14):7841-7845. doi:10.1073/pnas.141221698.
 298. Lian J, Lv S, Liu C, et al. Effects of serial passage on the characteristics and cardiac and neural differentiation of human umbilical cord wharton's jelly-derived mesenchymal stem cells. *Stem Cells Int.* 2016;2016. doi:10.1155/2016/9291013.
 299. Lee J, Kim HK, Rho JY, Han YM, Kim J. The human OCT-4 isoforms differ in their ability to confer self-renewal. *J Biol Chem.* 2006;281(44):33554-33565. doi:10.1074/jbc.M603937200.
 300. Hsiao L-C, Perbellini F, Gomes RSM, et al. Murine cardiosphere-derived cells are

- impaired by age but not by cardiac dystrophic dysfunction. *Stem Cells Dev.* 2014;23(9):1027-1036. doi:10.1089/scd.2013.0388.
301. Furtado MB, Costa MW, Pranoto EA, et al. Cardiogenic Genes Expressed in Cardiac Fibroblasts Contribute to Heart Development and Repair. *Circ Res.* 2014;114(9):1422-1434. doi:10.1161/CIRCRESAHA.114.302530.
 302. Zhou J, Zhang Y, Wen X, et al. Telocytes accompanying cardiomyocyte in primary culture: Two- and three-dimensional culture environment. *J Cell Mol Med.* 2010;14(11):2641-2645. doi:10.1111/j.1582-4934.2010.01186.x.
 303. Mummery CL, van Achterberg TA, van den Eijnden-van Raaij AJ, et al. Visceral-endoderm-like cell lines induce differentiation of murine P19 embryonal carcinoma cells. *Differentiation.* 1991;46(1):51-60. doi:10.1111/j.1432-0436.1991.tb00865.x.
 304. Choi YS, Dusting GJ, Stubbs S, et al. Differentiation of human adipose-derived stem cells into beating cardiomyocytes. *J Cell Mol Med.* 2010;14(4):878-889. doi:10.1111/j.1582-4934.2010.01009.x.
 305. Condorelli G, Borello U, De Angelis L, et al. Cardiomyocytes induce endothelial cells to trans-differentiate into cardiac muscle: implications for myocardium regeneration. *Proc Natl Acad Sci U S A.* 2001;98(19):10733-10738. doi:10.1073/pnas.191217898\r191217898 [pii].
 306. Laugwitz K-L, Moretti A, Lam J, et al. Postnatal isl1+ cardioblasts enter fully differentiated cardiomyocyte lineages. *Nature.* 2005;433(7026):647-653. doi:10.1038/nature03215.
 307. Pfister O, Mouquet F, Jain M, et al. CD31- but not CD31+ cardiac side population cells exhibit functional cardiomyogenic differentiation. *Circ Res.* 2005;97(1):52-61. doi:10.1161/01.RES.0000173297.53793.fa.
 308. Burridge PW, Matsa E, Shukla P, et al. Chemically defined generation of human cardiomyocytes. *Nat Methods.* 2014;11(8):855-860. doi:10.1038/nmeth.2999.
 309. Lian X, Hsiao C, Wilson G, et al. Robust cardiomyocyte differentiation from human pluripotent stem cells via temporal modulation of canonical Wnt signaling. *Proc Natl Acad Sci U S A.* 2012;109(27):E1848-57. doi:10.1073/pnas.1200250109.
 310. Cohen ED, Tian Y, Morrissey EE. Wnt signaling: an essential regulator of cardiovascular differentiation, morphogenesis and progenitor self-renewal. *Development.* 2008;135(5):789-798. doi:10.1242/dev.016865.
 311. Pagliari S, Jelinek J, Grassi G, Forte G. Targeting pleiotropic signaling pathways to control adult cardiac stem cell fate and function. *Front Physiol.* 2014;5(July):1-10. doi:10.3389/fphys.2014.00219.
 312. Mummery CL, Zhang J, Ng ES, Elliott DA, Elefanty AG, Kamp TJ. Differentiation of human embryonic stem cells and induced pluripotent stem cells to cardiomyocytes: A methods overview. *Circ Res.* 2012;111(3):344-358. doi:10.1161/CIRCRESAHA.110.227512.
 313. Murry CE, Field LJ, Menasché P. Cell-based cardiac repair reflections at the 10-year point. *Circulation.* 2005;112(20):3174-3183. doi:10.1161/CIRCULATIONAHA.105.546218.
 314. Barile L, Messina E, Giacomello A, Marbán E. Endogenous Cardiac Stem Cells. *Prog Cardiovasc Dis.* 2007;50(1):31-48. doi:10.1016/j.pcad.2007.03.005.
 315. Behfar A, Zingman L V, Hodgson DM, et al. Stem cell differentiation requires a paracrine pathway in the heart. *FASEB J.* 2002;16(12):1558-1566. doi:10.1096/fj.02-0072com.
 316. Yuasa S, Itabashi Y, Koshimizu U, et al. Transient inhibition of BMP signaling by Noggin induces cardiomyocyte differentiation of mouse embryonic stem cells. *Nat Biotechnol.* 2005;23(5):607-611. doi:10.1038/nbt1093.
 317. Slager HG, Van Inzen W, Freund E, Van den Eijnden-Van Raaij AJ, Mummery CL. Transforming growth factor-beta in the early mouse embryo: implications for the regulation of muscle formation and implantation. *Dev Genet.* 1993;14(3):212-224.

- doi:10.1002/dvg.1020140308.
318. Cagavi E, Bartulos O, Suh CY, et al. Functional cardiomyocytes derived from isl1 cardiac progenitors via Bmp4 stimulation. *PLoS One*. 2014;9(12). doi:10.1371/journal.pone.0110752.
 319. Laflamme M a, Chen KY, Naumova A V, et al. Cardiomyocytes derived from human embryonic stem cells in pro-survival factors enhance function of infarcted rat hearts. *Nat Biotechnol*. 2007;25(9):1015-1024. doi:10.1038/nbt1327.
 320. Ménard C, Hagège AA, Agbulut O, et al. Transplantation of cardiac-committed mouse embryonic stem cells to infarcted sheep myocardium: A preclinical study. *Lancet*. 2005;366(9490):1005-1012. doi:10.1016/S0140-6736(05)67380-1.
 321. Monzen K, Shiojima I, Hiroi Y, et al. Bone morphogenetic proteins induce cardiomyocyte differentiation through the mitogen-activated protein kinase kinase kinase TAK1 and cardiac transcription factors Csx/Nkx-2.5 and GATA-4. *Mol Cell Biol*. 1999;19(10):7096-7105. doi:10.1128/MCB.19.10.7096.
 322. Sachinidis A, Fleischmann BK, Kolossov E, Wartenberg M, Sauer H, Hescheler J. Cardiac specific differentiation of mouse embryonic stem cells. *Cardiovasc Res*. 2003;58(2):278-291. doi:10.1016/S0008-6363(03)00248-7.
 323. Smits AM, van Vliet P, Metz CH, et al. Human cardiomyocyte progenitor cells differentiate into functional mature cardiomyocytes: an in vitro model for studying human cardiac physiology and pathophysiology. *Nat Protoc*. 2009;4(2):232-243. doi:10.1038/nprot.2008.229.
 324. Goumans MJ, de Boer TP, Smits AM, et al. TGF- β 1 induces efficient differentiation of human cardiomyocyte progenitor cells into functional cardiomyocytes in vitro. *Stem Cell Res*. 2008;1(2):138-149. doi:10.1016/j.scr.2008.02.003.
 325. Choi SH, Jung SY, Asahara T, Suh W, Kwon SM, Baek SH. Direct comparison of distinct cardiomyogenic induction methodologies in human cardiac-derived c-kit positive progenitor cells. *Tissue Eng Regen Med*. 2012;9(6):311-319. doi:10.1007/s13770-012-0336-6.
 326. Roggia C, Ukena C, Böhm M, Kilter H. Hepatocyte growth factor (HGF) enhances cardiac commitment of differentiating embryonic stem cells by activating PI3 kinase. *Exp Cell Res*. 2007;313(5):921-930. doi:10.1016/j.yexcr.2006.12.009.
 327. Paquin J, Danalache BA, Jankowski M, McCann SM, Gutkowska J. Oxytocin induces differentiation of P19 embryonic stem cells to cardiomyocytes. *Proc Natl Acad Sci U S A*. 2002;99(14):9550-9555. doi:10.1073/pnas.152302499.
 328. Fathi F, Murasawa S, Hasegawa S, Asahara T, Kermani AJ, Mowla SJ. Cardiac differentiation of P19CL6 cells by oxytocin. *Int J Cardiol*. 2009;134(1):75-81. doi:10.1016/j.ijcard.2008.01.046.
 329. Matsuura K, Nagai T, Nishigaki N, et al. Adult Cardiac Sca-1-positive Cells Differentiate into Beating Cardiomyocytes. *J Biol Chem*. 2004;279(12):11384-11391. doi:10.1074/jbc.M310822200.
 330. Yoon BS, Yoo SJ, Lee JE, You S, Lee HT, Yoon HS. Enhanced differentiation of human embryonic stem cells into cardiomyocytes by combining hanging drop culture and 5-azacytidine treatment. *Differentiation*. 2006;74(4):149-159. doi:10.1111/j.1432-0436.2006.00063.x.
 331. Fukuda K. Development of regenerative cardiomyocytes from mesenchymal stem cells for cardiovascular tissue engineering. *Artif Organs*. 2001;25(3):187-193. doi:10.1046/j.1525-1594.2001.025003187.x.
 332. Rangappa S, Fen C, Lee EH, Bongso A, Wei ESK. Transformation of adult mesenchymal stem cells isolated from the fatty tissue into cardiomyocytes. *Ann Thorac Surg*. 2003;75(3):775-779. doi:10.1016/S0003-4975(02)04568-X.
 333. Qian Q, Qian H, Zhang X, et al. 5-Azacytidine Induces Cardiac Differentiation of Human Umbilical Cord-Derived Mesenchymal Stem Cells by Activating Extracellular Regulated Kinase. *Stem Cells Dev*. 2012;21(1):67-75. doi:10.1089/scd.2010.0519.

334. Xu W, Zhang X, Qian H, et al. Mesenchymal stem cells from adult human bone marrow differentiate into a cardiomyocyte phenotype in vitro. *Exp Biol Med (Maywood)*. 2004;229(7):623-631. doi:229/7/623 [pii].
335. Naeem N, Haneef K, Kabir N, Iqbal H, Jamall S, Salim A. DNA methylation inhibitors, 5-azacytidine and zebularine potentiate the transdifferentiation of rat bone marrow mesenchymal stem cells into cardiomyocytes. *Cardiovasc Ther*. 2013;31(4):201-209. doi:10.1111/j.1755-5922.2012.00320.x.
336. Passier R, Oostwaard DW, Snapper J, et al. Increased cardiomyocyte differentiation from human embryonic stem cells in serum-free cultures. *Stem Cells*. 2005;23(6):772-780. doi:10.1634/stemcells.2004-0184.
337. Takahashi T, Lord B, Schulze PC, et al. Ascorbic acid enhances differentiation of embryonic stem cells into cardiac myocytes. *Circulation*. 2003;107(14):1912-1916. doi:10.1161/01.CIR.0000064899.53876.A3.
338. Martinez EC, Wang J, Gan SU, Singh R, Lee CN, Kofidis T. Ascorbic acid improves embryonic cardiomyoblast cell survival and promotes vascularization in potential myocardial grafts in vivo. *Tissue Eng Part A*. 2010;16(4):1349-1361. doi:10.1089/ten.TEA.2009.0399.
339. Wobus a M, Kaomei G, Shan J, et al. Retinoic acid accelerates embryonic stem cell-derived cardiac differentiation and enhances development of ventricular cardiomyocytes. *J Mol Cell Cardiol*. 1997;29(6):1525-1539. doi:S0022282897904338 [pii].
340. Zandstra PW, Bauwens C, Yin T, et al. Scalable production of embryonic stem cell-derived cardiomyocytes. *Tissue Eng*. 2003;9(4):767-778. doi:10.1089/107632703768247449.
341. Drab M, Haller H, Bychkov R, et al. From totipotent embryonic stem cells to spontaneously contracting smooth muscle cells: a retinoic acid and db-cAMP in vitro differentiation model. *FASEB J*. 1997;11(11):905-915.
342. Lengerke C, Wingert R, Beeretz M, et al. Interactions between Cdx genes and retinoic acid modulate early cardiogenesis. *Dev Biol*. 2011;354(1):134-142. doi:10.1016/j.ydbio.2011.03.027.
343. McBurney MW, Jones-Villeneuve EM, Edwards MK, Anderson PJ. Control of muscle and neuronal differentiation in a cultured embryonal carcinoma cell line. *Nature*. 1982;299(5879):165-167.
344. Ventura C, Maioli M. Opioid peptide gene expression primes cardiogenesis in embryonal pluripotent stem cells. *Circ Res*. 2000;87(3):189-194. doi:10.1161/01.RES.87.3.189.
345. Skerjanc IS. Cardiac and skeletal muscle development in P19 embryonal carcinoma cells. *Trends Cardiovasc Med*. 1999;9(5):139-143. doi:10.1016/S1050-1738(99)00017-1.
346. Jasmin, Spray DC, Campos de Carvalho AC, Mendez-Otero R. Chemical induction of cardiac differentiation in p19 embryonal carcinoma stem cells. *Stem Cells Dev*. 2010;19(3):403-412. doi:10.1089/scd.2009.0234.
347. Linke A, Müller P, Nurzynska D, et al. Stem cells in the dog heart are self-renewing, clonogenic, and multipotent and regenerate infarcted myocardium, improving cardiac function. *Proc Natl Acad Sci U S A*. 2005;102(25):8966-8971. doi:10.1073/pnas.0502678102.
348. Issa JP, Kantarjian H. Azacitidine. *Nat Rev Drug Discov*. 2005;Suppl:S6-7. <http://www.ncbi.nlm.nih.gov/pubmed/15962522>.
349. Stresemann C, Lyko F. Modes of action of the DNA methyltransferase inhibitors azacytidine and decitabine. *Int J Cancer*. 2008;123(1):8-13. doi:10.1002/ijc.23607.
350. Issa J-PJ. DNA methylation as a therapeutic target in cancer. *Clin Cancer Res*. 2007;13(6):1634-1637. doi:10.1158/1078-0432.CCR-06-2076.
351. Makino S, Fukuda K, Miyoshi S, et al. Cardiomyocytes can be generated from

- marrow stromal cells in vitro. *J Clin Invest*. 1999;103(5):697-705. doi:10.1172/JCI5298.
352. Kaur K, Yang J, Eisenberg C a, Eisenberg LM. 5-Azacytidine Promotes the Transdifferentiation of Cardiac Cells to Skeletal Myocytes. *Cell Reprogram*. 2014;16(5):1-7. doi:10.1089/cell.2014.0021.
 353. Wan Safwani WKZ, Makpol S, Sathapan S, Chua KH. 5-Azacytidine is insufficient for cardiogenesis in human adipose-derived stem cells. *J Negat Results Biomed*. 2012;11(1):3. doi:10.1186/1477-5751-11-3.
 354. Cao N, Liu Z, Chen Z, et al. Ascorbic acid enhances the cardiac differentiation of induced pluripotent stem cells through promoting the proliferation of cardiac progenitor cells. *Cell Res*. 2012;22(1):219-236. doi:10.1038/cr.2011.195.
 355. Choi K-M, Seo Y-K, Yoon H-H, et al. Effect of ascorbic acid on bone marrow-derived mesenchymal stem cell proliferation and differentiation. *J Biosci Bioeng*. 2008;105(6):586-594. doi:10.1263/jbb.105.586.
 356. Sato H, Takahashi M, Ise H, et al. Collagen synthesis is required for ascorbic acid-enhanced differentiation of mouse embryonic stem cells into cardiomyocytes. *Biochem Biophys Res Commun*. 2006;342(1):107-112. doi:10.1016/j.bbrc.2006.01.116.
 357. Li T-S, Hayashi M, Ito H, et al. Regeneration of infarcted myocardium by intramyocardial implantation of ex vivo transforming growth factor-beta-preprogrammed bone marrow stem cells. *Circulation*. 2005;111(19):2438-2445. doi:10.1161/01.CIR.0000167553.49133.81.
 358. Lim JY, Kim WH, Kim J, Park SI. Involvement of TGF-beta1 signaling in cardiomyocyte differentiation from P19CL6 cells. *Mol Cells*. 2007;24(3):431-436. doi:1151 [pii].
 359. McCulloch C a, Tenenbaum HC. Dexamethasone induces proliferation and terminal differentiation of osteogenic cells in tissue culture. *Anat Rec*. 1986;215:397-402. doi:10.1002/ar.1092150410.
 360. Jaiswal N, Haynesworth SE, Caplan a I, Bruder SP. Osteogenic differentiation of purified, culture-expanded human mesenchymal stem cells in vitro. *J Cell Biochem*. 1997;64(2):295-312. doi:10.1002/(sici)1097-4644(199702)64:2<295::aid-jcb12>3.0.co;2-i.
 361. Hamidouche Z, Haÿ E, Vaudin P, et al. FHL2 mediates dexamethasone-induced mesenchymal cell differentiation into osteoblasts by activating Wnt/beta-catenin signaling-dependent Runx2 expression. *FASEB J*. 2008;22:3813-3822. doi:10.1096/fj.08-106302.
 362. Chang PL, Blair HC, Zhao X, et al. Comparison of fetal and adult marrow stromal cells in osteogenesis with and without glucocorticoids. *Connect Tissue Res*. 2006;47(2):67-76. doi:10.1080/03008200600584074.
 363. Feng X-H, Derynck R. Specificity and Versatility in TGF-beta Signaling Through Smads TGF-beta: transforming growth factor-beta. *Annu Rev Cell Dev Biol*. 2005;21:659-693. doi:10.1146/.
 364. Moustakas A, Heldin C-HH. The regulation of TGFbeta signal transduction. *Development*. 2009;136(22):3699-3714. doi:136/22/3699 [pii]\n10.1242/dev.030338 [doi].
 365. Wu MY, Hill CS. TGF-?? Superfamily Signaling in Embryonic Development and Homeostasis. *Dev Cell*. 2009;16(3):329-343. doi:10.1016/j.devcel.2009.02.012.
 366. Shi Y, Massagué J. Mechanisms of TGF-beta signaling from cell membrane to the nucleus. *Cell*. 2003;113(6):685-700. doi:10.1016/S0092-8674(03)00432-X.
 367. Ikushima H, Miyazono K. TGFbeta signalling: a complex web in cancer progression. *Nat Rev Cancer*. 2010;10(6):415-424. doi:10.1038/nrc2853.
 368. Pardali E, Goumans MJ, ten Dijke P. Signaling by members of the TGF-beta family in vascular morphogenesis and disease. *Trends Cell Biol*. 2010;20(9):556-567. doi:10.1016/j.tcb.2010.06.006.

369. Akhmetshina A, Palumbo K, Dees C, et al. Activation of canonical Wnt signalling is required for TGF- β -mediated fibrosis. *Nat Commun.* 2012;3:735. doi:10.1038/ncomms1734.
370. Teekakirikul P, Eminaga S, Toka O, et al. Cardiac fibrosis in mice with hypertrophic cardiomyopathy is mediated by non-myocyte proliferation and requires Tgf- β . *J Clin Invest.* 2010;120(10):3520-3529. doi:10.1172/JCI42028.
371. Goumans MJ, Mummery C. Functional analysis of the TGF β receptor/Smad pathway through gene ablation in mice. *Int J Dev Biol.* 2000;44(3):253-265. doi:10.1002/stem.286.
372. Cai W, Guzzo RM, Wei K, Willems E, Davidovics H, Mercola M. A nodal-to-TGF β cascade exerts biphasic control over cardiopoiesis. *Circ Res.* 2012;111(7):876-881. doi:10.1161/CIRCRESAHA.112.270272.
373. Goumans M-J, de Boer TP, Smits AM, et al. TGF- β 1 induces efficient differentiation of human cardiomyocyte progenitor cells into functional cardiomyocytes in vitro. *Stem Cell Res.* 2008;1(2):138-149. doi:10.1016/j.scr.2008.02.003.
374. Abdel-Latif A, Zuba-Surma EK, Case J, et al. TGF- β 1 enhances cardiomyogenic differentiation of skeletal muscle-derived adult primitive cells. *Basic Res Cardiol.* 2008;103(6):514-524. doi:10.1007/s00395-008-0729-9.
375. FLANDERS K. Autoinduction of mRNA and protein expression for transforming growth factor- β s in cultured cardiac cells. *J Mol Cell Cardiol.* 1995;27(2):805-812. doi:10.1016/0022-2828(95)90087-X.
376. Nuclear Receptors Nomenclature C. A unified nomenclature system for the nuclear receptor superfamily. *Cell.* 1999;97(2):161-163. doi:10.1016/S0092-8674(00)80726-6.
377. Berger J, Moller DE. The mechanisms of action of PPARs. *Annu Rev Med.* 2002;53(1):409-435. doi:10.1146/annurev.med.53.082901.104018.
378. Michalik L, Auwerx J, Berger JP, et al. International Union of Pharmacology. LXI. Peroxisome proliferator-activated receptors. *Pharmacol Rev.* 2006;58(4):726-741. doi:10.1124/pr.58.4.5.
379. Westin S, Kurokawa R, Nolte RT, et al. Interactions controlling the assembly of nuclear-receptor heterodimers and co-activators. *Nature.* 1998;395(6698):199-202. doi:10.1038/26040.
380. Göttlicher M, Widmark E, Li Q, Gustafsson JA. Fatty acids activate a chimera of the clofibrilic acid-activated receptor and the glucocorticoid receptor. *Proc Natl Acad Sci U S A.* 1992;89(10):4653-4657. doi:10.1073/pnas.89.10.4653.
381. Brown PJ, Smith-Oliver T a, Charifson PS, et al. Identification of peroxisome proliferator-activated receptor ligands from a biased chemical library. *Chem Biol.* 1997;4(12):909-918. doi:DOI: 10.1016/S1074-5521(97)90299-4.
382. Brown P, Winegar D, Plunket K. A ureido-thioisobutyric acid (GW9578) is a subtype-selective PPAR α agonist with potent lipid-lowering activity. *J Med Chem.* 1999;42:3785-88.
383. Ding L, Liang X-G, Hu Y, Zhu D-Y, Lou Y-J. Involvement of p38MAPK and reactive oxygen species in icariin-induced cardiomyocyte differentiation of murine embryonic stem cells in vitro. *Stem Cells Dev.* 2008;17(4):751-760. doi:10.1089/scd.2008.0206.
384. Issemann I, Green S. Activation of a member of the steroid hormone receptor superfamily by peroxisome proliferators. *Nature.* 1990;347(6294):645-650. doi:10.1038/347645a0.
385. Kersten S, Desvergne B, Wahli W. Roles of PPARs in health and disease. *Nature.* 2000;405(6785):421-424. doi:10.1038/35013000.
386. Burkart EM, Sambandam N, Han X, et al. Nuclear receptors PPAR β and PPAR δ direct distinct metabolic regulatory programs in the mouse heart. *J Clin Invest.* 2007;117(12):3930-3939. doi:10.1172/JCI32578.
387. Kersten S. Integrated physiology and systems biology of PPAR α . *Mol Metab.*

- 2014;3(4):354-371. doi:10.1016/j.molmet.2014.02.002.
388. Leone TC, Weinheimer CJ, Kelly DP. A critical role for the peroxisome proliferator-activated receptor (PPAR) in the cellular fasting response: The PPAR-null mouse as a model of fatty acid oxidation disorders. *Proc Natl Acad Sci*. 1999;96(13):7473-7478. doi:10.1073/pnas.96.13.7473.
389. Gulick T, Cresci S, Caira T, Moore DD, Kelly DP. The peroxisome proliferator-activated receptor regulates mitochondrial fatty acid oxidative enzyme gene expression. *Proc Natl Acad Sci U S A*. 1994;91(23):11012-11016. <http://www.pubmedcentral.nih.gov/articlerender.fcgi?artid=45156&tool=pmcentrez&rendertype=abstract>.
390. Finck BN, Lehman JJ, Leone TC, et al. The cardiac phenotype induced by PPAR α overexpression mimics that caused by diabetes mellitus. *J Clin Invest*. 2002;109(1):121-130. doi:10.1172/JCI200214080.
391. Ding L, Liang X-G, Lou Y-J. Time-dependence of cardiomyocyte differentiation disturbed by peroxisome proliferator-activated receptor alpha inhibitor GW6471 in murine embryonic stem cells in vitro. *Acta Pharmacol Sin*. 2007;28(5):634-642. doi:10.1111/j.1745-7254.2007.00558.x.
392. Finck BN, Kelly DP. Peroxisome proliferator-activated receptor alpha (PPAR α) signaling in the gene regulatory control of energy metabolism in the normal and diseased heart. *J Mol Cell Cardiol*. 2002;34(10):1249-1257. doi:10.1006/jmcc.2002.2061.
393. Sanderson LM, Degenhardt T, Koppen A, et al. Peroxisome proliferator-activated receptor beta/delta (PPAR β/δ) but not PPAR α serves as a plasma free fatty acid sensor in liver. *Mol Cell Biol*. 2009;29(23):6257-6267. doi:10.1128/MCB.00370-09.
394. Handschin C, Spiegelman BM. PGC-1 coactivators, energy homeostasis, and metabolism. *Endocr Rev*. 2006.
395. Vega RB, Huss JM, Kelly DP. The coactivator PGC-1 cooperates with peroxisome proliferator-activated receptor alpha in transcriptional control of nuclear genes encoding mitochondrial fatty acid oxidation enzymes. *Mol Cell Biol*. 2000;20(5):1868-1876. doi:10.1128/MCB.20.5.1868-1876.2000.
396. Egan BM, Lu G, Greene EL. Vascular effects of non-esterified fatty acids: implications for the cardiovascular risk factor cluster. *Prostaglandins LeukotEssentFatty Acids*. 1999;60(0952-3278 (Print)):411-420.
397. Popeijus HE, van Otterdijk SD, van der Krieken SE, et al. Fatty acid chain length and saturation influences PPAR α transcriptional activation and repression in HepG2 cells. *Mol Nutr Food Res*. 2014;58(12):2342-2349. doi:10.1002/mnfr.201400314.
398. Moon HS, Batirel S, Mantzoros CS. Alpha linolenic acid and oleic acid additively down-regulate malignant potential and positively cross-regulate AMPK/S6 axis in OE19 and OE33 esophageal cancer cells. *Metabolism*. 2014;63(11):1447-1454. doi:10.1016/j.metabol.2014.07.009.
399. Liu Z, Xiao Y, Yuan Y, et al. Effects of oleic acid on cell proliferation through an integrin-linked kinase signaling pathway in 786-O renal cell carcinoma cells. *Oncol Lett*. 2013;5(4):1395-1399. doi:10.3892/ol.2013.1160.
400. Harvey K a, Walker CL, Xu Z, et al. Oleic acid inhibits stearic acid-induced inhibition of cell growth and pro-inflammatory responses in human aortic endothelial cells. *J Lipid Res*. 2010;51:3470-3480. doi:10.1194/jlr.M010371.
401. Toborek M, Lee YW, Garrido R, Kaiser S, Hennig B. Unsaturated fatty acids selectively induce an inflammatory environment in human endothelial cells. *Am J Clin Nutr*. 2002;75(1):119-125.
402. Schlich R, Lamers D, Eckel J, Sell H. Adipokines enhance oleic acid-induced proliferation of vascular smooth muscle cells by inducing CD36 expression. *Arch Physiol Biochem*. 2015;3455:1-7. doi:10.3109/13813455.2015.1045520.

403. Haeiwa H, Fujita T, Saitoh Y, Miwa N. Oleic acid promotes adaptability against oxidative stress in 3T3-L1 cells through lipohormesis. *Mol Cell Biochem.* 2014;386(1-2):73-83. doi:10.1007/s11010-013-1846-9.
404. Hatanaka E, Dermargos A, Hirata AE, et al. Oleic, Linoleic and Linolenic Acids Increase ROS Production by Fibroblasts via NADPH Oxidase Activation. *PLoS One.* 2013;8(4). doi:10.1371/journal.pone.0058626.
405. Tumova J, Malisova L, Andel M, Trnka J. Protective Effect of Unsaturated Fatty Acids on Palmitic Acid-Induced Toxicity in Skeletal Muscle Cells is not Mediated by PPAR δ Activation. *Lipids.* 2015;50(10):955-964. doi:10.1007/s11745-015-4058-0.
406. Gehrman W, W??rdemann W, Pl??tz T, J??rns A, Lenzen S, Elsner M. Antagonism between Saturated and Unsaturated Fatty Acids in ROS Mediated Lipotoxicity in Rat Insulin-Producing Cells. *Cell Physiol Biochem.* 2015;36(3):852-865. doi:10.1159/000430261.
407. Huang YS, Tseng YZ, Wu JC, Wang SM. Mechanism of oleic acid-induced gap junctional disassembly in rat cardiomyocytes. *J Mol Cell Cardiol.* 2004;37(3):755-766. doi:10.1016/j.yjmcc.2004.06.011.
408. Al-Shudiefat AAR, Sharma AK, Bagchi AK, Dhingra S, Singal PK. Oleic acid mitigates TNF- α -induced oxidative stress in rat cardiomyocytes. *Mol Cell Biochem.* 2013;372:75-82. doi:10.1007/s11010-012-1447-z.
409. Lin YK, Chen YC, Kao YH, et al. A monounsaturated fatty acid (oleic acid) modulates electrical activity in atrial myocytes with calcium and sodium dysregulation. *Int J Cardiol.* 2014;176(1):191-198. doi:10.1016/j.ijcard.2014.07.004.
410. Perdomo L, Beneit N, Otero YF, et al. Protective role of oleic acid against cardiovascular insulin resistance and in the early and late cellular atherosclerotic process. *Cardiovasc Diabetol.* 2015;14:75. doi:10.1186/s12933-015-0237-9.
411. Lopaschuk GD, Jaswal JS. Energy metabolic phenotype of the cardiomyocyte during development, differentiation, and postnatal maturation. *J Cardiovasc Pharmacol.* 2010;56(2):130-140. doi:10.1097/FJC.0b013e3181e74a14.
412. Lai L, Leone TC, Zechner C, et al. Transcriptional coactivators PGC-1 α and PGC-1 β control overlapping programs required for perinatal maturation of the heart. *Genes Dev.* 2008;22(14):1948-1961. doi:10.1101/gad.1661708.
413. Kolwicz SC, Purohit S, Tian R. Cardiac metabolism and its interactions with contraction, growth, and survival of cardiomyocytes. *Circ Res.* 2013;113(5):603-616. doi:10.1161/CIRCRESAHA.113.302095.
414. Lopaschuk GD, Spafford M a, Marsh DR. Glycolysis is predominant source of myocardial ATP production immediately after birth. *Am J Physiol.* 1991;261(6 Pt 2):H1698-H1705. <http://www.ncbi.nlm.nih.gov/pubmed/1750528>.
415. Breckenridge RA, Piotrowska I, Ng KE, et al. Hypoxic Regulation of Hand1 Controls the Fetal-Neonatal Switch in Cardiac Metabolism. *PLoS Biol.* 2013;11(9). doi:10.1371/journal.pbio.1001666.
416. Attardi G, Schatz G. Biogenesis of mitochondria. *Annu Rev Cell Biol.* 1988;4(1):289-333. doi:10.1002/jbt.20396.
417. Mayor F, Cuezva JM. Hormonal and metabolic changes in the perinatal period. *Biol Neonate.* 1985;48(0006-3126 (Print)):185-196.
418. Lehman JJ, Barger PM, Kovacs A, Saffitz JE, Medeiros DM, Kelly DP. Peroxisome proliferator-activated receptor gamma coactivator-1 promotes cardiac mitochondrial biogenesis. *J Clin Invest.* 2000;106(7):847-856. doi:10.1172/JCI10268.
419. Steinmetz M, Quentin T, Poppe A, Paul T, Jux C. Changes in expression levels of genes involved in fatty acid metabolism: upregulation of all three members of the PPAR family (a,c,d) and the newly described adiponectin receptor 2, but not adiponectin receptor 1 during neonatal cardiac development of the. *Basic Res*

- Cardiol.* 2005;100((3)):263-269.
420. Virbasius CMA, Virbasius J V., Scarpulla RC. NRF-1, an activator involved in nuclear-mitochondrial interactions, utilizes a new DNA-binding domain conserved in a family of developmental regulators. *Genes Dev.* 1993;7(12 A):2431-2445. doi:10.1101/gad.7.12a.2431.
 421. Chung S, Dzeja PP, Faustino RS, Perez-Terzic C, Behfar A, Terzic A. Mitochondrial oxidative metabolism is required for the cardiac differentiation of stem cells. *Nat Clin Pr Cardiovasc Med.* 2007;4 Suppl 1:S60-7. doi:ncpcardio0766 [pii]\r10.1038/ncpcardio0766.
 422. Lee SH, Wolf PL, Escudero R, Deutsch R, Jamieson SW, Thistlethwaite PA. Early expression of angiogenesis factors in acute myocardial ischemia and infarction. *N Engl J Med.* 2000;342(9):626-633. doi:10.1056/NEJM200003023420904.
 423. Cross HR, Opie LH, Radda GK, Clarke K. Is a high glycogen content beneficial or detrimental to the ischemic rat heart? A controversy resolved. *Circ Res.* 1996;78(3):482-491. doi:10.1161/01.RES.78.3.482.
 424. Sharov VG, Goussev a, Lesch M, Goldstein S, Sabbah HN. Abnormal mitochondrial function in myocardium of dogs with chronic heart failure. *J Mol Cell Cardiol.* 1998;30(9):1757-1762. doi:10.1006/jmcc.1998.0739.
 425. Sharov VG, Todor A V., Silverman N, Goldstein S, Sabbah HN. Abnormal mitochondrial respiration in failed human myocardium. *J Mol Cell Cardiol.* 2000;32(12):2361-2367. doi:10.1006/jmcc.2000.1266.
 426. Gong G, Liu J, Liang P, et al. Oxidative capacity in failing hearts. *Am J Physiol Heart Circ Physiol.* 2003;285(2):H541-8. doi:10.1152/ajpheart.01142.2002.
 427. Casademont J, Miró O. Electron transport chain defects in heart failure. *Heart Fail Rev.* 2002;7(2):131-139. <http://www.ncbi.nlm.nih.gov/pubmed/11988637>.
 428. Marin-Garcia J, Goldenthal MJ, Moe GW. Mitochondrial pathology in cardiac failure. *Cardiovasc Res.* 2001;49(1):17-26. doi:10.1016/S0008-6363(00)00241-8.
 429. Quigley a F, Kapsa RM, Esmore D, Hale G, Byrne E. Mitochondrial respiratory chain activity in idiopathic dilated cardiomyopathy. *J Card Fail.* 2000;6(1):47-55.
 430. Taegtmeyer H, Sen S, Vela D. Return to the fetal gene program: A suggested metabolic link to gene expression in the heart. In: *Annals of the New York Academy of Sciences.* Vol 1188. ; 2010:191-198. doi:10.1111/j.1749-6632.2009.05100.x.
 431. Leong HS, Grist M, Parsons H, et al. Accelerated rates of glycolysis in the hypertrophied heart: are they a methodological artifact? *Am J Physiol Endocrinol Metab.* 2002;282:E1039-E1045. doi:10.1152/ajpendo.00507.2001.
 432. Kreipke R, Wang Y, Miklas JW, Mathieu J, Ruohola-Baker H. Metabolic Remodeling in early development and cardiomyocyte maturation. *Semin Cell Dev Biol.* 2016;52:84-92. doi:10.1016/j.semcdb.2016.02.004.
 433. Lesnefsky EJ, Gudz TI, Moghaddas S, et al. Aging decreases electron transport complex III activity in heart interfibrillar mitochondria by alteration of the cytochrome c binding site. *J Mol Cell Cardiol.* 2001;33(1):37-47. doi:10.1006/jmcc.2000.1273.
 434. Biala AK, Dhingra R, Kirshenbaum LA. Mitochondrial dynamics: Orchestrating the journey to advanced age. *J Mol Cell Cardiol.* 2015;83:37-43. doi:10.1016/j.yjmcc.2015.04.015.
 435. Warburg O. Injuring of Respiration the Origin of Cancer Cells. *Science (80-).* 1956;123(3191):309-314. doi:10.1126/science.123.3191.309.
 436. Ito K, Suda T. Metabolic requirements for the maintenance of self-renewing stem cells. *Nat Rev Mol Cell Biol.* 2014;15(4):243-256. doi:10.1038/nrm3772.
 437. Vander Heiden MG, Cantley LC, Thompson CB. Understanding the Warburg effect: the metabolic requirements of cell proliferation. *Science.* 2009;324(5930):1029-1033. doi:10.1126/science.1160809.
 438. Munyon W, Merchant D. The relation between glucose utilization, lactic acid

- production and utilization and the growth cycle of L strain fibroblasts. *Exp Cell Res.* 1959;17:490–98. doi:10.1016/0014-4827(59)90069-2.
439. Wang T, Marquardt C, Foker J. Aerobic glycolysis during lymphocyte proliferation. *Nature.* 1976;261(5562):702-705. doi:10.1038/261702a0.
 440. Hedekov CJ. Early Effects of Phytohaemagglutinin on Glucose Metabolism of Normal Human Lymphocytes. *Biochem J.* 1968;110(2):373-380. <http://www.pubmedcentral.nih.gov/articlerender.fcgi?artid=1187214&tool=pmcentrez&rendertype=abstract>.
 441. Kondoh H, Leonart ME, Nakashima Y, et al. A High Glycolytic Flux Supports the Proliferative Potential of Murine Embryonic Stem Cells. *Antioxid Redox Signal.* 2006;0(0):61221112325011. doi:10.1089/ars.2007.9.ft-14.
 442. Moussaieff A, Rouleau M, Kitsberg D, et al. Glycolysis-Mediated Changes in Acetyl-CoA and Histone Acetylation Control the Early Differentiation of Embryonic Stem Cells. *Cell Metab.* 2015;21(3):392-402. doi:S1550-4131(15)00054-6 [pii]\r10.1016/j.cmet.2015.02.002.
 443. Suda T, Takubo K, Semenza GL. Metabolic regulation of hematopoietic stem cells in the hypoxic niche. *Cell Stem Cell.* 2011;9(4):298-310. doi:10.1016/j.stem.2011.09.010.
 444. Warr MR, Passegu?? E. Metabolic makeover for HSCs. *Cell Stem Cell.* 2013;12(1):1-3. doi:10.1016/j.stem.2012.12.005.
 445. Simsek T, Kocabas F, Zheng J, et al. The distinct metabolic profile of hematopoietic stem cells reflects their location in a hypoxic niche. *Cell Stem Cell.* 2010;7(3):380-390. doi:10.1016/j.stem.2010.07.011.
 446. DeBerardinis RJ, Mancuso A, Daikhin E, et al. Beyond aerobic glycolysis: transformed cells can engage in glutamine metabolism that exceeds the requirement for protein and nucleotide synthesis. *Proc Natl Acad Sci U S A.* 2007;104(49):19345-19350. doi:10.1073/pnas.0709747104.
 447. Lunt SY, Vander Heiden MG. Aerobic glycolysis: meeting the metabolic requirements of cell proliferation. *Annu Rev Cell Dev Biol.* 2011;27:441-464. doi:10.1146/annurev-cellbio-092910-154237.
 448. Dos Santos F, Andrade PZ, Boura JS, Abecasis MM, Da Silva CL, Cabral JMS. Ex vivo expansion of human mesenchymal stem cells: A more effective cell proliferation kinetics and metabolism under hypoxia. *J Cell Physiol.* 2010;223(1):27-35. doi:10.1002/jcp.21987.
 449. Hosios AM, Hecht VC, Danai LV, et al. Amino Acids Rather than Glucose Account for the Majority of Cell Mass in Proliferating Mammalian Cells. *Dev Cell.* 2016;36(5):540-549. doi:10.1016/j.devcel.2016.02.012.
 450. Schönfeld P, Schild L, Bohnensack R. Expression of the ADP/ATP carrier and expansion of the mitochondrial (ATP + ADP) pool contribute to postnatal maturation of the rat heart. *Eur J Biochem.* 1996;241(3):895-900.
 451. Folmes CDL, Nelson TJ, Martinez-Fernandez A, et al. Somatic oxidative bioenergetics transitions into pluripotency-dependent glycolysis to facilitate nuclear reprogramming. *Cell Metab.* 2011;14(2):264-271. doi:10.1016/j.cmet.2011.06.011.
 452. Wang Z, Yang Y, Xiang X, Zhu Y, Men J, He M. [Estimation of the normal range of blood glucose in rats]. *Wei Sheng Yan Jiu.* 2010;39(2):133-137, 142. <http://www.ncbi.nlm.nih.gov/pubmed/20459020>.
 453. Wolfensohn S, Lloyd M. *Handbook of Laboratory Animal Management and Welfare.* Third. lackwell Publishing Ltd; 2003.
 454. Chung S, Arrell DK, Faustino RS, Terzic A, Dzeja PP. Glycolytic network restructuring integral to the energetics of embryonic stem cell cardiac differentiation. *J Mol Cell Cardiol.* 2010;48(4):725-734. doi:10.1016/j.yjmcc.2009.12.014.
 455. Porter GA, Hom JR, Hoffman DL, Quintanilla RA, Bentley KL de M, Sheu SS.

- Bioenergetics, mitochondria, and cardiac myocyte differentiation. *Prog Pediatr Cardiol.* 2011;31(2):75-81. doi:10.1016/j.ppedcard.2011.02.002.
456. Cho YM, Kwon S, Pak YK, et al. Dynamic changes in mitochondrial biogenesis and antioxidant enzymes during the spontaneous differentiation of human embryonic stem cells. *Biochem Biophys Res Commun.* 2006;348:1472-1478. doi:10.1016/j.bbrc.2006.08.020.
 457. Norddahl GL, Pronk CJ, Wahlestedt M, et al. Accumulating mitochondrial DNA mutations drive premature hematopoietic aging phenotypes distinct from physiological stem cell aging. *Cell Stem Cell.* 2011;8(5):499-510. doi:10.1016/j.stem.2011.03.009.
 458. Inoue SI, Noda S, Kashima K, Nakada K, Hayashi JI, Miyoshi H. Mitochondrial respiration defects modulate differentiation but not proliferation of hematopoietic stem and progenitor cells. *FEBS Lett.* 2010;584(15):3402-3409. doi:S0014-5793(10)00531-4 [pii]\r10.1016/j.febslet.2010.06.036.
 459. Van Blerkom J. Mitochondria in early mammalian development. *Semin Cell Dev Biol.* 2009;20(3):354-364. doi:10.1016/j.semcdb.2008.12.005.
 460. Shyh-Chang N, Locasale JW, Lyssiotis CA, et al. Influence of threonine metabolism on S-adenosylmethionine and histone methylation. *Science (80-).* 2013;339(6116):222-226. doi:10.1126/science.1226603.
 461. De Sousa Andrade LN, De Lima TM, Curi R, De Lauro Castrucci AM. Toxicity of fatty acids on murine and human melanoma cell lines. *Toxicol Vitro.* 2005;19(4):553-560. doi:10.1016/j.tiv.2005.02.002.
 462. Cottet-Rousselle C, Ronot X, Leverve X, Mayol JF. Cytometric assessment of mitochondria using fluorescent probes. *Cytom Part A.* 2011;79 A(6):405-425. doi:10.1002/cyto.a.21061.
 463. Xu C. Characterization and Enrichment of Cardiomyocytes Derived From Human Embryonic Stem Cells. *Circ Res.* 2002;91(6):501-508. doi:10.1161/01.RES.0000035254.80718.91.
 464. Fijnvandraat AC, Van Ginneken ACG, Schumacher CA, et al. Cardiomyocytes purified from differentiated embryonic stem cells exhibit characteristics of early chamber myocardium. *J Mol Cell Cardiol.* 2003;35(12):1461-1472. doi:10.1016/j.yjmcc.2003.09.011.
 465. Van Laake LW, Van Hoof D, Mummery CL. Cardiomyocytes derived from stem cells. *Ann Med.* 2005;37(7):499-512. doi:N782Q30313536680 [pii]\r10.1080/07853890500327843.
 466. Wang C, Hu SM. Developmental regulation in the expression of rat heart glucose transporters. *Biochem Biophys Res Commun.* 1991;177(3):1095-1100. <http://www.ncbi.nlm.nih.gov/pubmed/1711843>.
 467. Studelska DR, Campbell C, Pang S, Rodnick KJ, James DE. Developmental expression of insulin-regulatable glucose transporter GLUT-4. *Am J Physiol - Endocrinol Metab.* 1992;263(1):E102-E106.
 468. Postic C, Leturque A, Printz RL, et al. Development and regulation of glucose transporter and hexokinase expression in rat. *Am J Physiol.* 1994;266(4 Pt 1):E548-59. http://www.ncbi.nlm.nih.gov/entrez/query.fcgi?cmd=Retrieve&db=PubMed&do pt=Citation&list_uids=8178975.
 469. Ding L, Liang X, Zhu D, Lou Y. Peroxisome proliferator-activated receptor alpha is involved in cardiomyocyte differentiation of murine embryonic stem cells in vitro. *Cell Biol Int.* 2007;31(9):1002-1009. doi:10.1016/j.cellbi.2007.03.013.
 470. Looijenga LHJ, Stoop H, De Leeuw HPJC, et al. POU5F1 (OCT3/4) identifies cells with pluripotent potential in human germ cell tumors. *Cancer Res.* 2003;63(9):2244-2250.
 471. Niwa H, Miyazaki J, Smith AG. Quantitative expression of Oct-3/4 defines differentiation, dedifferentiation or self-renewal of ES cells. *Nat Genet.*

- 2000;24(4):372-376. doi:10.1038/74199.
472. Masui S, Nakatake Y, Toyooka Y, et al. Pluripotency governed by Sox2 via regulation of Oct3/4 expression in mouse embryonic stem cells. *Nat Cell Biol.* 2007;9(6):625-U26. doi:10.1038/Ncb1589.
 473. Noguchi T, Camp P, Alix SL, et al. Myosin from failing and non-failing human ventricles exhibit similar contractile properties. *J Mol Cell Cardiol.* 2003;35(1):91-97. doi:10.1016/S0022-2828(02)00282-1.
 474. García-Castro M, Reguero JR, Batalla A, et al. Hypertrophic cardiomyopathy: Low frequency of mutations in the β -myosin heavy chain (MYH7) and cardiac troponin T (TNNT2) genes among Spanish patients. *Clin Chem.* 2003;49(8):1279-1285. doi:10.1373/49.8.1279.
 475. Epp TA, Dixon IMC, Wang H-Y, Sole MJ, Liew C-C. Structural organization of the human cardiac α -myosin heavy chain gene (MYH6). *Genomics.* 1993;18(3):505-509. doi:10.1016/S0888-7543(11)80006-6.
 476. Ching Y-H, Ghosh TK, Cross SJ, et al. Mutation in myosin heavy chain 6 causes atrial septal defect. *Nat Genet.* 2005;37(4):423-428. doi:10.1038/ng1526.
 477. Anderson P a, Malouf NN, Oakeley a E, Pagani ED, Allen PD. Troponin T isoform expression in humans. A comparison among normal and failing adult heart, fetal heart, and adult and fetal skeletal muscle. *Circ Res.* 1991;69(5):1226-1233. doi:10.1161/01.RES.69.5.1226.
 478. Boengler K, Schulz R, Heusch G. Connexin 43 signalling and cardioprotection. *Heart.* 2006;92(12):1724-1727. doi:10.1136/hrt.2005.066878.
 479. Eckardt D, Kirchhoff S, Kim JS, et al. Cardiomyocyte-restricted deletion of connexin43 during mouse development. *J Mol Cell Cardiol.* 2006;41(6):963-971. doi:10.1016/j.yjmcc.2006.07.017.
 480. Paulin D, Li Z. Desmin: A major intermediate filament protein essential for the structural integrity and function of muscle. *Exp Cell Res.* 2004;301(1):1-7. doi:10.1016/j.yexcr.2004.08.004.
 481. Capetanaki Y, Milner DJ, Weitzer G. Desmin in muscle formation and maintenance: knockouts and consequences. *Cell Struct Funct.* 1997;22(1):103-116. doi:10.1247/csf.22.103.
 482. Castelló A, Cadefau J, Cussó R, et al. GLUT-4 and GLUT-1 glucose transporter expression is differentially regulated by contractile activity in skeletal muscle. *J Biol Chem.* 1993;268(20):14998-15003. <http://www.ncbi.nlm.nih.gov/pubmed/8325875>.
 483. Pepino MY, Kuda O, Samovski D, Abumrad N a. Structure-Function of CD36 and Importance of Fatty Acid Signal Transduction in Fat Metabolism. *Annu Rev Nutr.* 2014;34:281-303. doi:10.1146/annurev-nutr-071812-161220.
 484. Coburn CT, Hajri T, Ibrahimi A, Abumrad NA. Role of CD36 in membrane transport and utilization of long-chain fatty acids by different tissues. *J Mol Neurosci.* 2001;16(2-3):117-21-7. doi:10.1385/JMN:16:2-3:117.
 485. Kim JJP, Miura R. Acyl-CoA dehydrogenases and acyl-CoA oxidases: Structural basis for mechanistic similarities and differences. *Eur J Biochem.* 2004;271(3):483-493. doi:10.1046/j.1432-1033.2003.03948.x.
 486. Kwon HS, Huang B, Unterman TG, Harris RA. Protein Kinase B- α Inhibits Human Pyruvate Dehydrogenase Kinase-4 Gene Induction by Dexamethasone Through Inactivation of FOXO Transcription Factors. *Diabetes.* 2004;53(4):899-910. doi:10.2337/diabetes.53.4.899.
 487. Lanza IR, Nair KS. Functional assessment of isolated mitochondria in vitro. *Methods Enzymol.* 2009;457:349-372. doi:10.1016/S0076-6879(09)05020-4.
 488. Braissant O, Foufelle F, Scotto C, Dauça M, Wahli W. Differential expression of peroxisome proliferator-activated receptors (PPARs): tissue distribution of PPAR- α , - β , and - γ in the adult rat. *Endocrinology.* 1996;137(1):354-366. doi:10.1210/endo.137.1.8536636.

489. Puigserver P, Wu Z, Park CW, Graves R, Wright M, Spiegelman BM. A cold-inducible coactivator of nuclear receptors linked to adaptive thermogenesis. *Cell*. 1998;92(6):829-839. doi:10.1016/S0092-8674(00)81410-5.
490. Cheng K, Ibrahim A, Hensley MT, et al. Relative roles of CD90 and c-kit to the regenerative efficacy of cardiosphere-derived cells in humans and in a mouse model of myocardial infarction. *J Am Heart Assoc*. 2014;3(5):e001260. doi:10.1161/JAHA.114.001260.
491. Attia RR, Connaughton S, Boone LR, et al. Regulation of pyruvate dehydrogenase kinase 4 (PDK4) by thyroid hormone: role of the peroxisome proliferator-activated receptor gamma coactivator (PGC-1 alpha). *J Biol Chem*. 2010;285(4):2375-2385. doi:10.1074/jbc.M109.039081.
492. Attia RR, Sharma P, Janssen RC, et al. Regulation of pyruvate dehydrogenase kinase 4 (PDK4) by CCAAT/enhancer-binding protein beta (C/EBPbeta). *J Biol Chem*. 2011;286(27):23799-23807. doi:10.1074/jbc.M111.246389.
493. Wende AR, Huss JM, Schaeffer PJ, Giguère V, Kelly DP. PGC-1 α Coactivates PDK4 Gene Expression via the Orphan Nuclear Receptor ERR α : a Mechanism for Transcriptional Control of Muscle Glucose Metabolism. *Mol Cell Biol*. 2005;25(24):10684-10694. doi:10.1128/MCB.25.24.10684-10694.2005.
494. Siu PM, Donley DA, Bryner RW, Alway SE. Citrate synthase expression and enzyme activity after endurance training in cardiac and skeletal muscles. *J Appl Physiol*. 2003;94(2):555-560. doi:10.1152/jappphysiol.00821.2002.
495. Qin S, Zhou W, Liu S, Chen P, Wu H. Icaritin stimulates the proliferation of rat bone mesenchymal stem cells via ERK and p38 MAPK signaling. 2015;8(5):7125-7133.
496. Delorme B, Dahl E, Jarry-Guichard T, et al. Expression pattern of connexin gene products at the early developmental stages of the mouse cardiovascular system. *Circ Res*. 1997;81(3):423-437. <http://www.ncbi.nlm.nih.gov/pubmed/9285645>.
497. Zhang Y, Liu C, Zhu L, et al. PGC-1alpha inhibits oleic acid induced proliferation and migration of rat vascular smooth muscle cells. *PLoS One*. 2007;2(11):e1137. doi:10.1371/journal.pone.0001137.
498. Johnston P V., Sasano T, Mills K, et al. Engraftment, differentiation, and functional benefits of autologous cardiosphere-derived cells in porcine ischemic cardiomyopathy. *Circulation*. 2009;120(12):1075-1083. doi:10.1161/CIRCULATIONAHA.108.816058.
499. Cheng K, Li TS, Malliaras K, Davis DR, Zhang Y, Marbán E. Magnetic targeting enhances engraftment and functional benefit of iron-labeled cardiosphere-derived cells in myocardial infarction. *Circ Res*. 2010;106(10):1570-1581. doi:10.1161/CIRCRESAHA.109.212589.
500. Duval C, Augé N, Frisach M-F, Casteilla L, Salvayre R, Nègre-Salvayre A. Mitochondrial oxidative stress is modulated by oleic acid via an epidermal growth factor receptor-dependent activation of glutathione peroxidase. *Biochem J*. 2002;367(Pt 3):889-894. doi:10.1042/BJ20020625.
501. Tabernero A, Lavado EM, Granda B, Velasco A, Medina JM. Neuronal differentiation is triggered by oleic acid synthesized and released by astrocytes. *J Neurochem*. 2001;79(3):606-616. doi:10.1046/j.1471-4159.2001.00598.x.
502. Rodríguez-Rodríguez RA, Tabernero A, Velasco A, Lavado EM, Medina JM. The neurotrophic effect of oleic acid includes dendritic differentiation and the expression of the neuronal basic helix-loop-helix transcription factor NeuroD2. *J Neurochem*. 2004;88(5):1041-1051. doi:10.1046/j.1471-4159.2003.02262.x.
503. Madsen L, Petersen RK, Kristiansen K. Regulation of adipocyte differentiation and function by polyunsaturated fatty acids. In: *Biochimica et Biophysica Acta - Molecular Basis of Disease*. Vol 1740. ; 2005:266-286. doi:10.1016/j.bbadis.2005.03.001.
504. Ghazvini Zadegan F, Ghaedi K, Kalantar SM, et al. Cardiac differentiation of mouse embryonic stem cells is influenced by a PPAR γ /PGC-1 α -FNDC5 pathway during

- the stage of cardiac precursor cell formation. *Eur J Cell Biol.* 2015;94(6):257-266. doi:10.1016/j.ejcb.2015.04.002.
505. Zorzano A, Liesa M, Palacín M. Role of mitochondrial dynamics proteins in the pathophysiology of obesity and type 2 diabetes. *Int J Biochem Cell Biol.* 2009;41(10):1846-1854. doi:10.1016/j.biocel.2009.02.004.
 506. Paltauf-Doburzynska J, Malli R, Graier WF. Hyperglycemic conditions affect shape and Ca²⁺ homeostasis of mitochondria in endothelial cells. *J Cardiovasc Pharmacol.* 2004;44(4):423-436. doi:10.1097/01.fjc.0000139449.64337.1b.
 507. Sauro VS, Strickland KP. Changes in oleic acid oxidation and incorporation into lipids of differentiating L6 myoblasts cultured in normal or fatty acid-supplemented growth medium. *Biochem J.* 1987;244(3):743-748. <http://www.pubmedcentral.nih.gov/articlerender.fcgi?artid=1148058&tool=pmcentrez&rendertype=abstract>.
 508. Lim JH, Gerhart-Hines Z, Dominy JE, et al. Oleic acid stimulates complete oxidation of fatty acids through protein kinase A-dependent activation of SIRT1-PGC1alpha complex. *J Biol Chem.* 2013;288(10):7117-7126. doi:10.1074/jbc.M112.415729.
 509. Ko IK, Lee SJ, Atala A, Yoo JJ. In situ tissue regeneration through host stem cell recruitment. *Exp Mol Med.* 2013;45(11):e57. doi:10.1038/emm.2013.118.
 510. Zimmermann W-H, Melnychenko I, Wasmeier G, et al. Engineered heart tissue grafts improve systolic and diastolic function in infarcted rat hearts. *Nat Med.* 2006;12(4):452-458. doi:10.1038/nm1394.
 511. Don CW, Murry CE. Improving survival and efficacy of pluripotent stem cell-derived cardiac grafts. *J Cell Mol Med.* 2013;17(11):1355-1362. doi:10.1111/jcmm.12147.
 512. Sackstein R, Merzaban JS, Cain DW, et al. Ex vivo glycan engineering of CD44 programs human multipotent mesenchymal stromal cell trafficking to bone. *Nat Med.* 2008;14(2):181-187. doi:10.1038/nm1703.
 513. Lo CY, Weil BR, Palka BA, Momeni A, Canty JM, Neelamegham S. Cell surface glycoengineering improves selectin-mediated adhesion of mesenchymal stem cells (MSCs) and cardiosphere-derived cells (CDCs): Pilot validation in porcine ischemia-reperfusion model. *Biomaterials.* 2016;74:19-30. doi:10.1016/j.biomaterials.2015.09.026.
 514. Hung SC, Pochampally RR, Hsu SC, et al. Short-term exposure of multipotent stromal cells to low oxygen increases their expression of CX3CR1 and CXCR4 and their engraftment in vivo. *PLoS One.* 2007;2(5). doi:10.1371/journal.pone.0000416.
 515. Tang YL, Zhu W, Cheng M, et al. Hypoxic preconditioning enhances the benefit of cardiac progenitor cell therapy for treatment of myocardial infarction by inducing CXCR4 expression. *Circ Res.* 2009;104(10):1209-1216. doi:10.1161/CIRCRESAHA.109.197723.
 516. Yan F, Yao Y, Chen L, Li Y, Sheng Z, Ma G. Hypoxic preconditioning improves survival of cardiac progenitor cells: Role of stromal cell derived factor-1 α -CXCR4 axis. *PLoS One.* 2012;7(7). doi:10.1371/journal.pone.0037948.
 517. Mayorga M, Kiedrowski M, Shamhart P, et al. Early upregulation of myocardial CXCR4 expression is critical for dimethylxallylglycine-induced cardiac improvement in acute myocardial infarction. *Am J Physiol Heart Circ Physiol.* 2016;310(1):H20-8. doi:10.1152/ajpheart.00449.2015.
 518. Feng Y, Huang W, Meng W, et al. Heat shock improves sca-1+ stem cell survival and directs ischemic cardiomyocytes toward a prosurvival phenotype via exosomal transfer: A critical role for HSF1/miR-34a/HSP70 pathway. *Stem Cells.* 2014;32(2):462-472. doi:10.1002/stem.1571.
 519. Hausenloy DJ, Yellon DM. Survival kinases in ischemic preconditioning and postconditioning. *Cardiovasc Res.* 2006;70(2):240-253.

- doi:10.1016/j.cardiores.2006.01.017.
520. Denli AM, Tops BBJ, Plasterk RH a, Ketting RF, Hannon GJ. Processing of primary microRNAs by the Microprocessor complex. *Nature*. 2004;432(7014):231-235. doi:10.1038/nature03049.
521. <http://www.mirbase.org/cgi-bin/browse.pl>.
522. Berezikov E, Guryev V, Van De Belt J, Wienholds E, Plasterk RHA, Cuppen E. Phylogenetic shadowing and computational identification of human microRNA genes. *Cell*. 2005;120(1):21-24. doi:10.1016/j.cell.2004.12.031.
523. Selbach M, Schwanhäusser B, Thierfelder N, Fang Z, Khanin R, Rajewsky N. Widespread changes in protein synthesis induced by microRNAs. *Nature*. 2008;455(7209):58-63. doi:10.1038/nature07228.
524. Gibbins D, Voinnet O. Control of RNA silencing and localization by endolysosomes. *Trends Cell Biol*. 2010;20(8):491-501. doi:10.1016/j.tcb.2010.06.001.
525. Lytle JR, Yario T a, Steitz J a. Target mRNAs are repressed as efficiently by microRNA-binding sites in the 5' UTR as in the 3' UTR. *Proc Natl Acad Sci U S A*. 2007;104(23):9667-9672. doi:10.1073/pnas.0703820104.
526. Bartel DP. MicroRNAs: Target Recognition and Regulatory Functions. *Cell*. 2009;136(2):215-233. doi:10.1016/j.cell.2009.01.002.
527. Kasabov N. *Springer Handbook of Bio-/Neuroinformatics*; 2014. doi:10.1007/978-3-642-30574-0.
528. Agarwal V, Bell GW, Nam JW, Bartel DP. Predicting effective microRNA target sites in mammalian mRNAs. *Elife*. 2015;4(AUGUST2015). doi:10.7554/eLife.05005.
529. Lall S, Grün D, Krek A, et al. A genome-wide map of conserved MicroRNA targets in *C. elegans*. *Curr Biol*. 2006;16(5):460-471. doi:10.1016/j.cub.2006.01.050.
530. Betel D, Wilson M, Gabow A, Marks DS, Sander C. The microRNA.org resource: Targets and expression. *Nucleic Acids Res*. 2008;36(SUPPL. 1). doi:10.1093/nar/gkm995.
531. Griffiths-Jones S, Saini HK, Van Dongen S, Enright AJ. miRBase: Tools for microRNA genomics. *Nucleic Acids Res*. 2008;36(SUPPL. 1). doi:10.1093/nar/gkm952.
532. Hata A. Functions of microRNAs in cardiovascular biology and disease. *Annu Rev Physiol*. 2013;75:69-93. doi:10.1146/annurev-physiol-030212-183737.
533. Small EM, Olson EN. Pervasive roles of microRNAs in cardiovascular biology. *Nature*. 2011;469(7330):336-342. doi:10.1038/nature09783.
534. Park CY, Choi YS, McManus MT. Analysis of microRNA knockouts in mice. *Hum Mol Genet*. 2010;19(R2). doi:10.1093/hmg/ddq367.
535. Fasanaro P, Greco S, Ivan M, Capogrossi MC, Martelli F. microRNA: Emerging therapeutic targets in acute ischemic diseases. *Pharmacol Ther*. 2010;125(1):92-104. doi:10.1016/j.pharmthera.2009.10.003.
536. Thum T, Condorelli G. Long noncoding RNAs and microRNAs in cardiovascular pathophysiology. *Circ Res*. 2015;116(4):751-762. doi:10.1161/CIRCRESAHA.116.303549.
537. Guo Z, Maki M, Ding R, Yang Y, Zhang B, Xiong L. Genome-wide survey of tissue-specific microRNA and transcription factor regulatory networks in 12 tissues. *Sci Rep*. 2014;4:5150. doi:10.1038/srep05150.
538. van Rooij E, Quiat D, Johnson BA, et al. A Family of microRNAs Encoded by Myosin Genes Governs Myosin Expression and Muscle Performance. *Dev Cell*. 2009;17(5):662-673. doi:10.1016/j.devcel.2009.10.013.
539. Olson EN. MicroRNAs as therapeutic targets and biomarkers of cardiovascular disease. *Sci Transl Med*. 2014;6(239):239ps3. doi:10.1126/scitranslmed.3009008.
540. Creemers EE, Tijssen AJ, Pinto YM. Circulating MicroRNAs: Novel biomarkers and

- extracellular communicators in cardiovascular disease? *Circ Res*. 2012;110(3):483-495. doi:10.1161/CIRCRESAHA.111.247452.
541. van Rooij E, Sutherland LB, Thatcher JE, et al. Dysregulation of microRNAs after myocardial infarction reveals a role of miR-29 in cardiac fibrosis. *Proc Natl Acad Sci U S A*. 2008;105(35):13027-13032. doi:10.1073/pnas.0805038105.
 542. Wang S, Aurora AB, Johnson B a., et al. The Endothelial-Specific MicroRNA miR-126 Governs Vascular Integrity and Angiogenesis. *Dev Cell*. 2008;15(2):261-271. doi:10.1016/j.devcel.2008.07.002.
 543. Dakhllallah D, Zhang J, Yu L, Marsh CB, Angelos MG, Khan M. MicroRNA-133a engineered mesenchymal stem cells augment cardiac function and cell survival in the infarct heart. *J Cardiovasc Pharmacol*. 2015;65(3):241-251. doi:10.1097/FJC.000000000000183.
 544. Boon R, Dimmeler S. Reviews: MicroRNAs in myocardial infarction. *Nat Rev Cardiol*. 2014:135-142. doi:10.1161/ATVBAHA.112.300137.
 545. Ivan M, Harris AL, Martelli F, Kulshreshtha R. Hypoxia response and microRNAs: No longer two separate worlds. *J Cell Mol Med*. 2008;12(5A):1426-1431. doi:10.1111/j.1582-4934.2008.00398.x.
 546. Qin Q, Furong W, Baosheng L. Multiple functions of hypoxia-regulated miR-210 in cancer. *J Exp Clin Cancer Res*. 2014;33(1):50. doi:10.1186/1756-9966-33-50.
 547. Hu S, Huang M, Li Z, et al. MicroRNA-210 as a novel therapy for treatment of ischemic heart disease. *Circulation*. 2010;122(11 SUPPL. 1). doi:10.1161/CIRCULATIONAHA.109.928424.
 548. Barile L, Lionetti V, Cervio E, et al. Extracellular vesicles from human cardiac progenitor cells inhibit cardiomyocyte apoptosis and improve cardiac function after myocardial infarction. *Cardiovasc Res*. 2014:1-24. doi:10.1093/cvr/cvu167.
 549. Fasanaro P, D'Alessandra Y, Di Stefano V, et al. MicroRNA-210 modulates endothelial cell response to hypoxia and inhibits the receptor tyrosine kinase ligand ephrin-A3. *J Biol Chem*. 2008;283(23):15878-15883. doi:10.1074/jbc.M800731200.
 550. Pulkkinen K, Malm T, Turunen M, Koistinaho J, Yl??-Herttuala S. Hypoxia induces microRNA miR-210 in vitro and in vivo. Ephrin-A3 and neuronal pentraxin 1 are potentially regulated by miR-210. *FEBS Lett*. 2008;582(16):2397-2401. doi:10.1016/j.febslet.2008.05.048.
 551. Signorelli SS, Volsi GL, Pitruzzella A, et al. Circulating miR-130a, miR-27b, and miR-210 in Patients With Peripheral Artery Disease and Their Potential Relationship With Oxidative Stress: A Pilot Study. *Angiology*. 2016;1(6):6. doi:10.1177/0003319716638242.
 552. Yan Y, Wang C, Zhou W, Shi Y, Guo P, Liu Y. Elevation of Circulating miR-210-3p in High-Altitude Hypoxic Environment. 2016;7(March). doi:10.3389/fphys.2016.00084.
 553. Chiong M, Wang Z V, Pedrozo Z, et al. Cardiomyocyte death: mechanisms and translational implications. *Cell Death Dis*. 2011;2(12):e244. doi:10.1038/cddis.2011.130.
 554. Elmore S. Apoptosis: a review of programmed cell death. *Toxicol Pathol*. 2007;35(4):495-516. doi:10.1080/01926230701320337.
 555. Strasser A, Jost PJ, Nagata S. The Many Roles of FAS Receptor Signaling in the Immune System. *Immunity*. 2009;30(2):180-192. doi:10.1016/j.immuni.2009.01.001.
 556. Czabotar PE, Lessene G, Strasser A, Adams JM. Control of apoptosis by the BCL-2 protein family: implications for physiology and therapy. *Nat Rev Mol Cell Biol*. 2014;15(1):49-63. doi:10.1038/nrm3722.
 557. Bialik S, Geenen DL, Sasson IE, et al. Myocyte apoptosis during acute myocardial infarction in the mouse localizes to hypoxic regions but occurs independently of p53. *J Clin Invest*. 1997;100(6):1363-1372. doi:10.1172/JCI119656.

558. Baldi A, Abbate A, Bussani R, et al. Apoptosis and post-infarction left ventricular remodeling. *J Mol Cell Cardiol.* 2002;34(2):165-174. doi:10.1006/jmcc.2001.1498.
559. Proskuryakov SY, Konoplyannikov AG, Gabai VL. Necrosis: A specific form of programmed cell death? *Exp Cell Res.* 2003;283(1):1-16. doi:10.1016/S0014-4827(02)00027-7.
560. Rock KL, Kono H. The inflammatory response to cell death. *Annu Rev Pathol.* 2008;3:99-126. doi:10.1146/annurev.pathmechdis.3.121806.151456.
561. Levine B, Yuan J. Autophagy in cell death: An innocent convict? *J Clin Invest.* 2005;115(10):2679-2688. doi:10.1172/JCI26390.
562. Levine B, Kroemer G. Autophagy in the Pathogenesis of Disease. *Cell.* 2008;132(1):27-42. doi:10.1016/j.cell.2007.12.018.
563. Zhang H, Bosch-Marce M, Shimoda LA, et al. Mitochondrial autophagy is an HIF-1-dependent adaptive metabolic response to hypoxia. *J Biol Chem.* 2008;283(16):10892-10903. doi:10.1074/jbc.M800102200.
564. Gatica D, Chiong M, Lavandero S, Klionsky DJ. Molecular mechanisms of autophagy in the cardiovascular system. *Circ Res.* 2015;116(3):456-467. doi:10.1161/CIRCRESAHA.114.303788.
565. Kanamori H, Takemura G, Goto K, et al. The role of autophagy emerging in postinfarction cardiac remodelling. *Cardiovasc Res.* 2011;91(2):330-339. doi:10.1093/cvr/cvr073.
566. Yan L, Vatner DE, Kim SJ, et al. Autophagy in chronically ischemic myocardium. *Proc Natl Acad Sci U S A.* 2005;102(39):13807-13812. doi:10.1073/pnas.0506843102.
567. Matsui Y, Takagi H, Qu X, et al. Distinct roles of autophagy in the heart during ischemia and reperfusion: Roles of AMP-activated protein kinase and beclin 1 in mediating autophagy. *Circ Res.* 2007;100(6):914-922. doi:10.1161/01.RES.0000261924.76669.36.
568. Dhesi P, Tehrani F, Fuess J, Schwarz ER. How does the heart (not) die? The role of autophagy in cardiomyocyte homeostasis and cell death. *Heart Fail Rev.* 2010;15(1):15-21. doi:10.1007/s10741-009-9137-y.
569. Boya P, Gonzalez-Polo, Rosa-Ana Casares N, Perfettini J-L, et al. Inhibition of Macroautophagy Triggers Apoptosis Inhibition of Macroautophagy Triggers Apoptosis †. *Mol Cell Biol.* 2005;25(3):1025-1040. doi:10.1128/MCB.25.3.1025.
570. Overholtzer M, Mailleux AA, Mouneimne G, et al. A Nonapoptotic Cell Death Process, Entosis, that Occurs by Cell-in-Cell Invasion. *Cell.* 2007;131(5):966-979. doi:10.1016/j.cell.2007.10.040.
571. Bergsbaken T, Fink SL, Cookson BT. Pyroptosis: host cell death and inflammation. *Nat Rev Microbiol.* 2009;7(2):99-109. doi:10.1038/nrmicro2070.
572. Sperandio S, de Belle I, Bredesen DE. An alternative, nonapoptotic form of programmed cell death. *Proc Natl Acad Sci U S A.* 2000;97(26):14376-14381. doi:10.1073/pnas.97.26.14376.
573. Sperandio S, Poksay K, de Belle I, et al. Paraptosis: mediation by MAP kinases and inhibition by AIP-1/Alix. *Cell Death Differ.* 2004;11:1066-1075. doi:10.1038/sj.cdd.4401465.
574. Maltese WA, Overmeyer JH. Methuosis: Nonapoptotic cell death associated with vacuolization of macropinosome and endosome compartments. *Am J Pathol.* 2014;184(6):1630-1642. doi:10.1016/j.ajpath.2014.02.028.
575. Nikolettou V, Markaki M, Palikaras K, Tavernarakis N. Crosstalk between apoptosis, necrosis and autophagy. *Biochim Biophys Acta - Mol Cell Res.* 2013;1833(12):3448-3459. doi:10.1016/j.bbamcr.2013.06.001.
576. Zhang JS, Li DM, Ma Y, et al. γ -Tocotrienol Induces Paraptosis-Like Cell Death in Human Colon Carcinoma SW620 Cells. *PLoS One.* 2013;8(2). doi:10.1371/journal.pone.0057779.
577. Galluzzi L, Maiuri M, Vitale I, et al. Cell death modalities: classification and

- pathophysiological implications Morphological Characterization of Cell Death. *Cell Death Differ.* 2007;14:1237-1243. doi:10.1038/sj.cdd.4402148.
578. Berghe T Vanden, Kaiser WJ, Bertrand MJM, Vandenabeele P. Molecular crosstalk between apoptosis, necroptosis and survival signaling. *Mol Cell Oncol.* 2015;3556(July 2015):00-00. doi:10.4161/23723556.2014.975093.
579. Li S, Xiao F, Shan P, et al. Overexpression of microRNA-133a inhibits ischemia-reperfusion-induced cardiomyocyte apoptosis by targeting DAPK2. - PubMed - NCBI. 2015;60(11):709-716. doi:10.1038/jhg.2015.96.
580. Zhang Y, Wang Z, Gemeinhart RA. Progress in microRNA delivery. *J Control Release.* 2013;172(3):962-974. doi:10.1016/j.jconrel.2013.09.015.
581. Frith JE, Porrello ER, Cooper-White JJ. Concise review: new frontiers in microRNA-based tissue regeneration. *Stem Cells Transl Med.* 2014;3(8):969-976. doi:10.5966/sctm.2014-0032.
582. Srinivas M, Cruz LJ, Bonetto F, Heerschap A, Figdor CG, de Vries IJM. Customizable, multi-functional fluorocarbon nanoparticles for quantitative in vivo imaging using 19F MRI and optical imaging. *Biomaterials.* 2010;31(27):7070-7077. doi:10.1016/j.biomaterials.2010.05.069.
583. Potier E, Ferreira E, Meunier A, et al. Prolonged hypoxia concomitant with serum deprivation induces massive human mesenchymal stem cell death. *Tissue Eng.* 2007;13(6):1325-1331. doi:10.1089/ten.2006.0325.
584. Deschepper M, Oudina K, David B, et al. Survival and function of mesenchymal stem cells (MSCs) depend on glucose to overcome exposure to long-term, severe and continuous hypoxia. *J Cell Mol Med.* 2011;15(7):1505-1514. doi:10.1111/j.1582-4934.2010.01138.x.
585. Zhuge J, Cederbaum AI. Serum deprivation-induced HepG2 cell death is potentiated by CYP2E1. *Free Radic Biol Med.* 2006;40(1):63-74. doi:10.1016/j.freeradbiomed.2005.08.012.
586. Lu C, Shi Y, Wang Z, et al. Serum starvation induces H2AX phosphorylation to regulate apoptosis via p38 MAPK pathway. *FEBS Lett.* 2008;582(18):2703-2708. doi:10.1016/j.febslet.2008.06.051.
587. Huang YC, Yang ZM, Chen XH, et al. Isolation of Mesenchymal stem cells from human placental decidua basalis and resistance to hypoxia and serum deprivation. *Stem Cell Rev Reports.* 2009;5(3):247-255. doi:10.1007/s12015-009-9069-x.
588. Ertas G, Ural E, Ural D, et al. Comparative analysis of apoptotic resistance of mesenchymal stem cells isolated from human bone marrow and adipose tissue. *ScientificWorldJournal.* 2012;2012:105698. doi:10.1100/2012/105698.
589. Kim HW, Haider HK, Jiang S, Ashraf M. Ischemic preconditioning augments survival of stem cells via miR-210 expression by targeting caspase-8-associated protein 2. *J Biol Chem.* 2009;284(48):33161-33168. doi:10.1074/jbc.M109.020925.
590. Kim HW, Jiang S, Ashraf M, Haider KH. Stem cell-based delivery of Hypoxamir-210 to the infarcted heart: Implications on stem cell survival and preservation of infarcted heart function. *J Mol Med.* 2012;90(9):997-1010. doi:10.1007/s00109-012-0920-1.
591. LeRoith D, Werner H, Beitner-Johnson D, Roberts CT. Molecular and cellular aspects of the insulin-like growth factor I receptor. *Endocr Rev.* 1995;16(2):143-163. doi:10.1210/edrv-16-2-143.
592. Jones JI, Clemmons DR. Insulin-like growth factors and their binding proteins: Biological actions. *Endocr Rev.* 1995;16(1):3-34. doi:10.1210/edrv-16-1-3.
593. Butt AJ, Firth SM, Baxter RC. The IGF axis and programmed cell death. In: *Immunology and Cell Biology.* Vol 77. ; 1999:256-262. doi:10.1046/j.1440-1711.1999.00822.x.

